



**HAL**  
open science

## ROS/RNS modulation in Systemic sclerosis treatment

Wioleta Marut

► **To cite this version:**

Wioleta Marut. ROS/RNS modulation in Systemic sclerosis treatment. Human health and pathology. Université René Descartes - Paris V, 2012. English. NNT : 2012PA05T079 . tel-01124101

**HAL Id: tel-01124101**

**<https://theses.hal.science/tel-01124101>**

Submitted on 30 Oct 2015

**HAL** is a multi-disciplinary open access archive for the deposit and dissemination of scientific research documents, whether they are published or not. The documents may come from teaching and research institutions in France or abroad, or from public or private research centers.

L'archive ouverte pluridisciplinaire **HAL**, est destinée au dépôt et à la diffusion de documents scientifiques de niveau recherche, publiés ou non, émanant des établissements d'enseignement et de recherche français ou étrangers, des laboratoires publics ou privés.

UNIVERSITÉ PARIS DESCARTES  
FACULTÉ DE MÉDECINE PARIS DESCARTES – SITE COCHIN

THÈSE  
pour obtenir le grade de  
DOCTEUR  
Sciences de la Vie et de la Santé  
Ecole Doctorale : Gc2iD  
Discipline: Immunologie

présentée et soutenue publiquement  
par madame Wioleta Marut  
le 15 novembre 2012

**ROS/RNS modulation in Systemic sclerosis treatment**

Jury:  
Dr Bernard WEILL, Président  
Pr Frédéric BATTEUX, Directeur de thèse  
Dr Phillipe Guilpain, Rapporteur  
Pr Gilbert Kirch, Rapporteur  
Pr Claus Jacob, Examineur  
Dr Amelie Servettaz, Examineur

*I dedicate this thesis to my  
husband and my beloved animals  
for their constant support and unconditional love*

## ACKNOWLEDGEMENTS

I would like to thank all those people who made this thesis possible and an unforgettable experience for me.

I would like to especially thank to my PhD supervisor, Frederic Batteux for supporting me during these past three years. Frederic is the funniest advisor and one of the smartest people I know.

Also I would like to express my very sincere gratitude to Mr. Bernard Weill for the essential contribution to this work.

I am very grateful to Frederic and Mr. Weill for their scientific advice, knowledge, and a lot of useful suggestions.

I also have to thank the members of my PhD committee, Professors Gilbert Kirsch and Philippe Guilpain for reviewing this work.

I will forever be thankful to Carole Nicco for her help, support and friendship. I could always count on her when I had a problems. She is my best role model for a scientist and mentor.

Remerciements également à Christiane Chereau, sans qui ce travail n'aurait pas abouti. Je la remercie pour sa gentillesse permanente et son soutien.

I also thank my best friend Mathilde for providing support and friendship that I needed.

The best outcome from these past three years is finding my best friend, soul-mate, and husband. Grzes has been a true and great supporter and has unconditionally loved me during my good and bad times.

## TABLE OF CONTENTS

<b>ABBREVIATIONS.....</b>	<b>7</b>
<b>PATHOGENESIS OF SYSTEMIC SCLEROSIS (SSC).....</b>	<b>10</b>
<b>I.1 Fibroblast dysfunction.....</b>	<b>10</b>
I.1.1  Intrinsic factors implicated in the fibroblast dysfunction .....	11
I.1.1.1  Activation of pro-collagen gene via TGF- $\beta$ signalling .....	11
I.1.1.2  CTGF - Connective tissue growth factor .....	14
I.1.1.3  Early growth response genes.....	14
I.1.1.4  Molecules involved in extracellular matrix degradation.....	15
I.1.1.5  Implication of ERK1/2 in fibrosis.....	16
I.1.1.6  Synthesis of free radicals.....	17
I.1.1.7  Synthesis of cytokines and chemokines .....	17
I.1.2  Extrinsic factors implicated in the fibroblast dysfunction .....	18
I.1.2.1  The role of cytokines.....	18
Interleukin-4 .....	18
Interleukin-13 .....	19
Interleukin-17 .....	19
Interferon $\gamma$ .....	20
I.1.2.2  Endothelin 1 .....	20
I.1.2.3  TGF- $\beta$ .....	21
I.1.2.4  PDGF.....	21
I.1.2.5  Serotonin .....	23
I.1.2.6  Angiotensin II.....	24
I.1.2.7  Notch proteins .....	25
<b>I.2 Endothelium dysfunction .....</b>	<b>26</b>
I.1.3  Vasculogenesis and angiogenesis .....	26
I.1.4  Dysregulation of vasculogenesis.....	27
I.1.4.1  Endothelin-1 .....	27
I.1.4.2  Nitric oxide (NO) .....	27
I.1.5  Dysregulation of angiogenesis.....	28
I.1.6  Local recruitment of leukocytes.....	30
I.1.7  The coagulation/fibrinolysis balance in systemic sclerosis .....	30
<b>Intervention of the immune system .....</b>	<b>30</b>
I.1.8  Innate immunity .....	31

I.1.9	Cellular adaptive immunity.....	32
I.1.10	Humoral adaptive immunity .....	33
I.1.10.1	Elements contributing to the activation of B cells.....	34
I.1.10.2	Role of autoantibodies in SSc.....	35
I.1.10.3	Autoantibodies relatively specific for SSc .....	36
I.1.11	Targeted therapy directed against B lymphocytes .....	39
	<b>Genetic and environmental factors.....</b>	<b>40</b>
I.1.12	Genetic factors .....	40
I.1.13	Environmental Factors .....	42
	<b>Animal models of SSc.....</b>	<b>42</b>
I.1.14	Inducible models of SSc .....	43
I.1.15	Spontaneous models.....	47
	<b>ROLE OF REACTIVE OXYGEN SPECIES (ROS) .....</b>	<b>48</b>
	<b>II.1 Sources of ROS.....</b>	<b>48</b>
	<b>The superoxide anion O<sup>•-</sup><sub>2</sub> .....</b>	<b>48</b>
	<b>Hydrogen peroxide (H<sub>2</sub>O<sub>2</sub>).....</b>	<b>51</b>
	<b>Hydroxyl radical (OH<sup>•</sup>).....</b>	<b>51</b>
	<b>Nitrogen oxide (NO<sup>•</sup>) .....</b>	<b>52</b>
	<b>II.1 Role and consequences of ROS .....</b>	<b>52</b>
I.1.16	Action on proteins.....	52
I.1.17	Effect on lipids .....	53
I.1.18	Action on DNA .....	53
I.1.19	Roles and effects of ROS in cellular metabolism .....	53
I.1.20	Antioxidants systems .....	55
I.1.20.1	Examples of enzymatic antioxidants systems .....	55
I.1.20.2	Examples of non-enzymatic antioxidant systems.....	56
I.1.21	The role of ROS/RNS in SSc.....	56
	<b>PERSONAL WORK .....</b>	<b>60</b>
	<b>III.1 Article 1 .....</b>	<b>62</b>
	<b>III.2 Article 2 .....</b>	<b>93</b>
	<b>III.3 Article 3 .....</b>	<b>122</b>

<b>DISCUSSION.....</b>	<b>154</b>
<b>CONCLUSIONS AND PERSPECTIVE .....</b>	<b>163</b>
<b>APPENDICES.....</b>	<b>165</b>
<b>REFERENCES .....</b>	<b>206</b>

## ABBREVIATIONS

<i>Ab</i>	Antibody
<i>AOPP</i>	Advanced Oxidation Protein Products
<i>AT II</i>	Angiotensin II
<i>AT<sub>1</sub>R</i>	Angiotensin II type 1 receptor
<i>CTGF</i>	Connective Tissue Growth Factor
<i>DPTTS</i>	Dipropyltetrasulfide
<i>EC</i>	Endothelial cells
<i>EP</i>	Epithelial cells
<i>Egr</i>	Early Growth Response Factor
<i>ETI</i>	Endothelin-1
<i>GSH</i>	Glutathion
<i>GVHD</i>	Graft-versus-host Disease
<i>HIF1</i>	Hypoxia-Induced Factor 1
<i>HOCl</i>	Hypochlorous acid
<i>IFN</i>	Interferon
<i>IL</i>	Interleukine
<i>KO</i>	Knock-Out
<i>LB</i>	Lymphocyte B
<i>LPS</i>	Lipopolysaccharide
<i>LT</i>	Lymphocyte T
<i>MCP-1</i>	Monocyte Chemoattractant Protein-1
<i>MMP</i>	Matrix Metalloproteinase
<i>NO</i>	Nitric oxide
<i>NKT</i>	Natural Killer T Cells
<i>OSCs</i>	Organosulfur compounds
<i>pDC</i>	plasmacytoid Dendritic Cell
<i>PDGF</i>	Platelet Derived Growth Factor
<i>PDGFR</i>	Platelet Derived Growth Factor Receptor
<i>(PHTe)<sub>2</sub>NQ</i>	3-bis(phenyltellanyl)naphthoquinone
<i>ROS</i>	Reactive Oxygen Species
<i>RNS</i>	Reactive nitrogen species

***SCID*** Severe Combined ImmunoDeficiency

***SSc*** Systemic Sclerosis

***SMA*** Smooth Muscle Actin

Smad

***TGF*** Transforming Growth Factor

***Th1*** lymphocyte T helper 1

***Th2*** lymphocyte T helper 2

***TIMP*** Tissue Inhibitor of Metalloproteinase

***TKI*** Tyrosine Kinase Inhibitor

***TLR*** Toll like Receptors

***TNF*** Tumor Necrosis Factor

***TSK*** Tight Skin

***VEGF*** Vascular Endothelial Growth Factor

***VEGFR*** Vascular Endothelial Growth Factor  
Receptor

## FIGURE LIST

<b>Figure 1.</b> Link between dysfunction of fibroblasts, endothelial cells, and immune cells in systemic sclerosis from J Varga, Nature Reviews Rheumatology, 2012.....	11
<b>Figure 2.</b> TGF $\beta$ Smad and non-Smad signaling pathways from initiation to nucleus. (a) Signal initiation (b) Smad-dependent pathway (c) Smad-independent pathway from Souchelnytskyi, Experimental Oncology, 2012.....	13
<b>Figure 3.</b> Link between Ras and ROS by Gabrielli, The Journal of biological Chemistry, 2005.....	16
<b>Figure 4.</b> IL-13 binding to the IL-13 receptor induces the activation of fibroblasts, differentiation into myfibroblasts, increased ECM deposition, and fibrosis from Fuschiotti, Cytokine, 2011. ....	19
<b>Figure 5.</b> Possible profibrotic pathways by angiotensin II by Dobrev, Circulation: Arrhythmia and Electrophysiology, 1995.....	25
<b>Figure 6.</b> Endothelial receptor tyrosine kinases involved in angiogenesis adapted from Alitalo, The Journal of Cell Biology, 1995.....	29
<b>Figure 7.</b> Angiogenesis in systemic sclerosis from Giacomelli, Autoimmunity Review, 2011. ....	30
<b>Figure 8.</b> Animal models of inducible and spontaneous SSc by Batteux, Current Opinion in Rheumatology, 2011. ....	47
<b>Figure 9.</b> Sources of ROS by Dawes, Trends in Cell Biology, 2005.....	52
<b>Figure 10.</b> Regulation of cancer cells and SSc fibroblasts proliferation adapted from P. Huang, Nature Reviews, Drug Discovery, 2009.....	58
<b>Figure 11.</b> Induction of murine SSc through daily intradermal injections of HOCl generating agents, by Batteux et al, Curr. Op Rheumatol, 2011.....	15

# Pathogenesis of systemic sclerosis (SSc)

---

Systemic sclerosis (SSc) is a rare connective tissue disease characterized by fibrosis of skin and internal organs, autoimmunity, and microcirculatory abnormalities [1, 2]. There are two widely recognized subsets of SSc, limited cutaneous (lcSSc) and diffuse SSc (dSSc). The main difference between these two subsets is the speed of disease progression, and the extent and severity of skin and internal organs. In lcSSc, skin thickening is confined to the face and extremities. In dcSSc, disease progression is very rapid, with the skin changes extending on the trunk, thighs, and upper arms. dcSSc is a more serious subset of the disease, with fatal visceral organ involvement.

SSc affects approximately 75.000-100.000 individuals in the United States. It affect four times more woman than man, and is more frequent in African-Americans than Caucasians [3]. Pathogenesis of SSc is complex and poorly understood. Factors causing dysfunction of fibroblasts, endothelial cells, and cells of the immune system have to be clarified (Figure 1). Among environmental factors, certain viruses, like cytomegalovirus [4] and certain chemicals such as solvents, silica, or pesticides may play a role in triggering the disease. In addition, several studies have shown that reactive oxygen species (ROS) [5-7] or TGF- $\beta$  [8, 9] may play a role in the initiation and progression of the disease. These new pathophysiological tracks open new therapeutic perspectives for this disease.

## ***1.1 Fibroblast dysfunction***

In SSc the excessive connective tissue fibrosis is the most characteristic pathological manifestation of the disease. In fibrotic tissue, normal architecture is replaced with a largely acellular, collagen-rich, stiff connective tissue, resulting in loss of functional

integrity. The key cellular moderator of fibrosis are myofibroblasts which are a differentiated and activated form of fibroblasts [10]. Myofibroblasts are responsible for increased collagen synthesis and deposition. Biochemical analysis of SSc skin shows increased accumulation of the main fibrillar collagens (Type I and III). Moreover, lesional skin has abundant fibrillin and elastin fibrils, and elevated levels of enzymes such as lysyl hydroxylase and lysyl oxidase. These enzymes catalyze post-translation collagen modifications [11].

**Figure 1.** Link between dysfunction of fibroblasts, endothelial cells, and immune cells in systemic sclerosis from J Varga, Nature Reviews Rheumatology, 2012.

SSc fibroblasts are characterized by abnormal growth, secretion of cytokines and chemokines, expression of cell-surface integrin adhesion molecules, and receptors for PDGF, CCL2, and TGF- $\beta$ . They differentiate into myofibroblasts which express alpha smooth muscle actin ( $\alpha$ -SMA) which is strongly associated with tissue fibrosis [12].

### **I.1.1 Intrinsic factors implicated in the fibroblast dysfunction**

#### **I.1.1.1 Activation of pro-collagen gene via TGF- $\beta$ signalling**

The family of transforming growth factor- $\beta$  (TGF- $\beta$ ) contain a large number of signaling proteins including TGF-isoforms, the factors that includes bone morphogenic proteins and activins. There are three isoforms of TGF- $\beta$  encoded by three different genes (TGF- $\beta$  1, 2, and 3). TGF- $\beta$  1 is synthesized by endothelial cells (EC), hematopoietic cells and connective tissue cells. TGF- $\beta$  2 is synthesized by epithelial and neuronal cells, and TGF- $\beta$  3 by mesenchymal cells. After secretion, all isoforms are stored in the extracellular

matrix as a complex of TGF- $\beta$ , the propeptide, and a protein called latent TGF- $\beta$ -binding protein. TGF- $\beta$  is released *in vivo* from the complex by the multifunctional matrix glycoprotein thrombospondin-1, and may also be activated by plasmin-mediated cleavage of the complex [13]. TGF- $\beta$  can signal through intracellular Smad proteins or through receptor serine/threonine kinases.

- TGF- $\beta$  signalling through Smad pathway:

The interaction of TGF- $\beta$  with its specific transmembrane receptors (like TGF $\beta$ RI) with serine-threonine kinase activity, induces a signal transduction involving intra-cytoplasmic Smad proteins. Ligand-induced phosphorylation of Smad2 and Smad3 allows them to form a heterocomplex with Smad4. This complex migrate into the nucleus where its regulates transcription of certain genes including type I collagen, plasminogen activator inhibitor-1,  $\alpha$ -SMA, and CTGF (Figure 2). Ligand-induced signal transduction through the Smad proteins is tightly controlled by endogenous inhibitors such as Smad7. Compared to healthy fibroblasts, fibroblasts from SSc patients are at the site of an abnormal nuclear accumulation of phosphorylated smad3 and a lack of smad7 expression. The lack of Smad7 helps to keep an abnormal production of collagen in SSc fibroblasts [14]. The imbalance of Smad 3 and Smad 7 in SSc fibroblasts might contribute to the initiation of the abnormal fibrogenic response.

Smad proteins are the most potent mediators of COL1A2 gene activation in SSc fibroblasts. Overexpression of Smad3 and Smad4 leads to the activation of COL1A2 promoter in normal fibroblasts via interaction with SBE (Smad Binding Element), and thus transcription of the COL1A2 gene.

**Figure 2.** TGF $\beta$  Smad and non-Smad signaling pathways from initiation to nucleus. (a) Signal initiation (b) Smad-dependent pathway (c) Smad-independent pathway from Souchelnytskyi, Experimental Oncology, 2012.

- TGF- $\beta$  signaling through non Smad pathway

Non-smad molecules activated by TGF- $\beta$  include protein kinase (the MAPKs p38 and JNK, focal adhesion kinase [FAK], and TGF- $\beta$  activated kinase 1), lipid kinases (such as PI3K and its downstream target, AKT), and the calcium-dependent phosphatase calcineurin (Figure 2) [15, 16]. Non-Smad pathway is involved in regulating cell proliferation, cytoskeletal rearrangement, ECM synthesis, and apoptosis.

- Role of TGF- $\beta$  in SSc

The expression of TGF- $\beta$  is elevated in scleroderma dermal fibroblasts, as well as in monocyte/macrophages and other infiltrating inflammatory cells [17]. TGF- $\beta$  is one of the most potent inducers of synthesis of extracellular matrix, and plays a central role in the process of fibrosis observed in SSc and other fibrosis diseases [18]. Several teams have demonstrated increased expression of type I and type II TGF- $\beta$  receptors in the fibroblasts from SSc patients [19, 20]. Pannu et al. have shown that aberrantly expressed TGF- $\beta$ -RI may drive an autocrine loop involved in the up-regulation of collagen and other matrix-related genes in SSc fibroblasts. In addition they demonstrated that imatinib mesylate blocks TGF- $\beta$ -induced activation of Smad1 and ERK-1/2 pathways in control fibroblasts and induces phosphorylation of Smad1 and ERK-1/2 in SSc fibroblasts [16].

The importance of TGF- $\beta$  in SSc has been confirmed by DNA microarray studies of SSc skin and SSc fibroblasts, in which TGF- $\beta$  signatures correlated with certain gene-expression subsets (34, 35). Moreover Milano et al. (36) have shown that the TGF- $\beta$ -responsive signature occurred only in a subset of skin biopsies from patients with diffuse

SSc. It was not increased in the patients with limited SSc, which suggests that fibrosis in these patients is driven by a different mechanism [21].

#### **I.1.1.2 CTGF - Connective tissue growth factor**

Connective tissue growth factor (CTGF) or CCN2 is a member of the CCN early-response gene family. CTGF is involved in essential cellular functions such as the maintenance of homeostasis, wound healing, control of cell growth, as well as the regulation of angiogenesis. Serum levels of CTGF are elevated in SSc patients, and SSc fibroblasts demonstrate overexpression of CTGF [22, 23]. Expression of CTGF can be regulated by TGF- $\beta$  and by many other factors (cAMP, angiotensin II) [24]. In vitro, CTGF can stimulate proliferation, chemotaxis and adhesion of fibroblasts, and increase synthesis of collagen. In animal models of SSc, CTGF level is associated with the development of fibrosis. Some authors have suggested that CTGF is essential to the maintenance of fibrosis, after it has been induced by a signal mediated by TGF- $\beta$  [23].

#### **I.1.1.3 Early growth response genes**

Egr-1 is the prototypical member of a family of zinc finger transcription factors. Expression of Egr-1 is induced at sites of acute injury and implicated in cell proliferation, differentiation, and survival. Egr-1 regulates gene expression of several pro-fibrotic factors like: TGF- $\beta$ , **platelet-derived growth factor (PDGF)**, CTGF, **vascular endothelial growth factor (VEGF)**, fibronectin, **tissue inhibitor of metalloproteinase (TIMP-1)**, and osteopontin. In Hep-G2 cells, Egr-1 induces epithelial-mesenchymal transition (EMT) by upregulating the expression of Snail. Abnormal expression of Egr-1 was found in several animal models of fibrosis. In normal skin and lung fibroblasts, forced expression of Egr-1 is sufficient to induce the increase of COL1A2 promoter activity and increase stimulation induce by TGF- $\beta$ . Subcutaneous injection of bleomycin induces fibrosis into the mice. This

leads to the accumulation of Egr-1 in skin fibroblasts and enhances TGF- $\beta$  signaling. Transgenic fibroblasts expressing Egr-1 have an **eight-fold increase** expression of NADPH oxidase-4 (NOX-4), which is involved in the generation of ROS. Egr-1 increase levels of NOX-4 in hypoxia condition. Some authors suggest that in SSc patients, hypoxia and TGF- $\beta$  might be responsible for overexpression of Egr-1 resulting in an increase activity of NOX-4 and production of ROS, which contribute to the progression of fibrosis. In addition, high levels of Egr-1 in peripheral mononuclear cells were found in SSc patients and is associated with pulmonary hypertension [25].

#### **I.1.1.4 Molecules involved in extracellular matrix degradation**

Fibroblasts are able of both synthesis and degradation of extracellular matrix (ECM). The amount of ECM in the tissue is controlled through the balance of ECM degradation enzymes - metalloproteinases (MMPs) and tissue inhibitors of metalloproteinases (TIMPs). MMPs and TIMPs are produced by mesenchymal cells (fibroblasts, myofibroblasts, endothelial cells), innate immunity cells (macrophages, monocytes, neutrophils), and metastatic cancer cells. MMPs are a family of at least 23 calcium-activated and zinc-dependent endopeptidases. They are essential for various biological processes such as embryonic development, morphogenesis, and tissue reproduction [26-28]. MMP-1 to 8 are the collagenases and play a major role in the digestion of type 1 collagen [29]. Too low or too high accumulation of ECM may result in different diseases such as connective tissue disorders or organ fibrosis. Numerous studies have shown overexpression of MMPs and TIMPs in SSc patients. In one study, authors have shown that SSc patients have higher serum concentrations of MMP-9 and TIMP-1. Moreover, they demonstrated that serum concentrations of MMP-9 is significantly higher in the diffuse type than the limited type of SSc [30]. Furthermore, expression of TIMP-1 in SSc fibroblasts is elevated and correlated

with disease severity in SSc patients. Auto-antibodies blocking anti-MMP1 and -3 were found in SSc patients, and their concentrations are correlated with the extent of cutaneous fibrosis, pulmonary and renal arterioles [28, 29, 31]. All these data suggest that an imbalance of MMP / TIMP could cause the development of fibrosis in SSc patients.

#### **I.1.1.5 Implication of ERK1/2 in fibrosis**

ERK 1/2 (extracellular signal-regulated kinases 1/2) is constitutively activated in SSc lungs and skin fibroblasts. This activation is accompanied by significant production of ROS via NADPH oxidase, and an abnormal accumulation of Ha-Ras protein in the cytoplasm. Accumulation of Ha-Ras proteins could be the result of a inhibition of their degradation by a proteasome as a result of ERK 1/2 activation. Svegliati et al highlight the importance of ERK 1/2, ROS and Ha-Ras protein in the induction and maintenance of "Scleroderma" phenotype fibroblasts (Figure 3). They have shown that *in vitro*, "scleroderma" phenotype fibroblasts obtained from SSc patients are rapidly reversible (after 1-2 days). In more recent work, the authors linked ERK1/2 activation to PDGF receptor signaling. They showed that extrinsic activation of PDGF receptor is required to maintain long-term activation of ERK and "scleroderma" phenotype, associated with activation of antibody (Ab) anti-receptor PDGF [32, 33]. Another studies have shown activation of ERK1/2 by TGF- $\beta$  in many cells type, and its important role for the CTGF and collagen stimulation [34].

**Figure 3.** Link between Ras and ROS by Gabrielli, The Journal of biological Chemistry, 2005.

#### **I.1.1.6 Synthesis of free radicals**

SSc fibroblasts spontaneously synthesize a large quantities of free radicals (superoxide anions  $O_2^{\bullet-}$  and  $H_2O_2$ ), molecules that stimulate fibroblast proliferation and collagen synthesis [7]. This synthesis appears to be independent from IL4, CTGF and TGF- $\beta$ , and could be partly dependent on the platelet derived growth factor (PDGF) [33]. Moreover, this increase oxidative stress could results from an inbalance between prooxidants and antioxidants system observed in SSc fibroblasts.

#### **I.1.1.7 Synthesis of cytokines and chemokines**

Fibroblasts are involved in the recruitment of leukocytes in the tissues by secreting chemokines and cytokines (IL-1, IL-6, tumor necrosis factor- $\alpha$  (TNF- $\alpha$ ), IL-8, monocyte chemo-attractant protein-1 (MCP-1), and PDGF). They promote the migration of circulating lymphocytes through the endothelial barrier and their accumulation in the dermis [35-37].

*In vitro* data suggest that some cytokines secreted by fibroblasts are directly involved in the dysfunction of fibroblasts by the autocrine activation.

- Interleukin-1 $\alpha$ : Fibroblasts from scleroderma patients aberrantly synthesize the IL1 $\alpha$  active precursor form (pro-IL-1 $\alpha$ ). The blocking of the synthesis of IL-1 results in a reduction of IL-6 and collagen synthesis, and reduces the transcription of PDGF in these fibroblasts [38].

- MCP 1: This chemokine also appears to have a direct effect in stimulating the synthesis of collagen, according to data obtained in a murine model of bleomycin-induced fibrosis [35].

## I.1.2 **Extrinsic factors implicated in the fibroblast dysfunction**

### I.1.2.1 **The role of cytokines**

#### ***Interleukin-4***

Interleukin-4 (IL-4) is a cytokine associated with B cell activation and T cell polarization to the Th2 phenotype. IL-4 have distinct roles in the regulation of tissue remodeling and fibrosis. Recent study suggest that IL-4 isa major factor of fibrosis induction [39]. The level of IL-4 is found increased in the bronchoalveolar lavage fluids of patients with idiopathic pulmonary fibrosis (IPF) [40], in the pulmonary interstitium of individulas with cryptogenic fibrosis alveolitis [41], and in peripheral blood mononuclear cells of those suffering from periportal fibrosis [42]. Increased serum levels of IL-4 [43] and IL-4–producing T cells were observed in patients with SSc [44] as well as in mice with bleomycin-induced skin sclerosis and lung fibrosis [45]. TSK-1 mice harboring the tight skin (TSK) mutation. TSK-1 spontaneously develop skin fibrosis and express a large quantities of IL-4 receptors. As a consequences, TSK-1 mice have a constitutive activation of IL- 4 signaling pathways [46]. This excess of IL-4 seems to have a pathogenic role, since treatment of TSK mice with anti IL-4 prevents collagen deposition in the dermis [47]. In SSc, IL-4 is mostly produced by CD4 + T cells and monocytes. Mice deficient for T-bet, a Th1 initiating factor, show increased and faster development of fibrosis with an exaggerated immune response and a constitutive elevation of IL-13 (45, 46 revue from bleo hocl). In humans, IL-4 stimulates proliferation of fibroblasts, increases deposition of extracellular matrix in the tissues, and is involved in the pathogenesis of SSc [48]. In addition, IL-4 stimulates the synthesis of pro-fibrotic cytokines such as MCP-1 by fibroblasts [39].

### ***Interleukin-13***

IL-13 is an immunoregulatory cytokine secreted by activated Th2 cells. IL-13 is involved in the pathogenesis of many fibrotic diseases, including SSc, and appears to be necessary in the effector phase of fibrosis and inflammation. IL-13 and IL-4 share many functional activities, because they exploit the same signaling pathways (IL-4Ra/Stat6) [49]. IL-13, like IL-4, can induce the expression of collagen type 1 in the skin fibroblasts. Thus, the pro-fibrotic effects of IL-13 are due to direct activation of fibroblasts or mediated by TGF- $\beta$ , whereas the maintenance of the type-2 immune response and the activation of proinflammatory mediators are important contributors to the chronic nature of fibrotic disorders (Figure 3).

**Figure 4.** IL-13 binding to the IL-13 receptor induces the activation of fibroblasts, differentiation into myofibroblasts, increased ECM deposition, and fibrosis from Fuschiotti, Cytokine, 2011.

IL-13 stimulates macrophages to produce TGF- $\beta$  by several different mechanisms including the production of latent and up-regulation of MMPs and also through IL-13R $\alpha$ 2 signaling. Transgenic IL-13 mice have exacerbated pulmonary fibrosis with high levels of TGF- $\beta$  [50]. Moreover, in SSc-bleomycin mice, mRNA levels of IL-13 were increased in the damaged skin, and expression of IL-13 receptor - IL-13R-2 was increased in mononuclear cells and macrophages infiltrating the skin. Finally, IL-13 deficient mice did not develop skin fibrosis after daily injection of bleomycin, showing involvement of IL-13 in the development of cutaneous fibrosis [50].

### ***Interleukin-17***

Recent study suggests that patients with SSc have strikingly increased frequencies of Th17 cells. Th17 cells are cells that secrete Interleukin-17 (IL-17). IL-17 is a cytokine family of six members (IL-17A-F). IL-17A and IL-17F are implicated in a variety of autoimmune

diseases, such as rheumatoid arthritis, multiple sclerosis, inflammatory bowel disease, asthma, and psoriasis. IL-17A and IL-17F have similarities in their amino acid sequence, and both bind to the same receptor: IL-17R type A. The effect of IL-17 in SSc is still poorly understood. It was recently shown that expression of IL-17A, but not IL-17F was significantly increased in the skin and serum of SSc patients [65]. On the contrary, the IL-17R type A is under-expressed in skin fibroblasts from SSc patients compared to normal fibroblasts, which is caused by activation of the intrinsic TGF- $\beta$  pathway in these cells. According to Nakashima study, IL-17A has an anti-fibrotic effect via down-regulation of type I collagen and CTGF through the microRNAs. IL-17A receptor signaling is suppressed by the intrinsic activation of TGF- $\beta$ 1 in SSc fibroblasts, which may amplify the increased collagen accumulation and fibrosis in SSc [51]. By contrast, Yoshizaki et al have shown that IL-17 has a pro-fibrotic effect. They demonstrated in bleomycine-induced fibrosis mice that L-selectin and ICAM-1 regulate Th17 cell accumulation into the skin and lung, leading to the development of fibrosis [52].

### ***Interferon $\gamma$***

Interferon-gamma is produced by Th1 lymphocytes and is a negative regulator of fibroblast activation. IFN- $\gamma$  inhibits the proliferation of fibroblasts and differentiation into myofibroblasts. There is a lot of studies showing the capability of IFN- $\gamma$  to selectively inhibit collagen synthesis [53, 54]. Another studies in SSc have shown that some fibroblasts from SSc patients are resistant to the inhibitory effect of IFN- $\gamma$ .

### **I.1.2.2 Endothelin 1**

Endothelin-1 (ET-1) is a potent vasomodulatory peptide produced by endothelial cells, macrophages, fibroblasts, and other type of cells. In addition to its vasomodulatory effects, ET-1 can induce the transformation of fibroblasts into myofibroblasts via the endothelin

receptors A (ETRA) and B (ETRB) [55]. ET-1 can induce collagen synthesis by activation of CTGF. The expression of ET-1 and its receptors is elevated in the skin from SSc patients [56]. Serum concentrations of endothelin-1 is increased in SSc patients [57]. Moreover, blockade of the endothelin receptors (ET-A and ETB) with bosentan significantly reduces overexpression of  $\alpha$ -SMA and ECM concentration by SSc fibroblasts [58].

### **I.1.2.3 TGF- $\beta$**

TGF- $\beta$  is a pleiotropic cytokine, recognized as a master regulator of pathological fibrosis. This cytokine is clearly involved in the activation and survival of fibroblasts, and synthesis of collagen [59]. TGF- $\beta$  can lead to transformation of normal fibroblasts into activated myofibroblasts and increase the synthesis of extracellular matrix [8]. Moreover TGF- $\beta$  increases the synthesis of CTGF by fibroblasts and as a consequence the synthesis of collagen [60]. Nevertheless, SSc fibroblasts do not produce themselves TGF- $\beta$  [61] and the level expression of TGF- $\beta$  is variable [62]. TGF- $\beta$  is originally secreted by endothelial cells, or by inflammatory cells present in the dermis in the first stage of the disease. It has also been shown that the skin of patients with SSc contained varying amounts of three isoforms of TGF- $\beta$  according the stage of disease [63]. Isoforms 1 and 2 are found in a large amount in the dermis at an early stage of the disease, a coexisting infiltration of the dermis by inflammatory cells. In fibrosis stage, these isoforms are absent, as in the skin of control subjects. It seems likely that TGF- $\beta$  plays a role in the induction of fibrosis at an early stage of the disease, but is less involved in the fibrosis [63, 64].

### **I.1.2.4 PDGF**

Platelet-derived growth factor (PDGF) is a major mitogen for many cell types of mesenchymal origin, e.g. fibroblasts and smooth muscle cells. PDGF is a dimeric peptide

secreted by various cell types such as platelets, fibroblasts, and smooth muscle cells. PDGF induces migration, differentiation and transformation of various cell types. PDGF participates in the regulation of apoptosis in part through the generation of ROS. Five isoforms of PDGF are described: PDGF AA, AB, BB, CC, DD. Many cells express PDGF, but the degree of expression is variable from one cell type to the other (Figure 3) [65]. For example, PDGF B is mainly synthesized by endothelial cells, megakaryocytes and neurons [66]. PDGF A and PDGF C are mainly secreted by epithelial cells, muscle cells and neural progenitors. PDGF D appears to be mainly synthesized by fibroblasts and smooth muscle cells. The PDGF receptors are formed by the association of two chains with tyrosine kinases: two  $\alpha$  chains, two  $\beta$  chains or a heterodimer formed by  $\alpha$  and  $\beta$  chain [65]. Activation of PDGFR induces phosphorylation of MAP kinases (Erk1/2, p38, JNK), Ras activation and the expression of genes such as Egr-1, c-fos, c-jun. Abnormalities of PDGF or their receptors have been identified in tumor process, various vascular diseases (atherosclerosis, pulmonary hypertension) and fibrosis [66, 67]. Svegliati et al have shown that stimulatory antibodies to the PDGFR selectively induced the Ha-Ras-ERK1/2 pathway and the stimulation of ROS cascades. This cascade of events increase the production of collagen type I and conversion of normal fibroblasts into activated myofibroblast [32, 33]. In mice, activation of PDGFR leads to progressive fibrosis of the skin suggesting the role of this signaling pathway in the development of fibrosis [68]. Fibroblasts from SSc patients constitutively synthesize PDGF AA under the autocrine stimulation by IL1 $\alpha$  [38], whereas normal fibroblasts do not synthesize PDGF AA, stimulated with mitogens *in vitro*. PDGF AA concentrations were found increased in the alveolar lavage of SSc patients [69]. In addition, expression of PDGF receptor  $\alpha$  was increased on the surface of fibroblasts from SSc patients. Activation of PDGFR could be inhibited by synthetic molecules inhibiting tyrosine kinases (TKI), including imatinib, axitinib, sunitinib, dasatinib, sorafenib and the

nilotinib. These molecules were initially developed for cancer treatment to inhibit signals proliferation via bcr/abl and c-kit and for some of them by inhibiting VEGFR and noangiogenesis. Imatinib has been successfully tested in a murine model of lung hypertension [70]. Others have shown that imatinib could reduce the synthesis of collagen and fibronectin in human skin fibroblasts [71, 72]. Recently, our team provided a new data on the activation of PDGFR in SSc and the effectiveness of certain TKI molecules to coneracts fibrosis, vascular abnormalities and activation of immune system in mouse model of SSc [73].

#### **I.1.2.5 Serotonin**

Serotonin (5-Hydroxytryptamine, 5-HT) is a hormone released upon the activation of platelets. Normally, plasma level of 5-HT is very low because circulating 5-HT is stored in platelets, but in SSc patients upon platelets activation, plasma level of 5-HT is significantly increased [74]. Serotonin is known to increase proliferation of fibroblasts and synthesis of collagen I. For example, 5-HT stimulates the proliferation of fibroblasts isolated from pulmonary hypertensive animals [75]. Seven distinct families of 5-HT receptors have been identified (5-HT1–5-HT7). Among them, two receptor subtypes, 5-HT2A and 5-HT2B, have been shown to play a role in the lung fibrosis. Large amounts of serotonin 5-HT2B receptor is expressed in the lung of patients with pulmonary fibrosis, and 5-HT2A and B receptors are induced in the lungs after intratracheal instillation of bleomycin, a molecule inducing pulmonary fibrosis. Inhibition of these receptors decreases fibrosis induced by bleomycin. Moreover, inhibition of the serotonin receptors on human fibroblasts reduce synthesis of collagen by inhibiting one of TGF- $\beta$  dependent pathways involving Smad proteins. In 2011, studies conducted in different murine models of SSc demonstrated that serotonin

induced platelet synthesis of extracellular matrix via activation of 5-HT<sub>2B</sub> by a TGF- $\beta$  dependent mechanism [76]. Thus, serotonin can be a mediator linking vascular injury, platelet activation, and fibrosis in SSc.

#### **I.1.2.6 Angiotensin II**

Angiotensin II (ANG II) is a profibrotic component of the renin angiotensin system (RAS) and plays a critical role in controlling of cardiovascular homeostasis. The RAS is a critical regulator of sodium balance, extracellular fluid volume, vascular resistance, and, ultimately, arterial blood pressure.

ANG II is profibrotic molecule produced by activated fibroblasts and macrophages and exerts its effect by inducing NADPH oxidase activity and by stimulation of TGF $\beta$ 1 production. This leads to the proliferation of fibroblast and then differentiation into active myofibroblasts. Moreover, ANG II increases TGF $\beta$ 1 signaling by increasing the level of smad 2/3 [77, 78]. In addition to its implication in various cardiovascular diseases, ANG II is also involved in cardiac fibrosis and in hypertensive heart disease [79]. ANG II plays an important role in the development of hepatic, lung, and renal fibrosis [80, 81].

Angiotensin II acts by binding to two receptor subtypes, angiotensin type I (AT<sub>1</sub>R) and type II (AT<sub>2</sub>R) receptors. AT<sub>1</sub>R mediates the profibrotic effects of ANG II by stimulating fibroblasts proliferation, cardiomyocytes hypertrophy and by increasing apoptosis of endothelial cells [82]. AT<sub>1</sub>R can induce fibrosis through the Shc/Grb2/SOS protein complex which activates Ras protein. This phenomenon initiates mitogen-activated protein kinase (ERK 1/2, p38, JNK) phosphorylation cascades which are centrally involved in fibrosis remodeling [83]. The JAK/STAT pathway, activating transcription factors such as activator protein-1 (AP-1) and nuclear factor- $\kappa$ B (NF- $\kappa$ B) are also activated by ANG

II(Figure 4). Both pathways lead to the proliferation and differentiation of fibroblasts, and synthesis of collagen.

**Figure 5.** Possible profibrotic pathways by angiotensin II by Dobrev, *Circulation: Arrhythmia and Electrophysiology*, 1995.

#### **I.1.2.7 Notch proteins**

The Notch pathway is an evolutionary conserved signalling mechanism that regulates cellular fate and development in various cell types. The main function of the Notch proteins is the regulation of many processes such as proliferation, differentiation, and apoptosis. Notch mutation has been demonstrated in *Drosophila* in the early twentieth century. "Partial loss of function" of Notch had resulted in the formation of notches ("Notch") at the end of the wings of fruit flies. At the end of the 30s, Poulson showed that the total loss of Notch function resulted in embryonic lethal phenotype characterized by an overproduction of neurons, called phenotype "neurogenic" [73]. Subsequently, four Notch proteins (Notch1 to 4) have been described in mammals. They have non-redundant functions during embryogenesis. An increasing amount of evidence suggests that the Notch pathway is implicated in the development of fibrosis that characterizes SSc in both rodent and human. Indeed, Notch1 is activated in the lesional skin of SSc patients and in their fibroblasts. Mice with ROS-induced SSc, bleomycin-induced SSc and *Tsk1*-mice also display elevated levels of intracellular portion of Notch receptors NICD (Notch Intra-Cellular Domain) in skin and lungs. This accumulation of NICD is associated with the overactivation of ADAM17 (TACE), a proteinase involved in Notch activation through the first cleavage of the Notch receptor. Moreover, treating mice with DAPT, a  $\gamma$ -secretase inhibitor that blocks the release of NICD, can reduce the collagen content in skin and lungs

and the production of autoantibodies, thus preventing the development of SSc in the different mouse models. Similarly, treating SSc-mice with Notch siRNA prevented dermal thickening and fibrosis [225].

### ***1.2 Endothelium dysfunction***

Vascular injury appears to be one of the earliest clinical manifestations in SSc and can be a crucial initiating event in the pathology of SSc. More than 90% of SSc patients present Raynaud's phenomenon and reversible and transient digital ischemia. This cause changes in the cellular metabolism and the generation of reactive oxygen species (ROS) by ischemia-reperfusion. Early apoptosis of endothelial cells is highlighted in the skin biopsies of patients, resulting in a loss of integrity of the endothelial barrier. Endothelial dysfunction has also consequences for the recruitment of inflammatory cells, changes in the coagulation / fibrinolysis balance, and abnormal vascular tone. In addition, endothelial abnormalities may contribute to the phenomenon of fibrosis in SSc [84].

#### **I.1.3 Vasculogenesis and angiogenesis**

In adults, blood vessels formation and repair are mediated via two different processes: vasculogenesis and angiogenesis. Vasculogenesis is describes by the formation of new vessels by circulating EP (bone marrow-derived endothelial progenitor cells) independent from pre-existing vessels [85]. Angiogenesis is a process of sprouting of differentiated EC from pre-existing vessels. It involves the proliferation and migration of mature endothelial cells. Stabilization of vessel wall by pericytes is the final process of angiogenesis and leads to a functional network of new capillary [86].

## **I.1.4 Dysregulation of vasculogenesis**

### **I.1.4.1 Endothelin-1**

Endothelin-1 (ET-1) is a typical endothelial cell-derived product. ET-1 receptors are expressed by various cells, including fibroblasts, monocytes and endothelial cells. ET-1 promotes fibroblasts synthesis of collagen, and thus provide the link between fibrosis and vasculopathy [87]. ET-1 exerts vasoconstrictor action through stimulation of ETA receptors in vascular smooth muscle and vasodilator action through stimulation of ETB receptors in endothelial cells. In SSc patients, increased production of ET-1 and decreased production nitric oxide and PGI<sub>2</sub> suggest contribution of ET-1 to the vasoconstrictive tendency in SSc [ ]. However, a number of other studies have shown no difference in endothelin levels in patients with Raynaud's phenomenon [89]. This indicates that increased endothelin levels may be rather a marker of endothelial damage than a reflect of enhanced susceptibility to vasoconstriction .

### **I.1.4.2 Nitric oxide (NO)**

Nitric oxide is an important vasodilator of vascular smooth muscle, constitutively secreted by endothelial cells. NO inhibits vascular smooth muscle cell proliferation via inhibition of mitogenic proteins TGF- $\beta$  and PDGF, and elevation of cyclic guanosine monophosphate (cGMP) [90]. The role of NO in the pathogenesis of SSc is complex. Plasma values of NO measured in patients are discordant from one study to another [91]. Moreover, the role of NO is ambivalent because it may interact with other reactive oxygen forms like superoxide anion to form the highly toxic species peroxynitrite. By contrast, NO can also limit cytokine-induced endothelial cell activation, adhesion of monocyte, and inhibits the release of inflammatory cytokine like IL-6 and IL-8 from endothelial cells. Therefore, NO

production in SSc may contribute to the pathogenesis of arteriolar intimal proliferation and may have a prominent role in pathogenesis of the disease.

### **I.1.5 Dysregulation of angiogenesis**

Angiogenesis is a multistep process under the control of angiogenesis inducers and inhibitors. Under normal conditions, the levels of angiogenesis inducers and inhibitors are balanced and angiogenesis does not occur in healthy tissues. Under inflammatory states or in hypoxic environment like Systemic sclerosis, angiogenic growth factors are induced which leads to the initiation of angiogenesis. Tissue ischemia leads to the expression of vascular endothelial growth factor (VEGF), PDGF, and basic fibroblast growth factor (bFGF), which have been characterized as key molecules in angiogenesis (Figure 5).

VEGF is a pro-angiogenic factor, which controls several molecular and cellular steps in the angiogenesis process. It causes proliferation and migration of endothelial cells, and stabilization of the lumina to form new vessels. Patients with early SSc have elevated level of VEGF in the serum [123]. VEGF and its receptors VEGFR-1 and VEGFR-2 are overexpressed in the skin of SSc patients [124]. However, the role of VEGF in the pathogenesis of SSc is unknown, although some authors have suggested that local hypoxia in the skin could be a contributing factor to increase of VEGF in some patients [125]. Other pro-angiogenic mediators like PDGF "Placental Growth Factor" (PIGF) and "Fibroblast Growth Factor-2" (FGF-2) also have elevated plasma levels compared to healthy subjects:

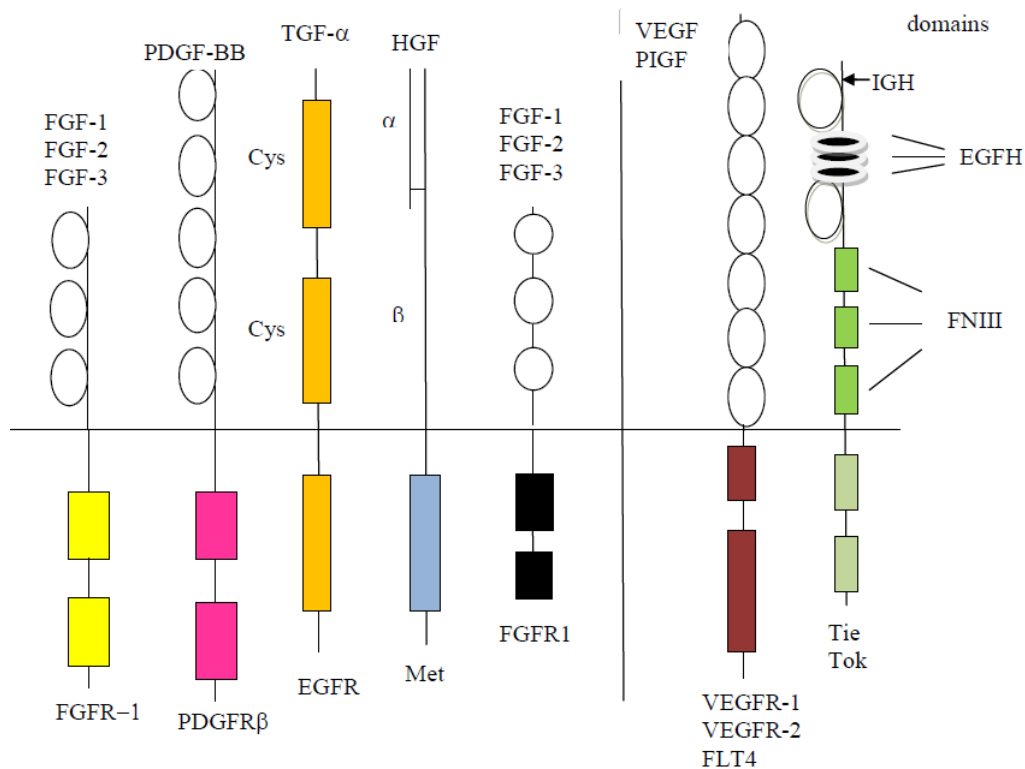


**Figure 6.** Endothelial receptor tyrosine kinases involved in angiogenesis adapted from Alitalo, *The Journal of Cell Biology*, 1995.

The concentration of anti-angiogenic factors is also increased in the serum of some SSc patients, like: angiostatin, CXCL4, thrombospondin, and IL-4 [126]. It remains to determine whether deregulation of pro and anti-angiogenic factors is cause or consequence of vascular disease in SSc.

Angiogenic growth factors such as GM-CSF or VEGF can stimulate the release of endothelial progenitor cells (EPC) from the bone marrow into the blood in response to stress or damage related signals. EPC migrate through the bloodstream to the sites of vascular injury, where they contribute to the formation of neovessels or the repair of damaged vessels.

Recent studies have shown that the chemokine stromal-cell derived factor-1 (SDF-1) has a major role in the recruitment and retention of endothelial progenitor cells expressing the

SDF-1 receptor, and probably has an important role in triggering cell arrest and emigration into the angiogenic niches (Figure 6).

Several recent studies have evaluated involvement of endothelial progenitor cells in SSc but the results on quantification and properties of these cells are contradictory, probably because the surface markers used in experiments are not the same in each study. Del Papa et al have shown that the rate of endothelial progenitor cells CD45-CD133 + was significantly lower in SSc patients than in healthy subjects [127]. Other team has shown increased angiogenic potency of monocytic endothelial progenitor cells in SSc patients [92].

#### I.1.6 **Local recruitment of leukocytes**

After *in vitro* activation endothelial cells from scleroderma patients, are capable to secrete MCP-1 and RANTES, two chemokines that attract monocytes and macrophages [93].

#### I.1.7 **The coagulation/fibrinolysis balance in systemic sclerosis**

An increase of coagulability is observed in SSc patients. Many clotting factors are present in excess in plasma of SSc patients like: dermatan sulfate, thrombin, antithrombin, and von Willebrand factor (vWF). Meanwhile, there is a deficiency in D-dimer, suggesting a defect in fibrinolysis in these patients [ ].

**Figure 7.** Angiogenesis in systemic sclerosis from Giacomelli, Autoimmunity Review, 2011.

### ***Intervention of the immune system***

Innate immunity and adaptive immunity play an important role in the pathogenesis of SSc. At an early phase of the sclerotic process, leukocyte activation is visible in the peripheral blood and damaged tissue, where it is directly involved in the induction of tissue damage.

### I.1.8 **Innate immunity**

Recently accumulating and mounting evidence points toward the importance of immune cells in SSc pathogenesis.

Monocytes and macrophages have been demonstrated in the skin of patients in the first stage of SSc [95]. These cells were also observed in a mouse model of SSc secondary to Graft versus Host Disease [96]. Monocytes and macrophages express on their surface a large amounts of antigen presenting molecules and they can induce the activation of LT. Mast cells are increased in the skin of patients at an early phase of the sclerotic process compared to healthy skin [97]. These cells release IL-4 and histamine, two compound involved in the fibrotic process. In murine models of fibrosis induced by bleomycin, a mast cell deficiency delayed the appearance of skin fibrosis [98]. Overexpression of CD163, a marker for M2 macrophages found on TLR4 activated monocytes in SSc patients with interstitial lung disease along with the increase production of CCL18 and IL-10 [99]. Interestingly, the expression of CD163 is also increase in diseased SSc skin [100]. Another study identified a circulating TLR4 ligand in SSc sera [101]. They have shown that ligation of TLR4 induces an increased production of IL-10 in SSc monocyte-derived dendritic cells [102]. Moreover, overproduction of IL-10 is partly related to the increased level of profibrotic CCL-18. In SSc patients, the expression of TLR3 in the skin is higher than in healthy controls. *In vivo* administration of several TLR ligands, especially TLR3, through a transcutaneous pump, induces fibrosis progression in mouse model of SSc [103]. Activation of TLR stimulates several inflammatory mediators, such as IL-1, IL-6 and TNF $\alpha$  in macrophages and dendritic cells. Activation of these and other inflammatory mediators, through TLR sensors, may collaborate to upregulate fibrotic mediators such as TGF $\beta$  and IL-13.

### I.1.9 Cellular adaptive immunity

Several arguments favor the role of T lymphocyte in the pathogenesis of SSc, especially in the initial phase of the disease. Infiltrating T cells, predominately CD4+, are the major lymphocytes seen in the involved skin of Systemic sclerosis patient [104]. The importance of this cells is correlated with a short diseased period and high inflammatory skin score. In fact, skin biopsies performed at the late stage of the disease with advanced fibrosis showed only moderate inflammatory infiltrates [63]. The perivascular infiltrates are predominantly CD3<sup>+</sup> and CD4<sup>+</sup> T cells that express the activation markers - HLA-DR and CD25, and secrete fibrogenic cytokines and chemokines [105]. T cells found in the affected tissues have restricted TCR specificities, suggesting an oligoclonal T cells expansion [106]. However, it is unclear whether these clones are activated nonspecifically by cytokines or chemokines or specifically by unknown antigens. In the skin, the recruitment of lymphocytes occurs through adhesion molecules. In 2010, Sato's team studied the role of various adhesion molecules in mice treated with bleomycin induced-SSc [52]. They shown that the L-selectin and ICAM-1 regulates accumulation of Th2 and Th17 cells in the skin and lungs. Both, Th2 and Th17 had a pro-fibrotic properties. In contrast, Th1 infiltrate appears to be regulated by P-selectin and PSGL-1, and have the property of inhibiting the development of fibrosis in this model. Th1/Th2 cytokine balance in SSc patients is still unclear. Several studies have shown conflicting results. On the one side, high levels of IL-4 were found in the serum of SSc patients [107]. In addition, a microarray analysis of the transcriptome of circulating lymphocytes of patients with scleroderma in 2006 showed high levels of GATA-3, a factor involved in the Th2 polarization. On the other side a profile of Th1 gene expression was observed in peripheral blood mononuclear cells of SSc patients [108]. Finally, proteomic analysis of bronchoalveolar lavage of patients confirms the predominance of Th2-type cytokines. Moreover, mice deficient in T-bet, a transcription

factor, specific for the activation of Th1 lymphocytes, develop exacerbated fibrosis in response to bleomycin injections [109].

Inducible costimulator ICOS, expressed on activated T Cells, and its ligand ICOSL on antigen-presenting cells, has recently been implicated in the pathogenesis of SSc. Indeed, ICOS deficiency reduces lung and skin fibrosis induced by bleomycin injection. In contrast, the ICOS-ligand deficiency increases the fibrotic process. The authors have shown that the severity of fibrosis was correlated with the expression levels of ICOS-ligand in B lymphocytes and macrophages [110]. Thus, ICOS-ligand plays a regulatory role in the activation of antigen-presenting cells in bleomycin-induced fibrosis.

Other studies have shown the role of activated T lymphocyte upon contact with fibroblast, in the production of collagen type I by cultured dermal fibroblasts from patients with diffuse systemic sclerosis (SSc) and healthy controls. They found that production of type I collagen by skin fibroblasts is inhibited by membranes from activated T cells [111]. This inhibitory effect is mediated by a direct contact between LT and fibroblasts, and dependent on a prior *in vitro* activation of T Cells. The same team has recently shown that Th-1 cells inhibit collagen production by skin fibroblasts, through the membrane associated tumor necrosis factor alpha [112]. Only anti-CD3 activated T Cells can reduce collagen synthesis by fibroblasts in SSc patients. These two last works shown the complexity of cellular interactions in SSc.

#### **I.1.10 Humoral adaptive immunity**

Abnormalities of B lymphocytes in SSc have been known for several years. They are characterized by the hypergammaglobulinemia, the production of autoantibodies, and the hyperactivity of B lymphocytes. More recently, anomalies on various B cells populations were identified.

### **I.1.10.1 Elements contributing to the activation of B cells**

The role of B lymphocyte in the development of fibrosis has been explored by studies in several animal model of SSc. Those mice produce autoantibodies against SSc-specific target autoantigens including topoisomerase I (scl70), fibrillin 1, type I collagen, and Fc-receptors [40]. Saito et al have shown that in bleomycin-induced fibrosis mice, deficiency of CD19 suppresses fibrosis and autoantibodies production by inhibiting TLR4 signals. Constitutive CD19 tyrosine phosphorylation is increased in TSK B cells compared with wild-type B cells . Chronically activated TSK B cells *in vivo*, and the cytokines produced by those cells may participate in the induction of skin fibrosis in TSK mice. In this animal model, the down-regulation of B-cell function decreased skin thickness [ , 114]. Saito et al. shown that CD19 expressed by B lymphocytes is abnormally activated and overexpress in SSc patients [115].

Furthermore, memory B cells from SSc patients show overexpression of CD80 and CD86, that are critical co-stimulatory molecules of B cells activation. To up-regulate the expression of CD80 and CD86, activation of B cells is required. This results indicate, that SSc memory B cells are chronically activated *in vivo*, possibly due to overexpression of CD19.

Another molecule, BAFF, is also involved in B cell homeostasis. BAFF is overexpressed in the blood and skin of SSc patients. Indeed, as patients with systemic lupus erythematosus or Sjögren's syndrome, SSc patients have elevated serum level of soluble BAFF compared to healthy control [116-118]. The level of BAFF correlate with the severity of skin disease. Further, expression of BAFF receptor on B cells is increased in SSc patients. SSc B cells overexpressing BAFF receptor, have a higher ability to produce IgG and IL-6, showing that BAFF signaling might contribute to the development of SSc. The evidence of T cell polarization toward a Th2 response play an important role in the

development of tissue fibrosis. The activation of B lymphocyte and humoral response are facilitated by the Th2 environment characterized by overproduction of IL-4, IL-5, IL-6, IL-10 and IL-13. These cytokines promote the production of antibodies by the B lymphocyte, and as we have already seen, they stimulate synthesis of collagen by fibroblasts. Moreover, B cells might influence the Th1/Th2 balance by regulating dendritic cells function. Activated B cells produce IL-10 which inhibits the production of IL-12 by dendritic cells, and promotes Th2 differentiation. That suggests a critical role of B cells for the development of Th2 response. IL-6 produced by B lymphocyte can also induce the production of collagen and glycosaminoglycans by dermal fibroblasts. Several studies have shown a high level of IL-6 in the skin and in the serum of SSc patients. These results indicate that this cytokine may play a role in the development of fibrosis via its pro-inflammatory activity [119]. Fibroblasts from scleroderma patients produce four times more IL-6 than fibroblasts from healthy controls. In Tsk1 mice, B lymphocytes stimulated with anti-IgM Ig and CD40-Ig produced significantly higher levels of IL-6 than B lymphocytes from control mice [113]. The B lymphocytes also secrete activated TGF- $\beta$ , which amplifies the excessive production of extracellular matrix proteins by fibroblasts [120].

#### **I.1.10.2 Role of autoantibodies in SSc**

Autoimmune disorders in SSc patients are characterized by activation of the immune system. This activation leads to lymphocyte activation and cytokine secretion, and to the production of specific autoantibodies. SSc patients have specific autoantibodies against a variety of self antigens which are not associated with other autoimmune diseases. Antinuclear autoantibodies are observed at the first diagnosis in more than 95% of SSc patients. Some of the autoantibodies are associated with distinct disease severity and

activity, including skin involvement, internal organ manifestations and prognosis. Anti-topoisomerase I antibodies (anti-topo I) and anti-centromere antibodies (ACA) are the classic autoantibodies associated with SSc [121]. Furthermore, antibodies against several other structures (including U3RNP, PM/Scl, snRNP, mitochondrial components, antigens present on endothelial cells and fibroblasts, and extracellular antigens) can also be detected in SSc serum [122]. However, the contribution of SSc-specific autoantibodies in the pathogenesis of SSc is not clearly demonstrated.

### **I.1.10.3 Autoantibodies relatively specific for SSc**

- **Anti-centromere antibodies**

Anti-centromere antibodies (ACA) were described in 1980 by Moroi et al. ACA are detected in the serum of 20 to 30% of scleroderma patients. The presence of these antibodies is correlated with certain clinical signs: limited cutaneous involvement, calcinosis, and Raynaud's syndrome. The presence of ACA can develop pulmonary hypertension but not pulmonary fibrosis. ACA-positive SSc patients have a more promising prognosis than patients with autoantibodies related to diffuse form of the disease. So far, no pathogenic role of ACA has been demonstrated [123, 124].

- **Anti-topoisomerase I antibodies**

Autoantibodies against a chromatin-associated protein were described for the first time in SSc patients in 1979. Anti-topoisomerase I antibodies (ATA) are highly associated with the dcSSc disease subset. ATA have been found in approximately 40% of patients with dSSc, and in less than 10% of lcSSc patients [125]. ATA are associated with pulmonary fibrosis, cardiac and musculoskeletal involvement, increased mortality, and with higher risk of developing malignancies. SSc patients with undetectable ATA have milder disease and better survival. Recent studies have shown that ATA positive patients earlier

developed Raynaud's phenomenon syndrome and have approximately double rate of lung fibrosis compared with anti-CENP patients [126]. Another recent studies have shown that anti-topoisomerase I is able to bind to the fibroblasts membrane, and induce adhesion of monocyte to fibroblasts and their activation [121].

- **Anti-RNA polymerase III antibodies**

These antibodies are detected approximately in 15% of patients with SSc. They are associated with the diffuse form of the disease, especially with renal involvement, and a poor prognosis. Their presence may be associated with the anti-DNA topoisomerase-1. Their determination in the serum of patients may have a prognostic value in the context of scleroderma renal crisis. Their pathogenicity has not been demonstrated yet [127].

- **Anti-Th/To antibodies**

Antibodies to Th/To are directed against subunits of the ribonuclease mitochondrial RNA processing and ribonuclease P complexes. Those antibodies were recently detected in patients with localized scleroderma [128]. Anti-Th/To are present in 2 to 5% of SSc patients and are relatively specific for SSc. They are associated with limited skin involvement but high risk of organ involvement and therefore a worse prognosis.

- **Anti-endothelial cell antibodies (AECA)**

Autoantibodies against endothelial cell antigens were found in 25–85% of patients with SSc, but were also detected in other connective tissue diseases. They are more frequently found in patients with a diffuse form of SSc, digital ulcers, severe Raynaud's phenomenon, pulmonary fibrosis and / or cardiac disease. Their antigenic targets are being identified. Several studies have demonstrated a pathogenic role of AECA. In SSc patients, AECA can induce EC activation *in vitro*, resulting in the expression of adhesion molecules and release of cytokines and chemokines [129].

- **Fibroblasts antibodies (AFA)**

AFA were identified in the serum of SSc patients in the 1980s [130]. Since then, AFA have been well characterized. They can be detected by ELISA in the serum from 46 to 58% of SSc patients [131]. They are more common in patients with diffuse form. They can be also detected by indirect immunofluorescence and flow cytometry. After binding to their ligands, some of AFA are internalized. *In vitro*, they induce the expression of adhesion molecules such as ICAM-1, and cytokines (IL1, IL6) by fibroblasts [132]. A recent study revealed alpha-enolase as a primary target antigen of AFA from SSc patients [133].

- **Fibrillin-1 antibodies**

Fibrillin is a major component of the extracellular matrix microfibrils. A polymorphism in the fibrillin gene (FBN1) is associated with development of SSc in some populations. Anti-fibrillin-1 antibody can be detected in patients with SSc most commonly in dcSSc but also in lcSSc or MCTD. The prevalence of these Abs effect varies according to the ethnic background of patients, since they are present in 94% of Choctaw Indians, 87% of Japanese patients and only 4% of subjects of African-American origin. Sera from patients with diffuse SSc or calcinosis, Raynaud's, or mixed connective tissue disease also had significantly higher frequencies of anti-fibrillin-1 Abs than sera from healthy controls or patients with other connective tissue diseases [134].

- **Anti-platelet-derived growth factor receptor antibodies (anti-PDGFR)**

PDGFR autoantibodies might have a pathogenic role in SSc patients. PDGFR expression is increased by pathological TGF- $\beta$  signaling, and binding of anti-PDGFR to the PDGFR ligand results in amplification of the Ras-extra-cellular signal-regulated kinase (ERK) and 1/2-reactive oxygen species (ROS) cascade. Thus, it leads to increased collagen production

[135]. Recent study reported autoantibodies against PDGFR in patients with SSc, but not in healthy controls or patients with rheumatoid arthritis, idiopathic pulmonary fibrosis or primary Raynaud's phenomenon [32]. Moreover, higher levels of those autoantibodies were detected among those with skin or lung fibrosis.

- **Vascular receptor antibodies**

Angiotensin II and endothelin-1 induce synthesis of collagen through target receptor stimulation in fibroblasts. Anti-angiotensin II type 1 receptor (anti-AT1R) and endothelin-1 type A receptor (anti-ETAR) autoantibodies were detected in the sera of SSc patients. Higher levels of both autoantibodies were associated with more severe disease manifestations and predicted mortality [136].

#### **I.1.11 Targeted therapy directed against B lymphocytes**

Recently, four clinical trials and four case studies suggest the possible use of the chimeric monoclonal anti-CD20 (Rituximab) in SSc patients [137-140]. This study included patients with the diffuse form of SSc and most of them were positive for anti-Scl 70 autoantibodies (anti-DNA-topoisomerase-1). In 3 of 4 trials, a significant improvement of Rodnan score in histological (reduction of B cell infiltrate in the skin, myofibroblasts and collagen deposition) and biological changes (serum concentration of IL-6 and BAFF ) has been reported. Those patients had relatively heterogeneous clinical forms (disease duration, severity, lung / heart involvement). They have received different immunosuppressive treatments in the past, and Rituximab doses used in those trials were highly variable. Therefore further studies, with more homogeneous groups of patients should be performed to precise the conclusions about the effectiveness of Rituximab in SSc.

## ***Genetic and environmental factors***

### **I.1.12 Genetic factors**

SSc is not a disease determined only by genetic factors. Nevertheless, it has been suggested that genetic risk factors predispose individuals to the onset of SSc [141, 142]. Many genes might interact to promote or influence on the clinical and serological manifestations of the disease (diffuse or limited cutaneous, vascular or fibrotic, anti-centromere Ab or anti-DNA topoisomerase-1). Fibrillin 1 is one of candidate genes that may promote fibrosis. Some polymorphisms in this gene were identified in the North American Indians Choctaw population, where the prevalence of SSc is very high [143]. Moreover, this gene is duplicated in TSK-1/+ mice which spontaneously develop cutaneous fibrosis [144]. However, this polymorphism was not found in other populations. Gene mutations encoding type II receptor of "bone morphogenetic proteins" (BMP) have been identified in familial forms of idiopathic pulmonary arterial hypertension. Gene mutations encoding "activin receptor-like- kinase-1 "(ALK-1) have been identified in pulmonary hypertension associated with Rendu-Osler Syndrome [145]. So far, these mutations have not been demonstrated in the SSc. There is no gene of the major histocompatibility complex (MHC) which confers increased susceptibility to develop SSc. However, many studies have shown associations between certain alleles of MHC genes and certain subgroups of SSc patients. In 2009, GENISOS (Genetic versus Environment In Scleroderma Outcome Study) demonstrated that the HLA DRB1\*0802 and DQA1\*0501 alleles were death predictive factors in SSc patients. A polymorphism at position 945 of the CTGF gene promoter has recently been demonstrated in two different groups in patients with SSc [146]. Study from few years, shows several single nucleotide polymorphisms

(SNPs) enriched in SSc patients compared with healthy controls. The SNPs were usually selected based on their locus in a gene involved in SSc pathogenesis. Using these strategies, several novel genetic risk factors were identified: STAT4, CD247, IRF5, Hepatocyte Growth Factor (HGF), and OX40L [147].

**STAT4** is a transcription factor playing a role in the differentiation of T lymphocyte. It also induces the transcription of type I IFN in activated monocytes. Its role as a mediator of inflammation in SSc was confirmed by development a moderate fibrosis after induction of SSc through the injections of bleomycin into STAT4 *-/-* mouse.

**CD247** play an important role in the immune system by encoding the T-cell coreceptor CD3 zeta, a component of the T-cell receptor complex. Low expression of CD247 may lead to defect in the immune response [148].

**IRF5** is a member of the IFN regulatory factors, which are critical components of virus-induced immune activation and type I IFN regulation. IRF5 was identified as a susceptibility gene for SSc. IRF5 rs4728142 [149]. IRF5 rs2004640 T allele was found to be associated with SS in the French Caucasian population [150, 151].

**HGF** is an antifibrotic factor involved in regenerating damaged tissue by promoting angiogenesis and by inhibiting fibrosis. A recent Japanese study have shown that the *HGF* -1652 TT genotype occurs significantly more frequently in SSc patients with end-stage lung disease compared with healthy controls (41% vs 8%).

**OX40L** is tumor necrosis factor superfamily-4, natural ligand of OX40 present on T cells and influences T-cell survival and expansion. OX40L binding partner OX40 is over-expressed in the serum of patients with SSc than in healthy controls [147]. In addition, analysis of clinical phenotypes demonstrated associations of OX40L variants with lcSSc and dcSSc, antitopoisomerase antibody and anticentromere antibody profiles [152].

### I.1.13 **Environmental Factors**

There is a lot of evidences of the association between systemic sclerosis and certain environmental risk factors, including exposures to vinyl chloride, silicone breast implants, organic solvents, and other agents such as epoxy resins and pesticides [153]. However, a meta-analysis did not find association between particular silicone breast implants and connective tissue [154].

Two viruses have attracted particular attention in SSc and are the subjects of several works: the Parvovirus B19 and the cytomegalovirus (CMV). DNA from parvovirus B19 was detected in the skin and bone marrow of SSc patients. However this finding was made in a small number of patients and no viral protein was found in those patients [154, 155]. Nevertheless, this virus remains a major candidate due to its capacity to fibroblasts activation [156]. More convincing arguments suggest a possible involvement of CMV in SSc. There is a structural homology between the viral protein UL94 and NAG 2, a membrane proteins expressed by human EC and normal fibroblasts [4]. It has been shown that anti-UL94 Ab were able to bind to EC and fibroblasts and induce their activation with transcription of adhesion molecules, cytokines, TGF- $\beta$ , and CTGF [157]. In addition, these Abs induced apoptosis of EC. Structural homology was also observed between another protein of CMV (UL 70) and the DNA topoisomerase I [158].

### ***Animal models of SSc***

Animal models of systemic sclerosis (SSc) have provided valuable insights into the causative mechanisms and the pathogenesis of SSc [159]. Several mouse models are available to study different aspects of the SSc disease related to fibrosis, vasculopathy, inflammation and autoimmunity (Figure 8). Since none of these models can reproduce all

features of human SSc, a critical selection of animal models is very important for successful *in vivo* studies.

#### I.1.14 **Inducible models of SSc**

Bleomycin was originally used as a cancer antibiotic that has established itself as a potent initiator of tissue injury and fibrosis in mice. Daily subcutaneous injection of bleomycine during 4 weeks induces skin and lung fibrosis [98]. Nevertheless, in contrast to the human SSc, in bleomycin-treated mice there is a few signs of autoimmunity and no evidence of microvasculopathy. Cutaneous changes are localized to the injected skin area and remain at least for 6 weeks after the last bleomycin treatment. Histological analysis of the skin and lungs from those mice shows an inflammatory infiltrate composed mainly of CD4 + T cells and mast cells. The extracellular matrix contains large amounts of TGF $\beta$  which is produced by fibroblasts and infiltrating cells like macrophages [160, 161]. The mechanisms involved in fibrosis induced by bleomycin seems to be complex and is probably caused by direct toxicity of the molecule, as well as by the effect of secondary mediators. Indeed, bleomycin induces the synthesis of ROS, especially superoxide anion and hydroxyl radical which also participate in its toxicity. Indeed, injections of SOD, an enzyme that converts superoxide anions into the less toxic H<sub>2</sub>O<sub>2</sub>, reduce the accumulation of collagen in the dermis if those injections are made at the same time as the bleomycin injection. Bleomycin model was developed 10 years ago by Yamamoto et al, and since that time, was extensively used by several groups, providing substantial and valuable information about the pathogenesis of human SSc [98]. However, this molecule acts by a complex mechanisms still poorly understood and probably acts through different pathways at least for the initial phase – to those involved in human SSc diseases.

- **Hypochlorous acid (HOCl)**

There is a lot of studies showing an important role of ROS in pathogenesis of SSc. Diseased fibroblasts from SSc patients produces a large amounts of ROS which activate collagen synthesis. The study conducted in our laboratory reproduced diffuse subset of SSc by subcutaneous injections of HOCl to BALB/c mice during around 6 weeks. Those daily injections induce localized cutaneous and lung fibrosis along with the production of antitopoisomerase-I antibodies in the serum, and numerous features which characterize diffuse cutaneous SSc in humans [162]. Moreover injections of HOCl increase number of B and CD4+ T cells in the spleen and total levels of IgG and IgM antibody in the serum. Inflammatory changes observed after HOCl injections are also observed in early stages of SSc patients. In the skin, HOCl induce myofibroblasts which increase proliferation rate and collagen production. High amounts of endothelial microparticles, sVCAM-1 and sE-selectin in HOCl mice shows the involvement of endothelial cells damage in this model. Subcutaneous HOCl stimulates fibroblasts to produce ROS which increase phosphorylation of ERK1/2 and activate Ras pathway. Moreover ROS production also induces the differentiation of fibroblast into  $\alpha$ -SMA-expressing myofibroblasts which stimulate the production of type-I collagen, leading to skin fibrosis [163]. This model leads to development of skin and lung fibrosis and production of antitopoisomerase I antibodies, which characterized general features of SSc in humans.

- **MRL / lpr mice deficient in IFN receptor-gamma**

MRL / lpr mice, deficient in IFN receptor-gamma, develop erythema and fibrosis with collagen accumulation in the skin, kidneys, liver, lungs, and salivary glands compared to the mice expressing IFN receptor [164]. Histological analysis also shows extensive thrombosis of small vessels.

- **FRA-2 transgenic mice**

Overexpression of FRA-2 was observed in the skin of SSc patients, suggesting that this transcription factor exerted an important role in vascular abnormalities and fibrosis. Maurer et al has developed a model based on overexpression of this transcription factor. FRA-2 mice (Fos-related antigen-2) have a microangiopathy and progressive cutaneous fibrosis [165]. These events are preceded by apoptosis of endothelial cells. FRA-2 is a transcription factor belonging to the family of AP-1 (activation factor-1) and its expression is independent of TGF-and PDGF.

- **Fli-1 mouse**

Fli-1 ("Friend leukemia integration factor-1") plays an inhibitory role in the expression proteins of the extracellular matrix. Fli-1 is involved in vascular development. Fli-1 <sup>-/-</sup> mice have an increased in vascular permeability, similar to that observed in SSc patients, as well as abnormalities in the formation of collagen fibrils [166].

- **Wnt-10b mouse**

Wnt proteins are involved in the tissue remodeling processes and fibrosis. Wnt-10b plays a role in adipogenesis and osteoblastogenesis. A new transgenic mouse model - Wnt-10b was recently described by J. Varga team. These mice develop dermal fibrosis, large deposits of collagen, fibroblast and myofibroblast accumulation [167].

- **Mice exposed to Vinyl Chloride**

Injection of vinyl chloride, an organic solvent into BALB / cJ mice retired breeder. Those mice developed skin fibrosis and inflammatory infiltrate. Exposure to vinyl chloride increases quantitatively circulating cells of fetal origin in the mice. This substance may have a role in the activation of fetal cells, which in turn are involved in the development of

fibrosis. This model is interesting because it is based on a cascade of events similar to humans [168].

- **Tight skin-2 mouse model**

The autosomal-dominant Tsk-2 mutants are developed by administration of the mutagenic agent ethylnitrosourea (ENU) [169]. The mutation is located in chromosome 1. Only heterozygous animals survive and develop the Tsk2 phenotype characterized by several biochemical and histological abnormalities similar to those in the skin of SSc patients.

Moreover, increased expression and accumulation of collagen were found in the skin of those mice. The molecular mechanisms, leading to fibrosis of the skin and internal organs are still unknown. In addition, Tsk-2 mice display inflammatory cell infiltrates in the affected tissue as well as autoimmunity including the presence of several autoantibodies against nuclear antigens including antitopoisomerase-I, anticentromere and anti-dsDNA antibodies [170].

- **Graft Versus Host disease (GVHD) - induced systemic sclerosis**

Chronic Graft-versus-Host Disease (GvHD) emerges from allo-reactive processes between donor-derived immune cells and host cell populations. Scl-GvHD can be induced through transfer of splenocytes and-bone marrow cells from B10.D2 donor mice into BALB/c RAG2<sup>-/-</sup> knockout (RAG2 KO) recipient mice, which are deficient in mature T and B cells. Those mice developed a skin thickness, particularly in the extremities, progressive fibrosis involving internal organs such as kidney and small intestine, but not lungs [96]. Those changes are observed already after 3-4 weeks. Histological analysis of the skin shows an inflammatory infiltrate of macrophages, monocytes, CD4<sup>+</sup>, CD8<sup>+</sup> T cells, and fibrosis with accumulation of extracellular matrix.

**Figure 8.** Animal models of inducible and spontaneous SSc by Batteux, *Current Opinion in Rheumatology*, 2011.

In these mice, except for fibrosis, they are other clinical abnormalities like vasculitis, alopecia and diarrhea resulting in loss of weight. Early immune activation and SSc-specific circulating autoantibodies such as antinuclear antibodies (ANAs) and anti-topoisomerase I antibodies (anti-Scl-70) were also detected in those mice. This model is based on immune system activation and therefore can be used to study the role of immune system in the fibrosis development and to test new approaches therapeutic targeting CD4 + T cells. A second model of SSc associated with GVHD was established by transferring splenocytes and-bone marrow cells of mice B10.D2 to BALB / c mice after lethal  $\gamma$ -irradiation of recipients [171]. This model eliminates the use of BALB / c RAG mice, but requires an irradiation step. Those mice develop the same abnormalities like in the previous model.

#### 1.1.15 Spontaneous models

- **UCD-200 chicken**

UCD-200 chickens spontaneously develop diffuse fibrosis, mononuclear cell infiltration, and vascular damage in visceral organs [172]. Additionally, antinuclear antibodies, anticardiolipin antibodies and rheumatoid factors are found in the serum. Nevertheless, more than half of the animals died before 10 weeks. Moreover, studies on this model are very expensive compared to that with mice because of breeding difficulties and size of those animals.

- **Tight skin-1 mouse model**

Tight skin-1 (Tsk-1) mice are heterozygous for a mutation in the fibrillin-1 (fbn-1) gene. Tsk-1 mice spontaneously developed skin fibrosis and autoimmunity [144]. This model shares many characteristics with fibrosis in human SSc. Nevertheless, there is no increase in rate of apoptosis of endothelial cells. In addition, mechanisms of those anomalies remain unclear and are probably very different from those seen in human SSc. However, the genetic background and autoimmunity make the Tsk1 mice a useful model for SSc which has been extensively studied in the past years.

## **Role of reactive oxygen species (ROS)**

A radical is an atom or a group of atoms that have one or more unpaired electrons. However, this state is transient and ends either by accepting another electron by the molecule or by the transfer of the free electron on another molecule. Radicals have extremely high chemical reactivity, which explains their anormal biological activities that inflicts destructive impact on cells. The term "reactive oxygen species" includes oxygen free radicals itself (superoxide anion  $O_2^{\bullet-}$ , hydroxyl radical  $OH^{\bullet}$ ), but also some non-radical reactive oxygen species with high toxicity (hydrogen peroxide  $H_2O_2$ , peroxynitrite ONOO) [173, 174]. Figure 9 shows different ROS generated by the cells.

**Figure 9.** Sources of ROS by Dawes, Trends in Cell Biology, 2005.

### ***II.1 Sources of ROS***

#### ***The superoxide anion $O_2^{\bullet-}$***

The superoxide anion is formed by adding one electron to an oxygen molecule:

$O_2 + e^- \rightarrow O_2^{\bullet -}$ . This radical has a short half-life by spontaneous dismutation accelerated by superoxide dismutase. It is not very toxic by itself, but can react with hydrogen peroxide or nitric oxide and result in the generation of strong oxidants (hydroxyl radical and peroxynitrite). Four cellular enzyme systems can lead to the formation of  $O_2^{\bullet -}$ :

- **Mitochondrial respiratory chain**

The mitochondrial respiratory chain is made up of several enzymes grouped inside of the inner membrane of the mitochondrion. It allows to oxidize NADH and succinate generated in Krebs cycle. In the respiratory chain, electrons accepted from substrates are passed through the chain of electron carriers. This drives proton pumping through the inner mitochondrial membrane to intermembrane space. Those events results in the transmembrane potential gradient generation. The return of protons to mitochondrial matrix is coupled to the regeneration of ATP. Electrons flow through respiratory chain terminates on molecular oxygen leading to the formation of  $H_2O$ :



However, there is leakage of electrons at each stage of transport and some  $O_2$  molecules will undergo a reduction by one electron, resulting in the formation of superoxide anion  $O_2^{\bullet -}$ :  $O_2 + 1e^- \rightarrow O_2^{\bullet -}$ . This mitochondrial superoxide anion production is continuous and ubiquitous.

- **NADPH-Cytochrome P450**

Cytochromes P450 constitute one of the largest superfamilies of enzyme hemoproteins [175]. Some cytochromes are located in the endoplasmic reticulum (microsomal cytochromes class), and play a role in the metabolism of xenobiotics. The others are located in the mitochondria (mitochondrial class) and some participate in steroid

metabolism. In all cases, cytochromes are associated with the electron transfer chain using NADPH as an electron source. These reactions may generate superoxide anions  $O_2^{\bullet -}$  :



- **Family of NADPH oxidases**

This family is also called NOX family ("superoxide-producing NADPH oxidase ") and constitutes seven members: NOX 1-5, and two DUOX1. Certain enzymes are ubiquitous (NOX4), while the others are only expressed preferentially in certain cell types such as phagocytes (NOX2) [176]. The phagocytic NADPH oxidase is a complex enzyme composed of membrane proteins (gp91phox (or NOX2) and p22phox) and cytosolic proteins (p47 phox, p67phox, p40phox). Activation of the membrane complex requires a presence of phosphorylated cytosolic proteins and a RAC - small G protein. These events occur during the activation of phagocytes (monocytes, macrophages, neutrophils and eosinophils) and finally allow the following reaction ("oxidative burst"), which is essential in innate immunity:

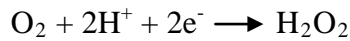


- **Xanthine oxidoreductase**

This enzyme is the main enzyme of purine degradation pathway. There are two forms of these enzymes: xanthine dehydrogenase reduces  $NAD^+$  and xanthine oxidase which reduces the molecular oxygen and form preferably superoxide anions  $O_2^{\bullet -}$ . Xanthine dehydrogenase is converted into oxidase through sulfhydryl oxidation especially during the ischemia-reperfusion phenomenon [6].

## ***Hydrogen peroxide (H<sub>2</sub>O<sub>2</sub>)***

The hydrogen peroxide production may result directly from the molecular oxygen reduction, under the action of different enzymes (e.g. glucose oxidase):



H<sub>2</sub>O<sub>2</sub> can also be formed from O<sup>•-</sup><sub>2</sub> after spontaneous dismutation or dismutation accelerated by superoxide dismutase (SOD).

Three types of SOD have been described in eukaryotic cells [177]:

- Cytosolic copper/zinc SOD (Cu/ZnSOD)=SOD1
- Mitochondrial manganese SOD (MnSOD)=SOD2
- Glycosylated extracellular copper/zinc SOD=SOD3

These enzymes catalyze the following reaction:  $2\text{O}^{\bullet-}_2 + 2\text{H}^+ \rightarrow \text{H}_2\text{O}_2 + \text{O}_2$ .

Hydrogen peroxide is a toxic derivative as it diffuses through the membrane. H<sub>2</sub>O<sub>2</sub> may interact with metal ions forming the highly reactive hydroxyl radical.

## ***Hydroxyl radical (OH<sup>•</sup>)***

Hydroxyl radical can be formed by interaction of H<sub>2</sub>O<sub>2</sub> with metal cations during cell lysis (hemolysis, rhabdomyolysis):



Reactions between different types of ROS can also lead to OH<sup>•</sup> formation:



Finally, myeloperoxidase, the enzyme located in the azurophilic granules of neutrophils and monocytes, catalyzes a reaction leading to the  $\text{OH}^\bullet$  production.

### ***Nitrogen oxide (NO)***

NO is synthesized from L-arginine by NO synthase (NOS). It is an important physiological signalling molecule, potent vasodilator, and oxidative stress mediator. In mammals, there are three isoforms of NO synthase enzyme:

- NO synthase-1 or neuronal
- NO synthase 2 or inducible
- NO synthase 3 or endothelial

Unlike the other two isoforms, NO synthase 2 is not constitutively expressed but is induced by  $\text{IFN-}\gamma$ ,  $\text{TNF-}\alpha$ , IL-1, IL-6, including LPS. NO production is physiological and plays a major role in vascular tone. However, at high concentrations, NO becomes deleterious to the cells, especially by reaction with superoxide anions ( $\text{O}_2^{\bullet-}$ ) to form the strong oxidant, peroxynitrite ( $\text{ONOO}^\bullet$ ).

## ***II.1 Role and consequences of ROS***

Reactive derivatives of oxygen can interact with each other, but also with all types of cell components: proteins, lipids, carbohydrates, DNA. These effects depend on their own reactivity, their preferential affinity for a particular substrate, their quantity and their ability to diffuse.

### **I.1.16 Action on proteins**

The radical forms can act on the main chain of the protein leading to its fragmentation. The interaction can also be located on the side chain. Particularly sensitive are sulfur residues

of methionine and cysteine. Reaction with aromatic amino acids (tyrosine, tryptophan, phenylalanine) leads to the formation of dityrosine or nitrotyrosine. Other amino acids are less sensitive and only strong ROS like HOCl may interact with lysine or arginine and lead to the formation of carbonyl groups [178]. These changes cause conformational changes, fragmentation or bonds between proteins and are thus likely to alter the activity of proteins.

#### **I.1.17 Effect on lipids**

ROS interactions with lipids lead to lipid peroxidation. The biological implications are of high importance for cells since all membranes are mainly composed of lipids. Peroxidation of the mitochondrial membrane can lead to such severe processes like apoptosis. Lipid peroxidation can also result in the formation of toxic byproducts such as malone dialdehyde (MDA) [179].

#### **I.1.18 Action on DNA**

ROS can cause oxidation of bases in deoxyribonucleotides, resulting in changes in the structure of base rings (for example oxidation of guanine leading to the formation of 8-oxo-guanine) or the oxidation of the sugar backbone resulting in the breakage of a single or double stranded DNA. Changes can also cause DNA-lipid or DNA-protein cross-links [180].

#### **I.1.19 Roles and effects of ROS in cellular metabolism**

Neutrophils and macrophages produce large amounts of  $O_2^{\bullet-}$  and  $H_2O_2$  via activation of NADPH oxidase complex [181, 182]. This enzyme is a key component of the antimicrobial arsenal. NADPH oxidase deficiency is responsible for immune deficiency in humans, the chronic granulomatous disease. ROS, especially  $H_2O_2$ , are also involved in cell cycle regulation [183]. Thus, low levels of ROS promote cell proliferation via the

activation of ERK [184]. A higher level of ROS, other "mitogen-activated protein kinases" (MAP kinases) and "stress activating protein kinases" (SAPK) are activated and promote apoptosis [185]. The proliferation of tumor cells is also regulated by  $H_2O_2$  (see Figure 10 below) [183].

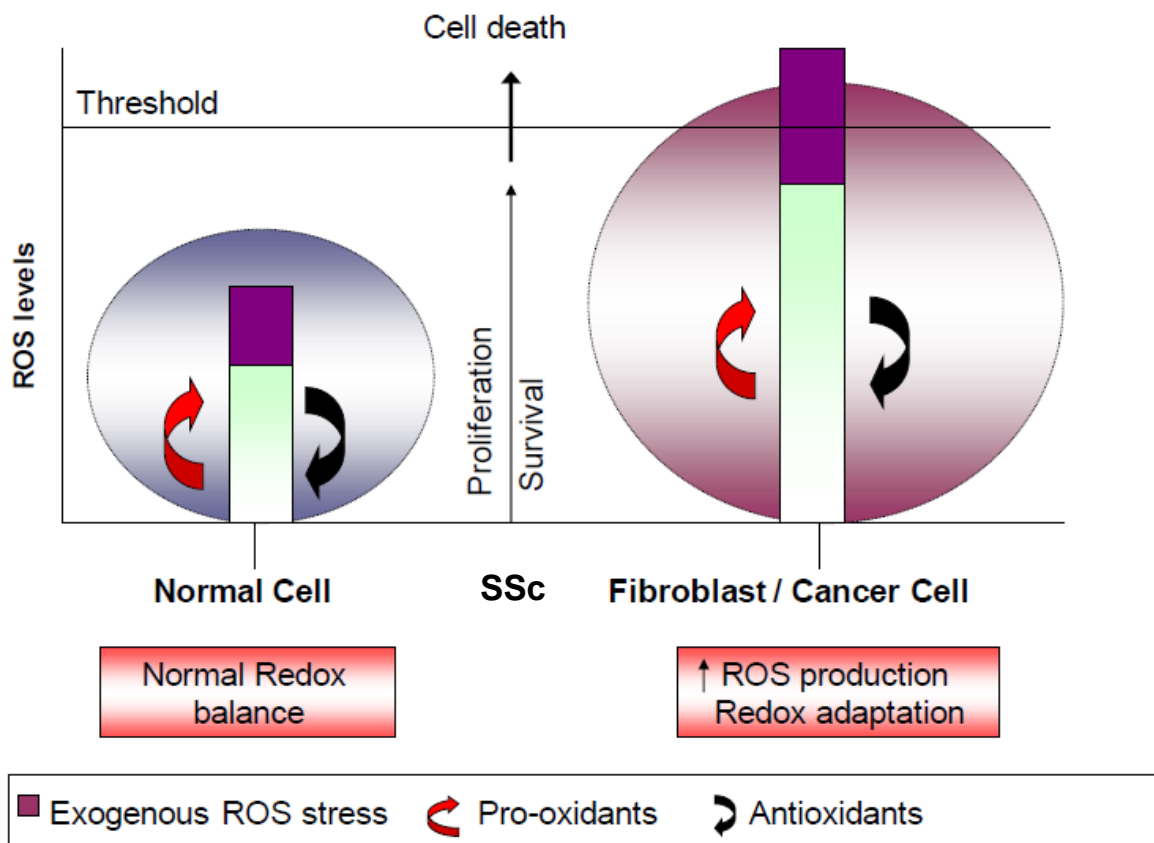


**Figure 10.** Regulation of cancer cells and SSc fibroblasts proliferation adapted from P. Huang, Nature Reviews, Drug Discovery, 2009.

ROS can also work as intracellular signal messenger. NO can indeed activate guanylate cyclase and oxidative modifications of intracellular proteins (modification of tyrosine and cysteine in particular) involved in signal transduction. ROS can also activate certain transcription factors such as nuclear factor- $\kappa$  B (NF- $\kappa$  B) and c-fos [186]. ROS are also involved in the process of VEGF dependent angiogenesis. Signal transduction of VEGF depends on the formation of ROS via endothelial NADPH oxidase [187]. Finally,

alongside the classic ROS, NO exerts specific functions in vessels: vasodilatation, antithrombotic and cytoprotective [91].

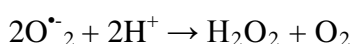
### I.1.20 **Antioxidants systems**

Constant production of ROS in aerobic organisms could be damaging in the absence of powerful antioxidant systems. Even under physiological conditions, a significant fraction of  $O_2$  is converted to ROS. The concentration of  $O_2^{\bullet-}$  and  $H_2O_2$  in cells does not exceed  $10^{10}$ - $10^{11}$  M and  $10^7$ - $10^9$  M, respectively [188].

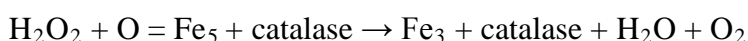
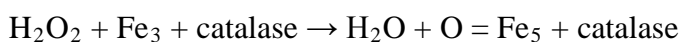
#### I.1.20.1 **Examples of enzymatic antioxidants systems**

In eukariotic cells following antioxidant systems exist:

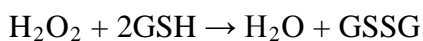
Superoxide dismutase (SOD), ubiquitous enzymes that catalyze reaction:



Catalase, an enzyme detoxifying  $H_2O_2$  is located mainly in the liver and kidney peroxysomes [189], whose synthesis is proportional to the  $H_2O_2$  concentration:



Glutathione peroxidase, catalyzes the detoxification of  $H_2O_2$  and lipid hydroperoxides (ROOH), and is using glutathione (GSH) as a cofactor.



The GSH system is the most powerful antioxidant systems of aerobic organisms. GSH is present in almost all eukaryotic cells. It is synthesized from L-glutamate, L-cysteine and L-glycine by the glutamylcysteine synthetase and GSH [190]. The antioxidant functions of GSH are related to its thiol group (-SH) which can be oxidized (GSSG). GSH serves to cofactor glutathione peroxidase, but also to dehydroascorbate reductase that regenerates

the antioxidant ascorbate. GSH can also directly detoxify ROS. Over 95% of GSH are under the reduced form. A change in the GSH/GSSG ratio can lead to serious disruption of cell homeostasis. Maintaining the reduced form of GSH depends on glutathione reductase, which depends on a balance of NADPH / NADP under the influence of G6PD (glyco-6-phosphate dehydrogenase).

#### **I.1.20.2 Examples of non-enzymatic antioxidant systems**

- Vitamin C and E

Vitamin E at the membrane (lipophilic) and vitamins C predominantly cytosolic (hydrophilic) eliminate the hydroxyl radicals.

- Ubiquinone (coenzyme Q10)

A vitamin having a significant role in the production of energy at the respiratory chain, and having an antioxidant role in protecting cells against damaging effects of free radicals [188].

#### **I.1.21 The role of ROS/RNS in SSc**

Many studies show an important role of ROS in the development of SSc. Stress induced on the endothelium by reactive nitrogen species or oxygen free radicals is locally generated by the inflammatory process and by frequent episodes of reperfusion injury (Raynaud's phenomenon). These stress may contribute to the inflammation and activation of the endothelium favoring the fibrotic process in SSc. ROS have been demonstrated to be cell transducers of collagen-gene expression, fibroblast proliferation, and myofibroblast phenotype conversion in SSc [5-7]. Recently, a number of studies have suggested that ROS plays a significant role in the progression of fibrosis in SSc. The biological consequences of free radicals overproduction was investigated by Avouac J et al. They found a higher levels of 8-hydroxy-2'-deoxyguanosine (8-oxodG), a biomarker of endogenous oxidative

damage to DNA in the blood of a large cohort of SSc patients [191]. Svegliati et al. had shown that PDGF, by stimulating ROS and Erk1/2 induced post-transcriptionally Ha-Ras protein. High level of ROS, Ha-Ras protein and activation of Erk1/2 stimulate collagen synthesis [33]. Another study, has shown that Silica can exert their effects in part through the oxidative stress. Silica can directly induce ROS formation on its surface, especially through the Fenton reaction, and indirectly through phagocytic cells activation. Furthermore, in mice, several studies emphasize the link between pulmonary fibrosis induced by the inhalation of silica and oxidative stress [192, 193]. Subcutaneous injections of bleomycin into the mice induce skin and lung fibrosis [98]. Study of this mouse model has shown the involvement of ROS in the development of cutaneous fibrosis resulting in lesions close to those observed in human SSc [194]. Spanish toxic oils Syndrome, which shares similarities with SSc also appears mediated by free radicals [195]. Over the past decade, numerous studies have reported increased oxidative stress in patients with SSc. It has been shown that the sera of patients contained higher amounts of oxidized proteins (carbonyls groups, advanced oxidation protein products (AOPP)) [196], and markers of lipid peroxidation. Lipid oxidation was directly observed in erythrocyte membranes of SSc patients [197]. This decreases the plasticity of erythrocytes, and could thus aggravate microcirculatory abnormalities. An Italian team has demonstrated a synthesis of large quantities of  $O_2^{\bullet-}$  by monocytes and fibroblasts in SSc patients [7, 198]. In both cell types, the synthesis of ROS is self-sustaining and dependent on a NADPH oxidase. The same team work suggests that synthesis of collagen in fibroblasts is dependent on the synthesis of ROS [33].

For nitric oxide, several studies attest to quantitative differences in the serum between SSc patients and healthy controls, but as stated previously, the results of these studies are contradictory. However that can be explain by differences in diseased subset, inflammatory

disorders, and different patients treatment. In most biological condition NO is oxidized to nitrate ( $\text{NO}_3^-$ ) and nitrite ( $\text{NO}_2^-$ ). Many studies shows overproduction of NO in SSc patients, increased plasma levels of  $\text{NO}_3^-/\text{NO}_2^-$ , and elevated nitration of plasma proteins, a marker of ONOO<sup>-</sup> production [199]. Abnormality in NO metabolism was demonstrated in the tight-skin (TSK-1/+) mouse model of fibrosis. Decreased activity of NOS was detected in TSK-1/+ mouse tissue compared to wild type mice, suggesting an abnormal NO metabolism. Also the expression of endothelial NOS was significantly reduced in TSK-1/+ mice [200]. Immunohistological studies of SSc skin also shown that as the disease progresses to the later fibrotic stages, the production of eNOS is downregulated, while iNOS is upregulated. Nitrated proteins are also found in the SSc skin associated with sites of inflammation [3, 4]. Another studies are showing NO acting as an antifibrotic effector in animal models of experimental fibrosis [201, 202]. NO has been shown to inhibit adhesion molecule expression, adhesion of platelet, and smooth muscle cell proliferation. Release of NO is dependent on the integrity of vascular endothelium. Under pathological states, endothelium dysfunction leads to constitutive NO synthesis and release. In SSc, the basal release of NO might be a potent chemical barrier that protects the vascular endothelium from oxidation injury. For example, in a mouse model of pulmonary fibrosis, a loss of NO bioactivity in eNOS knock-out mice, resulted in prolonged fibrosis [201]. Moreover, other study also shows reduced fibrotic content using transgenic mice overexpressing eNOS after bleomycin-induced fibrosis [202]. In contrary, other studies show harmful role of NO in SSc. A UK team have shown how the progression of the disease can change the NO synthase from the endothelial to the inducible form [203]. Moreover, cells in the damage skin express nitrotyrosine which indicate free radical injury [203, 204]. During the initial proinflammatory state of SSc NO and  $\text{O}_2^{\bullet-}$  is increased by the presence of macrophages or activated fibroblasts. Free radicals produced by

inflammatory cells can react with NO produced by iNOS to form peroxynitrite  $\text{ONOO}^-$  that may favour endothelial cells apoptosis [205]. In SSc, low concentration of NO contribute to the survival of endothelial cells whereas high level of NO induce the apoptosis of endothelial cells.

## Personal work

---

In this chapter, I will present my work on the effect of ROS/RNS modulators in Systemic sclerosis (SSc).

Several reports have suggested that reactive oxygen and nitrogen species are involved in SSc pathogenesis. SSc fibroblast from skin and internal organs overproduce ROS that trigger the proliferation of fibroblasts and the synthesis of type I collagen leading to the initiation and progression of SSc [7, 206, 207]. The role of ROS in the initiation of SSc has been evidenced in our laboratory. Our studies demonstrated that sera from SSc patients can induce not only the production of ROS by endothelial cells but also the proliferation of fibroblasts [208]. Moreover, by studying the involvement of ROS in the pathogenesis of SSc, a new chemically induced murine model of SSc was developed by injection of HOCl. This model presents all features characterizing SSc in human, among others skin and visceral fibrosis, vascular disease and autoimmunity diseases [162]. These are strong arguments confirming an important role of ROS in the pathophysiology of SSc. Thus, we decided to test new therapeutic approaches in the HOCl induced SSc murine model.

As in human SSc, skin fibroblasts from SSc mice constitutively produce large amounts of ROS. We have used this property to selectively induce apoptosis in the diseased fibroblast of SSc mice (Article 1, 2). Indeed, the organotelluride catalyst-(PHTE)<sub>2</sub>NQ and natural organosulfur compound-DPTTS are able of increasing ROS production by fibroblasts and inducing a lethal oxidative stress specifically in SSc fibroblasts. This phenomenon has no impact on normal fibroblasts that present normal levels of ROS and a normal oxidant/antioxidant status.

Many studies have also proved an importance of nitrogen species in the pathogenesis of SSc [206, 207]. In patients with SSc, the serum level of nitric oxide is significantly

increased [206]. Furthermore, NO can combine with other free radicals like superoxide anion ( $O^{\bullet}_2$ ) to form the highly cytotoxic peroxynitrite ( $ONOO^-$ ) that contributes to inflammation, fibrosis and apoptosis of endothelial cells. Production of NO by endothelial cells or by fibroblasts can be stimulated by angiotensin II, the main peptide of the renin-angiotensin system (RAS) [205]. The level of angiotensin II is increased in SSc patients as well as in our HOCl mouse model and can promote proliferation of fibroblasts, fibrosis, and inflammation [209]. These observations led us to test irbesartan, an angiotensin II type I receptor antagonist ( $AT_1$  RA) in the murine model of SSc (Article 3).

ROS/RNS modulators investigated during my thesis affect not only fibrosis process but also vascular tone (Article 3) and immune system (Articles 2 and 3), which are important in the initiation of SSc.

In conclusion, a new animal model based on chronic exposure to ROS and with many similarities to the human disease, allowed me to study new therapeutic approaches in SSc based on the cytotoxic action of pro-oxidative compounds -  $(PHTE)_2NQ$  and DPTTS - and on the anti-nitrosative effect of irbesartan. These new therapeutic strategies open interesting perspectives in the treatment of SSc, where the therapeutic arsenal is currently still limited.

### ***III.1 Article 1***

## **The organotelluride catalyst (PHTE)<sub>2</sub>NQ prevents HOCl – induced systemic sclerosis in the mouse**

Wioleta Marut<sup>1</sup>, Niloufar Kavian<sup>1</sup>, Amélie Servettaz<sup>1,2</sup>, Carole Nicco<sup>1</sup>, Lalla Ba<sup>3</sup>,  
Christiane Chéreau<sup>1</sup>, Claus Jacob<sup>3</sup>, Bernard Weill<sup>1</sup>, Frédéric Batteux<sup>1</sup>

*Journal of investigative dermatology, 2012 (Published)*

SSc fibroblasts from HOCl mice produce a large amounts of ROS that stimulate their proliferation and synthesis of type I collagen.

Cancer cells, like SSc fibroblasts also overproduce ROS that may participate to the proproliferative phenotype of those cells. Indeed, chronic exposure to low levels of ROS leads to carcinogenesis and tumor progression. However, when the oxidative burst reach a certain level, for example upon treatment with cytotoxic drugs, this burst can leads to the apoptosis of cancer cells [183]. By analogy to cancer cells which can be killed by pro-oxidant molecules through increased level of ROS above a lethal threshold, we tested the effectiveness of pro-oxidative organotellurium compound (PHTE)<sub>2</sub>NQ on SSc fibroblasts.

(PHTE)<sub>2</sub>NQ selectively kills activated SSc skin fibroblasts *in vitro* obtained from from HOCl treated mice but have no effect on normal skin fibroblasts from healthy mice.

(PHTE)<sub>2</sub>NQ amplifies the production of ROS by SSc fibroblasts which can not be detoxified due to low concentration of glutathione (GSH) observed in the diseased fibroblasts. By contrast, normal fibroblasts with a normal oxidative/antioxidant status resist to the action of (PHTE)<sub>2</sub>NQ.

*In vivo* HOCl treated mice were injected intravenously with (PHTE)<sub>2</sub>NQ once per week during six weeks. We observed the reduction of dermal thickness in the SSc mice treated with (PHTE)<sub>2</sub>NQ. Disease improvement was confirmed by histological analysis of skin and lung. (PHTE)<sub>2</sub>NQ reduces the collagen content in the skin and in the lung and inhibits differentiation of fibroblasts into myofibroblasts in SSc mice. Furthermore, *in vivo* treatment with (PHTE)<sub>2</sub>NQ resulted in a reduction of vascular abnormalities through the reduction of nitrite and also the level of oxidized protein-AOPP generated by SSc fibroblasts which can induce the production of reactive oxygen species by fibroblasts and endothelial cells, and thus enhance the vascular damage by increase the apoptosis of endothelial cells [162]. In addition, overproduction of ROS by SSc fibroblasts allows the production of oxidized intracellular proteins like oxidized DNA-topoisomerase-1 and then favour the breach of tolerance to DNA topoisomerase I and favour autoimmunity induction. As a consequence of the reduction of AOPP in the sera, HOCl mice treated with (PHTE)<sub>2</sub>NQ have a significantl decreased in the anti-DNA topoismerase I Ab concentration in the sera.

In conclusion, our results show that the organotelluride catalyst (PHTE)<sub>2</sub>NQ can interact with intracellular ROS generated in SSc fibroblasts to selectively kill them. This property lead to the clinical and biological improvement in HOCl treated SSc mice administrated with (PHTE)<sub>2</sub>NQ.

**The Organotelluride Catalyst (PHTe)2NQ Prevents HOCl – Induced Systemic Sclerosis in the Mouse**

Wioleta Marut<sup>1,4</sup>, Niloufar Kavian<sup>1,4</sup>, Amélie Servettaz<sup>1,2</sup>, Carole Nicco<sup>1</sup>, Lalla Ba<sup>3</sup>, Mandy Doering<sup>3</sup>, Christiane Chéreau<sup>1</sup>, Claus Jacob<sup>3</sup>, Bernard Weill<sup>1</sup>, Frédéric Batteux<sup>1</sup>.

<sup>1</sup>Université Paris Descartes, Sorbonne-Paris-Cité,

Faculté de Médecine, EA 1833 et Laboratoire d'immunologie biologique, Hôpital Cochin AP-HP, 75679 Paris cedex 14, France.

<sup>2</sup> Faculté de Médecine de Reims, Service de Médecine Interne, Maladies Infectieuses, Immunologie Clinique, Hôpital Robert Debré, 51092 Reims cedex, France.

<sup>3</sup> Division of Bioorganic Chemistry, School of Pharmacy, Saarland University, PO Box 151150, D-66123, Saarbrücken, Germany.

<sup>4</sup> These authors contributed equally to this work.

Address correspondence to: Dr. Frédéric Batteux, Laboratoire d'Immunologie, UPRES EA 1833, 8 rue Méchain 75679 Paris cedex 14, France. Tel: +33 (0) 1.58.41.20.09; Fax: +33 (0) 1.58.41.20.08; e-mail: frederic.batteux@cch.aphp.fr

Key words: Tellurium, oxidative stress, Scleroderma, fibrosis

## **ABSTRACT**

Systemic sclerosis (SSc) is a connective tissue disorder characterized by skin and visceral fibrosis, microvascular damages and autoimmunity. HOCl-induced mouse SSc is a murine model that mimics the main features of the human disease, in particular the activation and the hyperproliferation rate of skin fibroblasts. We demonstrate here the efficiency of a tellurium-based catalyst 2,3-bis(phenyltellanyl)naphthoquinone ((PHTE)<sub>2</sub>NQ) in the treatment of murine SSc, through its selective cytotoxic effects on activated SSc skin fibroblasts.

SSc mice treated by (PHTE)<sub>2</sub>NQ displayed a significant decrease in lung and skin fibrosis and in alpha-Smooth Muscle Actin ( $\alpha$ -SMA) expression in the skin compared to untreated mouse SSc animals. Serum concentrations of advanced oxidation protein products, nitrate, and anti-DNA topoisomerase-I autoantibodies were increased in SSc mice but were significantly reduced in SSc mice treated by (PHTE)<sub>2</sub>NQ. To assess the mechanism of action of (PHTE)<sub>2</sub>NQ, the cytotoxic effect of (PHTE)<sub>2</sub>NQ was compared in normal and in mouse SSc skin fibroblasts. ROS production is higher in mouse SSc fibroblasts than in normal fibroblasts and was still increased by (PHTE)<sub>2</sub>NQ to reach a lethal threshold and kill mouse SSc fibroblasts. Therefore, the effectiveness of (PHTE)<sub>2</sub>NQ in the treatment of mouse SSc seems to be linked to the selective pro-oxidative and cytotoxic effects of (PHTE)<sub>2</sub>NQ on hyperproliferative fibroblasts.

## **INTRODUCTION**

Systemic sclerosis (SSc) is an autoimmune disease of unknown aetiology, characterized by fibrosis of the skin and of internal organs, vascular dysfunction, and dysimmunity (LeRoy and Medsger, 2001). However, the mechanisms that underlie the

clinical manifestations of the disease remain unclear (Gabrielli and Avvedimento, 2009). Several reports have shown that reactive oxygen species (ROS) are involved in the pathogenesis of SSc (Simonini et al., 1999; Sambo et al., 2001; Allanore et al., 2004; Ogawa et al., 2006; Servettaz et al., 2007; Avouac et al., 2010). Indeed, skin fibroblasts in SSc patients spontaneously produce large amounts of ROS that trigger collagen synthesis (Sambo et al., 1999; Sambo et al., 2001). Intradermal injection of specific ROS-generating substances can reproduce the main features of local and systemic mouse SSc, depending on the type of ROS generated (Servettaz et al., 2009). In addition, anti-PDGFR autoantibodies (AAbs) found in SSc patients also trigger the production of ROS (Svegliati Baroni et al., 2006). Recently, we have reported that sera from patients with SSc can induce not only the production of ROS by endothelial cells but also by the proliferation of fibroblasts (Servettaz et al., 2007). The release of ROS by fibroblasts and endothelial cells can activate several processes that trigger the development of SSc. In fact, ROS can oxidize specific SSc antigens such as DNA-topoisomerase-1 and lead to this autoantigen's breach of tolerance (Casciola-Rosen et al., 1997; Servettaz et al., 2009). The autoimmune phenomenon can be amplified by the inflammatory reaction that results from the overproduction of ROS. This fibrotic process may also be related to the imbalance of the oxidant/antioxidant status in SSc. For instance, *in vitro* studies have shown that ROS triggers the differentiation of fibroblasts into myofibroblasts, either directly or through the activation of the ADAM17/NOTCH pathway (Kavian et al., 2010), and also through the release of TGF- $\beta$  from activated cells (Bellocq et al., 1999). Finally, ROS can stimulate the growth of dermal fibroblasts through the activation of the RAS pathway, which explains the hyperproliferative properties of SSc skin fibroblasts (Svegliati Baroni et al., 2005). However, if intracellular ROS can stimulate cell growth, they can also induce cell death beyond a certain threshold, as seen in tumor cells (Laurent et al., 2005; Lonkar and Dedon,

2010; Morgan and Liu, 2010, Coriat et al., 2011). Interestingly, some catalytic agents called 'sensor/effector' multifunctional redox catalyst, can modulate the intracellular redox balance by generating more reactive oxidants or by targeting cysteine residues in proteins. Those molecules seem to be particularly effective and selective (Fry and Jacob, 2006). Among the 'sensor/effector' multifunctional redox catalyst agents, quinone- and chalcogen (selenium, tellurium)-containing agents have shown an in vitro cytotoxic activity against various type of tumor cells (Doering et al., 2010; Lilienthal et al., 2011, Coriat et al., 2011). Those observations have prompted us to try these new cytotoxic organotelluride catalysts in the treatment of mouse SSc.

The organotelluride catalyst, (PHTE)<sub>2</sub>NQ, is a prototypical member of this newly described family (Fry and Jacob, 2006; Shabaan et al., 2009; Ba et al., 2010; Jamier et al., 2010). Within this family of compounds, (PHTE)<sub>2</sub>NQ has been the most widely studied compound in vitro on tumor cells (Doering et al., 2010; Jamier et al., 2010) and it has also been the only one used in vivo on mice (Coriat et al., 2011). Intracellular oxygen radicals and H<sub>2</sub>O<sub>2</sub> associate with the quinone moiety of the (PHTE)<sub>2</sub>NQ and strongly oxidized cellular thiols in a reaction catalyzed by the tellurium part of the molecule. This reaction significantly increases the intracellular level of ROS. Therefore, cells already overproducing H<sub>2</sub>O<sub>2</sub> that are treated with (PHTE)<sub>2</sub>NQ are likely to significantly increase their intracellular concentration of ROS over its cytotoxic level, to ultimately get pushed over a critical "life and death (redox) threshold" (Fry and Jacob, 2006; Mecklenburg et al., 2009). Since mouse SSc fibroblasts produce high amounts of H<sub>2</sub>O<sub>2</sub>, as opposed to normal fibroblasts, we hypothesize that (PHTE)<sub>2</sub>NQ could selectively kill disease fibroblasts in murine HOCl-induced SSc (Servettaz et al., 2009) and inhibit the development of the disease.

## RESULTS

### **(PHTE)<sub>2</sub>NQ exerted cytotoxic effects on normal and SSc fibroblasts in vitro**

Fibroblasts from normal mice and from HOCl-mice were exposed in vitro to increasing amounts of (PHTE)<sub>2</sub>NQ (Supplementary data, Figure 7) to assess the cytotoxic properties of this ‘sensor/effector’ multifunctional redox catalyst agent on those different types of fibroblasts. In the presence of 1 μM (PHTE)<sub>2</sub>NQ, the rate of viability of normal fibroblasts was 72% (P = 0.0001 vs untreated fibroblasts) and 68% with 4 μM (PHTE)<sub>2</sub>NQ (P = 0.0001 vs untreated fibroblasts; Figure 1a). (PHTE)<sub>2</sub>NQ had a more powerful cytotoxic effect on diseased SSc fibroblasts than on normal fibroblasts. In the presence of 1 μM (PHTE)<sub>2</sub>NQ, the rate of viability of SSc fibroblast was 45% (P = 0.0001 vs untreated fibroblasts and vs normal fibroblasts) and 30% with 4 μM (PHTE)<sub>2</sub>NQ (P = 0.0001 vs untreated fibroblasts and vs normal fibroblasts; Figure 1a).

### **(PHTE)<sub>2</sub>NQ exerted pro-oxidative effects in vitro**

The basal production of H<sub>2</sub>O<sub>2</sub> was increased by 56% in SSc fibroblasts compared to normal fibroblasts (P = 0.001). Production of NO was also higher in SSc fibroblasts than in normal fibroblasts (P = 0.01). Incubation of normal fibroblasts and SSc fibroblasts with increasing amounts of (PHTE)<sub>2</sub>NQ dose-dependently increased the production of H<sub>2</sub>O<sub>2</sub> (P = 0.009 and P = 0.001, respectively) and of NO (P = 0.018 in both cases; Figures 1b and c).

### **Imbalance of GSH metabolism in fibroblasts**

Glutathione is an essential cofactor of H<sub>2</sub>O<sub>2</sub> catabolism. The basal level of GSH was decreased by 22% in SSc fibroblasts compared to normal fibroblasts (P = 0.0032). The level of intracellular glutathione was higher (P = 0.0001) in normal fibroblasts following

exposure to 1  $\mu\text{M}$  (PHTE)<sub>2</sub>NQ than in untreated normal fibroblasts. By contrast, the treatment of diseased SSc fibroblasts by (PHTE)<sub>2</sub>NQ failed to increase the level of intracellular glutathione (Figure 1d).

### **Modulations of H<sub>2</sub>O<sub>2</sub> metabolism in SSc fibroblasts**

We next investigated the mechanism of action of (PHTE)<sub>2</sub>NQ using specific modulators of the enzymatic and non enzymatic systems involved in H<sub>2</sub>O<sub>2</sub> catabolism. Hydrogen peroxide is converted into H<sub>2</sub>O by two sets of enzymes, catalase and the GSH/GPx system. The latter uses reduced glutathione as cofactor. Depleting GSH with BSO significantly increased H<sub>2</sub>O<sub>2</sub> production in SSc fibroblasts ( $P = 0.0007$ ) and in normal fibroblasts ( $P = 0.0029$ ; Figure 2a). Moreover, incubation with (PHTE)<sub>2</sub>NQ in association with BSO increased H<sub>2</sub>O<sub>2</sub> production by 10.9% in normal fibroblasts and by 22% in SSc fibroblasts versus BSO alone ( $P = 0.001$ , data not shown). By contrast, adding NAC, a precursor of GSH, decreased H<sub>2</sub>O<sub>2</sub> production in normal fibroblasts ( $P = 0.04$ ) but had no effect on SSc fibroblasts (Figure 2a). On the other hand, specific inhibition of catalase by aminotriazol (ATZ) or addition of exogenous catalase, had no effect on the levels of H<sub>2</sub>O<sub>2</sub> in normal and SSc fibroblasts (Figure 2a). Depleting GSH with BSO significantly decreased the viability of SSc fibroblasts ( $P = 0.0026$ ) and of normal fibroblasts ( $P = 0.017$ ). By contrast, specific inhibition of catalase by aminotriazol (ATZ) had no effect on the viability of normal and SSc fibroblasts (Figure 2b). Moreover, addition of suboptimal doses of BSO and of (PHTE)<sub>2</sub>NQ added their effects worked jointly to kill SSc fibroblasts more efficiently than normal fibroblasts alone ( $P = 0.0168$ ) (Figure 2c).

### **Determination of cell death pathway in normal and SSc fibroblasts**

Fibroblasts from normal and HOCl-mice were incubated with 1, 2 and 4  $\mu\text{M}$  of (PHTE)<sub>2</sub>NQ for 12 h, 24 h, 36 h or 48 h. The highest cytotoxic effect of (PHTE)<sub>2</sub>NQ was observed at a concentration of 4  $\mu\text{M}$ . At this concentration the viability was decreased by 73% for SSc fibroblasts and only by 14.2% for normal fibroblasts ( $P = 0.001$ ). A kinetic analysis of cell death between 12 h and 48 h indicated that the (PHTE)<sub>2</sub>NQ effects are mainly mediated through a necrotic process (Figure 3).

### **(PHTE)<sub>2</sub>NQ decreased both skin and lung fibrosis in mice with SSc**

Clinically, HOCl-induced SSc in mice (HOCl-mice) is associated with an increase in dermal thickness that's significantly reduced by (PHTE)<sub>2</sub>NQ ( $P = 0.0001$  vs untreated SSc mice; Figure 4a). Histopathological analysis of skin (Figure 4c) and lung (Figure 5a) biopsies stained with hematoxylin and eosin, and lung biopsy stained by Sirius Red (Figure 5c), confirmed the dermal thickness reduction and evidenced a decrease in fibrosis in both tissues (Figure 4c, 5a, 5c). (PHTE)<sub>2</sub>NQ reduced the accumulation of type I collagen induced by HOCl in the skin versus untreated mice (Figures 4b). We also investigated the effects of (PHTE)<sub>2</sub>NQ in the bleomycin model and found the data to yield similar results to those gained by the HOCl model in terms of skin fibrosis. However, no lung fibrosis was observed after 5 weeks of bleomycin injections (Supplementary data, Figure 8).

Furthermore,  $\alpha$ -SMA staining in skin sections showed that HOCl-treated SSc animals displayed increased numbers of myofibroblasts ( $9.53\% \pm 0.483$  of positive area) compared to PBS-injected mice ( $2.46\% \pm 0.555$  of positive area,  $P = 0.0001$ ) (Figures 4e and 4f). The number of myofibroblasts was reduced by 47.6% after treating HOCl-mice with (PHTE)<sub>2</sub>NQ ( $P = 0.0005$ ). (PHTE)<sub>2</sub>NQ also reduced the concentration of type I collagen in the lungs of HOCl- mice by 26.7% ( $P = 0.0106$ ; Figures 5a and 5b).

### **Decrease of dermal thickness in SSc mice through (PHTE)<sub>2</sub>NQ curative treatment**

(PHTE)<sub>2</sub>NQ decreased dermal thickness when administered as a curative treatment. Mice with SSc were treated with (PHTE)<sub>2</sub>NQ (10 mg/kg of (PHTE)<sub>2</sub>NQ), which was administered intravenously once a week during 2 weeks. After 2 weeks, the dermal thickness in treated mice was significantly less than in the untreated group (P = 0.0151) (Figure 4d).

### **(PHTE)<sub>2</sub>NQ reduced the concentration of serum AOPP and nitrite production**

Advanced oxidation protein products (AOPP), a marker of systemic oxidative stress, increased in the sera of HOCl-mice compared to PBS control mice (P = 0.0001; Figure 6a). Treatment of HOCl-mice with (PHTE)<sub>2</sub>NQ reduced the levels of AOPP by 40%, compared to untreated SSc animals (P = 0.0001; Figure 6a). The level of nitrite in the sera, a marker of systemic nitrosative stress, increased in HOCl-mice compared to PBS control mice (P = 0.0006; Figure 6b). Treatment with (PHTE)<sub>2</sub>NQ in HOCl-mice reduced the levels of serum nitrite by 18% compared to untreated SSc mice (P = 0.039 ; Figure 6b).

### **(PHTE)<sub>2</sub>NQ reduced serum concentration of anti-DNA topoisomerase I Abs**

The sera of HOCl-mice contained significantly higher amounts of DNA-topoisomerase I Abs than the sera of mice treated with PBS (P = 0.0008). The level of anti-DNA topoisomerase I Abs significantly reduced in HOCl-mice treated with (PHTE)<sub>2</sub>NQ compared to untreated HOCl-mice (P = 0.04; Figures 6c).

## **DISCUSSION**

In this report, inspired by recent results obtained - by us and others - in cancer therapy using selective pro-oxidative molecules, we demonstrates that organotelluride catalysts can

combine with endogenous oxidative species generated 'naturally' in mouse SSc fibroblasts to selectively kill cells through a necrotic process.

Primary fibroblasts extracted from areas diseased skin areas, display an elevated basal level of ROS that is amplified by (PHTE)<sub>2</sub>NQ to generate a lethal oxidative burst in contrast with healthy fibroblasts that display a normal level of endogenous ROS and resist to the action of (PHTE)<sub>2</sub>NQ. The cytotoxic effects of ROS result from an imbalance between their rate of production and the activity of various detoxification systems (Laurent et al., 2005). Indeed, in SSc fibroblasts, the level of GSH is low and is not modified by (PHTE)<sub>2</sub>NQ, whereas, in normal fibroblasts, this level is higher and is raised by (PHTE)<sub>2</sub>NQ. Thus, when normal fibroblasts are exposed to (PHTE)<sub>2</sub>NQ, pro-oxidative activity of the compound is counterbalanced by the rise of GSH and no oxidative stress can be induced. In contrast, in diseased fibroblasts, (PHTE)<sub>2</sub>NQ induces a huge increase in ROS that is not counterbalanced by the low level of induced GSH and thus, reaches a lethal threshold. Because the level of endogenous ROS in SSc fibroblast is close to that threshold, the exposure to ROS-generating, redox modulating agents such as (PHTE)<sub>2</sub>NQ, enhances the rate of cell death. Since normal fibroblasts are not targeted by (PHTE)<sub>2</sub>NQ, that data could have important clinical implications (Amstad et al., 1991, Rodriguez et al., 2000, Hussain et al., 2004, Laurent et al., 2005).

The depletion of GSH by BSO, and the consecutive increase of (PHTE)<sub>2</sub>NQ toxicity in SSc and normal fibroblasts, confirms the role of the GSH pathway in mediating the cytotoxic effects of (PHTE)<sub>2</sub>NQ. In contrast, blocking the catalase pathway or adding PEG catalase, showed that this pathway has no effect on cell survival whatever the considered cell type is. Thus, H<sub>2</sub>O<sub>2</sub>-mediated (PHTE)<sub>2</sub>NQ toxicity is controlled by the glutathione pathway and not by the catalase pathway, as already observed with several cytotoxic

molecules (Jing et al., 1999; Hussain et al., 2004; Laurent et al., 2005; Alexandre et al., 2006). These findings are significant, since they seem to identify disturbances in the GSH household (and subsequent increases in ROS levels), rather than ROS generation per se, as the prime activity of such redox modulating agents.

In SSc, the local oxidative stress is associated with a systemic oxidative state, as demonstrated by the significant increase in the serum concentrations of advanced oxidation protein products, and of nitrite, in HOCl-treated SSc mice that are compared to PBS injected animals. Therefore, (PHTE)<sub>2</sub>NQ induces a lethal oxidative burst in cells with increased levels of intracellular ROS, but it is not a systemic pro-oxidative molecule, as already observed in various cancer models (Fry and Jacob, 2006; Doering et al., 2010; Coriat et al., 2011). Several reports have linked the intracellular oxidative burst and the initiation of the immune response in human or in murine models of SSc (Simonini et al., 1999; Harðardo et al., 2010). Indeed, local generation of HOCl or hydroxyl radicals triggers the production of anti-DNA-topoisomerase-1 autoantibodies, and consequently, the generation of peroxynitrite triggers the production of anti-centromeric protein B Abs. The mechanism through which the breach of tolerance to DNA-topoisomerase-1 occurs following exposure to HOCl or hydroxyl radicals, is related to the oxidation and cleavage of DNA-topoisomerase 1 within the cells (Servettaz et al., 2009). The selective destruction of diseased fibroblasts that chronically produce high levels of intracellular ROS by (PHTE)<sub>2</sub>NQ, probably explains the decreased concentration of circulating oxidized proteins in the sera, and especially of oxidized DNA-topoisomerase-1 anti-DNA-topoisomerase-1 Abs. Furthermore, oxidized topoisomerase-1 exerts a proproliferative effect on fibroblasts and increases the intracellular level of H<sub>2</sub>O<sub>2</sub> in fibroblasts and

endothelial cells. The decrease of circulating oxidized proteins linked to the selective destruction of diseased fibroblasts also explains the decrease in fibroblast proliferation.

One of the major consequences of the oxidative stress in diseased fibroblasts is their transformation into myofibroblasts and their increased production of type I collagen (Sambo et al., 2001; Toullec et al., 2010). As for autoantibodies and fibroblast proliferation, the selective destruction of diseased mouse SSc fibroblasts by (PHTE)<sub>2</sub>NQ is followed by the decrease in the numbers of myofibroblasts. These phenomena were associated with the inhibition of the development of mouse SSc because they were correlated with a decrease in the concentration of type I collagen in the skin of treated animals.

Altogether, our results show for that the organotelluride catalyst (PHTE)<sub>2</sub>NQ can interact with intracellular ROS generated in SSc fibroblasts to selectively kill the cells. This observation suggests a new therapeutic strategy in SSc, based on the modulation of the intracellular redox state of the activated fibroblasts. Indeed, new molecules such as (PHTE)<sub>2</sub>NQ, could help selectively eliminate the activated cells responsible for the development of skin and visceral fibrosis and, indirectly, be used for autoimmunity. Preliminary data suggest that the molecule is not only efficient as a preventive treatment, but as a curative treatment of SSc as well.

## **MATERIALS & METHODS**

### **Animals and chemicals**

Specific pathogen-free, 6 week-old female BALB/c mice were used in all experiments (Harlan, Gannat, France). All mice were housed in autoclaved ventilated cages with sterile food and water ad libitum. They were given humane care according to the guidelines of

our institution. HOCl administration was performed as previously described (Servettaz et al., 2009). Briefly, 300  $\mu$ l of HOCl were injected subcutaneously (s.c.) into the back of the mice 5 days per week during 6 weeks. One week after the end of the injections, the animals were sacrificed by cervical dislocation. Serum and tissue samples were collected from each mouse and stored at  $-80^{\circ}\text{C}$  until used or fixed in 10% acetic acid formol for histopathological analysis. For (PHTE)<sub>2</sub>NQ administration, BALB/c mice treated with HOCl (n=10) or not (n=7) were injected intravenously (i.v.) with (PHTE)<sub>2</sub>NQ (10 mg/kg per injection diluted in PBS once per week for 6 weeks). As the control group, BALB/c mice treated with HOCl (n=10) and those that were not (n=7), were injected intravenously (i.v.) with sterilized PBS once per week for 6 weeks. All cells were cultured as reported previously (Servettaz et al., 2009). All chemicals were from Sigma-Aldrich (France, Saint Quentin Fallavier), except when specified. The detailed synthesis of (PHTE)<sub>2</sub>NQ appears in the supplemental data.

### **Isolation of fibroblasts from the skin of mice**

HOCl or PBS were injected in the same skin area in all the mice. Skin samples were then collected from that area for experimental purposes. The samples were digested with “Liver Digest Medium” (Invitrogen Life Technologies, Grand Island, NY) for 1 h at  $37^{\circ}\text{C}$ . After three washes in complete medium, cells were seeded into sterile flasks, and isolated fibroblasts were cultured in DMEM/Glutamax-I supplemented with 10% heat-inactivated fetal calf serum and antibiotics, at  $37^{\circ}\text{C}$  in a humidified atmosphere containing 5%  $\text{CO}_2$ .

### **Viability Assays**

Isolated normal and SSc fibroblasts ( $4 \times 10^3$  cells/well) (Costar, Corning, Inc., Corning, NY) were incubated in 96-well plates with complete medium alone, or with 1, 2 or 4  $\mu\text{M}$

of (PHTE)<sub>2</sub>NQ for 48 h at 37°C. The number of viable cells was evaluated by the crystal violet assay. In brief, cells were stained in 0.5% crystal violet and 30% ethanol in PBS for 30 min at room temperature. After two washes in PBS, the stain was dissolved in 50% ethanol and absorbance was measured at 560 nm on a microplate reader (Fusion, PerkinElmer, Wellesley, MA). Results are expressed as percentage of viable treated cells compared to untreated cells.

### **H<sub>2</sub>O<sub>2</sub> and NO production and levels of intracellular reduced glutathione**

Isolated normal and SSc fibroblasts (2×10<sup>4</sup> cells/well) were seeded in 96-well plates (Costar) and incubated for 24 h at 37°C with either medium alone or with 0.5, 1 or 2 μM of (PHTE)<sub>2</sub>NQ. Levels of H<sub>2</sub>O<sub>2</sub> and NO were assessed spectrofluorometrically (Fusion, PerkinElmer, Wellesley, MA) using 2'-dichlorodihydrofluorescein diacetate (H<sub>2</sub>DCFDA) and diaminofluorescein-2 diacetate (DAF-2DA), respectively. Cells were incubated with 200 μM of H<sub>2</sub>DCFDA or 200 μM DAF-2DA in PBS for 1 hour at 37°C. The excitation and emission wavelengths used were 490 nm and 535 nm for H<sub>2</sub>DCFDA and 485 nm and 530 nm for DAF-2DA, respectively.

The levels of intracellular glutathione were assessed spectrofluorometrically using monochlorobimane staining. Cells were then washed and incubated with 50 μM monochlorobimane for 15 minutes at 37°C. The fluorescence intensity was measured with excitation and emission wavelengths of 380 and 485 nm, respectively. The intracellular H<sub>2</sub>O<sub>2</sub> and NO levels and the intracellular glutathione level were expressed as arbitrary units of fluorescence intensity normalized by the number of viable cells. The number of viable cells at the end of the experiments were evaluated by the crystal violet assay as described above.

### **Analysis of ROS metabolism of normal and SSc fibroblasts**

Isolated normal or SSc fibroblasts ( $2 \times 10^4$  cells/well) were seeded in 96-well plates and incubated for 24 h in complete medium alone or with the following molecules: 3.2 mM N-acetylcysteine (NAC), 1.6 mM BSO, 400  $\mu$ M ATZ or 20 U PEG-catalase. Cells were then washed three times with PBS and incubated with 100  $\mu$ l per wells of 200  $\mu$ M H<sub>2</sub>DCFDA for 30 min. Fluorescence intensity was read as described above. Intracellular H<sub>2</sub>O<sub>2</sub> levels were also expressed as described above.

### **Synergistic effect of BSO and (PHTE)<sub>2</sub>NQ on normal and SSc fibroblasts**

Isolated normal or SSc fibroblasts ( $2 \times 10^4$  cells/well ) were seeded in 96-well plates and incubated for 24 h in complete medium alone or with the following molecules: 0.8 mM BSO, 0.5  $\mu$ M (PHTE)<sub>2</sub>NQ, alone or in association. The number of viable cells at the end of the experiments were evaluated by the crystal violet assay as described above.

### **Analysis of cell death by Fluorescence-Activated Cell Sorting**

Cell death was analyzed by fluorescence-activated cell sorting (FACS)Canto™ II flow cytometer (Becton Dickinson, Franklin Lakes, NJ), using the Membrane Permeability/Dead Cell Apoptosis Kit with YO-PRO®-1 and Propidium iodide (PI) for Flow Cytometry (Invitrogen Life Technologies), under the manufacturer's recommendations. Briefly,  $1.2 \times 10^4$  normal or SSc fibroblasts isolated from the skin were incubated with 1, 2 or 4  $\mu$ M (PHTE)<sub>2</sub>NQ at 12 h, 24 h, 36 h, or 48 h. After the incubation period, the cells were collected, washed twice with PBS, stained on ice for 10 min with 1.5  $\mu$ M PI and 0.1  $\mu$ M YO-PRO®-1, and analyzed by flow cytometry.

### **Dermal thickness**

Skin thickness was measured one day before sacrifice with a calliper and expressed in millimeters (Servettaz et al., 2010).

### **Collagen content in skin and lung**

Skin was taken from the back region of mice with a punch (6 mm of diameter) and lung pieces, from each mouse, were diced using a sharp scalpel and then put into aseptic tubes, thawed, and mixed with pepsin (1:10 weight ratio) and 0.5 M acetic acid. Collagen content was assayed using the quantitative dye-binding Sircol method (Biocolor, Belfast, N. Ireland) (Burdick et al., 2005). The concentration values were read at 540 nm on a microplate reader (Fusion, PerkinElmer, Wellesley, MA, USA) versus a standard range of bovine collagen type I concentrations (supplied as a sterile solution in 0.5 M acetic acid).

### **Curative treatment**

BALB/c mice were injected s.c. with 300  $\mu$ l HOCl five days per week during five weeks to induce mouse SSc. SSc mice were then distributed randomly into two groups. The experimental group of treated mice (n=5) received 10 mg/kg of (PHTE)<sub>2</sub>NQ administered intravenously once a week during 2 weeks. The control group (n=5) received intravenous saline. Dermal thickness in SSc mice was measured after two weeks of treatment with (PHTE)<sub>2</sub>NQ.

### **Histopathological analysis**

Fixed lung and skin pieces were embedded in paraffin. A 5- $\mu$ m-thick tissue section was prepared from the mid-portion of the paraffin-embedded tissue and stained with either hematoxylin eosin or Sirius red. Slides were examined by a pathologist oblivious to the animal group assignment, via standard brightfield microscopy (Olympus BX60, Tokyo, Japan).

### **Analysis of $\alpha$ -SMA expression in mouse skin**

Expression of  $\alpha$ -SMA in mouse skin was analyzed by immunohistochemistry. Tissue sections were dewaxed then incubated with 200 mg/ml proteinase K for 15 min at 37°C for antigen retrieval. Specimens were then treated with 3% hydrogen peroxide for 20 min at 37°C to inhibit endogenous peroxidases and then blocked with BSA 5% for 30 min at 4°C. Sections were incubated with a 1:100 dilution of a monoclonal anti- $\alpha$ -smooth muscle Actin, Alkaline phosphatase conjugated (Cat. no. A-5691, Sigma- Aldrich). Antibody binding was visualised using Nitro blue tetrazolium chloride/5-bromo-4-chloro-3-indolyl phosphate (NBT/BCIP). The slides were examined by standard brightfield microscopy (Olympus BX60, Tokyo, Japan). Appropriate controls with irrelevant alkaline phosphatase-conjugated Ab were performed as control.

### **Determination of advanced oxidation protein product (AOPP) concentrations in sera**

AOPP were measured by spectrophotometry as previously described (Servettaz et al., 2009). Calibration used chloramine-T within the range of 0 to 100  $\mu\text{mol/l}$ . AOPP concentrations were expressed as  $\mu\text{mol/l}$  of chloramine-T equivalents.

### **Quantification of nitrite in mouse sera**

The concentration of nitrite was determined in sera by a spectrophotometric assay using oxidation catalysed by cadmium metal (Oxis, Portland, OR), which converts nitrate into nitrite. The total determined nitrite corresponds to NO production. The detection threshold for nitrite was 0.1  $\mu\text{mol/l}$  (Sastry et al., 2002).

### **Detection of serum auto-antibody**

Serum anti-DNA topoisomerase-1 IgG Abs were assayed by ELISA using purified calf thymus DNA topoisomerase-1 bound to the wells of a microtiter plate (Immunovision, Miami, FL). Plates were blocked with PBS-1% BSA and 100  $\mu$ l of 1:20 mouse serum were added and allowed to react for 1 h at room temperature. Bound Abs was detected with alkaline phosphatase-conjugated goat anti-mouse IgGAb and the reaction was developed by adding p-nitrophenyl phosphate. Optical density was measured at 405 nm using a Dynatech MR 5000 microplate reader (Dynex Technologies, Chantilly, VA).

### **Statistical Analysis**

All quantitative data was expressed as means  $\pm$  SEM. Data was compared using the Mann-Whitney nonparametric test or the Student's t paired test.

### **CONFLICT OF INTEREST**

The authors state no conflict of interest.

### **ACKNOWLEDGMENTS**

This work was supported by European Community's Seventh Framework Programme (FP7/2007-2013) under grant agreement 215009 RedCat for financial support.

### **REFERENCES**

Alexandre J, Batteux F, Nicco C, et al (2006). Accumulation of hydrogen peroxide is an early and crucial step for paclitaxel-induced cancer cell death both in vitro and in vivo. *Int. J. Cancer* 119: 41-48.

Allanore Y, Borderie D, Lemarechal H, et al (2004). Acute and sustained effects of dihydropyridine-type calcium channel antagonists on oxidative stress in systemic sclerosis. *Am J Med* 116: 595-600.

Amstad P, Peskin A, Shah G, et al. The balance between Cu,Zn-superoxide dismutase and catalase affects the sensitivity of mouse epidermal cells to oxidative stress. *Biochemistry* 1991: 30:9305-13.

- Avouac J, Borderie D, Ekindjian OG, et al (2010). High DNA oxidative damage in systemic sclerosis. *J Rheumatol* 37: 2540-47.
- Ba LA, Doering M, Jamier V, et al., (2010). Tellurium: an element with great biological potency and potential. *Org Biomol Chem* 8: 4203-16.
- Bellocq A, Azoulay E, Marullo S, et al (1999). Reactive oxygen and nitrogen intermediates increase transforming growth factor-beta1 release from human epithelial alveolar cells through two different mechanisms. *Am J Respir Cell Mol Biol* 21: 128-36.
- Burdick MD, Murray LA, Keane MP, et al (2005). CXCL11 attenuates bleomycin-induced pulmonary fibrosis via inhibition of vascular remodeling. *Am J Respir Crit Care Med* 171: 261-68.
- Casciola-Rosen L, Wigley F and Rosen A (1997). Scleroderma autoantigens are uniquely fragmented by metal-catalyzed oxidation reactions: implications for pathogenesis. *J Exp Med* 185: 71-79.
- Coriat R, Marut W, Leconte M, et al (2011). The organotelluride catalyst LAB027 prevents colon cancer growth in the mice. *Cell Death Dis* 2: e191; doi:10.1038/cddis.2011.73.
- Doering M, Ba LA and Lilienthal N (2010). Synthesis and selective anticancer activity of organochalcogen based redox catalysts. *J Med Chem* 14: 6954-63.
- Fry FH, Jacob C (2006). Sensor/effector drug design with potential relevance to cancer. *Curr Pharm Des* 12: 4479-99.
- Gabrielli A, Avvedimento EV, and Krieg T.N (2009). Scleroderma. *Engl J Med*: 7;360: 1989-2003.
- Harðardo H, Helvoort H, Vonk MC, et al (2010). Exercise in systemic sclerosis intensifies systemic inflammation and oxidative stress. *Scand J Rheumatol* 39: 63-70.
- Hussain SP, Amstad P, He P, et al (2004). p53-induced up-regulation of MnSOD and GPx but not catalase increases oxidative stress and apoptosis. *Cancer research* 64: 2350-56.
- Jamier V, Ba LA and Jacob C (2010). Selenium- and tellurium-containing multifunctional redox agents as biochemical redox modulators with selective cytotoxicity. *Chemistry* 16:10920-28.
- Jing Y, Dai J, Chalmers-Redman RM, et al (1999). Arsenic trioxide selectively induces acute promyelocytic leukemia cell apoptosis via a hydrogen peroxide-dependent pathway. *Blood* 94: 2102-11.
- Kavian N, Servettaz A, Mongaret C, et al (2010). Targeting ADAM-17/notch signaling abrogates the development of systemic sclerosis in a murine model. *Arthritis Rheum* 62: 3477-87.
- Laurent A, Nicco C, Chéreau C, et al (2005). Controlling tumor growth by modulating endogenous production of reactive oxygen species. *Cancer Res* 65: 948-56.

LeRoy EC and Medsger TAJ (2001). Criteria for the classification of early systemic sclerosis. *J Rheumatol* 28: 1573-76.

Lilienthal N, Prinz C, Peer-Zada AA, et al (2011). Targeting the disturbed redox equilibrium in chronic lymphocytic leukemia by novel reactive oxygen species-catalytic 'sensor/effector' compounds. *Leuk Lymphoma* 52: 1407-11.

Lonkar P and Dedon PC (2010). Reactive species and DNA damage in chronic inflammation: Reconciling chemical mechanisms and biological fates. *Int J Cancer*.

Mecklenburg S, Shaaban S, Ba LA, et al (2009). Exploring synthetic avenues for the effective synthesis of selenium- and tellurium-containing multifunctional redox agents. *Org Biomol Chem* 7: 4753-62.

Morgan MJ and Liu ZG (2010). Reactive oxygen species in TNF alpha-induced signaling and cell death. *Mol Cells* 30: 1-12.

Ogawa F, Shimizu K, Muroi E, et al (2006). Serum levels of 8-isoprostane, a marker of oxidative stress, are elevated in patients with systemic sclerosis. *Rheumatology (Oxford)* 45: 815-58.

Rodriguez AM, Carrico PM, Mazurkiewicz JE, et al (2000). Mitochondrial or cytosolic catalase reverses the MnSOD-dependent inhibition of proliferation by enhancing respiratory chain activity, net ATP production, and decreasing the steady state levels of H<sub>2</sub>O<sub>2</sub>. *Free Radic Biol Med* 29: 801-13.

Sambo P, Baroni SS, Luchetti M, et al (2001). Oxidative stress in scleroderma: maintenance of scleroderma fibroblast phenotype by the constitutive up regulation of reactive oxygen species generation through the NADPH oxidase complex pathway. *Arthritis Rheum* 44: 2653-64.

Sambo P, Jannino L, Candela M, et al (1999). Monocytes of patients with systemic sclerosis (scleroderma) spontaneously release in vitro increased amounts of superoxide anion. *J Invest Dermatol* 112: 78-84.

Sastry KV, Moudgal RP, Mohan J, et al (2002). Spectrophotometric determination of serum nitrite and nitrate by copper-cadmium alloy. *Anal Biochem* 306: 79-82.

Servettaz A, Guilpain P, Goulvestre C, et al (2007). Radical oxygen species production induced by advanced oxidation protein products predicts clinical evolution and response to treatment in systemic sclerosis. *Ann Rheum Dis* 66: 1202-29.

Servettaz A, Goulvestre C, Kaviani N, et al (2009). Selective oxidation of DNA topoisomerase 1 induces systemic sclerosis in the mouse. *J Immunol* 182: 5855-64.

Servettaz A, Kaviani N, Nicco C, et al (2010). Targeting the cannabinoid pathway limits the development of fibrosis and autoimmunity in a mouse model of systemic sclerosis. *Am J Pathol* 177: 187-96.

Shabaan S, Ba LA, Abbas M, et al (2009). Multicomponent reactions for the synthesis of multifunctional agents with activity against cancer cells. *Chem Commun* 31: 4702-24.

Simonini G, Matucci Cerinic M, et al (1999). Oxidative stress in Systemic Sclerosis. *Mol Cell Biochem* 196: 85-91.

Svegliati Baroni S, Santillo M, Bevilacqua F, et al (2006). Stimulatory autoantibodies to the PDGF receptor in systemic sclerosis. *N Engl J Med* 354: 2667-76.

Svegliati S, Canello R, Sambo P, et al (2005). Platelet-derived Growth Factor and Reactive Oxygen Species (ROS) Regulate Ras Protein Levels in Primary Human Fibroblasts via ERK1/2. *J Biol Chem* 280(43): 36474-82.

Toullec A, Gerald D, Despouy G, Bourachot B, et al (2010). Oxidative stress promotes myofibroblast differentiation and tumour spreading. *EMBO Mol Med.* 2: 211-30.

## FIGURE LEGENDS

### Figure 1.

Effects of (PHTE)<sub>2</sub>NQ on normal and diseased SSc fibroblasts in vitro. Primary skin fibroblasts extracted from 3 different normal skins (normal fibroblasts) or 3 different diseased skins (SSc fibroblasts) were tested. (a) Cytotoxic effects of (PHTE)<sub>2</sub>NQ on normal and diseased SSc fibroblasts in vitro. Cytotoxicity was assayed using the crystal violet method. Results are expressed as the percentage of viable treated cells compared with untreated cells. (b) Production of hydrogen peroxide by fibroblasts incubated with increasing concentrations of (PHTE)<sub>2</sub>NQ. H<sub>2</sub>O<sub>2</sub> levels were analyzed spectrofluorimetrically using H<sub>2</sub>DCFDA. (c) Production of nitric oxide (NO) by fibroblasts incubated with increasing concentrations of (PHTE)<sub>2</sub>NQ. NO levels were analyzed spectrofluorimetrically using DAF-2DA (d) Intracellular Glutathione levels in fibroblasts treated with various concentrations of (PHTE)<sub>2</sub>NQ. GSH levels were analyzed spectrofluorimetrically using monochlorobimane. Statistics: \*P < 0.05, \*\*P < 0.01, \*\*\*P < 0.001, NS - not significant.

### Figure 2.

Modulation of H<sub>2</sub>O<sub>2</sub> metabolism by (PHTE)<sub>2</sub>NQ in SSc fibroblasts. (a) percentage of H<sub>2</sub>O<sub>2</sub> production by treated fibroblasts compared with untreated fibroblasts in the presence of specific modulators of the enzymatic systems involved in ROS metabolism. The concentrations used were: 3.2 mM N-acetylcysteine (NAC), 0.8 mM BSO, 400 μM ATZ, 20 U catalase. (b) Viability of normal and SSc fibroblasts in the presence of, 3.2 mM N-acetylcysteine (NAC), 0.8 mM BSO, 400 μM ATZ, 20 U catalase. (c) Cytotoxic effects of (PHTE)<sub>2</sub>NQ on normal and diseased SSc fibroblasts in vitro. Cytotoxicity was assayed using the crystal violet method. Results are expressed as percentage of viable treated cells compared with untreated cells. Statistics: \*P < 0.05, \*\*P < 0.01, \*\*\*P < 0.001.

### **Figure 3.**

Analysis of cell death by Fluorescence-Activated Cell Sorting. Apoptosis/necrosis was analyzed by flow cytometry using the Membrane Permeability/Dead Cell Apoptosis Kit with YO-PRO®-1 and Propidium iodide (PI) on isolated normal and SSc fibroblast treated with 4 μM of (PHTE)<sub>2</sub>NQ for 48 h (a). Necrotic cells are PI positive and YO-PRO®-1 positive or negative. Apoptotic cells are PI negative and YO-PRO®-1 positive. Viable cells are negative for both dyes. Analysis of cell death is presented over 48 h (b).

### **Figure 4.**

Effect of (PHTE)<sub>2</sub>NQ on skin fibrosis induced by HOCl in BALB/c mice. Subcutaneous injections of HOCl or PBS were performed every day for 6 weeks in the back of mice and intravenous injections of (PHTE)<sub>2</sub>NQ (10 mg/kg) were performed once a week for 6 weeks (n = 7 to 10 mice per group as described in the materials and methods section). (a) Dermal thickness, as measured on skin sections in the injected areas of BALB/c mice. (b) Collagen content in 4-mm punch biopsy of skin as assayed by the Sircol method. (c)

Representative skin sections comparing dermal fibrosis in the injected areas from BALB/c mice. 1: PBS, 2: (PHTE)<sub>2</sub>NQ, 3: HOCl, 4: HOCl + (PHTE)<sub>2</sub>NQ. Tissue sections were stained with H&E. Scale bar = 100 μm (Olympus DP70 Controller). (d) Curative treatment of SSc mice with (PHTE)<sub>2</sub>NQ. (e) Percentage of positive areas for αSMA (f) αSMA expression in mouse skin by immunohistochemistry. Statistics: \*P < 0.05, \*\*\*P < 0.001.

### Figure 5.

Effect of (PHTE)<sub>2</sub>NQ on lung fibrosis induced by HOCl in BALB/c mice. Subcutaneous injections of HOCl or PBS were performed every day for 6 weeks in the back of mice and intravenous injections of (PHTE)<sub>2</sub>NQ (10 mg/kg) were performed once a week for 6 weeks (n = 7 to 10 mice per group as described in the materials and methods section). (a) Representative lung sections from BALB/c mice. 1: PBS, 2: (PHTE)<sub>2</sub>NQ, 3: HOCl, 4: HOCl+(PHTE)<sub>2</sub>NQ. Tissue sections were stained with H&E. Scale bar = 100 μm (Olympus DP70 Controller). (b) Collagen content in lung as assayed by the Sircol method. (c) Sirius Red staining for lung sections, 1: PBS, 2: (PHTE)<sub>2</sub>NQ, 3: HOCl, 4: HOCl + (PHTE)<sub>2</sub>NQ. Statistics: \*P < 0.05.

### Figure 6.

Effect of the organotellurium compound (PHTE)<sub>2</sub>NQ on AOPP, nitrite concentration, and anti-DNA topoisomerase 1 Abs in mice sera. HOCl or PBS was injected subcutaneously every day for 6 weeks in the back of mice. (PHTE)<sub>2</sub>NQ (10mg/kg) was similarly injected once a week for 6 weeks (n =7 to 10 mice per group as described in the materials and methods section). Sera were collected at the time of sacrifice. (a) Serum concentration of AOPP in the sera of mice. (b) Serum concentration of nitrite in the sera of mice. (c) Levels

of serum anti-DNA-topoisomerase 1 Abs. Values are means +/- SEM of data gained from all mice in the experimental or control groups. Statistics: \*P < 0.05, \*\*\*P < 0.001.

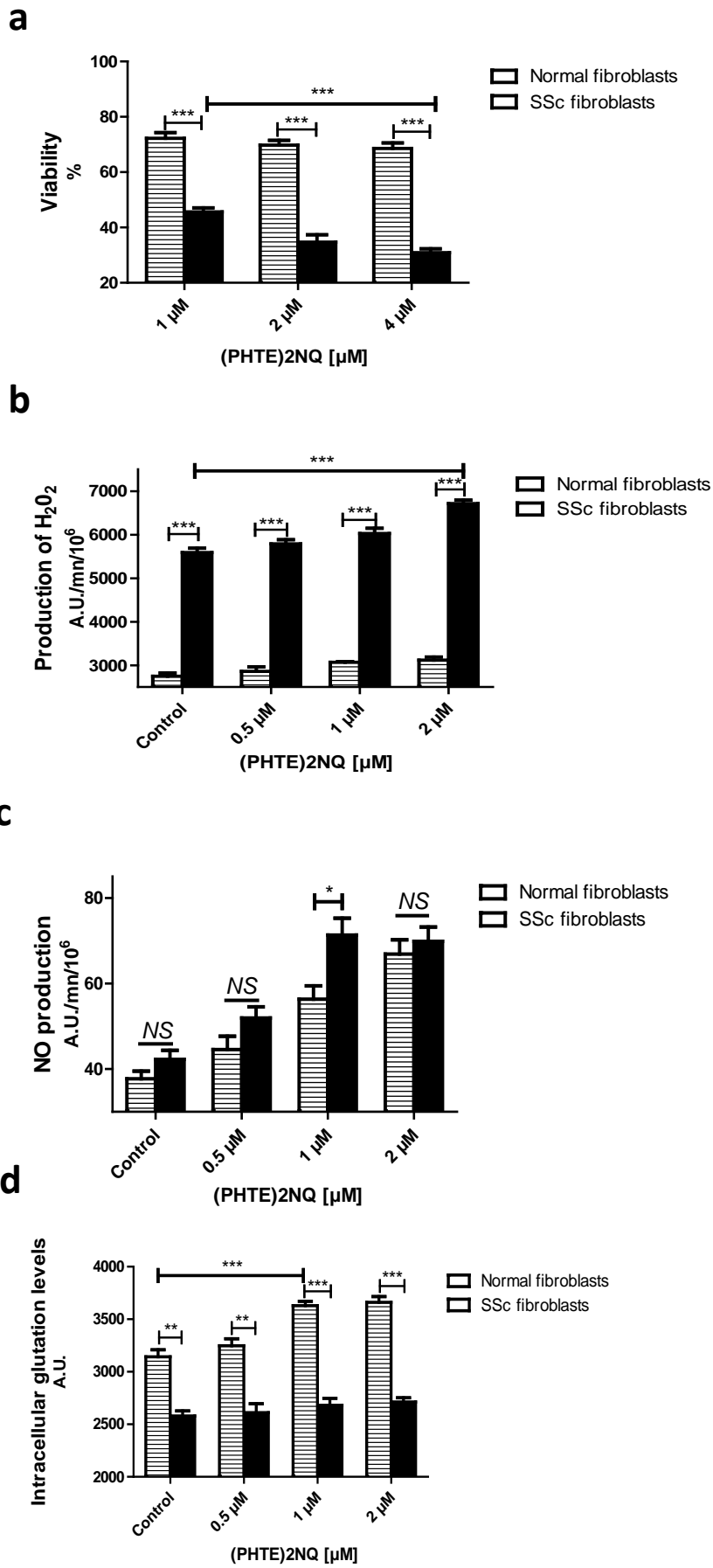
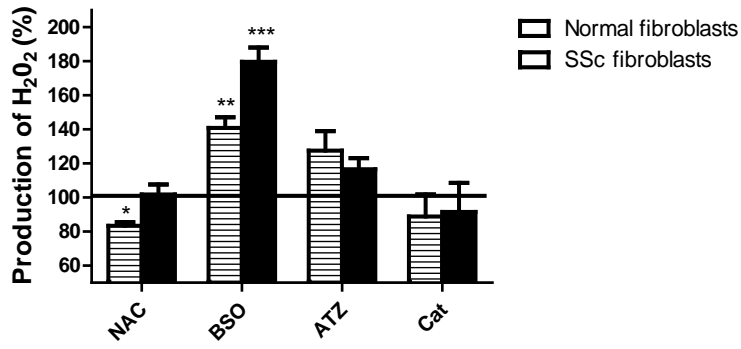
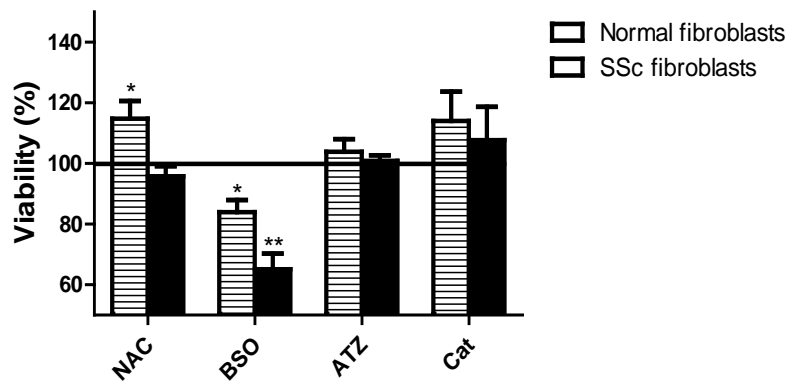


**Figure 1.**

**a**



**b**



**c**

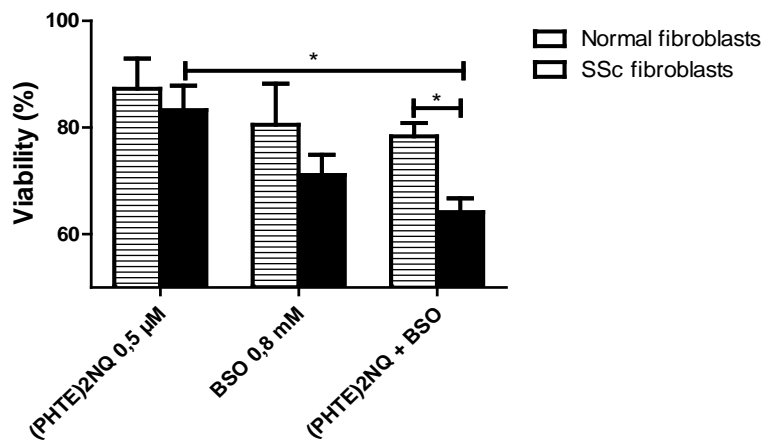


**Figure 2.**

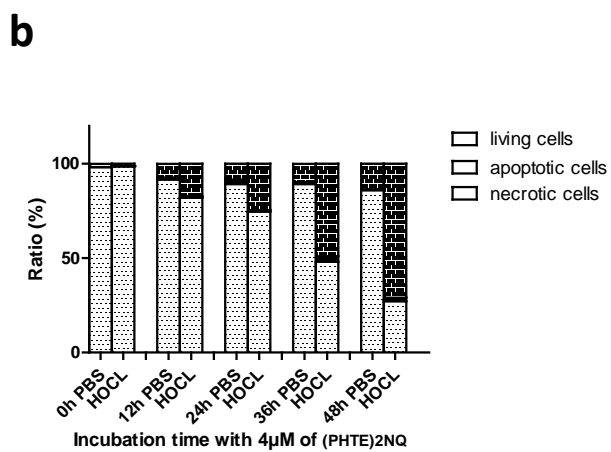
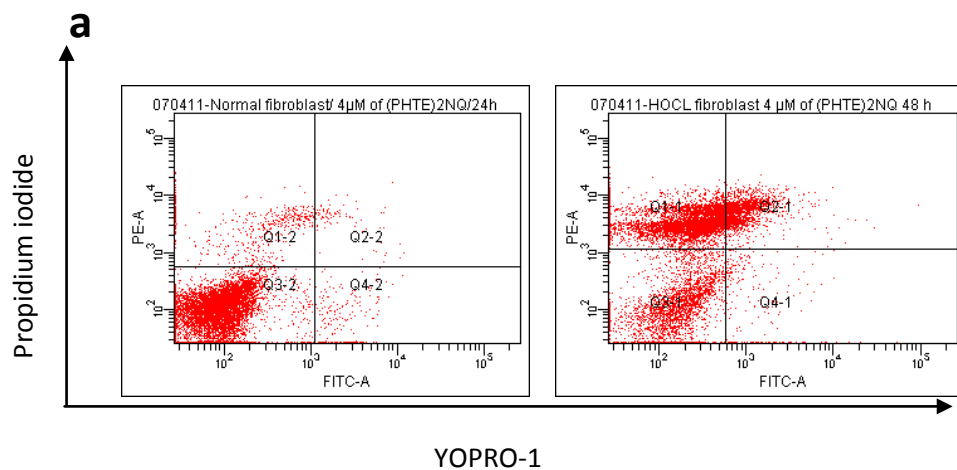


**Figure 3.**

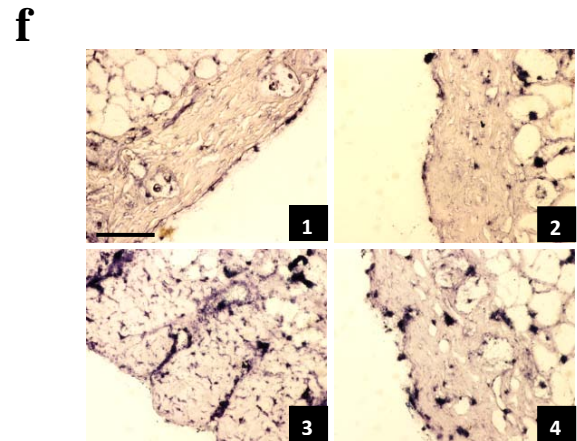
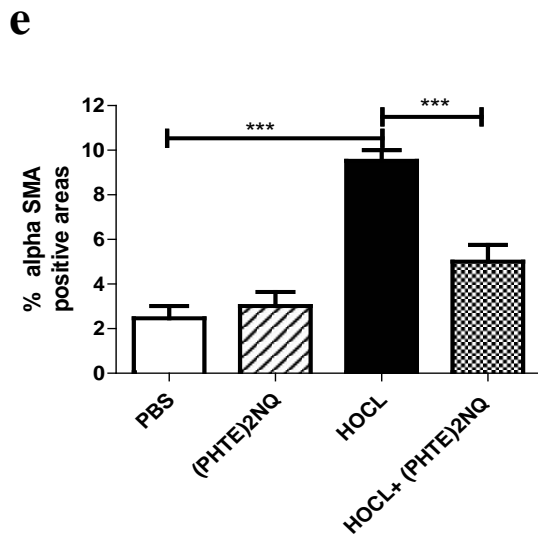
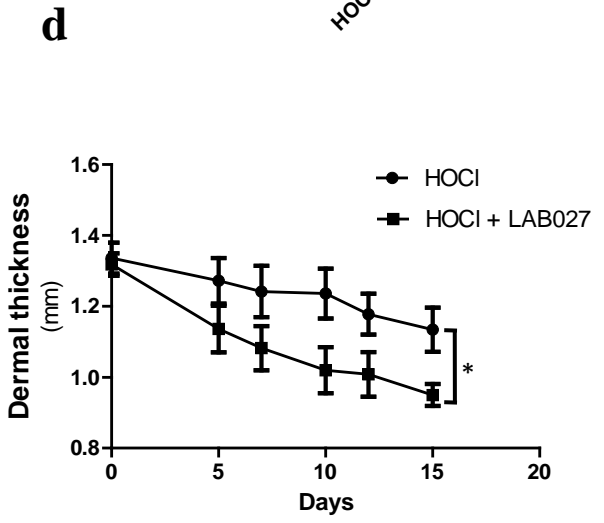
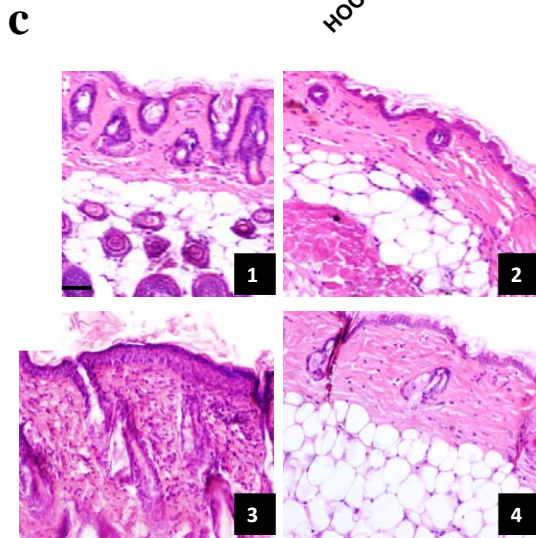
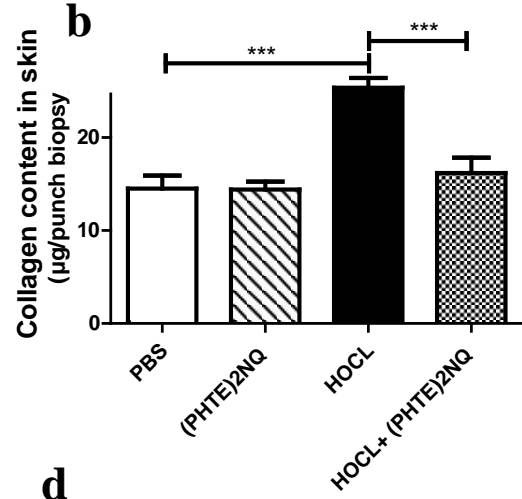
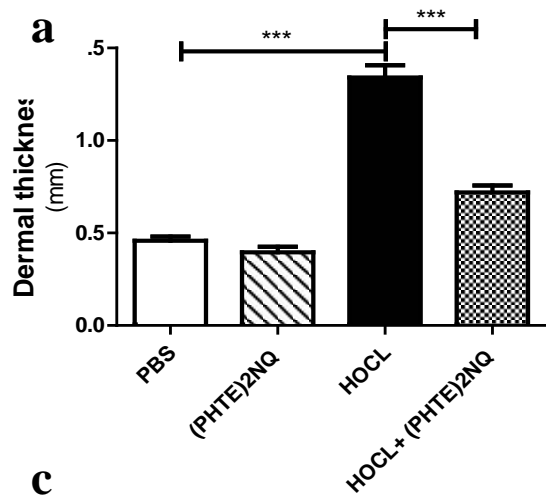


**Figure 4.**

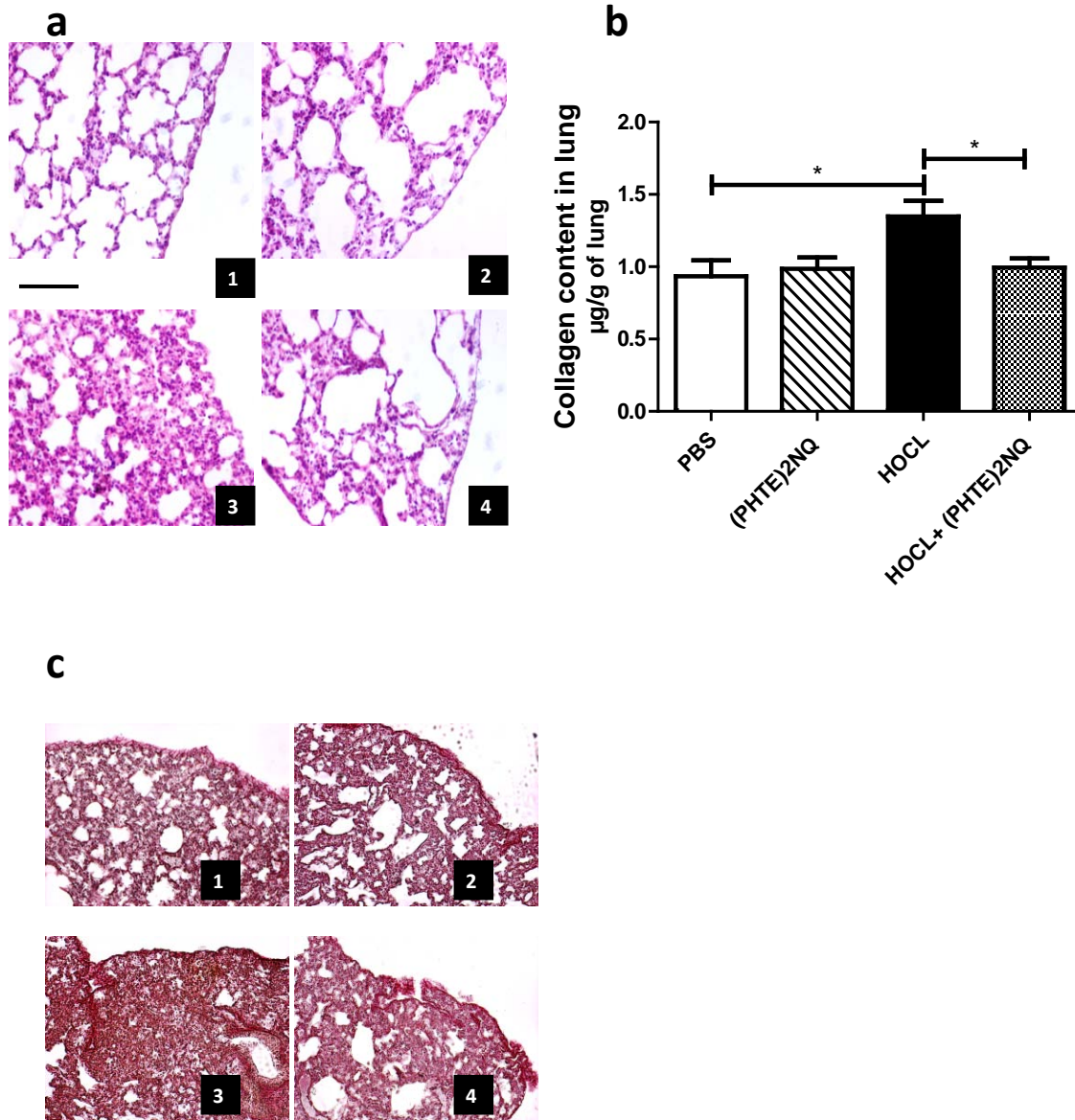
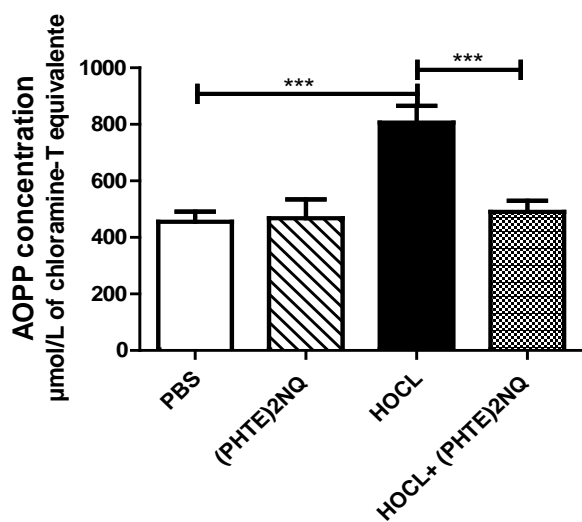
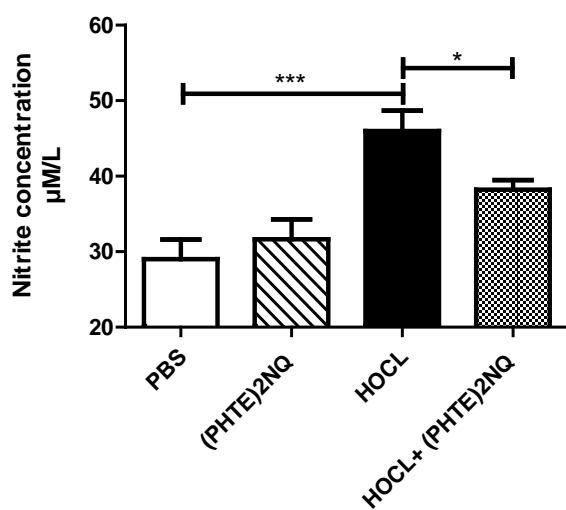


**Figure 5.**

a



b



c

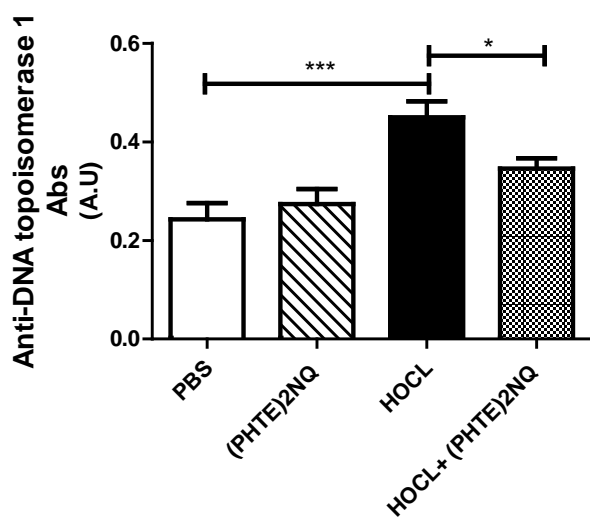


Figure 6.

### ***III.2 Article 2***

## **The natural organosulfur Dipropyltetrasulfide**

### **Prevents Systemic Sclerosis in the mice**

Wioleta Marut<sup>1</sup>, Vincent Jamier<sup>1</sup>, Niloufar Kavian<sup>1</sup>, Amélie Servettaz<sup>1,2</sup>, Paul Winyard<sup>3</sup>,  
Paul Eggleton<sup>3</sup>, Awais Anwar<sup>4</sup>, Carole Nicco<sup>1</sup>, Christiane Chéreau<sup>1</sup>, Bernard Weill<sup>1</sup>,  
Frédéric Batteux<sup>1</sup>

*Arthritis & Rheumatism, 2012*

In this study we have demonstrated the efficiency of the natural organosulfur compound - dipropyltetrasulfide (DPTTS) in a mouse model of HOCl-induced SSc. DPTTS, naturally found in *Allium* vegetable, is a pro-oxidative molecule known in the medicine from its beneficial properties.

To assess the mechanism of action of this compound in our SSc mouse model, the cytotoxic effect of DPTTS was compared in normal and SSc skin fibroblasts. ROS production was higher in SSc fibroblasts than in normal fibroblasts and was still increased by DPTTS to reach a lethal threshold and kill mouse SSc fibroblasts.

*In vivo*, in HOCl induced fibrosis mice, DPTTS presented significant decrease in dermal thickness and collagen concentration in the skin and in the lung compared to untreated SSc mice. In addition, DPTTS reduces expression of phosphorylated Smad2 and 3 in the skin of SSc mice which inhibit synthesis of collagen type I. Serum concentrations of advanced oxidation protein products was also significantly reduced in SSc mice treated by organosulfur molecule. Moreover, DPTTS affects also immune system, decreases

proliferation of lymphocyte T and B activated with LPS and CD3/CD28, inhibits the production of auto-antibodies, and decreases the levels of main profibrotic cytokines - IL-4 and IL-13 produced by activated T cells.

This work demonstrates that DPTTS can combine with endogenous oxidative species overproduced by SSc fibroblasts to selectively kill them. Organosulfur compounds are natural compounds already used in medicine. Therefore, DPTTS could be an interesting compound to use in the treatment of SSc.

## **The natural organosulfur Dipropyltetrasulfide**

### **Prevents Systemic Sclerosis in the mice**

Wioleta Marut<sup>1</sup>, Vincent Jamier<sup>1</sup>, Niloufar Kaviani<sup>1</sup>, Amélie Servettaz<sup>1,2</sup>, Paul Winyard<sup>3</sup>, Paul Eggleton<sup>3</sup>, Awais Anwar<sup>4</sup>, Carole Nicco<sup>1</sup>, Christiane Chéreau<sup>1</sup>, Bernard Weill<sup>1</sup>, Frédéric Batteux<sup>1</sup>.

<sup>1</sup>Université Paris Descartes, Faculté de Médecine, EA 1833 et Laboratoire d'immunologie biologique, Hôpital Cochin AP-HP, 75679 Paris cedex 14, France.

<sup>2</sup> Faculté de Médecine de Reims, Service de Médecine Interne, Maladies Infectieuses, Immunologie Clinique, Hôpital Robert Debré, 51092 Reims cedex, France.

<sup>3</sup> Peninsula Medical School, University of Exeter, Ex2 Exeter, England.

<sup>4</sup> ECOspray Ltd., Grange Farm Hilborough, Norfolk IP26 5BT, United Kingdom.

Address correspondence to: Dr. Frédéric Batteux, Laboratoire d'Immunologie, UPRES EA 1833, 8 rue Méchain 75679 Paris cedex 14, France. Tel: +33 (0) 1.58.41.20.09; Fax: +33 (0) 1.58.41.20.08; e-mail: frederic.batteux@cch.aphp.fr

Key words: polysulfide, DPTTS, oxidative stress, reactive oxygen species, systemic sclerosis, fibrosis



## **ABSTRACT**

**Objective:** The pro-oxidative organosulfur molecule Dipropyltertrasulfide (DPTTS) is a natural compound found in *Allium* vegetable and devoted with antibiotic and anti-cancer properties. The aim of this study was to evaluate the efficiency of DPTTS in a recently described mouse model of HOCl-induced SSc.

**Methods:** The pro-oxidative effects of DPTTS and their anti-proliferative and cytotoxic consequences were evaluated in vitro on mouse normal and SSc skin fibroblasts. The anti-fibrotic and immunomodulating properties of iv injection of DPTTS were evaluated in vivo in HOCl-induced SSc.

**Results:** In vitro, the ROS production was higher in mouse SSc fibroblasts than in normal fibroblasts and was still increased by DPTTS to reach a cytostatic and cytotoxic threshold that kills mouse SSc fibroblasts.

SSc mice treated with DPTTS presented significant decrease in dermal thickness and collagen concentration in the skin compared to untreated SSc mice. Serum concentrations of advanced oxidation protein products, and hydrogen sulfide were significantly reduced in SSc mice treated by organosulfur molecule. Moreover, in vivo treatment of HOCl mice with DPTTS reduced splenic B cell count, inhibited auto-antibodies production, decreased CD3/CD28 and LPS induced splenocytes proliferation and decreased the production of IL-4 and IL-13 produced by activated T cells.

**Conclusions:** We demonstrate that the natural organosulfur compound DPTTS prevents skin fibrosis in the mouse by the selective killing of diseased fibroblasts and its immunomodulating properties. Therefore, the natural vegetable-derived compound DPTTS could be a safe and effective treatment of SSc.

Systemic sclerosis is a connective tissue disease characterised by fibrosis of skin and visceral organs, vascular disorders and dysimmunity (1). The pathogenesis of systemic sclerosis is not fully understood yet (2). Nevertheless, lot of evidence suggested that oxidative stress and inflammation play an important role in the initiation and development of this disease (3-5). In early stage of systemic sclerosis, activated fibroblasts constitutively produce a high amounts of reactive oxygen species (ROS) which caused the synthesis of type I collagen, and in consequence leads to fibrosis (4). Released of highly toxic reactive oxygen species by activated fibroblasts and endothelial cells also induce an inflammatory process that favour the recruitment of inflammatory cells and the production of cytokines that increase the profibrotic process (6). Involvement of the immune system in the pathogenesis of SSc is also reflected by circulating auto-antibodies, like anti-topoisomerase I Abs which are presents in many patients with diffuse SSc. Release of ROS by SSc fibroblasts can oxidized DNA-topoisomerase-1 and contributes to the breach of tolerance towards the auto-antigen. Moreover, auto-Abs against platelet-derived growth factor receptor frequently found in SSc patients can also induce the production of ROS. Altogether these observations demonstrate the key role played by the overproduction of ROS by diseased fibroblasts on SSc pathogenesis. If intracellular ROS can stimulate cell growth and fibrosis, ROS can also lead to cell death at certain level. It has been recently demonstrated that ROS generating molecules like arsenic trioxide can selectively kills diseased fibroblasts and be used to improve signs of fibrosis in two mouse models of SSc. However, the compounds used so far displayed several side effects that limit their use to severe forms of SSc. Dipropyltertrasulfide (DPTTS) is a natural organosulfur compound (OSC), found in *Allium* vegetable. This compound has pro-oxidative properties and is used as an antibiotic or anti-mitotic agent (7, 8). Polysulfides like DPTTS are already considered as a promising new class of antibiotic for resistant bacteria (9). In this study, we

have investigated the effect of DPTTS on the skin fibrosis and immune dysregulations in HOCl-induced SSc in the mouse.

## **MATERIALS AND METHODS**

**Animals and chemicals.** Six week-old female BALB/c mice were used in all experiments (Harlan, Gannat, France). All mice received humane care according to our institutional guidelines. Mice were divided into control and experimental groups. A total of 300  $\mu$ l of a solution generating HOCl was injected intra-dermally into the back of the mice everyday during 6 weeks. DPTTS was injected intravenously (i.v.) two times per week (6 mg/kg per injection diluted in PBS, n=8). Controls group received injection of PBS. One week after the end of the injections, the animals were sacrificed by cervical dislocation. Serum and tissue samples were collected from each mouse and stored at  $-80^{\circ}\text{C}$  until use.

**HOCl generation:** HOCl was produced by adding 166  $\mu$ l of NaClO solution (2.6% as active chlorine) to 11.1 ml of  $\text{KH}_2\text{PO}_4$  solution (100 mM (pH 6.2)). HOCl concentration was determined by spectrophotometry at 280 nm. The optical density of the HOCl solution at 280 nm should be between 0.7-0.9, and the amount of Sodium hypochlorite and/or  $\text{KH}_2\text{PO}_4$  solution must be adjusted for that. All cells were cultured as reported previously (10). All chemicals were from Sigma-Aldrich (France) except specifically specified.

**Synthesis of dipropyltetrasulfide.** Dipropyltetrasulfide (DPTTS) was synthesized from propylmercaptan and sulfur chloride ( $\text{S}_2\text{Cl}_2$ ). A solution of 10 mM each propylmercaptan and pyridine in 25 ml anhydrous diethyl ether was stirred at  $-78^{\circ}\text{C}$ . A solution of 10 mM sulfur monochloride in 50 ml anhydrous diethyl ether was added drop wise over 0.5 h. The reaction mixture was stirred for additional 0.5 h and another solution of 10 mM propylmercaptan and pyridine in 25 ml anhydrous diethyl ether was added drop wise over 0.5 h and reaction mixture was further stirred for 1 h. The reaction was stopped by adding

25 ml of H<sub>2</sub>O and mixture was brought to room temperature. The mixture was washed with 0.5 M NaOH until pH was neutral. The organic phase was dried over MgSO<sub>4</sub>, filtered and evaporated to yield a yellow oil with strong onion smell. The respective compound was purified by column chromatography using petrol ether: chloroform (95:3) as eluent. Characterization was done by NMR (Bruker (Rheinstetten) type DRX 500 and Avance 500); <sup>1</sup>H NMR (500MHz, CDCl<sub>3</sub>): δ1.02(6H, t, J=7.4Hz), 1.79(m,4H), 2.91(4H,t,J=7.4Hz). The purity of compound was confirmed by GC- MS and HPLC (80%MeOH:H<sub>2</sub>O) (11).

**Isolation of fibroblasts from the skin of mice.** At the time of sacrifice, fragments from HOCl-treated diseased skin and from PBS-treated control skin were collected from HOCl- and PBS-treated mice, respectively. Fragment of skin were digested with “Liver Digest Medium” (Invitrogen) for 1 h at 37°C. After three washes, cells were seeded into sterile flasks and isolated fibroblasts were cultured in DMEM/Glutamax-I supplemented with 10% heat-inactivated fetal calf serum and antibiotics at 37°C in humidified atmosphere with 5% CO<sub>2</sub>.

**In vitro cells proliferation and viability assays.** Isolated normal and SSc fibroblasts (4×10<sup>3</sup> cells/well) (Costar, Corning, Inc., Corning, NY) were incubated in 96-well plates with complete medium, and various dose of DPTTS (10 to 40 μM) for 48 h at 37°C. Cell proliferation was determined by pulsing the cells with [<sup>3</sup>H] thymidine (1 μCi/well) during the last 16 hours of culture. Cell viability was evaluated by the crystal violet assay (Alexandre et al., 2006). Results are expressed as percentage of viable treated cells compared to untreated cells.

**ROS production and levels of intracellular reduced glutathione.** 4×10<sup>4</sup> cells/well of isolated normal and SSc fibroblasts were coated in 96-well plates (Costar) and incubated

for 48 hours at 37°C with either medium alone or with 2.5, 5, 10, 20 or 40 µM of DPTTS. Levels of ROS and GSH were assessed spectrofluorometrically (Fusion, PerkinElmer, Wellesley, MA) using 2'-dichlorodihydrofluorescein diacetate (H<sub>2</sub>DCFDA) and monochlorobimane, respectively. Cells were incubated with 200 µM of H<sub>2</sub>DCFDA for 1h or 50 µM monochlorobimane in PBS for 15 minutes at 37°C. The intracellular ROS and the intracellular glutathione level were expressed as arbitrary units of fluorescence intensity normalized by the number of viable cells. The number of viable cells at the end of the experiments was evaluated by the crystal violet assay as described above.

**Modulation of ROS metabolism in normal and SSc fibroblasts.** Isolated primary fibroblasts ( $2 \times 10^4$  cells/well) from normal and SSc mice were seeded in 96-well plates and incubated for 12 hours in complete medium alone or with the following molecules: 3.2 mM N-acetylcysteine (NAC), 1.6 mM BSO, 20 U PEG-catalase, 400 µM AT, or 8 µM DDC. DPTTS (30 µM) was added in the last 16 hours. Cells were then washed three times with PBS and incubated with 100 µl per wells of 200 µM H<sub>2</sub>DCFDA for 30 min. Intracellular H<sub>2</sub>O<sub>2</sub> levels were expressed as described above.

**Fluorescence-Activated Cell Sorting Analysis of cell death.** Apoptosis and necrosis were analyzed by the fluorescence-activated cell sorting (FACS)Canto™ II flow cytometer (Becton Dickinson, Franklin Lakes, NJ), using the Membrane Permeability/Dead Cell Apoptosis Kit with YO-PRO®-1 and Propidium iodide (PI) for Flow Cytometry (Invitrogen) under the manufacturer's recommendations. Briefly, of Isolated normal and SSc fibroblast ( $1.2 \times 10^4$ ) were incubated with 40 µM of DPTTS for various times (5 h, 10 h, 15 h and 24h). After the incubation period, cells were collected, washed two times with PBS, stained for 10 minutes on ice with 1.5 µM PI and 0.1 µM YO-PRO®-1 and analyzed by flow cytometry.

**Dermal thickness.** Skin thickness was measured on the back of the mice in the area of intra-dermal injection one day before the sacrifice. Dermal thickness was measured with a calliper and expressed in millimeters (10).

**Measurements of collagen content in skin and lung.** Skin was taken with a punch (6 mm of diameter) and lung pieces were diced using a sharp scalpel, mixed with pepsin (1:10 weight ratio) and 0.5 M acetic acid at room temperature. After 3 days, collagen content was assayed using the quantitative dye-binding Sircol method (Biocolor, Belfast, N. Ireland) (12, 13).

**Ex vivo skin fibroblasts proliferation.** Primary normal and SSc fibroblasts from mice treated or not with DPTTS ( $4 \times 10^3$  cells/well) (Costar, Corning, Inc., Corning, NY) were incubated in 96-well plates with complete medium, for 48 h at 37°C. Cell proliferation was determined by pulsing the cells with [3H] thymidine (1  $\mu$ Ci/well) during the last 16 hours of culture like described above.

**Histopathological analysis.** A 5- $\mu$ m-thick tissue section was prepared from the mid-portion of paraffin-embedded skin and lung pieces and stained with hematoxylin eosin. Slides were examined by standard bright field microscopy (Olympus BX60, Tokyo, Japan) by a pathologist who was blinded to the assignment of the animal.

**Analysis of  $\alpha$ -SMA and pSmad2/3 expression in mouse skin.** Expression of  $\alpha$ -SMA and pSmad2/3 in mouse skin was analyzed by immunohistochemistry. Tissue sections were deparaffinized and rehydrated, then incubated with 200  $\mu$ g/ml proteinase K for 15 min at 37°C for antigen retrieval. Specimens were then treated with 3% hydrogen peroxide for 10 min at 37°C to inhibit endogenous peroxidases and then blocked with BSA 5% for 1h at

4°C. Sections were incubated with a 1:100 dilution of a monoclonal anti- $\alpha$ -smooth muscle Actin, Alkaline phosphatase conjugated antibody (Sigma- Aldrich) and with a 1:100 monoclonal antibody directed to Phospho-Smad2/3 (Cell Signaling Technology, USA) for a 2h at room temperature. Section incubated with pSmad2/3, were then incubated with HRP-conjugated secondary goat anti-rabbit (Rockland, USA) for 1 hour at room temperature. Antibody binding for  $\alpha$ SMA staining was visualised using Nitro blue tetrazolium chloride/5-bromo-4-chloro-3-indolyl phosphate (NBT/BCIP) and for pSmad2/3 using diaminobenzidine tetrahydrochloride (DAB) as a chromogen. The slides were examined by standard brightfield microscopy (Olympus BX60, Tokyo, Japan). Appropriate controls with irrelevant alkaline phosphatase-conjugated and HRP-conjugated Ab were performed as control.

**Determination of advanced oxidation protein product (AOPP) concentrations in sera.**

AOPP were measured by spectrophotometry as previously described (10). Calibration used chloramine-T within the range of 0 to 100  $\mu$ mol/l.

**Detection of serum anti-DNA topoisomerase-1 IgG Abs.** Serum levels of anti-DNA topoisomerase-1 IgG Abs were detected by ELISA using coated DNA topoisomerase-1 purified from calf thymus (Immunovision, USA). Optical density was measured at 405 nm using a Dynatech MR 5000 microplate reader (Dynex Technology, USA).

**Flow cytometric analysis and splenocytes proliferation.** Spleen cells suspensions were prepared after hypotonic lysis of erythrocytes. Splenocyte (10<sup>6</sup> cells) were incubated with anti-B220-PE antibody diluted 1:200 for 30 minutes at 4°C. Cells were then analyzed with a FACS Canto flow cytometer (BD Biosciences). For spleen cell proliferation, B and T cells were purified from splenocytes by MACS, and were coated 96-well plates. Briefly, splenic B or T cell suspensions (2 x 10<sup>5</sup> cells) were cultured with 10  $\mu$ g/ml of LPS

(Boehringer, Mannheim) for B cells, or with 2.5 µg/ml precoated anti-CD3 and 1 µg/ml precoated anti-CD28 mAb for T cells. Cell proliferation was determined as described above.

**Determination of IL-4 and IL-13.** MACS purified splenic T cells ( $2 \times 10^5$  cells per well) were cultured in 96-well plate in complete medium for 48 hrs at RT in the presence of 5 µg/ml concanavalin A. Cytokines were measured from the collected supernatants by ELISA (R&D System, USA) following the manufacturer's instructions. Results are expressed in ng/ml.

**Statistical Analysis.** All quantitative data were expressed as means  $\pm$  SEM. Data were compared using one-way ANOVA plus the Tukey test for the comparisons of mean among multiple groups. P value of less than 0.05 was considered as significant.

**CONFLICT OF INTEREST.** The authors state no conflict of interest.

**ACKNOWLEDGMENTS.** This work was supported by European Community's Seventh Framework Programme (FP7/2007-2013) under grant agreement 215009 RedCat for financial support.

## **RESULTS**

DPTTS exerted in vitro anti-proliferative and cytotoxic effects on normal and SSc fibroblasts. Fibroblasts from normal and SSc-mice were exposed in vitro to increasing amounts of DPTTS from 10-40 µM. Compared to untreated normal fibroblasts, the proliferation rate of normal fibroblasts decreased to 82% ( $82.4\% \pm 1.4$ ,  $P < 0.01$ ) and 61% ( $61.1\% \pm 4.8$ ,  $P < 0.05$ , Figure 1A) when cells were incubated with 10 µM and 40 µM of DPTTS, respectively. Nevertheless, compared to untreated SSc fibroblasts, the proliferation rate of SSc fibroblasts decreased to 63% ( $62.9\% \pm 4.2$ ,  $P < 0.01$ ) and 5.1%

(5.1%±0.5,  $P < 0.001$ , Figure 1A) when cells were incubated with 10  $\mu\text{M}$  and 40  $\mu\text{M}$  of DPTTS, respectively.

In the presence of 10  $\mu\text{M}$  DPTTS, the viability of normal fibroblasts was 84% (84.3%±9.5,  $P < 0.05$ ) and 69% (69.4%±1.1,  $P < 0.001$ , Figure 1B) with 40  $\mu\text{M}$  of DPTTS. DPTTS had a more powerful cytotoxic effect on diseased SSc compare to untreated fibroblasts. Indeed, in the presence of 10  $\mu\text{M}$  DPTTS, the viability of SSc fibroblast decreased to 66% (66.1%±2.2,  $P < 0.001$  vs untreated fibroblasts and vs normal fibroblasts) and 8.6% with 40  $\mu\text{M}$  DPTTS (8.6%±4.7,  $P < 0.001$  vs untreated fibroblasts and vs normal fibroblasts, Figure 1B).

**DPTTS exerted pro-oxidative effects in vitro.** The basal production of ROS was increased by 39% in SSc fibroblasts compared to normal fibroblasts (4285 A.U.±241 vs 2658 A.U.±235,  $P < 0.05$ , Figure 1C). Incubation of normal fibroblasts with DPTTS did not increase significantly the production of ROS. In contrast, SSc fibroblasts with increasing amounts of DPTTS dose-dependently, increased the production of ROS by more than 50% (8595 A.U.±269 vs 4285 A.U.±241,  $P < 0.001$  for 40  $\mu\text{M}$  of DPTTS; Figure 1C). We also investigate the effect of DPTTS on reduced glutathione levels, which is an essential cofactor of  $\text{H}_2\text{O}_2$  catabolism. The basal level of reduced GSH was decreased by 166% in SSc fibroblasts compared to normal fibroblasts (-132 A.U.±43.8 vs 380 A.U. ±22.6  $P < 0.001$ , Figure 1D). The level of intracellular glutathione was significantly higher ( $P < 0.001$ ) in normal fibroblasts in the presence of DPTTS in all tested doses than in SSc fibroblasts (Figure 1D).

**Modulations of  $\text{H}_2\text{O}_2$  metabolism in SSc fibroblasts.** We next investigated the mechanism of DPTTS action using specific modulators of the enzymatic and non enzymatic systems involved in  $\text{H}_2\text{O}_2$  catabolism. Primary control or SSc fibroblasts were

incubated with or without DPTTS together with N-acetylcystein (NAC), buthionin sulfoximine (BSO), catalase, aminotriazole (AT) or diethyldithiocarbamate (DDC). Co-incubation of DPTTS with NAC, a precursor of GSH, significantly decreased H<sub>2</sub>O<sub>2</sub> production by 57% in normal fibroblasts and by 60% in SSc fibroblasts (P < 0.05 for normal and P < 0.01 for SSc fibroblasts, Figure 1E). Hydrogen peroxide is converted into H<sub>2</sub>O by catalase and the GSH/GPx system. Depleting GSH with BSO significantly increased H<sub>2</sub>O<sub>2</sub> production by 30% in SSc fibroblasts (P < 0.05) and by 31% in normal fibroblasts (P < 0.05). In addition, H<sub>2</sub>O<sub>2</sub> production by SSc fibroblasts co-incubated with DPTTS and BSO reached 7.92±0.4 A.U. compared to those incubated with BSO alone 5.48±0.08 A.U. or DPTTS alone 3.15±0.3 A.U. showing the additive effect of DPTTS and BSO (P < 0.05). On the other hand, addition of DPTTS along with the catalase inhibitor aminotriazol (ATZ) or with exogenous PEG-catalase or with the superoxide dismutase inhibitor DDC had no effect on the levels of H<sub>2</sub>O<sub>2</sub> in normal and SSc fibroblasts (Figure 1E). Depleting GSH by adding BSO to the culture medium with DPTTS significantly decreased the viability of SSc fibroblasts (P < 0.01). By contrast, specific inhibition of catalase by aminotriazol (ATZ) or of superoxide dismutase by DDC had no effect on the viability of normal and SSc fibroblasts (Figure 1F).

**DPTTS induced apoptosis in normal and SSc fibroblasts.** Fibroblasts extracted from the skin of normal and of SSc mice were incubated with 10, 20, and 40 µM of DPTTS for 5 h, 10 h, 15 h or 24h. The highest cytotoxic effect of DPTTS was observed after incubation with 40 µM. At this concentration and after 15h the viability was decreased by 38% for SSc fibroblasts and only by 14% for normal fibroblasts (P < 0.001, Figure 2A). A kinetic analysis of cell death between 5 h and 24 h indicated that DPTTS effects are mainly mediated through a apoptotic process (Figure 2B).

**DPTTS decreased skin and lung fibrosis in mice with SSc.** HOCl-induced SSc in mice (HOCl-mice) is associated with an increase in dermal thickness that is significantly reduced by DPTTS ( $P < 0.001$  vs untreated SSc mice, Figure 3A). Those results were confirmed by the histopathological analysis of the skin of control or HOCl-mice treated or not with DPTTS (Figure 3C). In vivo treatment with DPTTS significantly reduced the accumulation of type I collagen induced by HOCl in the skin ( $P < 0.01$ , Figures 3B) and in the lung ( $P < 0.05$ , Figures 4A) versus untreated mice. Histopathological analysis of lung biopsies stained with hematoxylin & eosin (Figure 4B) confirmed the reduction in lung fibrosis in HOCl-mice treated with DPTTS. Moreover, the high proliferation rate of fibroblasts isolated from HOCl-mice was significantly reduced by in vivo treatment with DPTTS ( $8729\text{cpm} \pm 445$  vs  $6842\text{cpm} \pm 420$ ,  $P < 0.01$ , Figure 3D).

**DPTTS reduced the expression of  $\alpha$ SMA and pSmad2/3 in HOCl mice.** The expression of  $\alpha$ SMA was significantly higher in fibrotic skin of HOCl-mice compared to PBS mice ( $22.6\% \pm 1.6$  positive area vs  $10.01\% \pm 0.8$ ,  $P < 0.01$ , Figure 3C). DPTTS decreased expression of  $\alpha$ SMA by 40% compared to HOCl treated mice ( $13.7\% \pm 0.4$  positive area vs  $22.6\% \pm 1.6$  positive area in untreated HOCl mice,  $P < 0.01$ , Figure 3C). pSmad 2/3 protein, a key molecule involved in TGF $\beta$ -induced fibrogenesis, was overexpressed in HOCl-mice versus PBS controls ( $24.5\% \pm 1.4$  positive area in HOCl mice vs  $5.8\% \pm 0.4$  positive area in PBS mice,  $P < 0.01$ , Figure 3C). In vivo administration of DPTTS downregulated pSmad2/3 expression in HOCl-mice ( $7.2\% \pm 2.1$  positive area vs  $24.5\% \pm 1.4$  positive area in untreated HOCl-mice,  $P < 0.01$ , Figure 3C).

DPTTS decreased the serum concentration of AOPP and anti-DNA topoisomerase 1 Abs in SSc mice. Advanced oxidation protein products (AOPP), a marker of systemic oxidative stress, increased in the sera of HOCl-mice compared to PBS control mice ( $P < 0.001$ ,

Figure 5). Treatment of HOCl-mice with DPTTS reduced the levels of AOPP by 28%, compared to untreated SSc mice ( $P < 0.05$ , Figure 5B). The sera of SSc-mice contained significantly higher levels of anti-DNA-topoisomerase I Abs than the sera from normal mice ( $1.96 \text{ A.U.} \pm 0.1$  vs  $1.39 \text{ A.U.} \pm 0.11$ ,  $P < 0.05$ , Figure 5A). DNA-topoisomerase-1 Abs were significantly decreased in the sera from SSc mice treated with DPTTS compared to untreated SSc mice ( $1.47 \text{ A.U.} \pm 0.09$  vs  $1.96 \text{ A.U.} \pm 0.1$ ,  $P < 0.05$ , Figure 5A).

DPTTS treatment decreased the level of B cells and the proliferation rate of B and T cells in SSc-mice. We next tested the effects of DPTTS on spleen cells population. Intra-dermal injection of HOCl significantly increased the numbers of splenic B cells compared to normal mice ( $40.3\% \pm 0.6$  vs  $34.1\% \pm 0.61$ ,  $P < 0.01$ , Figure 6A). DPTTS decreased the numbers of splenic B cells by 16% in SSc mice compared to untreated HOCl induced SSc-mice ( $34.7\% \pm 1.1$  vs  $40.3\% \pm 0.6$ ,  $P < 0.01$ , Figure 6A). We also investigated proliferation rate of splenic T cells after stimulation with pre-coated-anti-CD3/CD28 mAb, and B cells after stimulation with LPS. T and B cells isolated from SSc-mice had both higher proliferation rate than T and B cells isolated from normal mice. T cells isolated from SSc-mice in vivo treated with DPTTS and in vitro stimulated by anti-CD3 mAb, had a lower proliferation rate than T cells obtained from untreated SSc-mice and stimulated under the same conditions ( $5538 \text{ cpm} \pm 427$  vs  $10967 \text{ cpm} \pm 786$ ,  $P < 0.001$ , Figure 6B). In addition, B cells isolated from SSc-mice treated with DPTTS and stimulated with LPS also displayed significantly lower proliferation rate than B cells obtained from untreated SSc-mice ( $7625 \text{ cpm} \pm 851$  vs  $12380 \text{ cpm} \pm 1572$ ,  $P < 0.05$ , Figure 6C).

In vivo administration of DPTTS reduced the production of IL-4 and IL-13 in SSc-mice. Next, we tested the levels of IL-4 and IL-13 produced by splenic T-cells. SSc mice had a higher concentration of those 2 cytokines compared to control mice ( $1.03 \pm 0.09$  vs  $0.58 \pm 0.1$ ,  $P < 0.01$  for IL-4, Figure 6D,  $1.2 \pm 0.07$  vs  $0.63 \pm 0.15$ ,  $P < 0.01$  for IL-13, Figures

6E). DPTTS decreased the levels of IL-4 in SSc mice by 37% ( $P < 0.05$ , Figure 6D), and of IL-13 by 36% ( $P < 0.05$ , Figure 6E). Results are expressed in ng/ml.

## DISCUSSION

In the present study, we have shown the effect of the natural organosulfur compound, DPTTS in the prevention of fibrosis development in a murine model of chemically-induced systemic sclerosis.

Several reports have emphasized the involvement of ROS in the pathogenesis of SSc. An increased oxidative stress occurs in diseased skin and lung fibroblasts during SSc. The reactive oxygen species locally generated favour the synthesis of type I collagen and the proliferation of fibroblasts through the activation of the RAS/MAPkinase pathways. Thus, the overproduction of ROS is one of the major actors of skin and lung fibrosis during SSc. Skin fibroblasts from the recently described model of SSc induced by daily injection of HOCl in mice skin durably decrease the level of reduced glutathione (GSH) in skin fibroblast and increased their production of ROS as observed in human SSc (3, 14). In our study, the pro-oxidant organosulfur compound, DPTTS, (15) additionally increase the level of ROS to generate a lethal oxidative burst in SSc fibroblasts. The cytotoxic effect of DPTTS occurs only in diseased fibroblasts, not in healthy fibroblasts with a normal level of endogenous reduced GSH and low level of ROS. Our results are in agreement with other studies on polysulfides compounds showing the pro-oxidant effect of these molecules. Hosono et al showed that diallyl-polysulfides lead to the ROS formation in cancer cells which also display increased level of ROS, causing  $\beta$ -tubulin oxidation and the disruption of the microtubule network leading to apoptosis of cancer cells (16). Moreover, the mechanism of action for DPTTS shows the role of the GSH pathway in mediating the cytotoxic effects of DPTTS. NAC, a GSH precursor, has a protective effect against DPTTS

in SSc-fibroblasts, while BSO, that depletes intracellular GSH, increases the cytotoxicity of organosulfur compound. The differences between normal and SSc fibroblasts in terms of basal oxidative stress and antioxidant enzyme levels have already been used to selectively kill SSc fibroblasts in vivo (17, 18).

Moreover, DPTTS decrease the level of oxidized protein-AOPP generated by SSc fibroblasts. AOPP could enhance the vascular damage by increase the apoptosis of endothelial cells (10). Moreover, ROS produced by SSc fibroblasts can oxidized different proteins, like anti-topoisomerase I, favouring the breach of tolerance towards this auto-antigen in SSc and the production of anti-DNA Topoisomerase I Abs (10). Selective destruction of SSc fibroblasts which chronically produce high levels of intracellular ROS by DPTTS explain decrease serum level of AOPP and of oxidized DNA topoisomerase I. Therefore, DPTTS could stop the induction of auto-immune reaction by the selective and early destruction of diseased fibroblasts.

Smad2 and Smad3 are transcription factors that are overexpressed in human SSc fibroblasts as well as in fibroblasts from HOCl-mice. Phosphorylated Smad2/3 activate genes coding for type I collagen which lead to fibrosis in several organs (19, 20). In vivo administration of DPTTS down-regulates the phosphorylation of Smad2/3 and contributes to decrease the accumulation of type I collagen in the skin of mice with HOCl-induced SSc compared to untreated HOCl mice. In addition, TGF $\beta$  which induced Smad2/3 phosphorylation is inhibited by a thiol antioxidant-NAC, GSH, and L-cysteine, which highlight the role of ROS in the activation of the Smad2/3 pathway (21). Therefore, in HOCl induced SSc in the mice, the selective deletion of fibroblast overexpressing ROS by DPTTS treatment decreased the number of cells with high phosphorylation levels of Smad2/3.

Another feature in SSc patients is an abnormal activation of immune cells, including T and B cells, infiltration of inflammatory cells, especially CD4<sup>+</sup> T cells in the skin and in the lungs along with increased levels of various pro-inflammatory and pro-fibrotic cytokines (6, 22). In vivo administration of DPTTS has an immunoregulatory effect in HOCl mice-induced SSc. Indeed, DPTTS significantly limits the expansion of B cells, reduction of the hyper-proliferation of CD3/CD28-activated T cells and the proliferation of LPS-activated B cells in HOCl treated mice. The role of onion-derived organosulfur on leukocytes has been the matter of controversies. Some reports describe their immunostimulatory properties (23) while other highlighted their cytotoxic effects on lymphocytes (24). However, both reports describes that organosulfur induce ROS production on organosulfur-exposed leukocytes (25). In our hand, the immunomodulating properties could be related to the high level of endogeneous ROS produced by activated autoreactive B and T cells that combines to the organosulfur-induced oxidative burst to inhibits lymphocytes proliferation as already described for treatment of SSc mice with the chemotherapeutic and pro-oxidative drug arsenic trioxide (26). The immunomodulatory properties of DPTTS are associated with the decreased in the splenic production of IL-4 and IL-13. The decrease level of those closely linked pro-fibrotic cytokines, elevated in the skin and in the serum of human and mouse SSc (22, 27), can, at least in part, explained the DPTTS anti-fibrotic effects observed in SSc mice.

Altogether, organosulfur compounds (OSCs), ubiquitous in *Allium* plants, are natural compounds with various health beneficial properties (7, 8). We demonstrate that organosulfur DPTTS can combine with endogenous oxidative species generated by SSc fibroblasts to selectively kill them by apoptotic process. This observation suggest that natural organosulfur compound could be used as a safe treatment of systemic sclerosis.

## **AUTHOR CONTRIBUTIONS**

Study conception and design. Marut, Janvier, Winyard, Eggleton, Weill, Batteux.

Acquisition of data. Marut, Janvier, Nicco, Chéreau, Winyard, Egglton, Weill, Batteux.

Analysis and interpretation of data. Marut, Janvier, Winyard, Eggleton, Weill, Batteux.

## REFERENCE

1. LeRoy EC, Medsger TA, Jr. Criteria for the classification of early systemic sclerosis. *The Journal of rheumatology*. 2001;28(7):1573-6.
2. Herrick AL, Worthington J. Genetic epidemiology: systemic sclerosis. *Arthritis research*. 2002;4(3):165-8.
3. Simonini G, Cerinic MM, Generini S, Zoppi M, Anichini M, Cesaretti C, et al. Oxidative stress in Systemic Sclerosis. *Molecular and cellular biochemistry*. 1999;196(1-2):85-91.
4. Sambo P, Baroni SS, Luchetti M, Paroncini P, Dusi S, Orlandini G, et al. Oxidative stress in scleroderma: maintenance of scleroderma fibroblast phenotype by the constitutive up-regulation of reactive oxygen species generation through the NADPH oxidase complex pathway. *Arthritis and rheumatism*. 2001;44(11):2653-64.
5. Lafyatis R, York M. Innate immunity and inflammation in systemic sclerosis. *Current opinion in rheumatology*. 2009;21(6):617-22.
6. Sato S, Fujimoto M, Hasegawa M, Takehara K. Altered blood B lymphocyte homeostasis in systemic sclerosis: expanded naive B cells and diminished but activated memory B cells. *Arthritis and rheumatism*. 2004;50(6):1918-27.
7. Groschel B, Bushman F. Cell cycle arrest in G2/M promotes early steps of infection by human immunodeficiency virus. *Journal of virology*. 2005;79(9):5695-704.
8. Kelkel M, Cerella C, Mack F, Schneider T, Jacob C, Schumacher M, et al. ROS-independent JNK activation and multisite phosphorylation of Bcl-2 link diallyl tetrasulfide-induced mitotic arrest to apoptosis. *Carcinogenesis*. 2012.
9. Busch C, Jacob C, Anwar A, Burkholz T, Aicha Ba L, Cerella C, et al. Diallylpolysulfides induce growth arrest and apoptosis. *International journal of oncology*. 2010;36(3):743-9.
10. Servettaz A, Goulvestre C, Kavian N, Nicco C, Guilpain P, Chereau C, et al. Selective oxidation of DNA topoisomerase 1 induces systemic sclerosis in the mouse. *J Immunol*. 2009;182(9):5855-64.
11. Lawson LD, Wang ZJ, Hughes BG. Identification and HPLC quantitation of the sulfides and dialk(en)yl thiosulfinates in commercial garlic products. *Planta Med*. 1991;57(4):363-70.

12. Burdick MD, Murray LA, Keane MP, Xue YY, Zisman DA, Belperio JA, et al. CXCL11 attenuates bleomycin-induced pulmonary fibrosis via inhibition of vascular remodeling. *Am J Respir Crit Care Med.* 2005;171:261–8.
13. Sue RD, Belperio JA, Burdick MD, Murray LA, Xue YY, Dy MC, et al. CXCR2 is critical to hyperoxia-induced lung injury. *J Immunol.* 2004;172:3860–8.
14. Herrick AL, Matucci Cerinic M. The emerging problem of oxidative stress and the role of antioxidants in systemic sclerosis. *Clinical and experimental rheumatology.* 2001;19(1):4-8.
15. Casella S, Leonardi M, Melai B, Fratini F, Pistelli L. The Role of Diallyl Sulfides and Dipropyl Sulfides in the In Vitro Antimicrobial Activity of the Essential Oil of Garlic, *Allium sativum* L., and Leek, *Allium porrum* L. *Phytotherapy research : PTR.* 2012.
16. Hosono T, Fukao T, Ogihara J, Ito Y, Shiba H, Seki T, et al. Diallyl trisulfide suppresses the proliferation and induces apoptosis of human colon cancer cells through oxidative modification of beta-tubulin. *The Journal of biological chemistry.* 2005;280(50):41487-93.
17. Marut WK, Kavian N, Servettaz A, Nicco C, Ba LA, Doering M, et al. The Organotelluride Catalyst (PHTE)(2)NQ Prevents HOCl-Induced Systemic Sclerosis in Mouse. *The Journal of investigative dermatology.* 2012.
18. Kavian N, Marut W, Servettaz A, Nicco C, Chereau C, Lemarechal H, et al. ROS-mediated killing of activated fibroblasts by arsenic trioxide ameliorates fibrosis in a murine model of SSc. *Arthritis and rheumatism.* 2012.
19. Takagi K, Kawaguchi Y, Kawamoto M, Ota Y, Tochimoto A, Gono T, et al. Activation of the activin A-ALK-Smad pathway in systemic sclerosis. *Journal of autoimmunity.* 2011;36(3-4):181-8.
20. Asano Y, Ihn H, Yamane K, Kubo M, Tamaki K. Impaired Smad7-Smurf-mediated negative regulation of TGF-beta signaling in scleroderma fibroblasts. *The Journal of clinical investigation.* 2004;113(2):253-64.
21. Li WQ, Qureshi HY, Liacini A, Dehnade F, Zafarullah M. Transforming growth factor Beta1 induction of tissue inhibitor of metalloproteinases 3 in articular chondrocytes is mediated by reactive oxygen species. *Free radical biology & medicine.* 2004;37(2):196-207.
22. Needleman BW, Wigley FM, Stair RW. Interleukin-1, interleukin-2, interleukin-4, interleukin-6, tumor necrosis factor alpha, and interferon-gamma levels in sera from patients with scleroderma. *Arthritis and rheumatism.* 1992;35(1):67-72.
23. Lau BH, Yamasaki T, Gridley DS. Garlic compounds modulate macrophage and T-lymphocyte functions. *Molecular biotherapy.* 1991;3(2):103-7.
24. Nakamura Y, Miyoshi N. Cell death induction by isothiocyanates and their underlying molecular mechanisms. *Biofactors.* 2006;26(2):123-34.
25. Zhang G, Wu H, Zhu B, Shimoishi Y, Nakamura Y, Murata Y. Effect of dimethyl sulfides on the induction of apoptosis in human leukemia Jurkat cells and HL-60 cells. *Bioscience, biotechnology, and biochemistry.* 2008;72(11):2966-72.

26. Kavian N, Marut W, Servettaz A, Laude H, Nicco C, Chereau C, et al. Arsenic trioxide prevents murine sclerodermatous graft-versus-host disease. *J Immunol.* 2012;188(10):5142-9.

27. Hasegawa M, Fujimoto M, Kikuchi K, Takehara K. Elevated serum levels of interleukin 4 (IL-4), IL-10, and IL-13 in patients with systemic sclerosis. *The Journal of rheumatology.* 1997;24(2):328-32.

## LEGENDS TO FIGURES

### Figure 1.

Effect of DPTTS on normal and diseased fibroblasts *in vitro*. Primary control- and SSc-fibroblasts were seeded in a 96-wells plate and exposed to various doses of DPTTS (10-40  $\mu$ M) or medium alone for 48 hours at 37°C. **A.** Proliferation of normal and SSc fibroblasts incubated with DPTTS. Cellular proliferation was measured by thymidine incorporation. **B.** Cytotoxic effects of DPTTS on normal and diseased SSc fibroblasts. Viability of fibroblasts were assessed by crystal violet assay. **C.** Production of reactive oxygen species levels were analyzed spectrofluorimetrically using H<sub>2</sub>DCFDA. **D.** Intracellular glutathione levels were analyzed spectrofluorimetrically using monochlorobimane. **E, F.** Primary control and SS fibroblasts (3 mice per group) were seeded in a 96-well plate in triplicate (2x10<sup>4</sup>/well) with various chemical and enzymatic modulators (NAC, BSO, Catalase, Aminotriazole, DDC) for 12 hours and exposed to DPTTS for 16 hours. Production of H<sub>2</sub>O<sub>2</sub> (**E**) and viability (**F**) were measured on a spectrofluorometer. Results are the means $\pm$ S.E.M. of three independent

experiments. Statistic: : \**P* < 0.05, \*\**P* < 0.01, \*\*\**P* < 0.001.

### Figure 2.

Pro-apoptotic effects of DPTTS analyzed by fluorescence-activated cells sorting. **A.** Normal and diseased fibroblasts were incubated with 40  $\mu$ M of DPTTS for various times

(5 h, 10 h and 15 h). Apoptosis/necrosis was analyzed by flow cytometry using the Membrane Permeability/Dead Cell Apoptosis Kit with YO-PRO-1 and Propidium iodide. Necrotic cells are PI positive and apoptotic cells are YO-PRO-1 positive. One of three representative experiment is shown. **B.** Kinetic apoptosis/necrosis evolution of normal and SSc fibroblasts treated with 40  $\mu$ M of DPTTS.

### **Figure 3.**

*In vivo* effect of DPTTS on skin fibrosis. BALB/c mice were injected intradermally with HOCl every day during 6 weeks and intravenously with DPTTS two times per week (6 mg/kg) (n=8 mice per group). **A.** Dermal thickness measured in the injected area of mice. **B.** Collagen content in the skin was measured by the Sircol method. **C.** Representative tissue sections comparing dermal fibrosis in the injected areas from BALB/c mice by H&E staining, the expression of  $\alpha$ SMA, and pSmad 2/3 in mouse skin by immunohistochemistry. Magnification is  $\times 50$  (Olympus DP70 Controller). **D.** Proliferation of fibroblast from normal control or SSc mice treated or not with DPTTS. Cellular proliferation was measured by thymidine incorporation. Values are means  $\pm$  SEM of data gained from all mice in the experimental or control groups. Statistic: \* $P < 0.05$ , \*\* $P < 0.01$ , \*\*\* $P < 0.001$ .

### **Figure 4.**

*In vivo* effect of DPTTS on lung fibrosis. BALB/c mice were injected intradermally with HOCl every day during 6 weeks and intravenously with DPTTS two times per week (6 mg/kg) (n=8 mice per group). **A:** Collagen content in the lungs was measured by the Sircol method. **B:** Representative lung sections from BALB/c mice. 1: PBS, 2: DPTTS, 3: HOCl, 4: HOCl+DPTTS Tissue sections were stained with H&E. Magnification is  $\times 50$  (Olympus

DP70 Controller). Values are means  $\pm$  SEM of data gained from all mice in the experimental or control groups. Statistic:  $*P < 0.05$ ,  $**P < 0.01$ .

**Figure 5.**

*In vivo* treatment with DPTTS inhibits the production of autoantibodies and exerts beneficial effects on local and systemic oxidative stress in HOCl-mice. **A.** Levels of anti-topoisomerase-1 Ab measured by ELISA. **B.** Serum AOPP levels ( $\mu\text{mol/l}$  of chloramin T equivalents). Values are means  $\pm$  SEM of data gained from all mice in the experimental and control groups. Statistics:  $*P < 0.05$ ,  $***P < 0.001$ .

**Figure 6.**

DPTTS exerts immunomodulating properties in mice with SSc. **A.** Splenic B cell numbers, as assessed by flow cytometry (millions of cells). **B.** Proliferation of splenic T cells activated by anti-CD3/CD28. **C.** Proliferation of splenic B cells activated by LPS. The level of IL-4 (**D**) and IL-13 (**E**) in supernatants of ConA activated splenic T cells. Values are means  $\pm$  SEM of data gained from all mice in the experimental and control groups. Statistics:  $*P < 0.05$ ,  $**P < 0.01$ ,  $***P < 0.001$ .

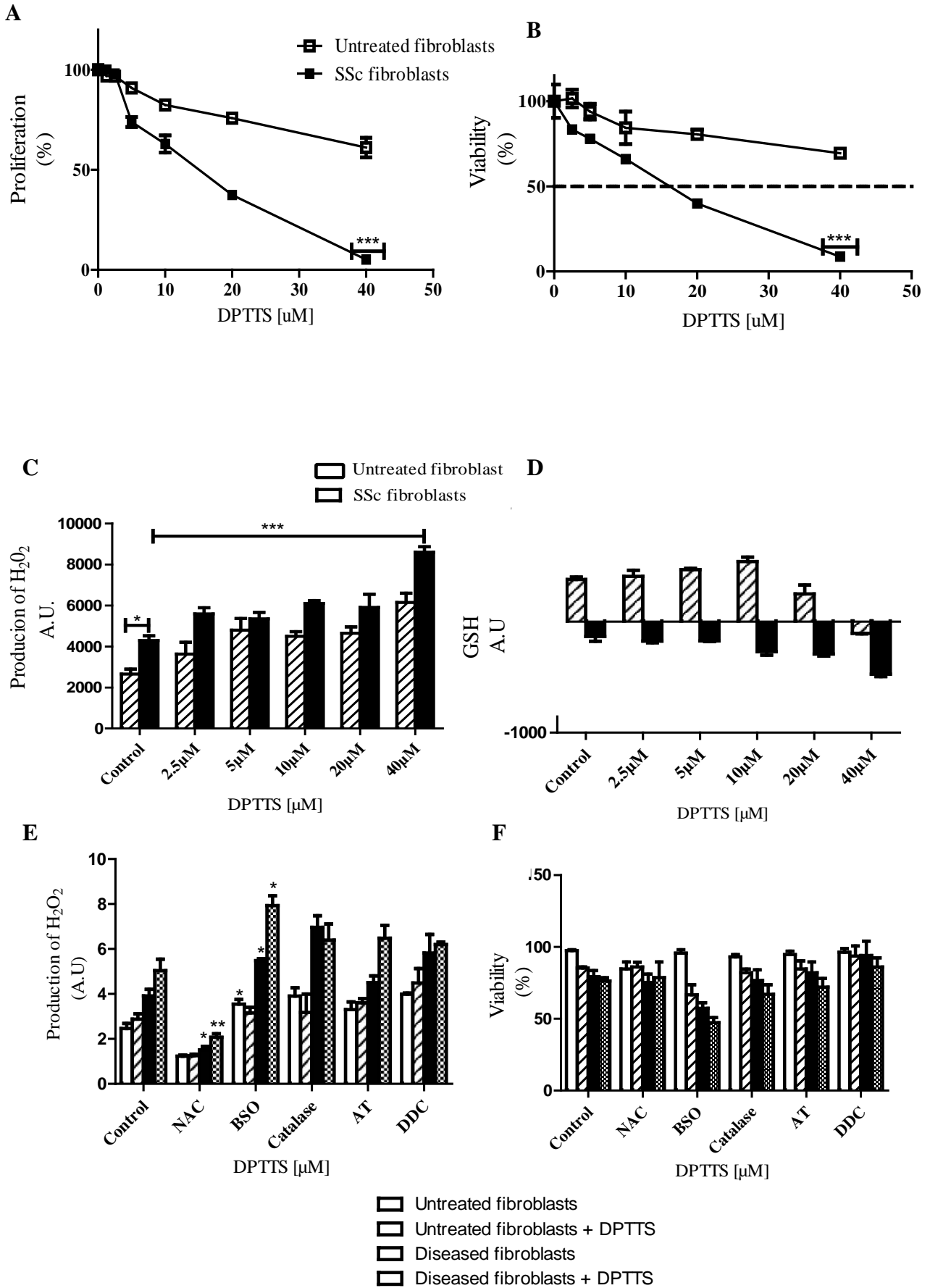
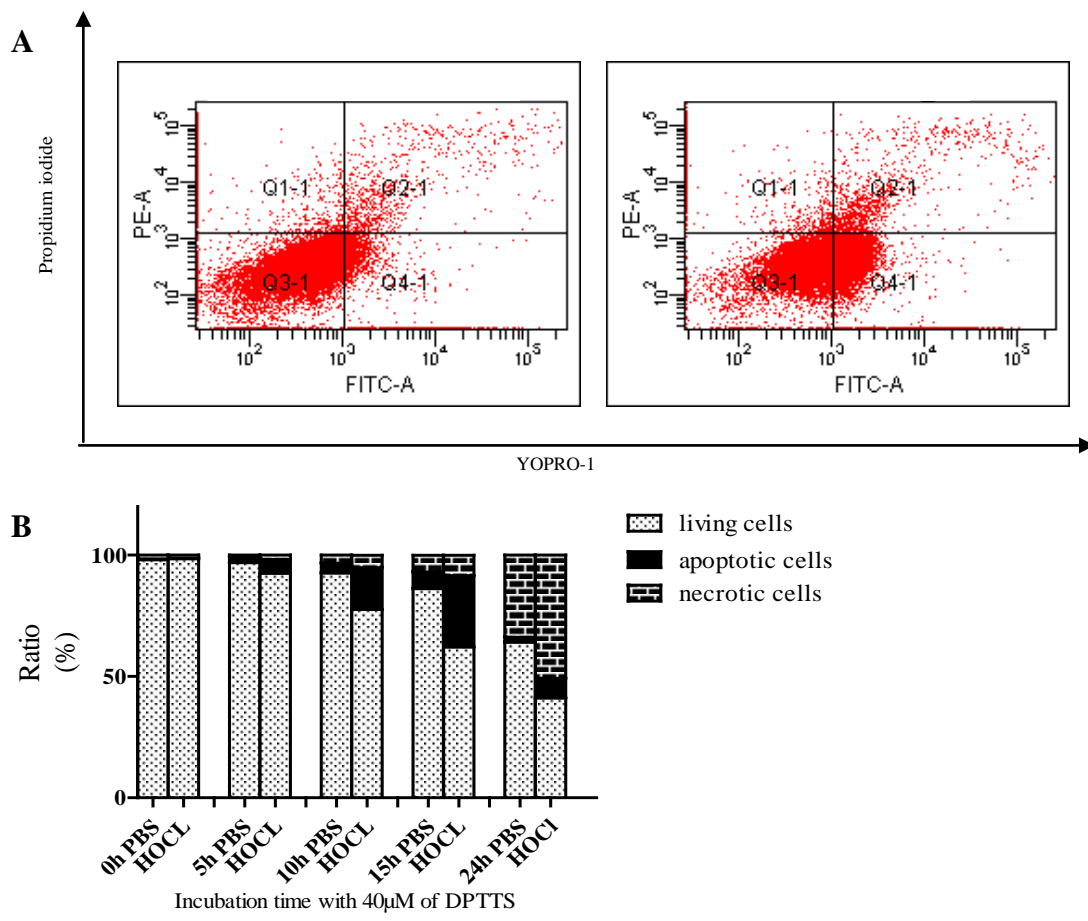
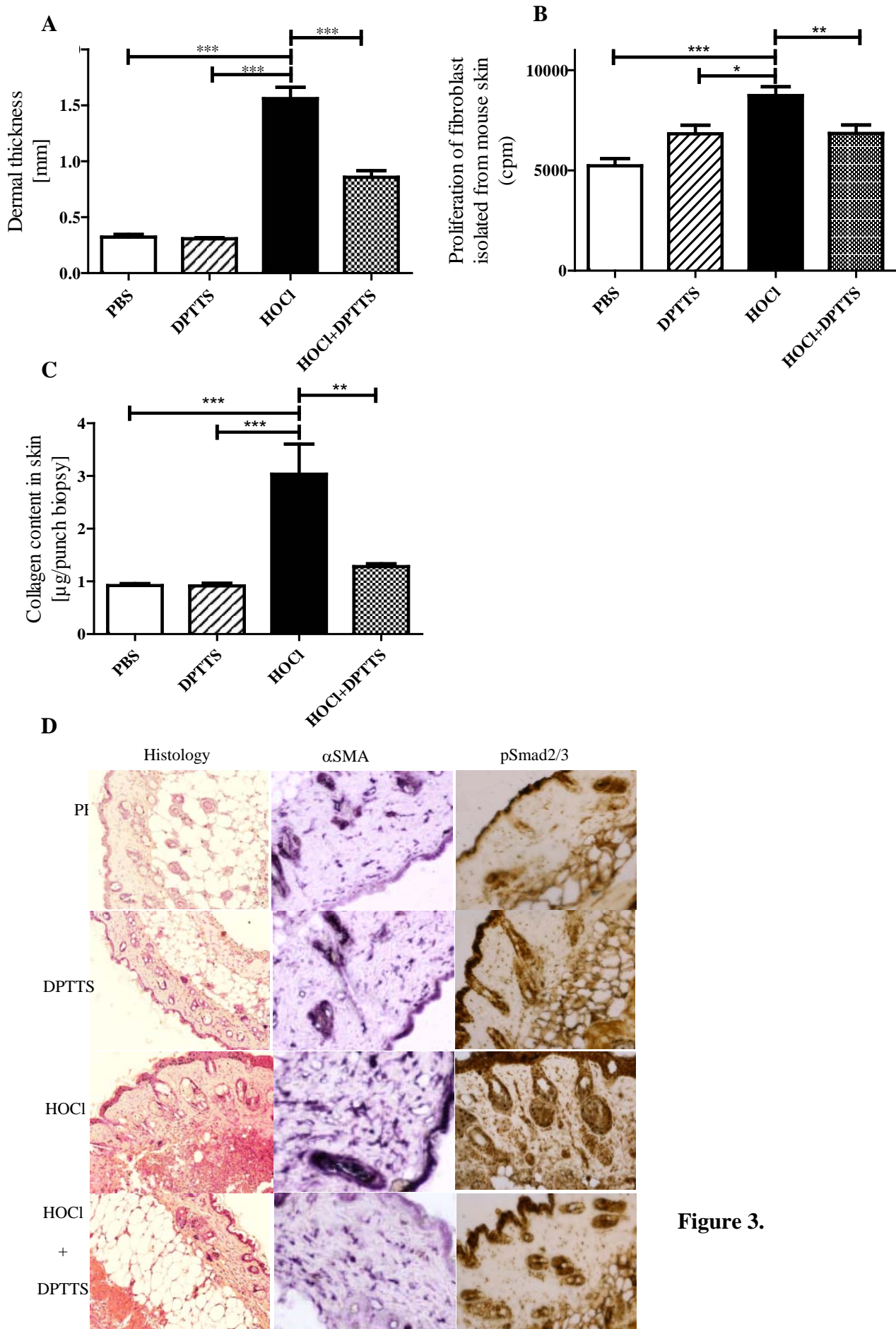


Figure1.



**Figure 2.**



**Figure 3.**

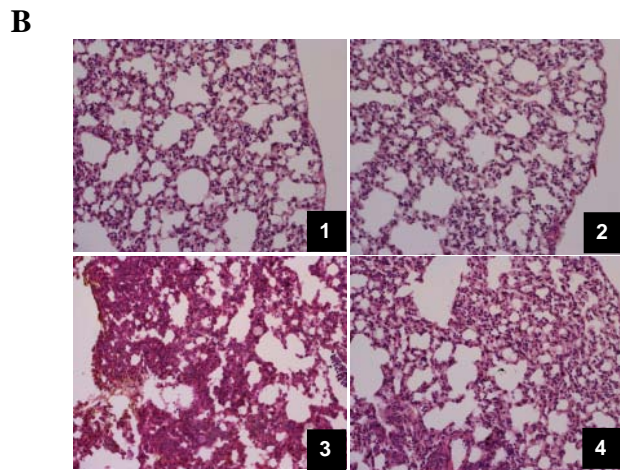
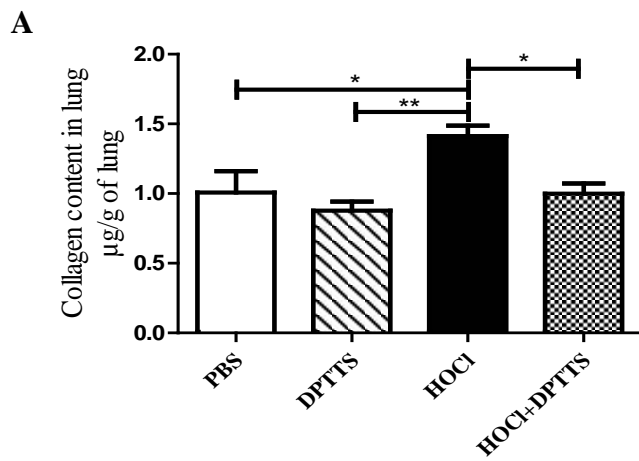


**Figure 4.**

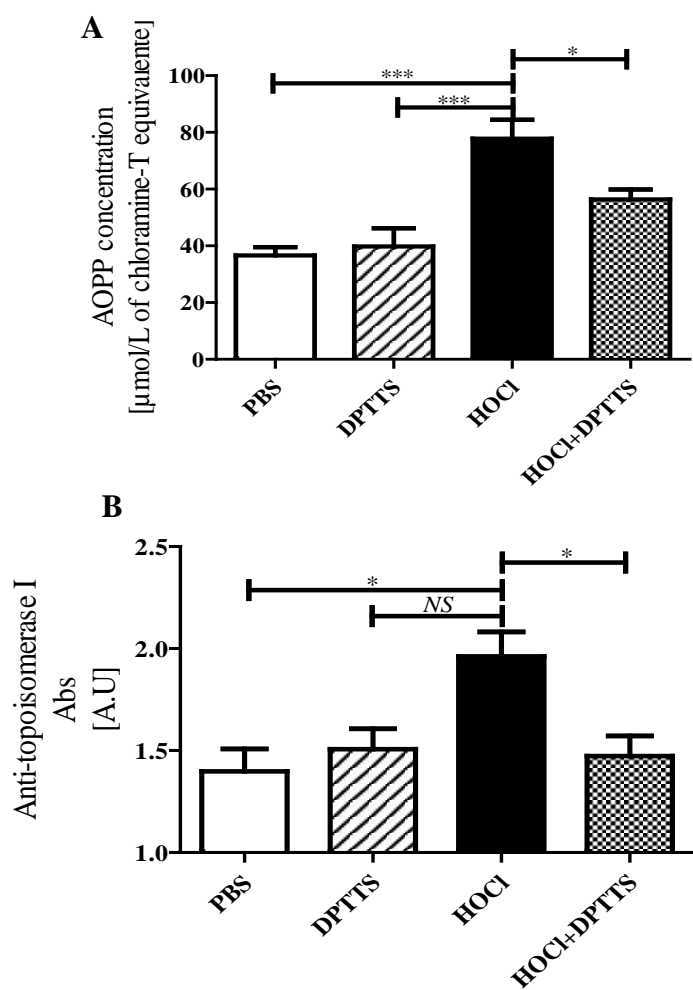


**Figure 5.**

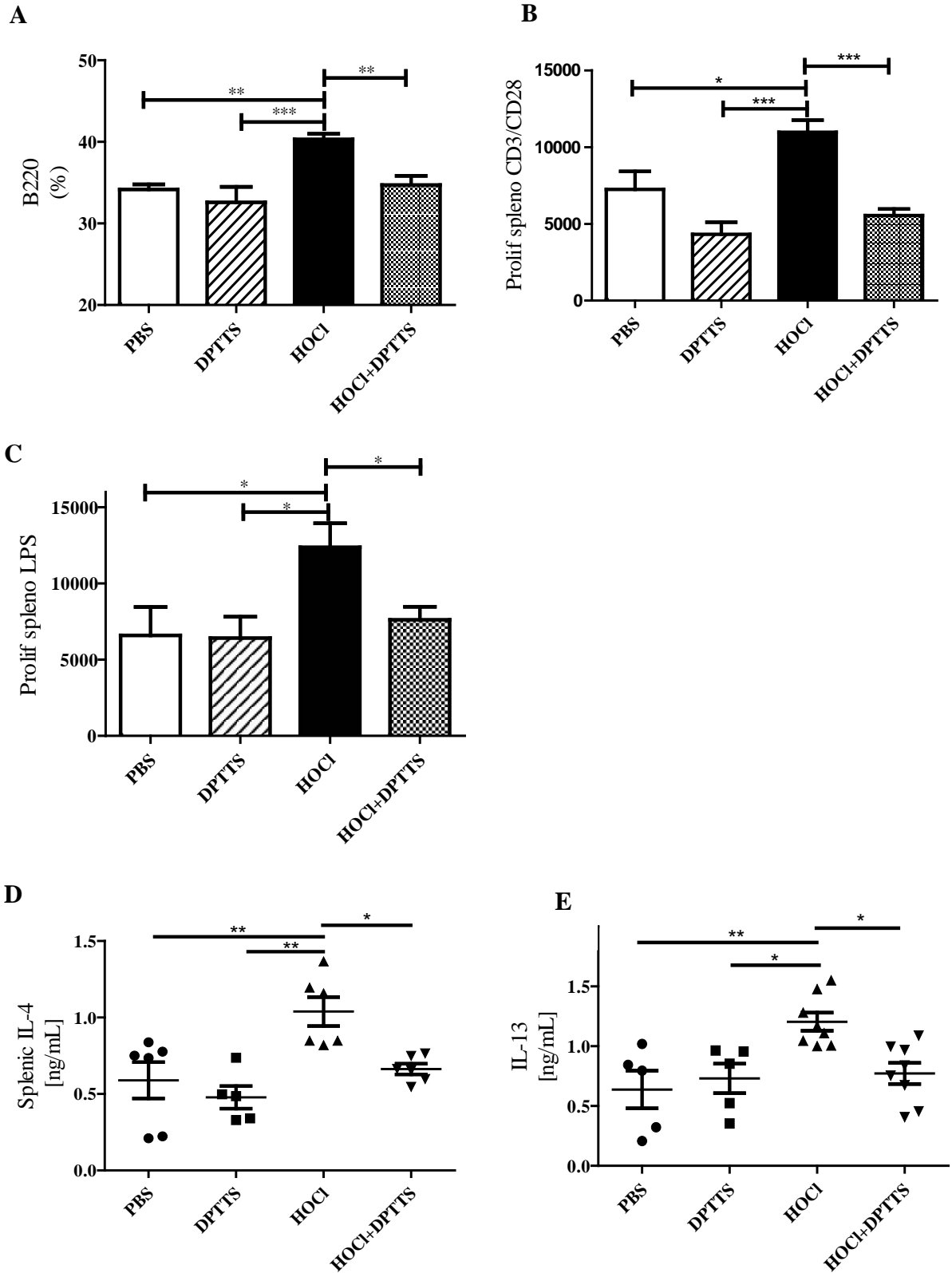


**Figure 6.**

### **III.3 Article 3**

## **Angiotensin II receptor blockade ameliorates systemic fibrosis in the mouse**

Wioleta Marut<sup>1\*</sup>, Niloufar Kaviani<sup>1\*</sup>, Amélie Servettaz<sup>1,2</sup>, Thong Hua-Huy<sup>3</sup>  
Carole Nicco<sup>1</sup>, Christiane Chéreau<sup>1</sup>, Bernard Weill<sup>1</sup>, Anh Tuan Dinh-Xuan<sup>3</sup>  
Frédéric Batteux<sup>1</sup>.

*Arthritis & Rheumatism, 2012 (Accepted)*

In this article, we have investigated the role of Angiotensin II in the mouse model of SSc. Angiotensin II, type I (AT<sub>1</sub>) is the main peptide of the renin angiotensin system (RAS). This molecule is involved in the pathogenesis of fibrotic disease by promoting fibrosis, proliferation, inflammation, and synthesis of nitric oxide. Further, angiotensin II activates Smad pathway which leads to expression of genes related to fibrosis [210]. AT<sub>1</sub> can induce the production of NO by various cells including fibroblasts and endothelial cells. In SSc patients, NO metabolism is distracted through overproduction of NO which can react with superoxide anions (O<sub>2</sub><sup>-</sup>) to form highly toxic peroxynitrite (ONOO<sup>-</sup>) [199, 211]. Constitutive overproduction of NO may contribute to vascular damage, increase fibroblasts proliferation and synthesis of type I collagen. As a consequence of this nitrostatic burst, SSc patients have increased level of nitrate and increased expression of the amino acid nitrosylated 3-nitrotyrosine (3-NT) in diseased tissue.

The antifibrotic effect of Irbesartan, an angiotensin II receptor antagonist, was evaluated in a mouse model of SSc induced by intradermal injection of hypochlorous acid in BALB/c

mice. Irbesartan significantly reduced dermal thickness and collagen concentration in the skin and lung of SSc mice compared to control mice. Moreover, *in vivo* administration of irbesartan displayed inhibition of exhaled nitric oxide, nitrates, E-selectin in the serum, and decreased expression of 3-NT in the skin and lung of HOCl mice, which contribute to the reduction of the nitrosative stress. In SSc, dysimmunity with the production of autoantibodies is a key feature of SSc. Irbesartan exerts an immuno-regulating effect in HOCl mice, reflected by the reduction in B cells, CD4 and CD8 T cell numbers in the spleens of SSc mice, and in the decrease in serum anti-DNA-topoisomerase-1Ab levels. In addition, irbesartan reduces the hyper-proliferation of CD3/CD28-activated T cells and the proliferation of LPS-activated B cells observed in HOCl-mice. AT<sub>1</sub> antagonist downregulate H-Ras which is a critical controller of T helper cell responses mostly by transmitting TCR signals that prime CD4 (+) T cells and trigger activation of B cell.

Previous study has connected skin fibrosis in SSc with stabilization of H-RAS oncogene and showed that its increase levels can directly stimulate phosphorylation of Smad2/3 and lead to the accumulation of collagen I. AT<sub>1</sub> receptor antagonist significantly reduces expression of phosphorylated Smad2 and 3 in the skin of SSc mice [212]. Our results are in agreement with a recent study showing that angiotensin II activates Smad signalling through the AT<sub>1</sub> receptor-mediated ERK1/2 MAPK pathway [210].

Our work highlights the important role of angiotensin II in the induction of fibrosis, autoimmunity, and vascular abnormalities in SSc. Our results suggest that AT<sub>1</sub> receptor antagonist could be tested as new therapeutic tools in SSc.

## **Angiotensin II receptor blockade ameliorates systemic fibrosis in the mouse**

Wioleta Marut<sup>1\*</sup>, Niloufar Kavian<sup>1\*</sup>, Amélie Servettaz<sup>1,2</sup>, Thong Hua-Huy<sup>3</sup>  
Carole Nicco<sup>1</sup>, Christiane Chéreau<sup>1</sup>, Bernard Weill<sup>1</sup>, Anh Tuan Dinh-Xuan<sup>3</sup>  
Frédéric Batteux<sup>1</sup>.

<sup>1</sup> Université Paris Descartes, Faculté de Médecine, EA 1833 et Laboratoire d'immunologie biologique, Hôpital Cochin, AP-HP, 75679 Paris cedex 14, France.

<sup>2</sup> Faculté de Médecine de Reims, Service de Médecine Interne, Maladies Infectieuses, Immunologie Clinique, Hôpital Robert Debré, 51092 Reims cedex, France.

<sup>3</sup> Département de Physiologie, Université Paris Descartes, Faculté de Médecine, Hôpital Cochin, AP-HP, 75679 Paris cedex 14, France.

This work was supported by European Community's Seventh Framework Programme (FP7/2007-2013) under grant agreement 215009 RedCat for financial support.

\* Equal contribution

Address correspondence to: Dr. Frédéric Batteux, Laboratoire d'Immunologie, EA

1833, 8 rue Méchain 75679 Paris cedex 14, France. Tel: +33 (0) 1.58.41.20.09; Fax: +33 (0) 1.58.41.20.08; e-mail: frederic.batteux@cch.aphp.fr

Key words: angiotensin II; irbesartan; fibrosis; systemic sclerosis; reactive oxygen species; nitric oxide.

## **ABSTRACT**

**Objective.** Systemic sclerosis (SSc) is characterized by microvascular damages, fibrosis of skin and visceral organs, and autoimmunity. Previous studies have shown that angiotensin II is involved in the synthesis of type I collagen. We investigated whether the blockade of angiotensin II receptor type-I (AT<sub>1</sub>R) by irbesartan reduces skin and lung fibrosis in two murine models of systemic systemic.

**Methods.** SSc was induced by daily intradermal injection of hypochlorous acid (HOCl) in the back of BALB/c mice (HOCl-SSc). Mice were treated daily with irbesartan by oral gavage.

**Results.** Irbesartan reduced dermal thickness, collagen concentration, smad 2/3 and  $\alpha$ SMA expression as well as fibroblast proliferation and H-Ras expression in the skin of HOCl-SSc mice that displayed less lung fibrosis, less inflammation, and a lower concentration of collagen in the lung than non treated mice. Exhaled nitric oxide, iNOS and 3-nitrosotyrosine expression in the lung were decreased following irbesartan. Moreover, irbesartan reduced the number and the proliferation of splenic B and T-cells, and the serum levels of anti-DNA-topoisomerase-1 autoantibodies.

**Conclusions.** Irbesartan, an AT<sub>1</sub>R antagonist, prevents fibrosis, inflammation and inhibits nitric oxide production in HOCl induced models of systemic fibrosis. This report extends the indication of an AT<sub>1</sub>R antagonist to SSc patients with diffuse fibrosis, especially those with lung involvement.

Systemic sclerosis (SSc) is a connective tissue disorder characterized by vascular alterations, extensive fibrosis and immunological dysregulations associated with specific autoantibodies (AABs). The involvement of visceral organs determines the prognosis of the disease. Despite progresses in the treatment of some visceral complications, no treatment has been designed to date that can cure SSc, in part because the mechanisms underlying the disease remain unclear.

On one hand, the vascular dysfunction in SSc triggers the sclerosis of skin and visceral organs (1). On the other hand, vascular complications often determine the rate of survival and the quality of life of patients (2). The levels of angiotensin II (AT) and its type 1 receptor AT<sub>1</sub>R are elevated in SSc (3) and could be pivotal in the development of the disease. This hypothesis has been strengthened by the observation that angiotensin II injected into the back of mice induces skin fibrosis (7). Moreover, angiotensinogen, the precursor of angiotensin II, synthesized in the liver upon inflammation (4) is also produced by fibroblasts and myofibroblasts through a ROS- (5) or a TGFβ1-mediated mechanism (6). Blockers of AT<sub>1</sub>R reduce the mortality linked to renal crisis and alleviate the vascular manifestations of SSc in addition to inducing vasodilation (7, 8). Therefore, AT which is the main peptide of the renin-angiotensin system (RAS), could be implicated in the pathophysiology of SSc with its functionally pleiotropic AT<sub>1</sub>R (9). AT is involved in the pathogenesis of fibrotic diseases by promoting vasoconstriction, cell proliferation, fibrosis, inflammation, and production of nitric oxide (10-14). Angiotensin II activates an early Smad signaling via the AT<sub>1</sub> receptor-mediated ERK1/2 MAPK pathway, leading to the accumulation of type I collagen (15).

The stimulation of AT<sub>1</sub>R by agonistic autoantibodies has been observed in severe vasculopathies associated with allograft rejection and pre-eclampsia (16, 17). In SSc, those

autoantibodies are associated with a high risk for the diffuse form of the disease and for the development of pulmonary hypertension, lung fibrosis, digital ulcers, and a higher rate of death related to these complications (7). Among the pathways engaged by the stimulation of AT<sub>1</sub>R, the regulation of the oxidative/nitrosative stress plays a key role (18). Particularly, AT and anti-AT<sub>1</sub>R agonistic autoantibodies can induce the production of nitric oxide (NO) that controls the vascular tone. In SSc, NO is overproduced and combines with reactive oxygen species to form the highly cytotoxic peroxynitrite (ONOO<sup>-</sup>) that contributes to inflammation, fibrosis and endothelial cell apoptosis (19, 20).

Those observations have prompted us to test irbesartan, an AT<sub>1</sub>R antagonist (AT<sub>1</sub>RA) used in the treatment of sclerodermal renal crisis (21), in the mouse model of systemic sclerosis induced by intradermal injections of HOCl that produces skin and lung fibrosis, vascular dysfunction and auto-immunity.

## **MATERIALS AND METHODS**

**Animals, cells and chemicals.** Six week-old female BALB/c mice were used in all experiments (Harlan, Gannat, France). Animals received humane care according to the guidelines of our institution. All mice were housed in autoclaved ventilated cages with sterile food and water ad libitum. All cells were cultured as reported previously (22). All chemicals were supplied from Sigma-Aldrich (Evry, France) except for irbesartan - Aprovel® (Sanofi-Aventis, Le Plessis Robinson, France).

**Experimental design.** Diffuse SSc was induced according to the protocol of Servettaz et al with minor modifications (23). Four hundred microliters (two injections of 200 µL) of a solution generating HOCl were prepared extemporaneously and injected intra-dermally into the shaved back of the mice, using a 27 gauge needle, everyday for 6 weeks (HOCl-

mice). HOCl was produced by adding NaClO solution (9.6 % as active chlorine) to KH<sub>2</sub>PO<sub>4</sub> solution (100 mM, pH 6.2) (24). HOCl concentration was determined by measuring the optical density of the solution at 292 nm, and then adjusted to obtain an OD between 0.7 and 0.9. Control groups received injections of 400 µl sterilized PBS (PBS-mice). Irbesartan was administered by oral gavage (50 mg/kg/day) 5 days per week during 6 weeks (n=8 mice per group). Dermal thickness was measured one day before sacrifice with a calliper and expressed in millimeters. The animals were sacrificed by cervical dislocation. Serum and tissue samples were collected from each animal and stored at – 80°C until used, or fixed in 10% acetic acid formol for histopathological analysis. In another set of experiments, limited SSc was induced by the injection of a solution generating peroxynitrites (ONOO-) (19) and irbesartan was administered as above.

**Histopathological analysis.** Fixed skin and lung pieces were embedded in paraffin. A 5-µm-thick tissue section was prepared from the mid-portion of the paraffin-embedded tissue and stained with hematoxylin eosin and with picro-sirius red for lung section.

**Collagen content in lung and skin.** Skin taken from the site of injection with a punch (6 mm of diameter) and lung pieces were diced using a sharp scalpel, put into aseptic tubes, and were then thawed and mixed with pepsin (1:10 weight ratio) and 0.5 M acetic acid. Collagen content was assayed using the quantitative dye-binding Sircol method (Biocolor, Belfast, N. Ireland) (25, 26).

**Isolation of skin fibroblasts, rate of proliferation and viability.** Primary fibroblasts were isolated from the skin of all mice (n=31) as previously described (27). Cell proliferation was determined by [<sup>3</sup>H]thymidine incorporation (27) and cell viability by the crystal violet assay as previously described (28).

**Flow cytometric analysis of splenocytes.** Spleen cells were isolated by disruption of spleens and erythrocytes lysed by hypotonic shock in a potassium acetate solution. Cells ( $1 \times 10^6$ ) were then incubated with the following antibodies diluted 1:200 for 30 min at 4°C: anti-B220-PE, anti-CD4-APC-Cy7, or anti-CD8-PE-Cy7 mAb (BD Pharmingen, Franklin, NJ). Spleen cell suspensions were subjected to three-color analysis on a FACSCanto II flow cytometer (BD Biosciences). All data were analyzed using Flow-Jo software (Tree Star, Ashland, USA).

**Spleen cell proliferation.** Spleen cell suspensions were prepared after hypotonic lysis of erythrocytes. Cells were cultured in RPMI 1640 supplemented with 10% heat-inactivated FCS (Invitrogen Life Technologies) as a complete medium. B and T cells were purified from splenocytes by MACS. The proliferation assay was conducted in 96-well flat-bottom plates. Briefly, splenic B or T cell suspensions ( $2 \times 10^5$  cells) were cultured in complete medium for 48 hrs in the presence of 10  $\mu$ g/ml LPS (Boehringer, Mannheim) for B cells, or with precoated anti-CD3 mAb (2.5  $\mu$ g/ml) for T cells. Cell proliferation was determined by pulsing the cells with [3H]thymidine (1  $\mu$ Ci/well) during the last 16 hrs of culture and by measuring the radioactivity incorporated by liquid scintillation counting.

**Western blot analysis of AT<sub>1</sub>R,  $\alpha$ SMA, 3-Nitrotyrosine (3-NT), iNOS and H-Ras proteins in the skin and lungs from mice and in activated splenocytes and HPMEC cells.**

Skin and lung samples taken from the injection sites of each mouse were incubated with 250  $\mu$ l of RIPA. Splenocytes were in vitro stimulated or not with LPS (10  $\mu$ g/ml) or with CD3/CD28 (2.5  $\mu$ g/ml) for 48 hours. HPMEC were stimulated with 5 ng/ml mouse TNF $\alpha$ (R&D) for 48 hours. HPMEC and splenocytes were treated with or without 20 and 40  $\mu$ M of irbesartan (Sigma-Aldrich, France). Then, cells were washed three times, then

incubated with 50  $\mu$ l of RIPA. Protein extracts (30  $\mu$ g total protein) were resolved by 10% SDS-PAGE and were blotted to PVDF membranes. Blots were blocked with 5% milk, and incubated with 1:500 mouse polyclonal anti-AGT<sub>1</sub>R (mouse skin, Sigma-Aldrich, France), 1:500 mouse monoclonal alpha-SMA (mouse skin, Sigma-Aldrich, France), 1:200 mouse monoclonal anti-nitrotyrosine (mouse skin, clone 1A6, Cell Signaling Technology, USA), 1:200 rabbit polyclonal anti-H-Ras Ab (mouse skin, lung and activated splenocytes, Santa Cruz Biotechnology, France), and 1:50.000 mouse anti- $\beta$ -actin mAb (Sigma-Aldrich, France), overnight at 4°C. Signals were developed using 1:1000 goat anti-mouse or goat anti-rabbit HRP-conjugated secondary antibody (Santa-Cruz Biotechnology, Paris, France). Immunoreactivities were revealed using ECL (Amersham) and densitometric analysis performed using ImageJ software (1.36 version). Results are expressed as arbitrary units defined as the densitometric intensity of the bands of the proteins tested divided by the densitometric intensity of the same bands labelled with mouse anti- $\beta$ -actin mAb.

**Immunohistochemistry of phospho-Smad2/3, angiotensin II, phospho-EGFR, and iNOS.** Five micrometer-thick sections were placed onto slides, deparaffinized and then rehydrated. Antigen retrieval was performed by incubating the sections with proteinase K (Dako, France) for 20 min in 37°C for phospho-Smad2/3, angiotensin II, phospho-EGFR, and with citrate buffer for iNOS. Sections were then treated with 3% H<sub>2</sub>O<sub>2</sub> for a period of 15 min in order to block endogenous peroxidase, and incubated in 5% bovine serum albumin for 30 min to block non-specific binding. Furthermore, they were incubated with 1:100 monoclonal antibody directed to phospho-Smad2/3 (Cell Signaling Technology, USA), with 1:100 iNOS antibody (Santa Cruz Biotechnology, France) for 2 hrs at room temperature or with 1:50 angiotensin II antibody (Novusbio, England), with 1:50 phospho-EGFR antibody (Sigma-Aldrich, France) overnight at 4°C. Sections were then incubated with HRP-labelled secondary goat anti-rabbit (Rockland, USA) for 1 hour at room

temperature. Irrelevant HRP-conjugated Abs were used as controls. Staining was finally visualized using diaminobenzidine tetrahydrochloride (DAB) as a chromogen. All slides were analyzed by two independent pathologists blinded with regard to the groups. Pictures were taken with a digital camera on a BX60 microscope (Olympus, France), using DP Manager Software, at x100 magnification. Immunostaining was analyzed using ImageJ Software (1.36 version; National Institute of Health) for quantitative assessment of staining positivity. Results are expressed as percents of positive skin area analysed with the ImageJ Software.

**Detection of serum autoantibodies.** Serum anti-DNA topoisomerase-1 IgG Abs were assayed by ELISA using purified calf thymus DNA topoisomerase-1 bound to the wells of a microtiter plate (Immunovision, USA) as previously described (29).

**Determination of IL13.** Splenic T cells purified by MACS ( $2 \times 10^5$  cells/well) were seeded in 96-well flat bottom plates and cultured in complete medium for 48 hrs in the presence of 5  $\mu\text{g/ml}$  concanavalin A. IL13 concentrations from the collected supernatants were measured by ELISA (E-bioscience, San Diego, USA). The concentrations were calculated from a standard curve according to the manufacturer's protocol. Results are expressed in  $\text{pg/ml}$ .

**Quantification of soluble E-selectin and nitrites in mouse sera.** Concentrations of serum sE-selectin were measured by ELISA using the Mouse sE-selectin/sCD62E Duo Set kit (R&D Systems, USA) following the manufacturer's instructions. The concentration of nitrites was determined in sera by a spectrophotometric assay using oxidation catalysed by cadmium metal (Oxis, Bioxytch, USA), which converts nitrates into nitrites (30). The total nitrites determined correspond to NO production. The detection threshold for nitrites was  $0.1 \mu\text{mol/l}$ .

**Cellular Production of H<sub>2</sub>O<sub>2</sub>, NO, and O<sub>2</sub><sup>°</sup>.** Human Pulmonary Microvascular Endothelial Cells (HPMEC, PromoCell, Heidelberg, Germany) (1x10<sup>4</sup> cells per well) were seeded in 96-well plates (Costar) and incubated for 48 hours with various concentrations of irbesartan or with culture medium alone. Levels of H<sub>2</sub>O<sub>2</sub>, NO, and O<sub>2</sub> were assessed spectrofluorometrically (Fusion, PerkinElmer, Wellesley, MA) using 2 - dichlorodihydrofluorescein diacetate (H2DCFDA), diaminofluorescein-2 diacetate (DAF-2DA), and dihydroethidium (DHE) respectively, as previously described (28).

**Exhaled nitric oxide measurement.** The level of nitric oxide exhaled by the mice was measured using a chemiluminescence NO analyzer (Sievers 280 NOATM, Sievers Instruments Inc., Boulder, CO, USA), as previously described (31). The analyzer was connected by 2 unidirectional valves system to a 300ml Plexiglas chamber (Figure 4F). Each mouse was placed in a Plexiglas chamber and allowed to rest for 5 minutes to accommodate with the chamber's environment. The chamber was flushed with NO-free air (Air Liquide, Puteaux, France) via a rodent ventilator (Harvard, USA) set to a flow rate of 800 ml/min (Vt: 5mL; respiratory rate 160/min) until the level of NO concentration reached zero (NO < 0.2 ppb) to set the baseline NO level. The chamber containing the mouse was then closed for 10 minutes during which exhaled NO produced by the mouse accumulated in the airtight chamber. To assess that mice were not exposed to hypoxia and/or hypercapnia, O<sub>2</sub> and CO<sub>2</sub> concentrations were measured in the chamber by an offline method using blood gas analyzer (Radiometer S.A.S., France). The CO<sub>2</sub> fraction was constantly less than 47 mmHg (37.7 ± 3.7) and the O<sub>2</sub> fraction more than 86 mmHg (100.5 ± 6.9) (data from 6 control mice). After 10 minutes, exhaled NO recording was started and continuously maintained for 20 seconds, until a stable plateau of NO was obtained for at least 5 seconds. Values were then recorded to calculate mean value of exhaled NO (ppb). We noted a small range (max – min) of exhaled NO used as an internal

control quality ( $\leq 0.5$  ppb and  $< 10\%$  of the mean). The mean of two measurement values was reported.

**Statistical Analysis.** All quantitative data are expressed as means  $\pm$  SEM. Data were compared using one-way ANOVA plus the Tukey post-hoc multiple-comparisons test for comparisons of means among multiple groups. An unpaired Student t test was used to compare two groups. All analyses were carried out using the GraphPad Prism 5.0 statistical software package, and a p value of less than 0.05 was accepted as statistically significant.

## RESULTS

**Irbesartan reduced skin fibrosis in mice with SSc.** In HOCl-mice, Irbesartan reduced dermal thickness by 60% ( $P < 0.001$ , Figure 1A) and skin collagen content by 20% ( $P < 0.05$ , Figure 1B) versus untreated HOCl-mice. Histopathological analysis confirmed the reduction in skin fibrosis in HOCl-mice (Figure 1C) and in ONOO—mice (Supplemental Figure 7).

Smad 2/3 protein was overexpressed in HOCl-mice versus PBS controls ( $19.52\% \pm 0.77$  positive areas in HOCl mice versus  $5.89\% \pm 0.15$  in PBS mice,  $P < 0.001$ , Figure 1C). Irbesartan reduced Smad 2/3 expression in the skin ( $13.41\% \pm 0.57$  positive areas) of HOCl-mice (versus  $19.57\% \pm 0.77$  in untreated HOCl-mice,  $P < 0.001$ , Figure 1C). The expression of  $\alpha$ Smooth Muscle Actin ( $\alpha$ -SMA) (Figure 1E) in fibrotic skin of HOCl-mice was higher than in PBS mice ( $24.12$  A.U.  $\pm 3.2$  versus  $8.15$  A.U.  $\pm 1.7$ ,  $P < 0.05$ ). Irbesartan downregulated  $\alpha$ -SMA expression by 77% compared to untreated HOCl-mice ( $5.66$  A.U.  $\pm 0.5$  versus  $24.12$  A.U.  $\pm 3.2$ ,  $P < 0.05$ ).

**Irbesartan reduced the expression of angiotensin II, AT<sub>1</sub>R, and phospho-EGFR in HOCl-mice.** The expression of AT (percent of positive areas) was significantly higher in fibrotic skin of HOCl-mice than in PBS mice ( $16.79\% \pm 0.53$  versus  $1.62\% \pm 0.47$ ,  $P < 0.01$ , Figure 1C). Irbesartan decreased AT expression by more than 80% in HOCl-mice ( $16.79\% \pm 0.53$  versus  $2.35\% \pm 1.1$ ,  $P < 0.01$ , Figure 1C). AT<sub>1</sub>R was overexpressed in HOCl-mice versus control PBS mice ( $24.1 \text{ A.U.} \pm 4.8$  versus  $5.8 \text{ A.U.} \pm 0.4$ ,  $P < 0.05$ , Figure 1E). In vivo administration of irbesartan downregulated AT<sub>1</sub>R expression in HOCl-mice ( $7.6 \text{ A.U.} \pm 0.4$  versus  $24.1 \text{ A.U.} \pm 4.8$  versus untreated HOCl-mice,  $P < 0.05$ , Figure 1E). Furthermore, the level of pEGFR was significantly higher in HOCl-mice ( $21.49\% \pm 2.5$ ) than in PBS mice ( $7.3\% \pm 0.66$ ,  $P < 0.01$ , Figure 1C). Irbesartan downregulated the expression of pEGFR in HOCl-treated mice versus untreated HOCl-mice ( $8.39\% \pm 1.05$  versus  $21.49\% \pm 2.5$ ,  $P < 0.01$ , Figure 1C).

**Irbesartan reduced the hyperproliferative phenotype of fibroblasts from the skin of HOCl-mice.** Skin fibroblasts isolated from HOCl-mice displayed a higher proliferation rate than fibroblasts obtained from mice injected with PBS ( $8557 \pm 774.3$  vs  $5218 \pm 536.7$ ,  $P < 0.01$ , Figure 1D). The proliferation rate of fibroblasts isolated from HOCl-mice treated with irbesartan was lower than that of fibroblasts isolated from mice injected only with HOCl ( $5996 \pm 378.7$  vs  $8557 \pm 774.3$ ,  $P < 0.05$ ).

Thus, irbesartan counteracted the hyperproliferative phenotype of HOCl-SSc fibroblasts. Ras GTPases (H-Ras) are activated in SSc skin fibroblasts and play a key role in regulating their proliferation rates (32, 33). By western blot analysis, we found that H-Ras was overexpressed in the skin of HOCl-mice compared to PBS-mice (Figure 1E) ( $28.6 \text{ A.U.} \pm 11$  versus  $3.64 \pm 0.5$ ,  $P < 0.01$ ). In HOCl-mice, H-Ras expression was reduced by 54% in irbesartan-treated mice compared to untreated animals (Figure 1E) ( $13.2 \text{ A.U.} \pm 2.2$  versus  $28.6 \text{ A.U.} \pm 11$ ,  $P < 0.01$ , ).

**Irbesartan reduced lung fibrosis in mice with SSc.** We next evaluated whether irbesartan could alter the systemic spreading of fibrosis in HOCl-mice. Irbesartan significantly reduced collagen content in the lungs ( $P < 0.05$ , Figure 2A) compared to untreated HOCl-mice. Histopathological analysis of lung biopsies stained with hematoxylin & eosin (Figure 2B) or Sirius Red (Figure 2C) confirmed the reduction in lung fibrosis in HOCl-mice treated with Irbesartan. As in the skin, HOCl induced H-Ras expression in the lungs compared to PBS-mice ( $P < 0.001$ , Figure 2D), but H-Ras expression was almost completely abolished in irbesartan-treated animals ( $P < 0.001$ , Figure 2D).

**Irbesartan exerted immunomodulating properties in mice with SSc.** The levels of anti- DNA-topoisomerase I Abs were higher in HOCl-mice than in PBS-mice ( $P < 0.05$ ) and reduced following treatment by irbesartan ( $P < 0.05$  versus HOCl-mice, Figure 3A).

We next tested the effects of irbesartan on splenic cell populations. Subcutaneous injections of HOCl increased the numbers of splenic B cells by 17% ( $P < 0.05$ ), of CD4+ T cells by 21% ( $P < 0.05$ ), and CD8+ T cells by 31% ( $P < 0.05$ ) compared to PBS-mice. Irbesartan decreased the numbers of splenic B cells by 14% ( $P < 0.05$ ), CD4+ T cells by 27% ( $P < 0.01$ ), and CD8+ T cells by 30% ( $P < 0.05$ ) in HOCl-mice versus untreated HOCl-mice (Figure 3B, 3C, 3D).

We also investigated the ex-vivo proliferation rate of splenic T and B cells upon stimulation with coated-anti-CD3 mAb or LPS. B cells isolated from HOCl-mice treated with irbesartan and stimulated with LPS displayed a lower proliferation rate than B cells obtained from untreated HOCl-mice ( $7047 \pm 663$  versus  $9541 \pm 588$ ,  $P < 0.05$ , Figure 3F). T cells isolated from HOCl-mice treated with irbesartan, then stimulated by anti-CD3 mAb, had a lower proliferation rate than T cells obtained from untreated HOCl-mice and

stimulated under the same conditions ( $25277 \pm 1736$  vs  $34181 \pm 1740$ ,  $P < 0.01$ , Figure 3E). H-Ras expression was dose-dependently decreased in anti-CD3 mAb- and in LPS-activated splenocytes incubated with irbesartan compared to untreated activated cells (Figures 3G). Next, we tested the level of IL13 produced by splenic T-cells, since IL13 is involved in the development of fibrosis in HOCl mice. SSc mice had higher serum concentrations of those cytokines than control mice ( $641 \pm 78.2$  versus  $318 \pm 36.3$ ,  $P < 0.01$ ) Irbesartan decreased the level of IL13 in HOCl mice by 40% ( $P < 0.01$ , data not shown).

**Irbesartan decreased the nitrosative stress in HOCl-mice.** HOCl-mice displayed higher levels of serum nitrites, a systemic marker of nitrosative stress, than PBS-mice (2.25-fold increase,  $P < 0.001$ , Figure 4A). Irbesartan reduced those levels by 30% ( $P < 0.05$  versus untreated HOCl-mice, Figure 4A). The tissular level of 3 nitrotyrosine (3NT) is a surrogate marker of the in vivo nitrosative stress (34). 3NT was significantly higher in the skin (8.7-fold increase,  $P < 0.01$ , Figure 4B) and in the lungs (6.05-fold increase,  $P < 0.01$ , Figure 4C) of HOCl-mice than in PBS-mice. In HOCl-mice, Irbesartan reduced the expression of 3NT in the skin (2.4-fold decrease,  $P < 0.05$ , Figure 4B) and in the lungs (2.4-fold decrease,  $P < 0.05$ , Figure 4C) of HOCl-mice. Immunohistochemistry showed that the number of iNOS-positive cells in the lungs was higher in HOCl-mice than in PBS mice ( $6.87 \pm 0.3$  versus  $0.068 \pm 0.009$ ,  $P < 0.001$ , Figure 4D). HOCl-mice treated with irbesartan showed a decreased number of iNOS-positive cells in the lungs ( $1.83 \pm 0.42$  versus  $6.87 \pm 0.3$ ,  $P < 0.001$  versus untreated HOCl-mice, Figure 4D). Exhaled NO is a relevant marker of in vivo lung inflammation and fibrosis in SSc patients (35). As in human, exhaled nitric oxide (NO) was significantly higher in HOCl-mice than in PBS-mice ( $3.22 \pm 0.18$  versus  $1.87 \pm 0.2$ ,  $P < 0.01$ , Figure 4E). Irbesartan significantly reduced the levels of exhaled NO in HOCl-mice ( $2.4 \pm 0.05$  versus  $3.22 \pm 0.18$ ,  $P < 0.05$  versus untreated HOCl-mice, Figure 4E). To gain further insight into the mechanism of inhibition

of NO production by irbesartan, the anti-oxidative effects of irbesartan were tested on Human Pulmonary Microvascular Endothelial Cells (HPMEC) in vitro. Incubation of HPMEC with increasing concentrations of irbesartan dose-dependently decreased the production of NO ( $P < 0.01$ ) (Figure 5A), of  $O_2^{\cdot -}$  ( $P < 0.05$ ) (Figure 5B), and of H<sub>2</sub>O<sub>2</sub> ( $P < 0.001$ ) (Figure 5C), and decreased iNOS expression in TNF- $\alpha$ -stimulated HPMEC (Figure 5D).

#### **Irbesartan decreased serum levels of soluble-E-selectin/sCD62E in HOCl-mice.**

Soluble-E-selectin is a relevant marker of in vivo vascular damages in SSc (36). HOCl-mice displayed higher levels (1.32-fold) of serum s-E-selectin ( $1.56 \pm 0.06$  pg/ml) than PBS-mice ( $1.19 \pm 0.04$  pg/ml,  $P < 0.01$ ) (Figure 5E). Irbesartan significantly reduced s-E-selectin levels in the sera of treated-HOCl-mice ( $1.28 \pm 0.06$  pg/ml) versus untreated HOCl-mice ( $1.56 \pm 0.06$  pg/mL,  $P < 0.05$ , Figure 5E).

## **DISCUSSION**

This report shows that Irbesartan, an angiotensin II type 1 receptor antagonist, prevents fibrosis in murine models of systemic sclerosis induced by reactive oxygen species, an observation consistent with the upregulation of AT and AT<sub>1</sub>R observed in HOCl-mice.

Irbesartan reduces fibrosis through inhibiting the accumulation of type I collagen in the skin and in the lung. This improvement is consecutive to the inhibition of fibroblast proliferation and differentiation into myofibroblasts, and to the decreased phosphorylation of smad3, a transcription factor implicated in the activation of the type I collagen gene. In addition, the phosphorylation of the epidermal growth factor receptor (EGFR) which occurs in the skin of HOCl-mice, is inhibited by Irbesartan. These data are in line with the observation that AT<sub>1</sub>R antagonists abrogate angiotensin II-induced connective tissue growth factor, collagen type-I and  $\alpha$ SMA expressions via a TGF $\beta$ -dependent Smad3

signalling pathway (15, 37, 38). This effect is reinforced by the activation through the AT<sub>1</sub>R pathway of the NADPH oxidase to produce ROS and to trigger collagen synthesis and fibrosis (39, 40). Similarly, the transactivation of EGFR by angiotensin II triggers the proliferation, the migration of fibroblasts and is abrogated by AT<sub>1</sub>R antagonist (41).

Another study has connected skin fibrosis in SSc with the stabilization of the oncogene H-Ras following the stimulation of ROS production by autoantibodies. Ras proteins are members of a large family of small membrane-bound GTPases which control profibrotic pathways engaged by TGF $\beta$ , angiotensin II, platelet-derived growth factor (PDGF) or ROS (42, 43). Recent reports have shown that increased levels of H-Ras protein can directly stimulate Smad2/3 signalling and collagen I accumulation (32). We found that irbesartan reduced the expression of H-Ras in the skin and lungs of SSc mice, which can also explain the reduction in fibrosis in HOCl-mice compared to untreated HOCl-mice.

Another feature in SSc patients is an abnormal activation of immune cells, including T and B cells, infiltration of inflammatory cells, especially CD4<sup>+</sup> T cells in the skin and in the lungs along with increased levels of various pro-inflammatory cytokines (44, 45). In HOCl-mice, irbesartan reduces the number of splenic B cells, of CD4<sup>+</sup> and CD8<sup>+</sup> T cells, the hyperproliferation of CD3/CD28-activated T cells and of LPS-activated B cells. These effects on B and T cells are in agreement with our observation that H-Ras expression is dose-dependently decreased in vitro by irbesartan in LPS- and in anti-CD3 mAb-activated splenocytes. Indeed, H-Ras transmits TCR signals that prime CD4 (+) T cells and trigger B cell activation (46), thus suggesting how irbesartan decreases the levels of anti-topoisomerase I Abs in the serum of HOCl-mice.

In addition to its immunomodulating properties, the antioxidant properties of irbesartan can explain its beneficial effect in HOCl-mice. Indeed, the high amounts of ROS

produced by endothelial cells and fibroblasts lead to the oxidation of proteins, in particular of DNA-topoisomerase I. The release of oxidized DNA-topoisomerase I into the bloodstream is a key event in the breach of immune tolerance in both mouse and human SSc (22). Therefore, the *in vivo* abrogation of the auto-immune response by irbesartan in HOCl-mice can be explained by its antioxidant properties that limits the oxidation of DNA-topoisomerase I and thus prevents the production of autoantigen.

Several reports have suggested that, in addition to reactive oxygen species, reactive nitrogen species are also involved in the pathogenesis of SSc (9, 15, 47-50). In patients, the serum levels of nitric oxide (NO) are significantly elevated, as evidenced by increased nitrate levels, increased expression of 3-nitrotyrosine in diseased tissue, and increased exhaled NO (49). NO can be either beneficial because of its vasodilating properties or deleterious when it combines with superoxide anions in an inflammatory context, to form highly toxic peroxynitrites responsible for vascular damages, fibrosis, and self-maintenance of reactive species production (50).

Inducible nitric oxide synthase (iNOS), an enzyme that allows the production of NO, is activated by cytokines, ligands of toll-like receptors or angiotensin II in various cell types, including endothelial cells and fibroblasts (51, 52). In contrast, AT<sub>1</sub>R antagonists prevent the nitrosative stress (53). In our hands, irbesartan decreases iNOS expression in the lung of HOCl-mice and the generation of ROS, resulting in a drop in the production of peroxynitrites and in a decrease in exhaled nitric oxide which is a highly relevant marker of the extent of lung involvement in systemic sclerosis (54). Nitric oxide is largely metabolized into nitrites, which are increased in the serum of patients with systemic sclerosis and also in HOCl-mice. The nitrosative stress induces vascular damages reflected by elevated serum levels of soluble E-selectine. Administration of irbesartan reduces the level of both serum nitrite and E-selectine in HOCl-mice, confirming the efficacy of an

AT<sub>1</sub>R blocker in the prevention of the systemic nitrosative stress in vivo and of its consequences on the vascular damages in HOCl-mice.

We also tested irbesartan in the model of peroxynitrite-induced SSc and found that the molecule is as effective in this model as in HOCl-mice on dermal thickness and collagen deposition in the skin.

In conclusion, in addition to its use in the treatment of sclerodermal renal crisis, irbesartan and other AT<sub>1</sub>R blockers should be evaluated as anti fibrotic and immunomodulating drugs in SSc patients with diffuse fibrosis.

## **ACKNOWLEDGMENTS**

The authors are grateful to Ms Agnes Colle for her excellent typing and editing of the manuscript.

## **AUTHOR CONTRIBUTIONS**

All authors were involved in drafting the article or revising it critically for intellectual content and all authors approved the final version to be published. Dr Batteux had full access to all of the data in the study and takes the responsibility for the integrity of the data and the accuracy of the data analysis.

Study conception and design. Marut, Kavian, Servettaz, Dinh-Xuan, Weill, Batteux.

Acquisition of data. Marut, Kavian, Hua-Huy, Nicco, Chéreau, Dinh-Xuan, Batteux.

Analysis and interpretation of data. Marut, Kavian, Servettaz, Weill, Dinh-Xuan, Batteux.

## **REFERENCES**

1. Botzoris V, Drosos AA. Management of Raynaud's phenomenon and digital ulcers in systemic sclerosis. *Joint, bone, spine. Rev Rhum* 2011;78(4):341-6.
2. Malcarne VL, Hansdottir I, McKinney A, Upchurch R, Greenbergs HL, Henstorf GH, et al. Medical signs and symptoms associated with disability, pain, and psychosocial adjustment in systemic sclerosis. *J Rheumatol* 2007;34(2):359-67.
3. Kawaguchi Y, Takagi K, Hara M, Fukasawa C, Sugiura T, Nishimagi E, et al. Angiotensin II in the lesional skin of systemic sclerosis patients contributes to tissue fibrosis via angiotensin II type 1 receptors. *Arthritis Rheum* 2004;50(1):216-26.
4. Ohtani R, Ohashi Y, Muranaga K, Itoh N, Okamoto H. Changes in activity of the renin-angiotensin system of the rat by induction of acute inflammation. *Life sciences* 1989;44(3):237-41.
5. Ohashi N, Urushihara M, Satou R, Kobori H. Glomerular angiotensinogen is induced in mesangial cells in diabetic rats via reactive oxygen species--ERK/JNK pathways. *Hypertension research : official journal of the Japanese Society of Hypertension* 2010;33(11):1174-81.
6. Uhal BD, Kim JK, Li X, Molina-Molina M. Angiotensin-TGF-beta 1 crosstalk in human idiopathic pulmonary fibrosis: autocrine mechanisms in myofibroblasts and macrophages. *Curr Pharm Des* 2007;13(12):1247-56.
7. Riemekasten G, Philippe A, Nather M, Slowinski T, Muller DN, Heidecke H, et al. Involvement of functional autoantibodies against vascular receptors in systemic sclerosis. *Ann Rheum Dis* 2011;70(3):530-6.
8. Fukasawa H, Furuya R, Ishigaki S, Kinoshita N, Isobe S, Fujigaki Y. Hyponatremia in a patient with scleroderma renal crisis: a potential role of activated renin-angiotensin system. *BMC Nephrol* 2012;13:47.
9. de Gasparo M, Catt KJ, Inagami T, Wright JW, Unger T. International union of pharmacology. XXIII. The angiotensin II receptors. *Pharmacol rev* 2000;52(3):415-72.
10. Stawski LS, Han R, Bujor AM, Trojanowska M. Angiotensin II induces skin fibrosis: a novel mouse model of dermal fibrosis *Arthritis Research & Therapy* 2012;14(4):R194.
11. Mezzano SA, Ruiz-Ortega M, Egido J. Angiotensin II and renal fibrosis. *Hypertension* 2001;38(3 Pt 2):635-8.
12. Watanabe T, Barker TA, Berk BC. Angiotensin II and the endothelium: diverse signals and effects. *Hypertension* 2005;45(2):163-9.
13. Hunyady L, Catt KJ. Pleiotropic AT1 receptor signaling pathways mediating physiological and pathogenic actions of angiotensin II. *Mol Endocrinol.* 2006;20(5):953-70.
14. Chappell MC. Angiotensin-converting enzyme 2 autoantibodies: further evidence for a role of the renin-angiotensin system in inflammation. *Arthritis Res Ther* 2010;12(3):128.

15. Wang W, Huang XR, Canlas E, Oka K, Truong LD, Deng C, et al. Essential role of Smad3 in angiotensin II-induced vascular fibrosis. *Circulation Research* 2006;98(8):1032-9.
16. Dragun D, Muller DN, Brasen JH, Fritsche L, Nieminen-Kelha M, Dechend R, et al. Angiotensin II type 1-receptor activating antibodies in renal-allograft rejection. *N Engl J Med* 2005;352(6):558-69.
17. Wallukat G, Homuth V, Fischer T, Lindschau C, Horstkamp B, Jupner A, et al. Patients with preeclampsia develop agonistic autoantibodies against the angiotensin AT1 receptor. *J Clin Invest* 1999;103(7):945-52.
18. Xia Y, Ramin SM, Kellems RE. Potential roles of angiotensin receptor-activating autoantibody in the pathophysiology of preeclampsia. *Hypertension* 2007;50(2):269-75.
19. Dooley A, Gao B, Bradley N, Abraham DJ, Black CM, Jacobs M, et al. Abnormal nitric oxide metabolism in systemic sclerosis: increased levels of nitrated proteins and asymmetric dimethylarginine. *Rheumatology (Oxford)* 2006;45(6):676-84.
20. Dooley A, Bruckdorfer KR, Abraham DJ. Modulation of fibrosis in systemic sclerosis by nitric oxide and antioxidants. *Cardiol Res Pract* 2012;2012:521958.
21. Walker KM, Pope J. Treatment of systemic sclerosis complications: what to use when first-line treatment fails--a consensus of systemic sclerosis experts. *Semi Arthritis Rheum* 2012;42(1):42-55.
22. Servettaz A, Goulvestre C, Kavian N, Nicco C, Guilpain P, Chereau C, et al. Selective oxidation of DNA topoisomerase 1 induces systemic sclerosis in the mouse. *J Immunol* 2009;182(9):5855-64.
23. Servettaz A, Goulvestre C, Kavian N, Nicco C, Guilpain P, Chéreau C, et al. Selective oxidation of DNA topoisomerase 1 induced systemic sclerosis in the mouse. *J Immunol* 2009;182(9):5855-64.
24. Dalle-Donne I, Rossi R, Giustarini D, Gagliano N, Lusini L, Milzani A, et al. Actin carbonylation: from a simple marker of protein oxidation to relevant signs of severe functional impairment. *Free Radic Biol Med* 2001;1:1075-83.
25. Burdick MD, Murray LA, Keane MP, Xue YY, Zisman DA, Belperio JA, et al. CXCL11 attenuates bleomycin-induced pulmonary fibrosis via inhibition of vascular remodeling. *Am J Respir Crit Care Med* 2005;171:261-8.
26. Sue RD, Belperio JA, Burdick MD, Murray LA, Xue YY, Dy MC, et al. CXCR2 is critical to hyperoxia-induced lung injury. *J Immunol* 2004;172:3860-8.
27. Servettaz A, Kavian N, Nicco C, Deveaux V, Chereau C, Wang A, et al. Targeting the cannabinoid pathway limits the development of fibrosis and autoimmunity in a mouse model of systemic sclerosis. *Am J Pathol* 2010;177(1):187-96.
28. Marut WK, Kavian N, Servettaz A, Nicco C, Ba LA, Doering M, et al. The Organotelluride Catalyst (PHTE)(2)NQ Prevents HOCl-Induced Systemic Sclerosis in Mouse. *J Invest Dermatol* 2012.

29. Kaviani N, Servettaz A, Mongaret C, Wang A, Nicco C, Chereau C, et al. Targeting ADAM-17/notch signaling abrogates the development of systemic sclerosis in a murine model. *Arthritis Rheum* 2010;62(11):3477-87.
30. Sastry KV, Moudgal RP, Mohan J, Tyagi JS, Rao GS. Spectrophotometric determination of serum nitrite and nitrate by copper-cadmium alloy. *Anal Biochem* 2002;306(1):79-82.
31. Delclaux C, Dinh-Xuan AT. [Art--and artefacts--of exhaled NO measurement in asthma]. *Rev Mal Respir* 2005;22(2 Pt 1):209-11.
32. Smaldone S, Olivieri J, Gusella GL, Moroncini G, Gabrielli A, Ramirez F. Ha-Ras stabilization mediates pro-fibrotic signals in dermal fibroblasts. *Fibrogenesis Tissue Repair* 2011;4(1):8.
33. Rosenbloom J, Saitta B, Gaidarova S, Sandorfi N, Rosenbloom JC, Abrams WR, et al. Inhibition of type I collagen gene expression in normal and systemic sclerosis fibroblasts by a specific inhibitor of geranylgeranyl transferase I. *Arthritis Rheum* 2000;43(7):1624-32.
34. Shimizu K, Ogawa F, Muroi E, Hara T, Komura K, Bae SJ, et al. Increased serum levels of nitrotyrosine, a marker for peroxynitrite production, in systemic sclerosis. *Clin Exp Rheumatol* 2007;25(2):281-6.
35. Tiev KP, Hua-Huy T, Kettaneh A, Allanore Y, Le-Dong NN, Duong-Quy S, et al. Alveolar concentration of nitric oxide predicts pulmonary function deterioration in scleroderma. *Thorax* 2012;67(2):157-63.
36. Gruschwitz MS, Hornstein OP, von Den Driesch P. Correlation of soluble adhesion molecules in the peripheral blood of scleroderma patients with their in situ expression and with disease activity. *Arthritis Rheum* 1995;38(2):184-9.
37. Yang F, Chung AC, Huang XR, Lan HY. Angiotensin II induces connective tissue growth factor and collagen I expression via transforming growth factor-beta-dependent and -independent Smad pathways: the role of Smad3. *Hypertension* 2009;54(4):877-84.
38. Ren X, Guan G, Liu G. Irbesartan ameliorates diabetic nephropathy by reducing the expression of connective tissue growth factor and alpha-smooth-muscle actin in the tubulointerstitium of diabetic rats. *Pharmacology* 2009;83(2):80-7.
39. Queisser N, Fazeli G, Schupp N. Superoxide anion and hydrogen peroxide-induced signaling and damage in angiotensin II and aldosterone action. *Biol Chem* 2010;391(11):1265-79.
40. Lijnen PJ, van Pelt JF, Fagard RH. Stimulation of reactive oxygen species and collagen synthesis by angiotensin II in cardiac fibroblasts. *Cardiovasc Therap* 2012;30(1):e1-8.
41. Yahata Y, Shirakata Y, Tokumaru S, Yang L, Dai X, Tohyama M, et al. A novel function of angiotensin II in skin wound healing. Induction of fibroblast and keratinocyte migration by angiotensin II via heparin-binding epidermal growth factor (EGF)-like growth factor-mediated EGF receptor transactivation. *J Biol Chem* 2006;281(19):13209-16.

42. Martinez-Salgado C, Fuentes-Calvo I, Garcia-Cenador B, Santos E, Lopez-Novoa JM. Involvement of H- and N-Ras isoforms in transforming growth factor-beta1-induced proliferation and in collagen and fibronectin synthesis. *Exp Cell Res* 2006;312(11):2093-106.
43. Schieffer B, Paxton WG, Chai Q, Marrero MB, Bernstein KE. Angiotensin II controls p21ras activity via pp60c-src. *Biol Chem* 1996;271(17):10329-33.
44. Sato S, Fujimoto M, Hasegawa M, Takehara K. Altered blood B lymphocyte homeostasis in systemic sclerosis: expanded naive B cells and diminished but activated memory B cells. *Arthritis Rheum* 2004;50(6):1918-27.
45. Needleman BW, Wigley FM, Stair RW. Interleukin-1, interleukin-2, interleukin-4, interleukin-6, tumor necrosis factor alpha, and interferon-gamma levels in sera from patients with scleroderma. *Arthritis Rheum* 1992;35(1):67-72.
46. Iborra S, Soto M, Stark-Aroeira L, Castellano E, Alarcon B, Alonso C, et al. H-ras and N-ras are dispensable for T-cell development and activation but critical for protective Th1 immunity. *Blood* 2011;117(19):5102-11.
47. Sambo P, Baroni SS, Luchetti M, Paroncini P, Dusi S, Orlandini G, et al. Oxidative stress in scleroderma: maintenance of scleroderma fibroblast phenotype by the constitutive up-regulation of reactive oxygen species generation through the NADPH oxidase complex pathway. *Arthritis Rheum* 2001;44(11):2653-64.
48. Servettaz A, Guilpain P, Goulvestre C, Chereau C, Hercend C, Nicco C, et al. Radical oxygen species production induced by advanced oxidation protein products predicts clinical evolution and response to treatment in systemic sclerosis. *Ann Rheum Dis* 2007;66(9):1202-9.
49. Takagi K, Kawaguchi Y, Hara M, Sugiura T, Harigai M, Kamatani N. Serum nitric oxide (NO) levels in systemic sclerosis patients: correlation between NO levels and clinical features. *Clin Exp Immunol* 2003;134(3):538-44.
50. Urtasun R, Conde de la Rosa L, Nieto N. Oxidative and nitrosative stress and fibrogenic response. *Clin Liver Dis* 2008;12(4):769-90, viii.
51. Forstermann U, Gath I, Schwarz P, Closs EI, Kleinert H. Isoforms of nitric oxide synthase. Properties, cellular distribution and expressional control. *Biochem Pharmacol* 1995;50(9):1321-32.
52. Sigusch HH, Campbell SE, Weber KT. Angiotensin II-induced myocardial fibrosis in rats: role of nitric oxide, prostaglandins and bradykinin. *Cardiovasc Res* 1996;31(4):546-54.
53. Fan Q, Liao J, Kobayashi M, Yamashita M, Gu L, Gohda T, et al. Candesartan reduced advanced glycation end-products accumulation and diminished nitro-oxidative stress in type 2 diabetic KK/Ta mice. *Nephrology, dialysis, transplantation : Official publication of the European Dialysis and Transplant Association - European Renal Association* 2004;19(12):3012-20.
54. Tiev KP, Le-Dong NN, Duong-Quy S, Hua-Huy T, Cabane J, Dinh-Xuan AT. Exhaled nitric oxide, but not serum nitrite and nitrate, is a marker of interstitial lung

disease in systemic sclerosis. Nitric oxide : biology and chemistry / official journal of the Nitric Oxide Society 2009;20(3):200-6.

## FIGURE LEGENDS

### Figure 1.

Effects of irbesartan on collagen content in the skin following intradermal injections of HOCl and oral administration of irbesartan (50 mg/kg/day) (n=8 mice per group). A: Dermal thickness in the injected areas of BALB/c mice. B: Collagen content in 6 mm punch biopsies of skin as measured by the quantitative dye-binding Sircol method. C: Representative tissue sections comparing dermal fibrosis in the injected areas from BALB/c mice by H&E staining. the expression of pSmad 2/3, AT<sub>1</sub>, and pEGFR expression in mouse skin by immunohistochemistry revealed with DAB. Magnification was ×50 (Olympus DP70 Controller). D: Spontaneous proliferation of fibroblasts isolated from the skin of mice. E: Western blot analysis showing expresion of AT<sub>1</sub>R, α-SMA, and H-Ras in the skin of two representative mice per group. Anti-β-actin mouse MoAb was used as internal control. Values are means ± SEM of data gained from all mice in the experimental and control groups. Statistics: \*P < 0.05, \*\*P < 0.01, \*\*\* P<0.001.

### Figure 2.

Effects of irbesartan on collagen content in the lungs of BALB/c mice. HOCl was injected intradermally and irbesartan orally administered (50 mg/kg/day) every day during 6 weeks (n=8 mice per group). A: Collagen content in the lungs was measured by the Sircol method. B: Representative lung sections from BALB/c mice. 1: PBS, 2: irbesartan, 3: HOCl, 4: HOCl+irbesartan. Tissue sections were stained with H&E. C: Picro-sirius Red staining for lung sections. Magnification is ×50 (Olympus DP70 Controller). D: Western

blot showing expression of H-Ras in the lungs of two representative mice per group. Anti- $\beta$ -Actin mouse MoAb was used as internal control. Values are means  $\pm$  SEM of data gained from all mice in the experimental and control groups. Statistics: \*P < 0.05, \*\*P < 0.01.

### **Figure 3.**

In vivo treatment with irbesartan inhibits the production of autoantibodies in HOCl-mice. A: Levels of anti-topoisomerase-1 Ab as measured by ELISA. B: Splenic B cell numbers, as assessed by flow cytometry (millions of cells). Values are means  $\pm$  SEM of data gained from all mice in the experimental and control groups. C: Splenic CD4 T cell numbers. D: Splenic CD8 T cell numbers. E: Proliferation of splenic T cells activated by anti-CD3/CD28. F: Proliferation of splenic B cells activated by LPS. G: Western blot analysis of H-Ras in splenocytes. Anti- $\beta$ -actin mouse MoAb was used as internal control. Values are means  $\pm$  SEM of data gained from all mice in the experimental and control groups. Statistics: \*P < 0.05, \*\*P < 0.01.

### **Figure 4.**

In vivo administration of irbesartan exerted beneficial effects on the local and systemic nitrosative stresses. A: Levels of nitrites in serum ( $\mu$ mol/g proteins). Western blot analysis of 3-nitrotyrosine (3-NT) expression in mouse skin B and in mouse lungs C. Anti- $\beta$ -actin mouse MoAb was used as internal control. D: Immunohistochemistry of lung sections stained with iNOS, and revealed with DAB. Magnification was  $\times 50$  (Olympus DP70 Controller). E: Level of exhaled nitric oxide measured by a chemiluminescence NO analyzer F: Sievers 280 NOATM, Sievers Instruments Inc., Boulder, CO, USA. Values are means  $\pm$  SEM of data gained from all mice in the experimental and control groups. Statistics: \*P < 0.05, \*\*P < 0.01.

### Figure 5.

Irbesartan decreased in vitro nitrosative and oxidative stresses. A: Production of NO, B: of  $O_2^{\circ-}$ , and C: of  $H_2O_2$  by HPMEC cells incubated for 48 hours with increasing concentrations of irbesartan. Levels of  $H_2O_2$ , NO, and  $O_2$  were assessed spectrofluorometrically using  $H_2DCFDA$ , DAF-2DA, and DHE, respectively. Results are expressed as arbitrary units of fluorescence intensity related to the number of viable cells evaluated by the crystal violet assay. as previously described (28). D: Expression of iNOS protein in HPMEC cells was analyzed by western blot. Anti- $\beta$ -actin mouse MoAb was used as internal control. E: Serum soluble E-selectin concentration (pg/ml) measured by ELISA. Results are the means  $\pm$  S.E.M. of three experiments performed in triplicates. Statistics: \*P < 0.05, \*\*P < 0.01, \*\*\*P < 0.001.

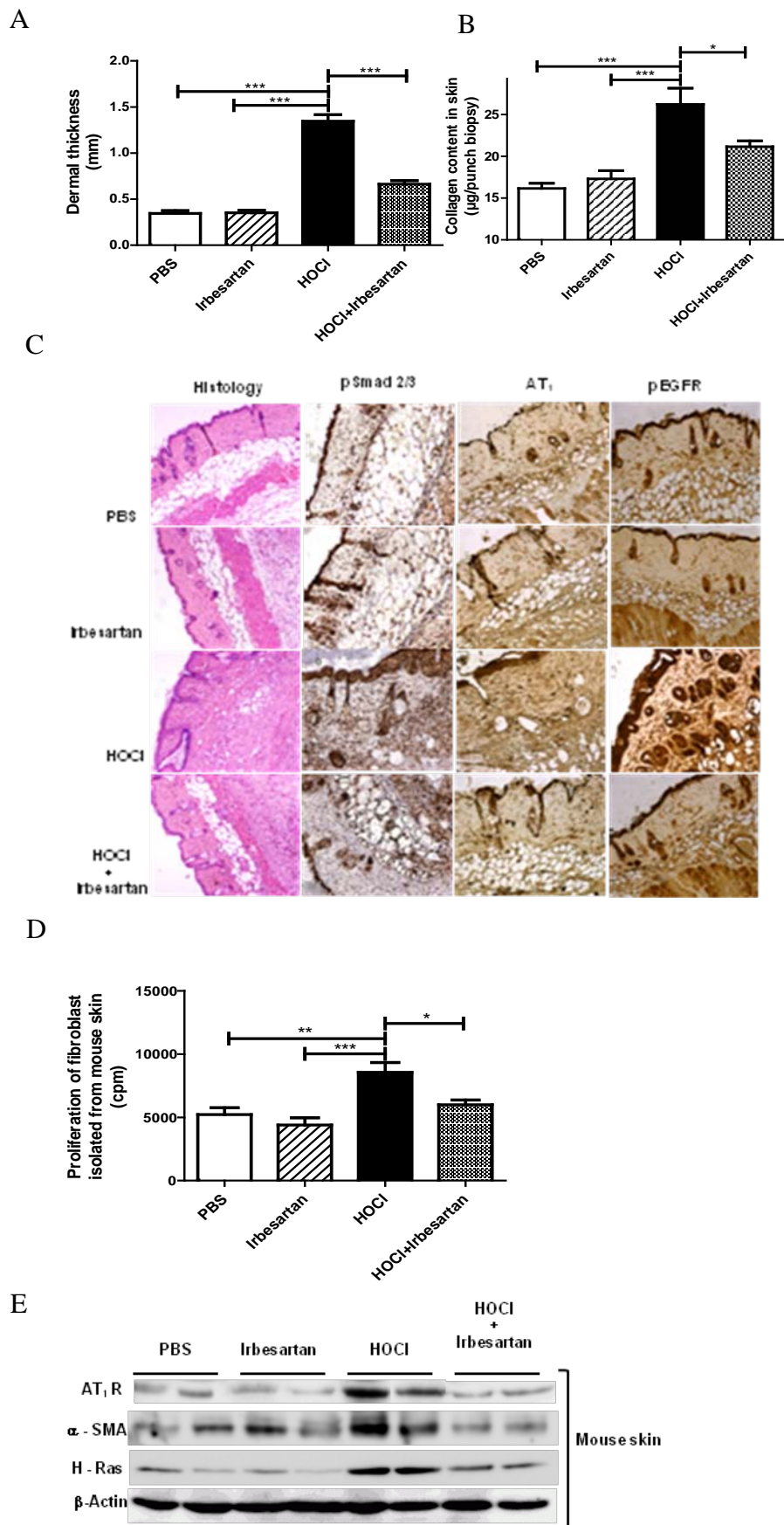


**Figure 1.**

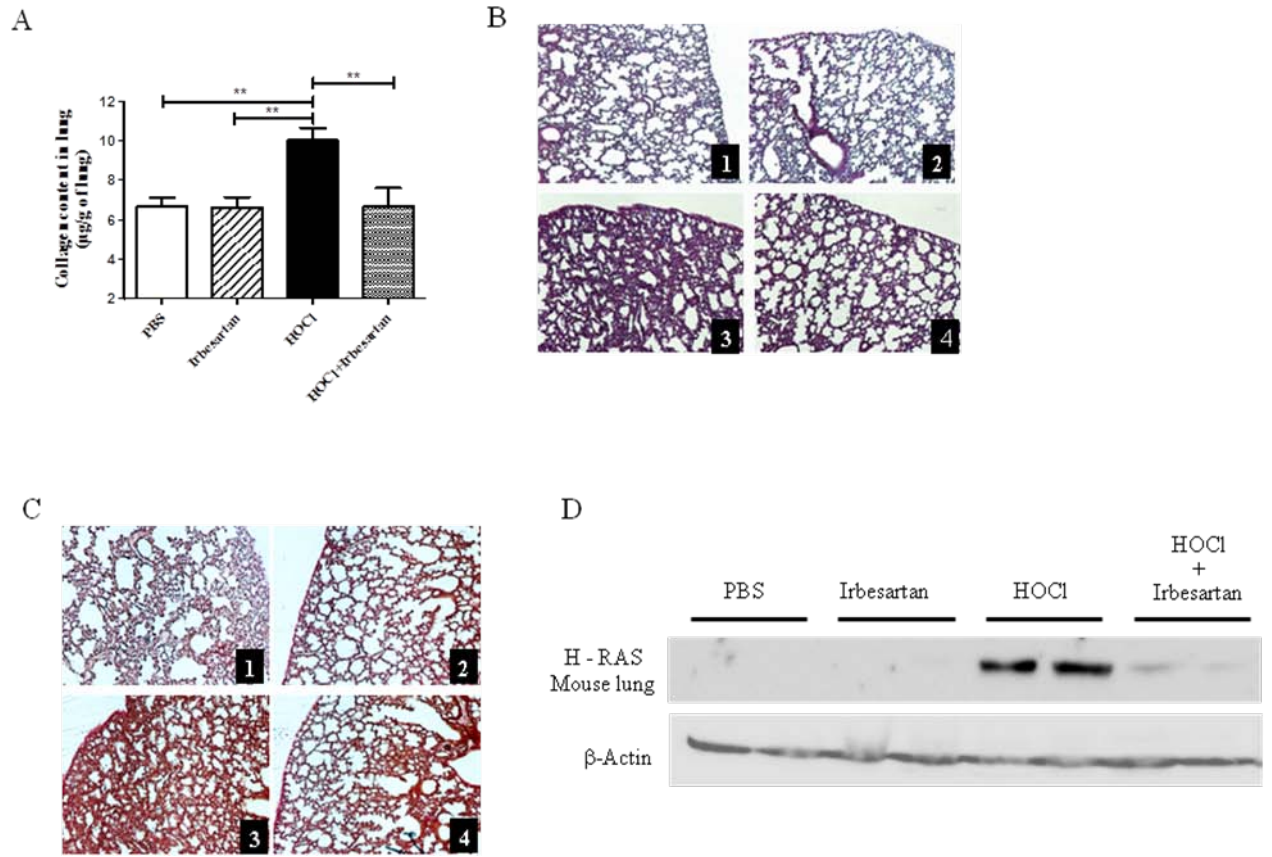


**Figure 2.**

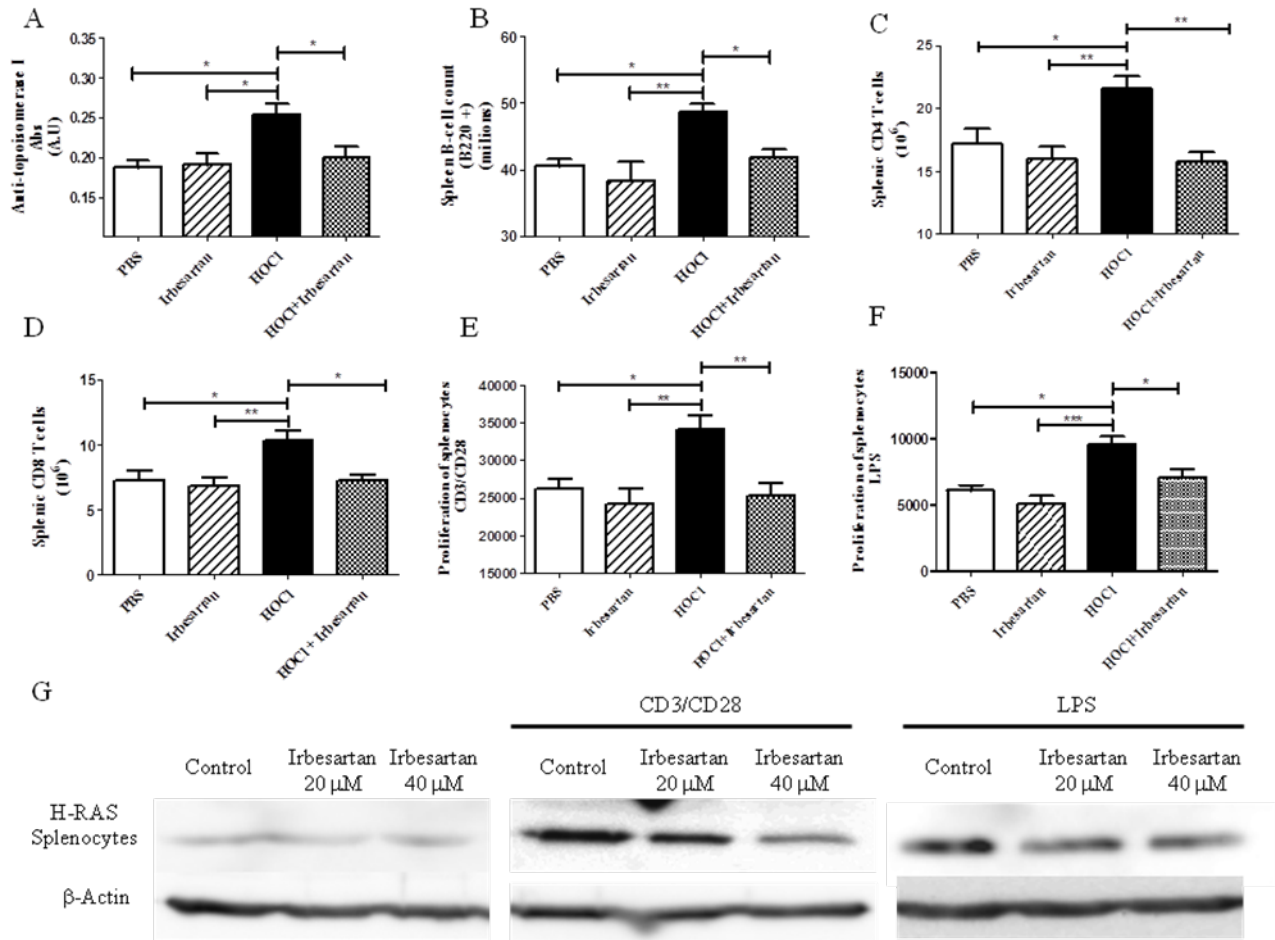


**Figure 3.**

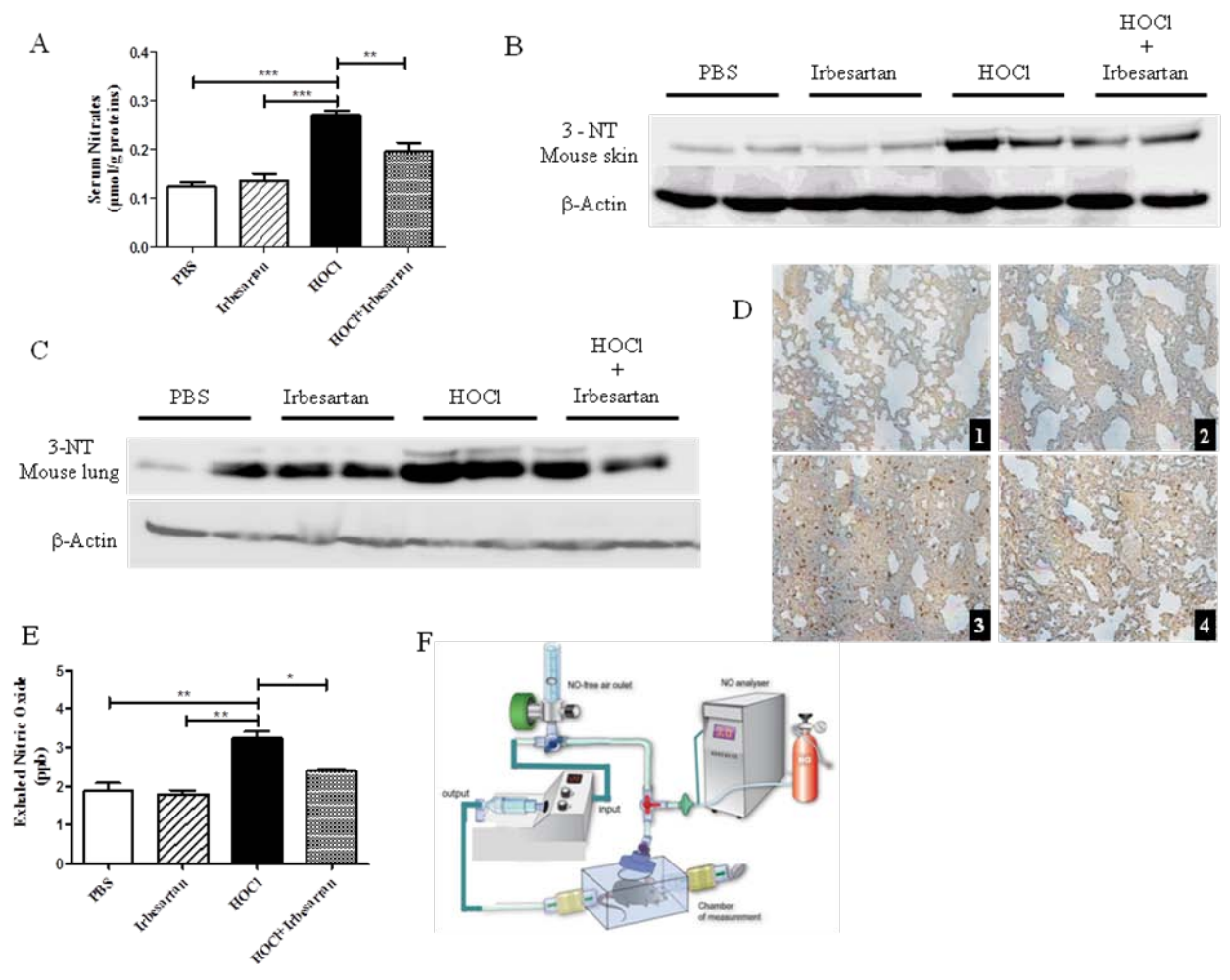


**Figure 4.**

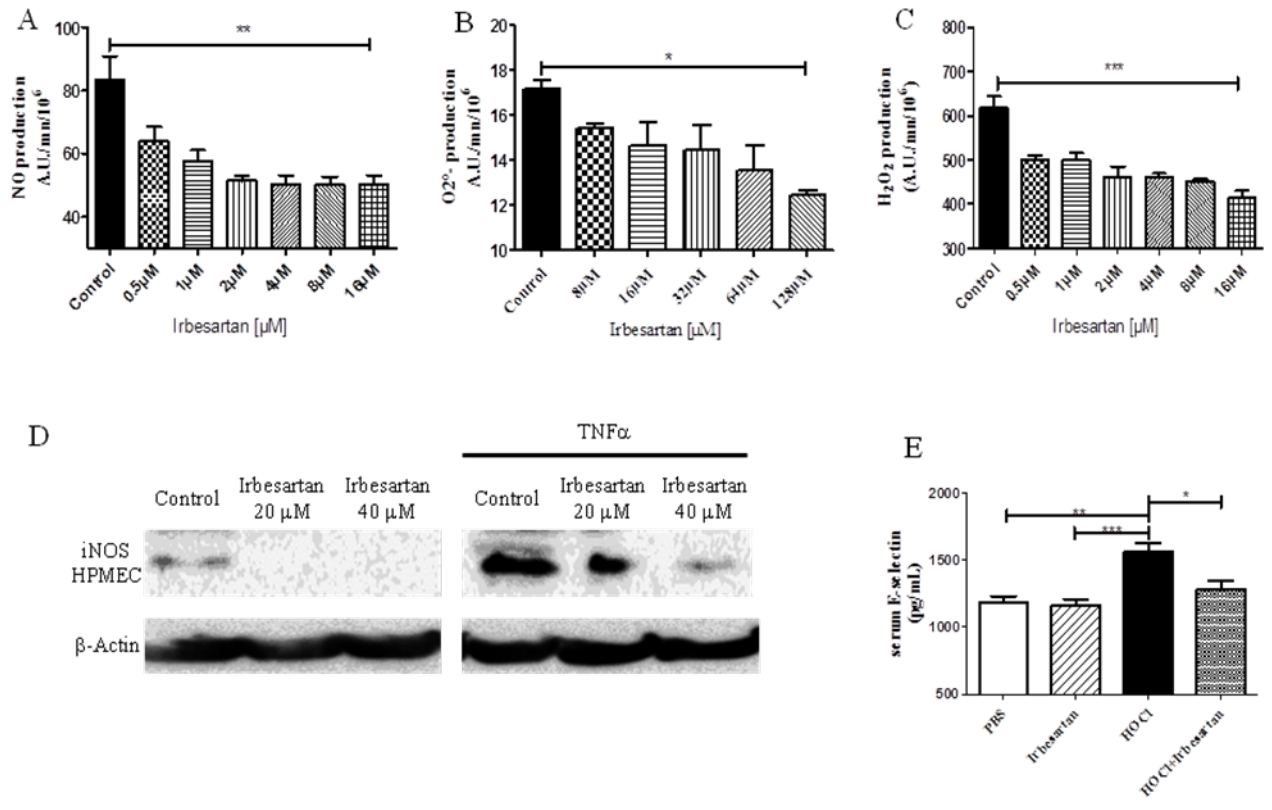


**Figure 5.**

## Discussion

---

Systemic sclerosis is a severe, immune-mediated disorder, the main features being microvascular damage, autoantibodies, and fibroblasts activation with fibrosis of the skin and visceral organs [213]. Despite significant efforts, the pathogenesis of SSc is still unclear, which is probably related to the complexity of factors involved in the pathophysiology of disease, but also its heterogeneity. Indeed, it is likely that the different clinical forms of the disease and its complications result from different mechanisms more or less distinct, making it difficult to understand. This gap in knowledge impairs the development of novel therapeutics able to modify the natural history of this disease.

Several years ago the pathogenesis of SSc was linked to the presence of a large excess of reactive oxygen species. This hypothesis, over the years, has been supported by several reports which documented the presence of an abnormal redox state in SSc patients [5, 6]. Oxidative stress appears to play a major role in SSc because it is able to modify the structure and antigenicity of proteins. Several clinical, epidemiological and biological arguments excuse the role of oxidative stress in early SSc. It is noteworthy that more than 90% of clinical patients have repeated ischemia-reperfusion phenomenon during the years preceding the development of SSc (approximately six years before the development of limited cutaneous SSc and approximately two years and a half before the development of diffuse SSc). This phenomenon generates a large amount of ROS, including  $O_2^{\bullet-}$  and  $ONOO^-$  [6, 7]. Epidemiologically, several toxics involved in triggering SSc exert their action through the generation of ROS. This is the case of silica, which directly induces ROS formation through the Fenton reaction, and indirectly through the activation of phagocytic cells. Syndrome toxic oils, which shares similarities with SSc, also seems to

involve free radicals. Finally, on a biological level, it has been shown that monocytes and fibroblasts of SSc patients produced large amounts of  $O^{\bullet-}_2$ .

Therapeutic options are limited. Therefore advances in medical understanding for the development of novel treatments are critical. The aim of this thesis is to update the role of oxidative stress in SS as a paradigm of fibrotic disorders.

In a previous work conducted in our laboratory, it was observed that the sera of SSc patients are able to induce oxidative stress. This stress is mediated by serum oxidized protein products (AOPP) which both induce fibroblasts proliferation and inhibit endothelial cells proliferation. In addition, sera from patients with lung fibrosis induce a higher proliferation rate of SSc fibroblasts and increased synthesis of  $H_2O_2$ , than those of SSc patients without pulmonary involvement. Sera from patients with serious vascular complications additionally induces NO release by endothelial cells, and strongly inhibit their growth. At the opposite, sera of patients with pulmonary fibrosis, they do not stimulate fibroblasts proliferation [208].

The correlation between ROS production induced by serum of SSc patients and clinical complications in these patients is a strong argument which favors the role of ROS in the pathogenesis of SSc. Therefore, in another study conducted in our laboratory, we decided to assess the extent, nature and consequences of oxidative stress in SSc. To study SSc on animal models, mice were exposed to different types of agents generating various types of ROS. We demonstrated a direct role for ROS in SSc and showed that the nature of the ROS dictates the form of SSc. Indeed, administration of peroxynitrites induced skin fibrosis and serum anti-CENP-B Abs that characterize limited SSc, whereas hypochlorite or hydroxyl radicals induced cutaneous and lung fibrosis and anti-DNA topoisomerase 1 autoantibodies that are characteristic of human diffuse SSc. Moreover, this work demonstrated that oxidized proteins, and especially oxidized DNA topoisomerase I,

generated in high amounts after exposition to agents generating ROS are directly involved in the spreading of the fibrosis from the skin to visceral organs through the systemic circulation. Thus leads to the increase release of oxidized DNA topoisomerase I, the production of anti-DNA-topoisomerase I Abs and the development of the diffuse form of SSc [162]. These observations are in agreement with previous studies, which demonstrated a direct link between the concentration of AOPP in the serum of SSc patients and the development of lung fibrosis.

**Figure 11.** Induction of murine SSc through daily intradermal injections of HOCl generating agents, by Batteux et al, *Curr. Op Rheumatol*, 2011.

Intradermal injections of agents generating hypochlorous acid (HOCl) to BALB/c mice induce cutaneous and lung fibrosis, characteristic kidney damages along with the production of serum anti-DNA-topoisomerase-1 Abs, all features that characterize diffuse cutaneous SSc in humans (Figure 11). Those experiments have shown implication of ROS in the development of SSc and provided a new and more representative murine model of SSc mimicking diffuse SSc. This new ROS-mediated murine model of SSc has allowed us to study a new therapeutic approach involving oxidative stress manipulation in the SSc.

SSc fibroblasts spontaneously produce large amounts of ROS, which at high concentration can damage cell structures, nucleic acids, lipids and proteins. We have used this properties to test the features of cytotoxic compounds - organotellurium compound- (PHTE)<sub>2</sub>NQ (Article 1) and natural organosulfur – dipropyltetrasulfide (DPTTS) (Article 2) in SSc. The balance of oxidants versus antioxidants system is crucial in the development of fibrotic diseases such as SSc. ROS can stimulate the growth and proliferation of fibroblasts to a certain threshold, beyond which they will induce apoptosis

(see Chapter 2). This property is also well known in cancer cells, where low levels of ROS lead to proliferation while high concentrations of ROS induced by cytotoxic anticancer drugs induce apoptosis [183]. (PHTE)<sub>2</sub>NQ is a pro-oxidant, cytotoxic molecule which has already been tested in our laboratory, in a mouse model of colon cancer. This study has shown that (PHTE)<sub>2</sub>NQ is able to increase intracellular levels of ROS in colon cancer cells and, as a consequence, selectively kill them (see Appendices, [240]). Dipropyltertrasulfide (DPTTS) is a natural sulfur compound isolated from *Allium*. Organosulfur compounds were already considered as a promising compound in medicine, as antibiotic for resistant bacteria or prooxidant agents for anti-cancer therapy [241]. For example, Hosono *et al* showed that an organosulfur compound (diallyl-tetrasulfide) that leads to ROS formation in cancer cells leading to  $\beta$ -tubulin oxidation and disruption of the microtubule network provoking apoptosis of cancer cells.

First, we explored the properties of (PHTE)<sub>2</sub>NQ and DPTTS *in vitro* on normal and SSc fibroblasts. Those molecules can combine with endogenous oxidative species generated ‘naturally’ in mouse SSc fibroblasts to selectively kill cells through a necrotic ((PHTE)<sub>2</sub>NQ ) or an apoptotic (DPTTS) process.

Cellular sensitivity to (PHTE)<sub>2</sub>NQ or to DPTTS is determined by the balance between the generation of ROS and their detoxification. Primary fibroblasts extracted from control and SSc mice were exposed to increases doses of (PHTE)<sub>2</sub>NQ or DPTTS. Production of H<sub>2</sub>O<sub>2</sub>, intracellular content of glutathione (GSH), and cells viability were measured in those cells. We observed differences in sensitivity between the two cell types, where (PHTE)<sub>2</sub>NQ or DPTTS significantly induces cell death of SSc fibroblasts and only slightly cell death of normal fibroblasts. This cell death involves an oxidative burst characterized by an overproduction of H<sub>2</sub>O<sub>2</sub> and a significant deficit in GSH. Indeed, SSc fibroblasts have an imbalance in the oxidant / antioxidant status which makes them particularly

sensitive to the action of cytotoxic, pro-oxidant molecules like (PHTE)<sub>2</sub>NQ or DPTTS. This phenomenon do not occurs in normal fibroblasts, with a normal oxidant / antioxidant status. To investigate more the mechanism of action of both molecules we decided to modulate the metabolism of ROS in the fibroblasts with various ROS modulators. N-acetylcysteine (NAC), a precursor of GSH, had a protective effect against the cells death induced by (PHTE)<sub>2</sub>NQ or DPTTS in SSc fibroblasts. Moreover, GSH-depleting agent BSO, intensified the cytotoxicity of those pro-oxidative molecules. These data explain an increased sensitivity of SSc fibroblasts to (PHTE)<sub>2</sub>NQ or DPTTS, which are deficient in GSH and overproduce ROS. Following these initial in vitro results, we decided to test the therapeutic properties of those compounds in an in vivo mouse model of SSc. In vivo, diseased skin fibroblasts are selectively killed by (PHTE)<sub>2</sub>NQ or DPTTS, while normal fibroblasts survive and grow in the place of the SSc fibroblasts. Thus, fibroblasts isolated from (PHTE)<sub>2</sub>NQ or DPTTS treated – SSc mice, display similar level of GSH approaching to fibroblasts from control mice. Therefore, despite its prooxidative activity, they paradoxically improves the antioxidant status of the SSc-skin. Indeed, as in human, mice SSc skin contains a mixed population of "diseased" myofibroblasts, the majority (about 70%) and normal fibroblasts minority (about 30%). Controrary to normal fibroblasts, treatment with those prooxidative molecules leads to the death of myofibroblasts, which overproduce H<sub>2</sub>O<sub>2</sub> and are deficient in GSH. For this reason, proxidative molecules - (PHTE)<sub>2</sub>NQ or DPTTS, have paradoxically antioxidant activity in the skin of SSc mice.

We have also observed the anti-oxidant effect of those compounds at the systemic level. The serum level of AOPP was reduced in mice treated with (PHTE)<sub>2</sub>NQ or DPTTS compared to untreated SSc mice. AOPP is generated in the skin by SSc fibroblasts that overproduce ROS, and are transported by the circulation into the tissues [208].

Since AOPP are released by SSc fibroblasts, the selective killing of those cells, early in the course of the disease, explain the decrease of AOPP level in the serum of SSc-mice treated with (PHTE)<sub>2</sub>NQ or DPTTS. Furthermore, in HOCl-induced SSc, AOPP can elicit the apoptosis of endothelial cells and cause vascular damages. *In vivo* treatment of SSc-mice with (PHTE)<sub>2</sub>NQ or DPTTS reduces the levels of AOPP. In addition, (PHTE)<sub>2</sub>NQ treatment reduces the concentration of nitrates, a marker of vascular activation and injury in murine and human SSc. Those results reflect the beneficial effect of (PHTE)<sub>2</sub>NQ and DPTTS on the vascular part of the disease.

One of the major consequences of the oxidative stress in diseased fibroblasts is their transformation into myofibroblasts expressing  $\alpha$ -SMA and their increased production of type I collagen [7]. The skin and lungs of patients with SSc contain myofibroblasts that displays an excessive rate of fibroblasts proliferation. The same observation has been made in the mouse model of HOCl induced SSc [162]. Selective destruction of SSc fibroblasts by (PHTE)<sub>2</sub>NQ or DPTTS is followed by the decrease in the numbers of myofibroblasts that correlate with down-regulation of  $\alpha$ -SMA, and decrease in the concentration of type I collagen in the skin and lung of treated SSc mice compared to untreated SSc mice.

Several reports have linked the intracellular oxidative burst and the initiation of the immune response in human or in murine models of SSc . Indeed, the high amounts of ROS lead to the oxidation of proteins, in particular of DNA-topoisomerase I. The oxidation of DNA-topoisomerase I is a key event in the breach of immune tolerance in both mice and human SSc and the released of high amounts of oxidized topoisomerase-1 favour the production of anti Topoisomerase I Abs. The selective destruction of SSc fibroblats that chronically produce high levels of intracellular ROS by (PHTE)<sub>2</sub>NQ or

DPTTS, explains the decreased release of oxidized DNA-topoisomerase-1, and in consequence the decrease production of anti-DNA-topoisomerase-1 Abs.

In addition, DPTTS treatment exerts an immuno-regulating effect in SSc mice, reflected by the reduction in B cell numbers in the spleens of treated mice and by the reduction in hyper-proliferation of CD3/CD28-activated T cells and the proliferation of LPS-activated B cells. The beneficial effect of DPTTS on the immune system also results in the decrease in spleen production of IL-4 and IL-13, two cytokines that trigger the synthesis of collagen in human skin fibroblasts, and whose concentrations are elevated in the skin and serum of SSc patients.

Article 1 and 2 shows that organotelluride catalyst (PHTE)<sub>2</sub>NQ and natural organosulfur DPTTS, can interact with intracellular ROS generated in SSc fibroblasts to selectively kill the cells. This observation suggests a new therapeutic strategy in SSc, which is based on the modulation of the intracellular redox state of the activated fibroblasts.

Various studies indicate an important role of nitrosative stress in SSc patients [7, 206, 207]. Nitric oxide (NO) is one of the most important mediators of the nitrosative stress and a relevant physiological signaling molecule. In SSc patients, the serum levels of NO are significantly elevated, as evidenced by increased nitrate levels, increased expression of 3-nitrotyrosine in diseased tissue, and increased exhaled NO [206]. NO can be either beneficial because of its vasodilating properties, or deleterious when combining with superoxide anions in an inflammatory context, to form the highly toxic molecule peroxynitrite that is responsible for vascular damages and fibrosis [207]. NO is synthesized from L-arginine by nitric oxide synthase (NOS). Increased levels of NO in SSc patients can be caused by excessive expression of NOS, especially of inducible nitric oxide synthase (iNOS). In various cell types, this enzyme is known to be activated by a variety of inflammatory signals such as cytokines and ligands of toll-like receptors [236].

In the Article 3, we shows that Irbesartan, a blocker of the angiotensin II type 1 receptor (AT<sub>1</sub>R), prevents fibrosis in a mice model of SSc, mostly through the inhibition of the nitrosative stress. Angiotensin II is able to stimulate the production of nitric oxide by various cells, including endothelial cells and fibroblasts [237]. Increasing doses of irbesartan progressively decrease iNOS expression in cytokine-activated human pulmonary microvascular endothelial cells [236]. As a consequence, the level of NO but also of hydrogen peroxide and of superoxide anions in cytokine-activated human pulmonary microvascular endothelial cells is also reduced by irbesartan. The peroxynitrites generated following the hyperproduction of NO can induce changes in the structure and function of normal proteins and lead to cell death and tissue damages [238]. 3-nitrotyrosine is a product of tyrosine nitration mediated by peroxynitrites and reflects the extent of tissular damages caused by the nitrosative stress [228]. 3-nitrotyrosine is increased in HOCl-mice, but down regulated in the skin and lungs by irbesartan. Additionally, *in vivo* administration of irbesartan abrogates the expression of iNOS in the lungs of SSc mice. As a consequence, exhaled nitric oxide, which is a highly relevant marker of the extent of lung involvement in systemic sclerosis, is reduced in HOCl-mice treated with irbesartan [239]. Nitric oxide is largely metabolized into nitrites, which are increased in the serum of SSc patients and also in HOCl-mice. The nitrosative stress induces vascular damages and elevated serum levels of soluble E-selectine. Administration of irbesartan reduces the level of both serum nitrite and E-selectine in HOCl-mice, confirming the efficacy of an AT<sub>1</sub>R blocker in the prevention of the systemic nitrosative stress *in vivo* and of its consequences on the vascular damages in HOCl-mice.

Moreover, administration of irbesartan *in vivo* down-regulates the phosphorylation of Smad2/3 and secondarily decreases the accumulation of type I collagen in the skin of HOCl-mice compared to untreated HOCl mice [242]. Phosphorylated Smad2 or Smad3

are transcription factors overexpressed in fibroblasts from HOCl-mice that activate genes coding for type I collagen, thus leading to fibrosis in several organs. Our results are in agreement with a recent study showing that angiotensin II activates Smad signalling through the AT<sub>1</sub> receptor-mediated ERK1/2 MAPK pathway, inducing the accumulation of type I collagen [210]. Another study has connected skin fibrosis in SSc with the stabilization of the oncogene H-Ras following the stimulation of ROS production by autoantibodies. Ras proteins are members of a large family of small membrane-bound GTPases which control profibrotic pathways engaged by TGFβ, angiotensin II, platelet-derived growth factor (PDGF) or ROS [212]. Recent reports have shown that increased levels of H-Ras protein can directly stimulate Smad2/3 signalling and type I collagen accumulation [212, 243]. We found that irbesartan reduced the expression of H-Ras in the skin and lungs of SSc mice, which can also explain the reduction in fibrosis in HOCl-mice compared to untreated HOCl-mice.

Irbesartan reduces an abnormal activation of immune cells through the reduction of number of splenic B cells, of CD4<sup>+</sup> and CD8<sup>+</sup> T cells [233, 234]. In addition, irbesartan reduces the hyper-proliferation of CD3/CD28-activated T cells and the proliferation of LPS-activated B cells observed in HOCl-mice. These effects on B

T cells are in agreement with our observation that H-Ras expression is dose-dependently decreased *in vitro* by irbesartan in LPS- and in anti-CD3 mAb-activated splenocytes. Indeed, H-Ras acts as a critical controller of T helper cell responses mostly by transmitting TCR signals that prime CD4 (+) T cells and trigger B cell activation [244]. This immunosuppressing effect of irbesartan can explain why the increased levels of anti-topoisomerase I Abs in the serum of the HOCl-mice are reduced by irbesartan. Moreover, the *in vivo* abrogation of the auto-immune response by irbesartan in HOCl-mice can also

be explained by its antioxidant properties that limits the oxidation of DNA-topoisomerase I and thus prevents the production of autoantigen.

Article 3 shows that in addition to the effectiveness of Irbesartan in the treatment of the renal crisis of SSc, irbesartan and other AT<sub>1</sub> R blockers should be evaluated as anti fibrotic and immunomodulating drugs in SSc patients with diffuse fibrosis.

## **Conclusions and perspective**

---

Our work confirms an important role of reactive oxygen / nitrogen species in the pathogenesis of SSc. Many studies confirmed that there is an increased oxidative stress in SSc patients [6, 7]. This phenomenon contributes directly to the deregulation of various signalling pathways leading to hyper-proliferative phenotype of fibroblasts and as a consequence to synthesis of collagen I and fibrosis. The importance of ROS in SSc has first been highlighted in our laboratory by showing that sera from SSc patients do not only induce ROS production by endothelial cells but also increase the proliferation of fibroblasts [245]. SSc is characterized by an abnormal proliferation of fibroblast which

differentiates into activated myofibroblasts that express alpha smooth muscle actin ( $\alpha$ -SMA).

To better understand the role of ROS in the SSc process we have conducted *in vivo* experiments. Injections of various types of ROS-inducing agents were performed on normal and immunodeficient mice. Those studies led us to develop new and more representative mice models of human SSc [162]. The importance of ROS encouraged us to test new therapeutic approaches using ROS modulators. SSc fibroblasts produce large amounts of ROS. We used this properties to selectively kill SSc fibroblasts with pro-oxidative compounds. We have demonstrated that cytotoxic molecules like organotellurium catalyst-(PHTE)<sub>2</sub>NQ and natural organosulfur-DPTTS can increase the level of ROS leading to a lethal oxidative stress in SSc fibroblasts but not in normal fibroblasts.

Moreover, various NO production may contribute to the development of SSc vascular disease by enhancing studies indicate an important role of nitrosative stress in SSc patients. platelet aggregation, upregulating endothelial and leucocyte adhesion molecules, and increasing wall thickness. Further, NO can enhance proliferation of fibroblasts, collagen synthesis, and production and activity of extracellular matrix. NO production is modulated by Angiotensin II. Our study have confirmed an important role NO production of in SSc. We have demonstrated that irbesartan, an angiotensin II receptor I antagonist, can decrease nitrosative stress which contributes to the decline of vascular disease, and skin and lung fibrosis in murine fibrosis model.

The current therapies arsenal does not propose molecules acting on ROS level. Our results open new perspectives for the SSc treatment.

## **Appendices**

---

In this chapter I will present the rest of publications in which I am co-author.

## Reactive Oxygen Species–Mediated Killing of Activated Fibroblasts by Arsenic Trioxide Ameliorates Fibrosis in a Murine Model of Systemic Sclerosis

Niloufar Kavian,<sup>1</sup> Wioleta Marut,<sup>2</sup> Amélie Servettaz,<sup>3</sup> Carole Nicco,<sup>2</sup> Christiane Chéreau,<sup>2</sup> Hervé Lemaréchal,<sup>4</sup> Didier Borderie,<sup>4</sup> Nicolas Dupin,<sup>1</sup> Bernard Weill,<sup>1</sup> and Frédéric Batteux<sup>1</sup>

**Objective.** In patients with systemic sclerosis (SSc), activated fibroblasts produce reactive oxygen species (ROS) that stimulate their proliferation and collagen synthesis. By analogy with tumor cells that undergo apoptosis upon cytotoxic treatment that increases ROS levels beyond a lethal threshold, we tested whether activated fibroblasts could be selectively killed by the cytotoxic molecule arsenic trioxide (As<sub>2</sub>O<sub>3</sub>) in a murine model of SSc.

**Methods.** SSc was induced in BALB/c mice by daily intradermal injections of HOCl. Mice were simultaneously treated with daily intraperitoneal injections of As<sub>2</sub>O<sub>3</sub>.

**Results.** As<sub>2</sub>O<sub>3</sub> limited dermal thickness and inhibited collagen deposition, as assessed by histologic examination and measurement of mouse skin and lung collagen contents. As<sub>2</sub>O<sub>3</sub> abrogated vascular damage, as shown by serum vascular cell adhesion molecule 1 level, and inhibited the production of autoantibodies,

interleukin-4 (IL-4), and IL-13 by activated T cells. These beneficial effects were mediated through ROS generation that selectively killed activated fibroblasts containing low levels of glutathione.

**Conclusion.** Our findings indicate that treatment with As<sub>2</sub>O<sub>3</sub> dramatically improves skin and lung fibrosis in a mouse model of SSc, providing a rationale for the evaluation of As<sub>2</sub>O<sub>3</sub> treatment in patients with SSc.

Disruption of the oxidant–antioxidant balance is a crucial step in the initiation and development of most systemic fibrotic diseases, particularly of liver, pancreatic, renal, and lung fibrosis (1–5). Systemic sclerosis (SSc) is a prototypic systemic fibrotic disease that involves the skin and visceral organs. The first stage of the disease consists of inflammation and the development of vascular abnormalities followed by the spreading of fibrosis. During this early stage, reactive oxygen species (ROS) overproduced by fibroblasts from the skin and internal organs trigger the proliferation of fibroblasts and the synthesis of type I collagen (4). The role of ROS in the initiation of SSc has recently been highlighted in a new murine model based on intradermal injections of HOCl-generating agents that induce skin and visceral fibrosis, vascular disease, and autoimmunity, which are all features that characterize SSc (6). The involvement of the immune system is reflected by the production of various autoantibodies. Autoantibodies to the platelet-derived growth factor receptor activate fibroblasts to produce ROS (7) and establish a loop that perpetuates the disease.

The early inflammatory process and the development of fibrosis caused by fibroblast proliferation and collagen production are stimulated by endogenous ROS up to a certain concentration, beyond which ROS induce

Supported by grants from Université Paris-Descartes and Cephalon. Dr. Kavian's work was supported by a grant from Assistance Publique-Hôpitaux de Paris.

<sup>1</sup>Niloufar Kavian, PharmD, Nicolas Dupin, MD, PhD, Bernard Weill, MD, PhD, Frédéric Batteux, MD, PhD: Université Paris Descartes, EA 1833, and Hôpital Cochin, AP-HP, Paris, France; <sup>2</sup>Wioleta Marut, MS, Carole Nicco, PhD, Christiane Chéreau, PharmD: Université Paris Descartes, EA 1833, Paris, France; <sup>3</sup>Amélie Servettaz, MD, PhD: Université Paris Descartes, EA 1833, Paris, France, and Hôpital Robert Debré, Reims, France; <sup>4</sup>Hervé Lemaréchal, PhD, Didier Borderie, MD, PhD: Hôpital Cochin, AP-HP, Paris, France.

Dr. Kavian and Ms Marut contributed equally to this work.

Dr. Batteux has received consulting fees, speaking fees, and/or honoraria from Cephalon (less than \$10,000).

Address correspondence to Frédéric Batteux, MD, PhD, Laboratoire d'Immunologie, EA 1833, Faculté de Médecine Paris Descartes, 27 Rue de Faubourg St. Jacques, 75679 Paris Cedex 14, France. E-mail: frederic.batteux@cch.aphp.fr.

Submitted for publication November 28, 2011; accepted in revised form May 1, 2012.

cell apoptosis. These contrasting effects of ROS have been clearly shown in cancer cells, since long-term exposure to low levels of ROS induces carcinogenesis and tumor progression, whereas the oxidative burst induced by cytotoxic drugs leads to the apoptosis of tumor cells (8).

Since SSC is associated with the activation of fibroblasts that overproduce ROS, we tested the therapeutic effect of the cytotoxic agent arsenic trioxide ( $\text{As}_2\text{O}_3$ ), which raises the intracellular level of ROS (9), in a murine model of SSC.  $\text{As}_2\text{O}_3$  is an inorganic trivalent salt that exhibits potent antitumor effects *in vitro* and *in vivo* (10,11), especially in the treatment of hematologic malignancies (12). It can affect many cellular functions, such as proliferation, apoptosis, differentiation, and angiogenesis, in various cell lines. Transformed keratinocytes (13) or activated autoimmune lymphocytes (14) can also be killed by ROS-mediated apoptosis triggered by  $\text{As}_2\text{O}_3$ . In this study, we evaluated the effects of  $\text{As}_2\text{O}_3$  on fibrotic, vascular, and immune dysregulation in mice with HOCl-induced SSC, an inflammatory model of SSC characterized by an early activation of fibroblasts by ROS.

## MATERIALS AND METHODS

**Isolation of fibroblasts from the skin of mice.** Fragments of diseased skin were collected from the backs of the mice at the time they were killed. Skin samples (from control mice and from mice with HOCl-induced SSC) were digested with Liver Digest Medium (Invitrogen) for 1 hour at 37°C. After 3 washes, cells were seeded in sterile flasks, and isolated fibroblasts (control or SSC) were seeded in 96-well plates (Corning Costar) and then cultured in Dulbecco's modified Eagle's medium/Glutamax I supplemented with 10% heat-inactivated fetal calf serum (FCS) and antibiotics.

**Measurement of intracellular levels of glutathione (GSH),  $\text{H}_2\text{O}_2$ , and  $\text{O}_2^-$  released by fibroblasts in response to *in vitro* treatment with  $\text{As}_2\text{O}_3$ .** Fibroblasts were coated in triplicate in 96-well microplates ( $8 \times 10^3$  cells/well) and incubated with complete medium for 24 hours at 37°C. Various doses of  $\text{As}_2\text{O}_3$  (0–40  $\mu\text{M}$ ) were added for the last 6 hours of culture. Levels of  $\text{H}_2\text{O}_2$ ,  $\text{O}_2^-$ , and GSH were assessed by spectrofluorometry (Fusion; PerkinElmer) using 2',7'-dichlorodihydrofluorescein diacetate ( $\text{H}_2\text{DCF-DA}$ ), dihydroethidium (DHE), and monochlorobimane (all from Molecular Probes), respectively. Cells were incubated with 200  $\mu\text{M}$   $\text{H}_2\text{DCF-DA}$ , DHE, or 50  $\mu\text{M}$  monochlorobimane in phosphate buffered saline (PBS) for 30 minutes at 37°C. Fluorescence intensity was read every hour for 6 hours. Results are expressed as arbitrary units (AU) of fluorescence intensity per million viable cells.

***In vitro* assay of  $\text{As}_2\text{O}_3$  cytotoxicity on mouse fibroblasts.** Fibroblasts were coated in triplicate ( $8 \times 10^3$  cells/well) and incubated with complete medium alone or with 10  $\mu\text{M}$   $\text{As}_2\text{O}_3$  for 48 hours at 37°C. The numbers of viable cells were

evaluated by crystal violet assay. Results are expressed as percentage viability among cells that were exposed to  $\text{As}_2\text{O}_3$  or left untreated.

**Modulation of ROS metabolism in fibroblasts from control mice and mice with HOCl-induced SSC.** Isolated fibroblasts from normal mice or mice with HOCl-induced SSC ( $2 \times 10^4$  cells/well) were seeded in 96-well plates and incubated for 24 hours in complete medium alone or with the following molecules: 3.2 mM *N*-acetylcysteine (NAC), 1.6 mM DL-buthionine-(*S,R*)-sulfoximine (BSO), 20 units polyethylene glycol (PEG)-catalase, 400  $\mu\text{M}$  aminotriazole, or 8  $\mu\text{M}$  diethyl dithiocarbamate (DDC).  $\text{As}_2\text{O}_3$  (10  $\mu\text{M}$ ) was added for the last 6 hours. Cells were then washed 3 times with PBS and incubated with 100  $\mu\text{l}$  per well of 200  $\mu\text{M}$   $\text{H}_2\text{DCF-DA}$  or 50  $\mu\text{M}$  monochlorobimane for 30 minutes.  $\text{H}_2\text{O}_2$  and GSH levels were expressed as described above.

**HOCl-induced SSC. Induction of SSC in BALB/c mice by intradermal injections of HOCl-generating solution.** Six-week-old female BALB/c mice were purchased from Harlan and maintained with food and water *ad libitum*. They were given humane care according to the guidelines of Université Paris Descartes. Mice were randomly distributed into experimental and control groups ( $n = 21$  per group). SSC was induced according to the protocol described by Servetaz et al (6), with minor modifications. A total of 400  $\mu\text{l}$  (2 injections of 200  $\mu\text{l}$  each) of a solution generating HOCl was prepared extemporaneously and injected intradermally into the shaved backs of the mice, using a 27-gauge needle, every day for 6 weeks (HOCl-injected mice). HOCl was produced by adding NaClO solution (9.6% active chlorine) to  $\text{KH}_2\text{PO}_4$  solution (100 mM; pH 6.2) (15). HOCl concentration was determined by measuring the optical density (OD) of the solution at 292 nm and then adjusted to obtain an OD between 0.7 and 0.9. Control mice received injections of 400  $\mu\text{l}$  of sterilized PBS (PBS-injected mice).

**Treatment of HOCl-injected mice with  $\text{As}_2\text{O}_3$ .** Mice were randomized and treated simultaneously with either HOCl-generating solution or PBS and intraperitoneal injections of either  $\text{As}_2\text{O}_3$  or vehicle alone for 6 weeks ( $n = 14$  per group). A stock solution was prepared extemporaneously by dissolving  $\text{As}_2\text{O}_3$  powder (Sigma-Aldrich) in 1M NaOH and diluting it 1:200 in PBS.  $\text{As}_2\text{O}_3$  was administered intraperitoneally 5 days a week at a dose of 5  $\mu\text{g}/\text{gm}$  body weight, which was the optimal dose previously determined by Bobé et al (14). Control mice received intraperitoneal PBS and NaOH (1:200) 5 days a week.

Three days after the last injection, animals were killed by cervical dislocation. Serum samples were collected and stored at  $-80^\circ\text{C}$ . The lungs were removed from each mouse, and a skin biopsy was performed on the back region with a punch (4 mm in diameter) involving the skin and the underlying muscle of the injected area. Mouse spleens were also collected, and splenocyte suspensions were prepared after hypotonic lysis of erythrocytes in potassium acetate solution.

**Assessment of collagen accumulation. Skin thickness.** The thickness of the skin on the shaved backs of the mice was measured (in millimeters) with a caliper 1 day before the mice were killed.

**Histopathologic analysis.** Fixed mouse lung and skin samples were embedded in paraffin. A 5- $\mu\text{m}$ -thick tissue section was prepared and stained with hematoxylin and eosin

(H&E) or with picosirius red. Slides were examined by standard brightfield microscopy (Olympus BX60) by a pathologist (FB) who was blinded with regard to treatment group.

**Collagen content in the mouse skin and lungs.** Mouse skin and lung samples were diced using a scalpel, placed into tubes, thawed, and mixed with pepsin (1:10 weight ratio) and 0.5M acetic acid overnight at room temperature under stirring. The collagen content assay was based on the quantitative Sircol dye-binding method (Biocolor).

**Immunohistochemical analysis of phospho-Smad2/3 in the diseased skin of mice.** Sections of diseased mouse skin were deparaffinized, and antigen retrieval was performed by incubating the slides with proteinase K (Dako) for 20 minutes. Slides were then incubated with 3% H<sub>2</sub>O<sub>2</sub> for 10 minutes, and then with 5% bovine serum albumin and 1% rabbit serum to block nonspecific binding. Slides were immunostained with a mouse monoclonal antibody directed to phospho-Smad2/3 (Cell Signaling Technology) for 1 hour. After washing in Tris buffered saline-Tween (TBST), slides were incubated with alkaline phosphatase-labeled rabbit anti-mouse secondary antibody (Rockland) for 1 hour. Staining was visualized with a diaminobenzidine solution kit (Sigma). Irrelevant isotype-matched antibodies were used as negative controls. All slides were analyzed by 2 independent pathologists (BW and FB) who were blinded with regard to treatment group. Images were obtained with a digital camera on an Olympus BX60 microscope using DP Manager software, at a magnification of  $\times 100$ , and analyzed using ImageJ Software version 1.36 (NIH Image, National Institutes of Health; online at <http://rsbweb.nih.gov/ij/>).

**Western blot analysis of  $\alpha$ -smooth muscle actin ( $\alpha$ -SMA) protein in mouse fibroblasts.** Mouse fibroblasts were isolated from skin biopsy specimens as described above. Proteins (30  $\mu$ g per well) were subjected to 10% polyacrylamide gel electrophoresis, transferred onto nitrocellulose membranes, blocked with 5% nonfat dry milk in TBST, and then incubated overnight at 4°C with an  $\alpha$ -SMA antibody (clone 1A4; Sigma). The membranes were then washed and incubated with a horseradish peroxidase-conjugated secondary antibody (Santa Cruz Biotechnology) for 1 hour. Immunoreactive signals were revealed with ECL (Amersham).

**Measurement of oxidized derivatives in mouse sera.** *Concentrations of advanced oxidation protein products.* The concentrations of advanced oxidation protein products were measured by spectrophotometry as previously described (16). The assay was calibrated using chloramine T.

*Nitrate levels.* Nitrate levels were measured by spectrophotometry using oxidation catalyzed by cadmium metal (Bioxytech assay kit; Oxis), which converts nitrates into nitrites. The detection limit for nitrites was 0.1  $\mu$ moles/liter.

**Measurement of intracellular GSH levels in fibroblasts from treated mice.** Fibroblasts were isolated from the skin of the mice (n = 10 per group) and seeded as described above. The levels of GSH were assessed by spectrofluorometry using monochlorobimane staining, as described above. The number of viable cells was evaluated by crystal violet assay.

**Determination of soluble vascular cell adhesion molecule 1 (sVCAM-1) concentrations in mouse sera.** Levels of sVCAM-1 in mouse sera were measured by enzyme-linked immunosorbent assay (ELISA) using a 1:800 dilution of sera and a mouse VCAM-1/CD106 DuoSet kit according to the recommendations of the manufacturer (R&D Systems).

#### Flow cytometric analysis of mouse spleen cell subsets.

Cell suspensions from mouse spleens were prepared after hypotonic lysis of erythrocytes in potassium acetate solution. Cells were incubated with the appropriate labeled antibody at 4°C for 30 minutes in PBS with 0.1% sodium azide and 5% normal rat serum. Flow cytometry was performed on a FACSCanto flow cytometer (BD Biosciences) using standard techniques. The monoclonal antibodies used were phycoerythrin [PE]-Cy7-conjugated anti-B220, biotin-conjugated anti-CD11b, PerCP-conjugated anti-CD4, and PE-Cy7-conjugated anti-CD8 monoclonal antibodies (all from BD Biosciences). Data were analyzed with FlowJo software (Tree Star).

#### Assays of serum immunoglobulins and autoantibodies.

Levels of anti-DNA topoisomerase I (anti-topo I) IgG antibodies were detected by ELISA on microtiter plates (Immuno Vision). Levels of total mouse IgG and IgM antibodies were measured using a standard ELISA as previously described (17). A 1:50 serum dilution was used for the determination of all antibodies.

**Determination of mouse splenocyte production of interleukin-4 (IL-4), IL-13, and interferon- $\gamma$  (IFN $\gamma$ ) by ELISA.** Mouse spleen cells were cultured in RPMI 1640 supplemented with antibiotics, Glutamax (Invitrogen Life Technologies), and 10% heat-inactivated FCS (Invitrogen Life Technologies) (complete medium). Spleen cell suspensions ( $2 \times 10^5$  cells) were seeded in 96-well flat-bottomed plates and cultured in complete medium for 48 hours in the presence of 5  $\mu$ g/ml concanavalin A. Supernatants were collected, and cytokine concentrations were determined by ELISA (for IL-4, IL-13, and IFN $\gamma$ ; eBioscience). Results are expressed as nanograms per milliliter.

**Analysis of IL-13 expression in mouse skin fibroblasts by reverse transcriptase-polymerase chain reaction (RT-PCR).** TRIzol reagent (Invitrogen) was used to extract RNA from skin fibroblasts isolated from mice (n = 7 per group). IL-13 complementary DNA (cDNA) was quantified by semiquantitative RT-PCR, using the following primers: forward 5'-CCTGGCTCTTGCTTGCCCTT-3' and reverse 5'-GGTCTTGTGTGATGTTGCTCA-3'. IL-13 cDNA levels were normalized to  $\beta$ -actin expression, using the following primers: forward 5'-GTGGGCCGCTCTAGGCACCAA-3' and reverse 5'-CTCTTTGATGTCACGCACGATTTC-3'.

**Statistical analysis.** Quantitative data were analyzed using GraphPad Prism software version 5, using one-way analysis of variance as appropriate, and are expressed as the mean  $\pm$  SEM. *P* values less than 0.05 were considered significant.

## RESULTS

**Cytotoxic and pro-oxidative effects of As<sub>2</sub>O<sub>3</sub> on fibroblasts from mice with HOCl-induced SSc in vitro.** Fibroblasts from control mice and mice with HOCl-induced SSc were exposed in vitro to increasing concentrations of As<sub>2</sub>O<sub>3</sub> (from 0 to 40  $\mu$ M). The basal production (without As<sub>2</sub>O<sub>3</sub>) of H<sub>2</sub>O<sub>2</sub> was increased by 34% in fibroblasts from mice with HOCl-induced SSc compared

to fibroblasts from normal mice ( $P = 0.035$ ) (Figure 1A). Incubation of control fibroblasts with low doses (2.5–10  $\mu\text{M}$ ) of  $\text{As}_2\text{O}_3$  did not significantly affect their production of  $\text{H}_2\text{O}_2$ . Only high doses of  $\text{As}_2\text{O}_3$  (20–40  $\mu\text{M}$ ) significantly increased  $\text{H}_2\text{O}_2$  production in those cells. In contrast, fibroblasts from mice with HOCl-induced SSc were hypersensitive to the oxidative effects of  $\text{As}_2\text{O}_3$ . At 2.5  $\mu\text{M}$  and 5  $\mu\text{M}$ ,  $\text{As}_2\text{O}_3$  increased the production of  $\text{H}_2\text{O}_2$  by fibroblasts from mice with HOCl-induced SSc by 34% and 64%, respectively, compared to that in untreated fibroblasts from

mice with HOCl-induced SSc ( $P = 0.06$  and  $P = 0.004$ , respectively) (Figure 1A). With  $\text{As}_2\text{O}_3$  concentrations from 10  $\mu\text{M}$  to 40  $\mu\text{M}$ , the production of  $\text{H}_2\text{O}_2$  by fibroblasts from mice with HOCl-induced SSc was increased by  $\geq 85\%$  ( $P = 0.025$  for fibroblasts from mice with HOCl-induced SSc treated with 10  $\mu\text{M}$   $\text{As}_2\text{O}_3$  versus untreated fibroblasts from mice with HOCl-induced SSc) (Figure 1A).

The basal level of GSH, an essential cofactor of  $\text{H}_2\text{O}_2$  catabolism, was decreased by 51% in fibroblasts from mice with HOCl-induced SSc compared to fibro-

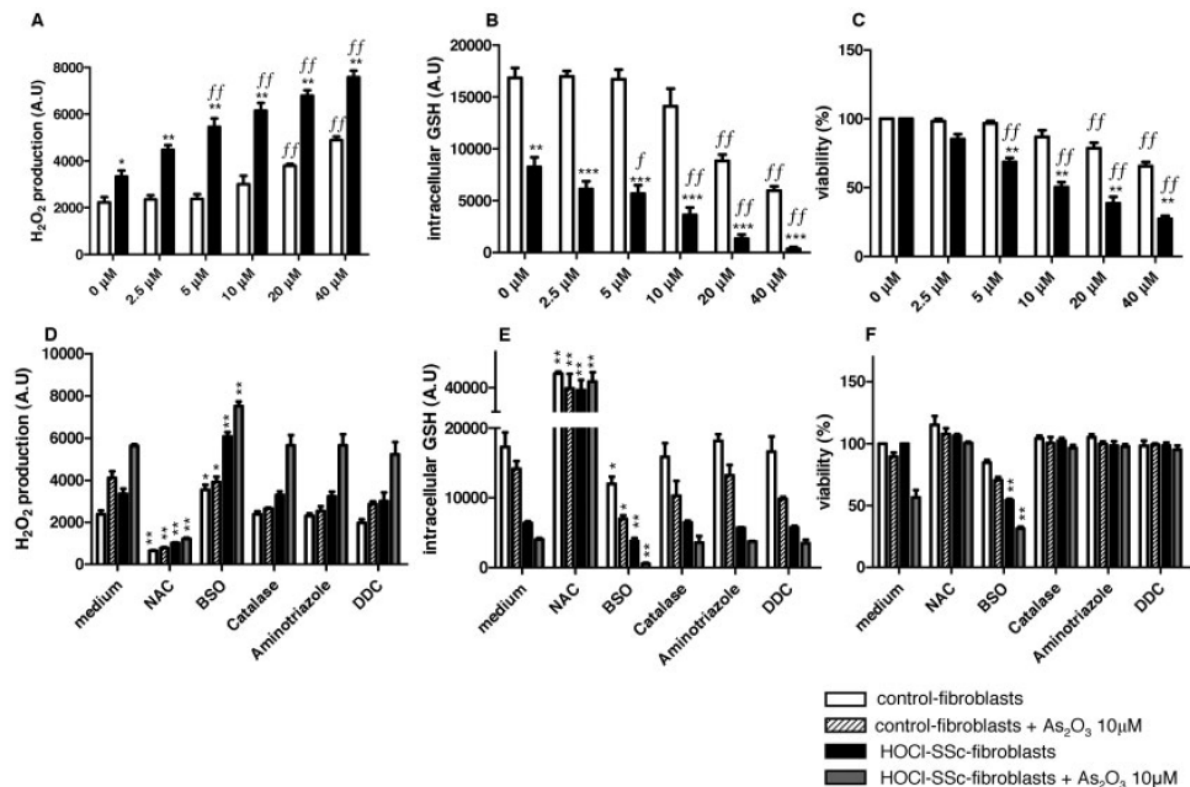


**Figure 1.** Dose-response effect and modulation of reactive oxygen species (ROS) metabolism in mouse fibroblasts treated with arsenic trioxide ( $\text{As}_2\text{O}_3$ ). A–C, Fibroblasts from control mice or mice with HOCl-induced systemic sclerosis (SSc) were seeded in a 96-well plate ( $8 \times 10^3$  cells/well) in triplicate and exposed to various doses of  $\text{As}_2\text{O}_3$  (ranging from 2.5 to 40  $\mu\text{moles/liter}$ ) or to medium alone for 6 hours. Production of  $\text{H}_2\text{O}_2$  (A), intracellular levels of glutathione (GSH) (B), and viability (C) were measured on a spectrofluorometer. Values are the mean  $\pm$  SEM ( $n = 3$  mice per group). \* =  $P < 0.05$ ; \*\* =  $P < 0.01$ ; \*\*\* =  $P < 0.001$ , versus fibroblasts from control mice treated with the same concentration of  $\text{As}_2\text{O}_3$ ;  $f = P < 0.05$ ;  $ff = P < 0.01$ , versus untreated fibroblasts from the same group (control mice or mice with HOCl-induced SSc). D–F, Fibroblasts from control mice or mice with HOCl-induced SSc were seeded in a 96-well plate ( $8 \times 10^3$  cells/well) in triplicate with various chemical and enzymatic ROS modulators (*N*-acetylcysteine [NAC], DL-buthionine-(*S,R*)-sulfoximine [BSO], catalase, aminotriazole, or diethyl dithiocarbamate [DDC]) for 24 hours and were given no additional treatment or were exposed to  $\text{As}_2\text{O}_3$  (10  $\mu\text{moles/liter}$ ) for the last 6 hours of culture. Production of  $\text{H}_2\text{O}_2$  (D), intracellular levels of GSH (E), and viability (F) were measured on a spectrofluorometer. Values are the mean  $\pm$  SEM ( $n = 3$  mice per group). \* =  $P < 0.05$ ; \*\* =  $P < 0.01$ , versus fibroblasts without ROS modulator. AU = arbitrary units.

blasts from control mice ( $P = 0.0007$ ) (Figure 1B).  $As_2O_3$  induced a reduction in the GSH content in fibroblasts from both control mice and mice with HOCl-induced SSc in a dose-dependent manner. In control mouse fibroblasts,  $As_2O_3$  had this effect only at high concentrations (from 10 to 40  $\mu M$ ), whereas in fibroblasts from mice with HOCl-induced SSc the molecule significantly decreased the intracellular GSH content at concentrations as low as 5  $\mu M$  ( $P = 0.042$ ) (Figure 1B).

We also investigated the effects of  $As_2O_3$  on  $O_2^-$  production. The basal production of  $O_2^-$  did not differ between fibroblasts from control mice and those from mice with HOCl-induced SSc (data not shown). The addition of  $As_2O_3$  to the culture medium did not affect the production of  $O_2^-$  by fibroblasts from control mice or mice with HOCl-induced SSc, even at high concentrations (data not shown).

$As_2O_3$  had a powerful cytotoxic effect on fibroblasts from mice with HOCl-induced SSc compared to fibroblasts from PBS-injected mice. Indeed, the rate of viability of fibroblasts from control mice was affected only slightly by in vitro treatment with  $As_2O_3$ , varying from 98% viability after treatment with 2.5  $\mu M$   $As_2O_3$  to 78% viability after treatment with 20  $\mu M$   $As_2O_3$  (Figure 1C). Inversely, the viability rate of fibroblasts from mice with HOCl-induced SSc in the presence of  $As_2O_3$  was 85% with 2.5  $\mu M$  ( $P = 0.059$  versus untreated fibroblasts from mice with HOCl-induced SSc), 68% with 5  $\mu M$  ( $P = 0.006$ ), 50% with 10  $\mu M$  ( $P = 0.003$ ), 38% with 20  $\mu M$  ( $P = 0.003$ ), and 27% with 40  $\mu M$  ( $P = 0.002$ ) (Figure 1C). After these dose-effect experiments were completed, a dose of 10  $\mu M$  was chosen for further experiments on the modulation of ROS metabolism by  $As_2O_3$ .

**Modulation of  $H_2O_2$  metabolism in mouse fibroblasts by  $As_2O_3$ .** Using specific modulators of enzymatic and nonenzymatic systems involved in  $H_2O_2$  metabolism, we investigated the mechanism of action of  $As_2O_3$ . Fibroblasts from control mice and from mice with HOCl-induced SSc were incubated with NAC, BSO, catalase, DDC, or aminotriazole, with or without 10  $\mu M$   $As_2O_3$ .

NAC, a precursor of GSH, significantly decreased the production of  $H_2O_2$  and increased the intracellular levels of GSH in untreated fibroblasts from control mice and mice with HOCl-induced SSc. Coincubation of  $As_2O_3$  with NAC decreased the production of  $H_2O_2$  by >70% in fibroblasts from both control mice and those with HOCl-induced SSc ( $P = 0.003$  for both cell types) (Figure 1D).  $As_2O_3$  and NAC increased the intracellular levels of GSH in fibroblasts from control

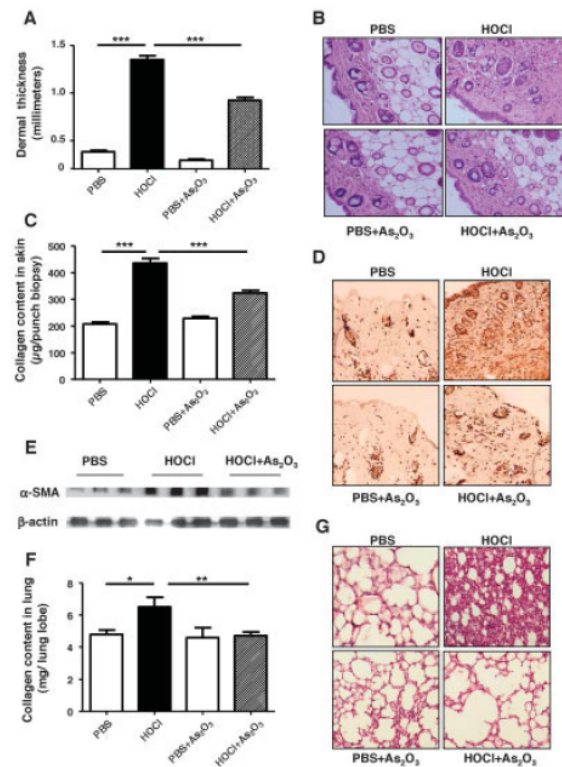


**Figure 2.** Reduction in skin and lung fibrosis in mice with HOCl-induced systemic sclerosis treated with arsenic trioxide ( $As_2O_3$ ). BALB/c mice received daily intradermal injections of HOCl or phosphate buffered saline (PBS) and were concomitantly treated with  $As_2O_3$  (5  $\mu g/gm$ ) or vehicle alone for 6 weeks ( $n = 10$  mice per group). **A**, Dermal thickness in the injected areas in the mice. **B**, Representative hematoxylin and eosin (H&E)-stained sections of mouse skin from the injected areas (viewed with an Olympus DP70 Controller). Original magnification  $\times 20$ . **C**, Collagen content in 6-mm punch biopsy specimens of mouse skin, as measured by the quantitative Sircol dye-binding method. **D**, Immunohistochemical analysis of phospho-Smad2/3 expression in mouse skin. Skin sections from the injected areas in the mice were stained with an anti-phospho-Smad2/3 antibody, and staining was revealed with diaminobenzidine. Original magnification  $\times 20$ . **E**, Western blot analysis of  $\alpha$ -smooth muscle actin ( $\alpha$ -SMA) in skin extracts from 3 representative mice (of 10 mice assessed). **F**, Collagen content in mouse lungs, as measured by the quantitative Sircol dye-binding method. **G**, Representative H&E-stained mouse lung sections. Original magnification  $\times 20$ . Values in **A**, **C**, and **F** are the mean  $\pm$  SEM. \* =  $P < 0.05$ ; \*\* =  $P < 0.01$ ; \*\*\* =  $P < 0.001$ , by Mann-Whitney paired U test.

mice by 180% and in fibroblasts from mice with HOCl-induced SSc by 800% ( $P < 0.001$  for both cell types) (Figure 1E).

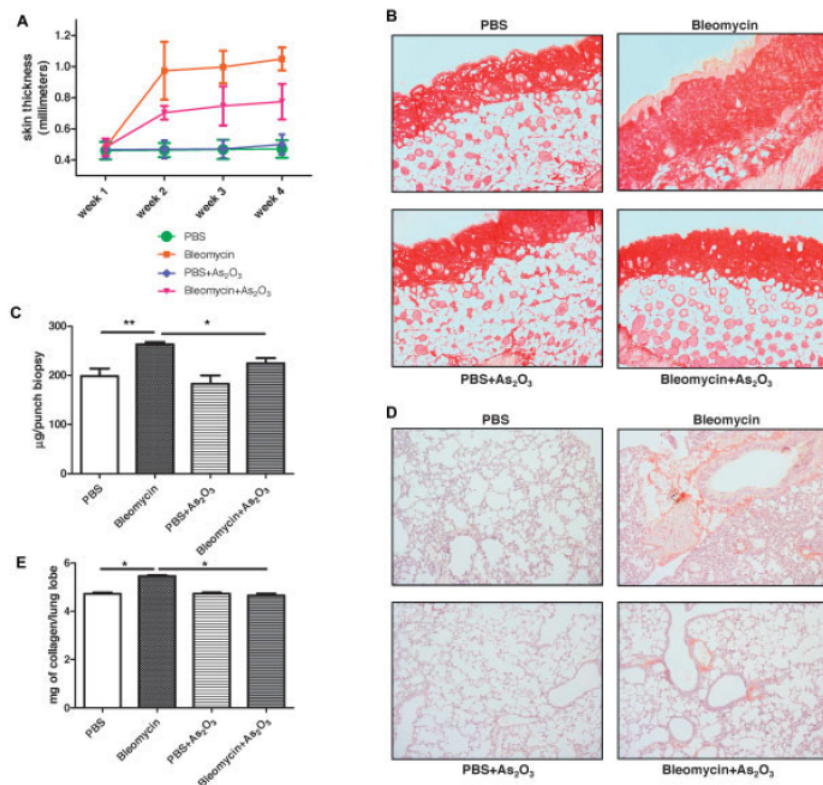


**Figure 3.** Reduction in skin and lung fibrosis in mice with bleomycin-induced systemic sclerosis treated with arsenic trioxide ( $\text{As}_2\text{O}_3$ ). BALB/c mice received daily subcutaneous injections of bleomycin (100  $\mu\text{g}/\text{ml}$ ) or phosphate buffered saline (PBS) and were concomitantly treated with  $\text{As}_2\text{O}_3$  (5  $\mu\text{g}/\text{gm}$ ) or vehicle alone for 5 weeks ( $n = 7$  mice per group). Images were obtained using a Nikon Eclipse 80i microscope and a Nikon Digital Sight DS-U3 camera. **A**, Dermal thickness in the injected areas in the mice. **B**, Representative picosirius red-stained sections of mouse skin from the injected areas. Original magnification  $\times 10$ . **C**, Collagen content in 6-mm punch biopsy specimens of mouse skin, as measured by the quantitative Sircol dye-binding method. **D**, Representative picosirius red-stained mouse lung sections. Original magnification  $\times 10$ . **E**, Collagen content in mouse lungs, as measured by the quantitative Sircol dye-binding method. Values in **A**, **C**, and **E** are the mean  $\pm$  SEM. \* =  $P < 0.05$ ; \*\* =  $P < 0.01$ , by Mann-Whitney paired U test.

In addition, incubation with BSO, a molecule that blocks the synthesis of GSH by selectively inhibiting gamma glutamyl cysteine synthetase, significantly increased the production of  $\text{H}_2\text{O}_2$  by fibroblasts from mice with HOCl-induced SSC ( $P = 0.002$  versus cells incubated without BSO) (Figure 1D) and, inversely, significantly decreased the concentration of GSH in those cells ( $P = 0.003$ ) (Figure 1E). Moreover, the mean  $\pm$  SEM  $\text{H}_2\text{O}_2$  production in fibroblasts from mice with HOCl-induced SSC that were cocultured with  $\text{As}_2\text{O}_3$  and BSO was  $7,522.9 \pm 206.9$  AU, while the mean  $\pm$  SEM  $\text{H}_2\text{O}_2$  production in these fibroblasts incubated with BSO alone was  $6,078 \pm 207.3$  AU, showing the additive

effect of  $\text{As}_2\text{O}_3$  and BSO ( $P = 0.0048$ ). We observed the same additive effect for intracellular levels of GSH in fibroblasts from mice with HOCl-induced SSC (mean  $\pm$  SEM  $3,797.1 \pm 429.37$  AU for BSO alone and  $528.3 \pm 118.1$  AU for BSO and  $\text{As}_2\text{O}_3$ ;  $P = 0.0042$ ).

Increasing the cellular levels of catalase, an enzyme that converts  $\text{H}_2\text{O}_2$  into  $\text{H}_2\text{O}$ , by adding PEG-catalase to medium culture with  $\text{As}_2\text{O}_3$  had no effect on  $\text{H}_2\text{O}_2$  cell production or GSH intracellular levels in either fibroblasts from control mice or fibroblasts from mice with HOCl-induced SSC ( $P = 0.127$  for  $\text{H}_2\text{O}_2$  production and  $P = 0.245$  for GSH level, in both groups) (Figures 1D and E). Blocking catalase with aminotri-

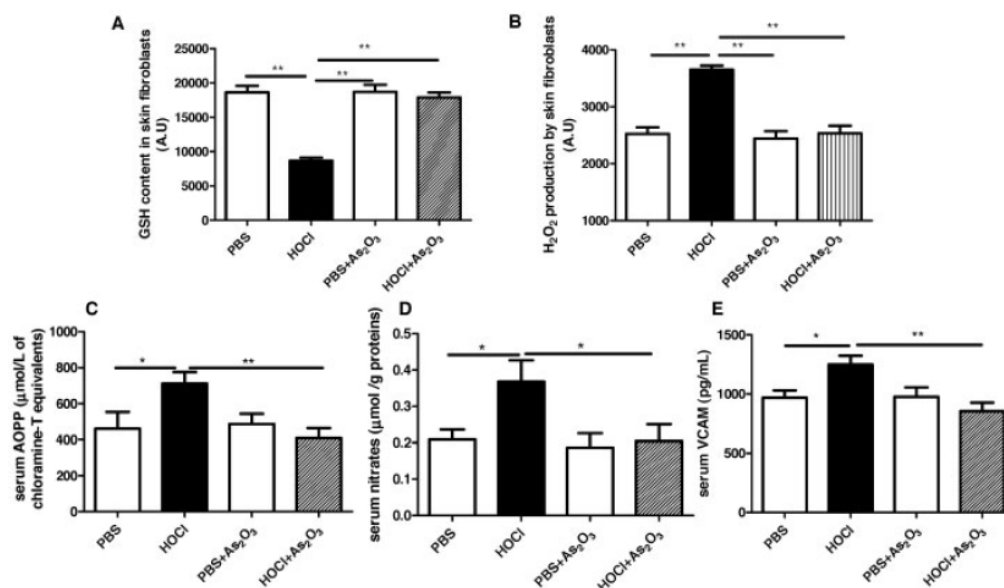


**Figure 4.** In vivo treatment with arsenic trioxide ( $\text{As}_2\text{O}_3$ ) exerts beneficial effects on local and systemic oxidative stress and abrogates endothelial injuries in mice with HOCl-induced systemic sclerosis. BALB/c mice received daily intradermal injections of HOCl or phosphate buffered saline (PBS) and were concomitantly treated with  $\text{As}_2\text{O}_3$  ( $5 \mu\text{g}/\text{g}$ ) or vehicle alone for 6 weeks ( $n = 10$  mice per group). **A**, Intracellular glutathione (GSH) levels in mouse skin fibroblasts. When mice were killed, fibroblasts were isolated from injected skin areas, and GSH levels were determined by spectrofluorometry. Results are expressed as optical density per viable cells. **B**, Levels of  $\text{H}_2\text{O}_2$  production by mouse skin fibroblasts, determined by spectrofluorometry. **C**, Serum levels of advanced oxidation protein products (AOPP) in the indicated groups of mice. **D**, Serum nitrate levels in the indicated groups of mice. **E**, Serum vascular cell adhesion molecule 1 (VCAM-1) concentrations in the indicated groups of mice. Values are the mean  $\pm$  SEM. \* =  $P < 0.05$ ; \*\* =  $P < 0.01$ , by Mann-Whitney paired U test. AU = arbitrary units.

zole did not affect the production of  $\text{H}_2\text{O}_2$  or GSH content in fibroblasts from control mice or mice with HOCl-induced SSc ( $P = 0.262$  for  $\text{H}_2\text{O}_2$  production and  $P = 0.312$  for GSH level, in both groups) (Figures 1D and E). Moreover, adding DDC, an inhibitor of superoxide dismutase, had no effect on either parameter, confirming that  $\text{O}_2^-$  is not involved in  $\text{As}_2\text{O}_3$  cytotoxicity. Taken together, these results indicate that  $\text{As}_2\text{O}_3$  selectively targets fibroblasts from mice with HOCl-induced SSc by depleting GSH and increasing  $\text{H}_2\text{O}_2$  production.

**Reduced skin and lung fibrosis in mice with HOCl-induced SSc treated with  $\text{As}_2\text{O}_3$ .** A significant increase in dermal thickness was observed in mice injected with HOCl compared to those injected with PBS ( $P < 0.001$ ) (Figure 2A). Dermal fibrosis was also significantly increased in HOCl-injected mice versus control mice, as demonstrated by the results of histopathologic analysis of the skin (Figure 2B) and by measurement of type I collagen concentration in skin extracts ( $P < 0.001$ ) (Figure 2C). In vivo treatment with  $\text{As}_2\text{O}_3$  reduced the dermal thickness, histologic signs of

fibrosis, and the accumulation of type I collagen in the skin of HOCl-injected mice ( $P = 0.023$ ) (Figures 2A, B, and C). The myofibroblast marker  $\alpha$ -SMA was overexpressed in the skin of HOCl-injected mice compared to that of PBS-injected mice and was significantly reduced by  $\text{As}_2\text{O}_3$  treatment (Figure 2E). Additionally, expression of phospho-Smad2/3, a key intracellular mediator of fibrosis, was strongly increased in the skin of HOCl-injected mice compared to the unaffected skin of control mice (mean  $\pm$  SEM  $23.2 \pm 2.9$  AU versus  $6.7 \pm 2.3$  AU;  $P = 0.0021$ ) (Figure 2D).  $\text{As}_2\text{O}_3$  treatment of HOCl-injected mice significantly reduced the expression of phospho-Smad2/3 in the skin (mean  $\pm$  SEM  $10.7 \pm 2.5$  AU;  $P = 0.0042$  versus untreated HOCl-injected mice) (Figure 2D).

As in some patients with SSc, lung fibrosis developed in the HOCl-injected mice. Figures 2F and G show the significant increase in type I collagen concentration in the lungs of HOCl-treated mice compared to control mice ( $P = 0.037$ ) and H&E-stained mouse lung biopsy specimens, respectively.  $\text{As}_2\text{O}_3$  abrogated the develop-

ment of lung fibrosis induced by HOCl, as shown by the weaker accumulation of type I collagen in the lungs of the As<sub>2</sub>O<sub>3</sub>-treated mice ( $P = 0.006$ ) (Figure 2F).

The antifibrotic effects of As<sub>2</sub>O<sub>3</sub> were confirmed in a mouse model of bleomycin-induced SSc. Indeed, skin thickness as well as the collagen content of the skin and lungs were significantly reduced in mice receiving bleomycin and concomitantly treated with As<sub>2</sub>O<sub>3</sub> compared to mice receiving bleomycin alone ( $P < 0.0001$  for skin thickness,  $P = 0.0127$  for skin collagen content, and  $P = 0.0079$  for lung collagen content) (Figures 3A, C, and E). Histopathologic analysis of mouse skin and lung sections confirmed these results (Figures 3B and D).

**Reduction in local and systemic oxidative stress and prevention of endothelial injuries in mice with HOCl-induced SSc by in vivo treatment with As<sub>2</sub>O<sub>3</sub>.** Because ROS are major mediators implicated in the development of SSc, and particularly in HOCl-induced SSc, we investigated the in vivo effects of As<sub>2</sub>O<sub>3</sub> on systemic oxidative stress markers at the local and systemic levels. We measured the intracellular levels of GSH, a major antioxidant involved in the cellular defense against ROS, in skin fibroblasts isolated from normal and diseased mice. Mice with HOCl-induced SSc displayed lower levels of GSH in their skin fibroblasts than did mice injected with PBS ( $P = 0.0049$ ) (Figure 4A). In vivo As<sub>2</sub>O<sub>3</sub> treatment of mice with HOCl-induced SSc prevented this decrease in GSH concentration ( $P = 0.003$ ); skin fibroblasts from treated mice displayed GSH levels similar to those observed in control mice (Figure 4A). In addition, fibroblasts isolated from mice with HOCl-induced SSc treated with As<sub>2</sub>O<sub>3</sub> displayed lower levels of H<sub>2</sub>O<sub>2</sub> than did fibroblasts isolated from untreated mice with HOCl-induced SSc (mean  $\pm$  SEM 2,535  $\pm$  131 AU versus 3,652  $\pm$  114 AU;  $P = 0.079$ ) (Figure 4B).

Mice with HOCl-induced SSc had higher serum levels of advanced oxidation protein products, a major marker of the systemic oxidative stress in SSc, than did mice treated with PBS ( $P = 0.048$ ) (Figure 4C). As<sub>2</sub>O<sub>3</sub> reduced the serum concentration of advanced oxidation protein products by 40% in mice exposed to HOCl ( $P = 0.0290$ ) (Figure 4C). The serum concentration of nitrates, a marker of nitrosative stress, reached 0.37  $\mu$ moles/gm of protein in mice with HOCl-induced SSc versus 0.21  $\mu$ moles/gm of protein in control mice ( $P = 0.04$ ) (Figure 4D). In vivo As<sub>2</sub>O<sub>3</sub> treatment of mice with HOCl-induced SSc decreased the concentration of nitrates to 0.20  $\mu$ moles/gm of protein ( $P = 0.042$ ) (Figure 4C). Mice with HOCl-induced SSc displayed higher serum levels of sVCAM-1 than did PBS-injected mice

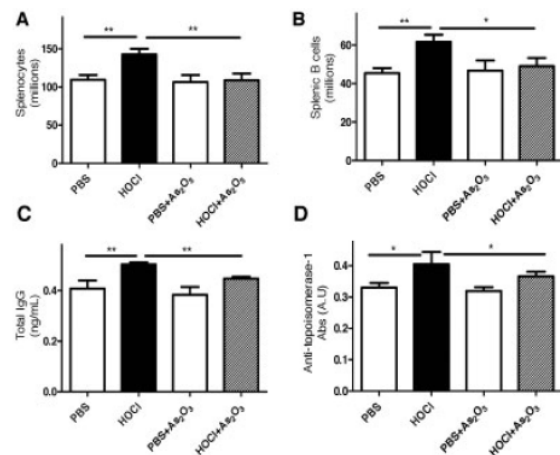


**Figure 5.** Inhibition of the production of autoantibodies in mice with HOCl-induced systemic sclerosis by in vivo treatment with arsenic trioxide (As<sub>2</sub>O<sub>3</sub>). BALB/c mice received daily intradermal injections of HOCl or phosphate buffered saline (PBS) and were concomitantly treated with As<sub>2</sub>O<sub>3</sub> (5  $\mu$ g/gm) or vehicle alone for 6 weeks. A, Total splenocyte numbers on the day mice were killed. B, Splenic B cell numbers, as assessed by flow cytometry, in the indicated groups of mice. C, Total serum IgG antibody levels, as determined by enzyme-linked immunosorbent assay (ELISA), in the indicated groups of mice. D, Serum anti-topoisomerase I antibody levels, as determined by ELISA, in the indicated groups of mice. AU = arbitrary units. Values are the mean  $\pm$  SEM. \* =  $P < 0.05$ ; \*\* =  $P < 0.01$ , by Mann-Whitney paired U test.

(mean  $\pm$  SEM 1,249  $\pm$  74 pg/ml versus 969  $\pm$  61 pg/ml;  $P = 0.026$ ) (Figure 4E). As<sub>2</sub>O<sub>3</sub> reduced serum sVCAM-1 levels in mice with HOCl-induced SSc ( $P = 0.024$ ) (Figure 4E).

**Down-regulation of the expansion of splenic B cells and decrease in the serum levels of anti-topo I autoantibodies in mice with HOCl-induced SSc after treatment with As<sub>2</sub>O<sub>3</sub>.** We next tested the effects of As<sub>2</sub>O<sub>3</sub> on mouse spleen cell populations. Mice with HOCl-induced SSc showed an increase in the total numbers of splenocytes ( $P = 0.039$ ) (Figure 5A), and in the numbers of splenic B cells ( $P = 0.035$ ) (Figure 5B), CD4<sup>+</sup> cells ( $P = 0.048$ ) (Figure 6A), and CD8<sup>+</sup> T cells ( $P = 0.006$ ) (Figure 6B), as compared to PBS-injected mice. As<sub>2</sub>O<sub>3</sub> inhibited the increase in splenic B cells ( $P = 0.043$ ) (Figure 5B), CD4<sup>+</sup> cells ( $P < 0.001$ ) (Figure 6A), and CD8<sup>+</sup> cells ( $P < 0.001$ ) (Figure 6B) in mice with HOCl-induced SSc.

Serum levels of total IgG were elevated in mice with HOCl-induced SSc compared to PBS-injected mice ( $P = 0.0048$ ) (Figure 5C), and treatment with As<sub>2</sub>O<sub>3</sub> led

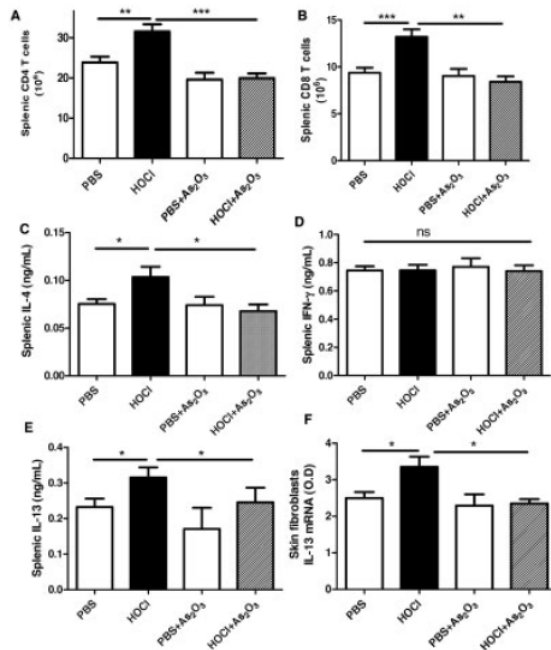


**Figure 6.** Reduction in the numbers of T splenocytes and the production of interleukin-4 (IL-4) and IL-13 by splenocytes in mice with HOCl-induced systemic sclerosis after *in vivo* administration of arsenic trioxide (As<sub>2</sub>O<sub>3</sub>). BALB/c mice received daily intradermal injections of HOCl or phosphate buffered saline (PBS) and were concomitantly treated with As<sub>2</sub>O<sub>3</sub> (5 μg/gm) or vehicle alone for 6 weeks. A, Splenic CD4 T cell numbers in the indicated groups of mice. B, Splenic CD8 T cell numbers in the indicated groups of mice. C, IL-4 concentrations in mouse spleen cell supernatants. D, Interferon-γ (IFNγ) concentrations in mouse spleen cell supernatants. NS = not significant. E, IL-13 concentrations in mouse spleen cell supernatants. F, IL-13 mRNA levels in mouse skin fibroblasts. OD = optical density. Values are the mean ± SEM. \* = *P* < 0.05; \*\* = *P* < 0.01; \*\*\* = *P* < 0.001, by Mann-Whitney paired U test.

to a decrease in this parameter in mice with HOCl-induced SSc (*P* = 0.001 versus untreated mice with HOCl-induced SSc) (Figure 5C). Levels of IgG antibodies directed against topo I were increased in the sera of the mice that had received HOCl injections for 6 weeks (*P* = 0.043) (Figure 5D) but not in the sera of mice with HOCl-induced SSc that were treated with As<sub>2</sub>O<sub>3</sub> (*P* = 0.05 versus untreated mice with HOCl-induced SSc).

**Reduction in the *ex vivo* production of IL-4 and IL-13 by spleen cells from mice with HOCl-induced SSc after *in vivo* administration of As<sub>2</sub>O<sub>3</sub>.** Supernatants of splenocytes from HOCl-injected mice contained higher concentrations of IL-4 and IL-13 than did supernatants

of splenocytes from normal mice (mean ± SEM 0.10 ± 0.03 versus 0.07 ± 0.01 ng/ml for IL-4 and 0.30 ± 0.07 versus 0.22 ± 0.06 ng/ml for IL-13; *P* = 0.044 and *P* = 0.045, respectively) (Figures 6C and E). Treatment of mice with HOCl-induced SSc with As<sub>2</sub>O<sub>3</sub> reduced the concentrations of both cytokines by 30% (*P* = 0.011 for IL-4 and *P* = 0.05 for IL-13) (Figures 6C and E). IFNγ production was not modified by either HOCl injections or As<sub>2</sub>O<sub>3</sub> treatment (Figure 6D). Moreover, As<sub>2</sub>O<sub>3</sub> abrogated the local production of IL-13 in the skin of HOCl-injected mice, as shown by IL-13 messenger RNA levels in fibroblasts (Figure 6F).

## DISCUSSION

In the present study, we demonstrated that As<sub>2</sub>O<sub>3</sub>, a common chemotherapeutic drug used to treat hematologic malignancies, inhibits the development of systemic fibrosis in a chemically induced murine model of SSc. We first investigated the mechanisms through which As<sub>2</sub>O<sub>3</sub> exerts this therapeutic effect. Among the factors that determine cellular susceptibility to As<sub>2</sub>O<sub>3</sub>, the balance between ROS generation and detoxification plays a major role (18). We observed that fibroblasts from mice with HOCl-induced SSc were more prone to As<sub>2</sub>O<sub>3</sub>-induced apoptosis than were fibroblasts from normal mice. This difference in susceptibility to arsenic between fibroblasts from mice with HOCl-induced SSc and those from normal mice correlates with the difference in oxidant/antioxidant status between the 2 cell types. Indeed, skin fibroblasts isolated from HOCl-injected mice showed a higher intracellular concentration of H<sub>2</sub>O<sub>2</sub> and a lower level of GSH than did skin fibroblasts from control mice. Moreover, NAC, a GSH precursor, had a protective effect against As<sub>2</sub>O<sub>3</sub>-induced apoptosis in fibroblasts from mice with HOCl-induced SSc, while BSO, which depletes intracellular GSH, increased arsenic cytotoxicity.

Our data on fibroblasts are consistent with the findings of previous studies of other cell types. In NB4 cells, GSH depletion increased the apoptosis triggered by arsenic (19), and H<sub>2</sub>O<sub>2</sub>-resistant Chinese hamster ovary cells have been shown to be less susceptible to As<sub>2</sub>O<sub>3</sub> (20). In addition, GSH can bind to arsenic and protect its target through the formation of a transient As(GS)<sub>3</sub> complex, thus explaining the enhanced susceptibility of fibroblasts from mice with HOCl-induced SSc to As<sub>2</sub>O<sub>3</sub> (21).

*In vivo*, diseased skin fibroblasts are selectively killed by arsenic, while normal fibroblasts survive and grow in their place. Thus, fibroblasts isolated from

As<sub>2</sub>O<sub>3</sub>-treated mice with HOCl-induced SSc displayed levels of GSH approaching those in fibroblasts from PBS-injected mice. Therefore, despite its pro-oxidative activity, As<sub>2</sub>O<sub>3</sub> paradoxically improves the antioxidant status in the skin of mice with HOCl-induced SSc.

This effect of As<sub>2</sub>O<sub>3</sub> was also observed at the systemic level. Advanced oxidation protein products are oxidized proteins generated by fibroblasts in the skin of mice with HOCl-induced SSc. Advanced oxidation protein products are responsible for the spreading of the disease from skin to visceral organs via systemic circulation (6). In the present study, levels of advanced oxidation protein products were decreased in As<sub>2</sub>O<sub>3</sub>-treated mice with HOCl-induced SSc compared to untreated mice. Since advanced oxidation protein products are released by fibroblasts from mice with HOCl-induced SSc, the selective killing of those cells early in the course of the disease explains the decrease in serum advanced oxidation protein product levels observed in the mice with HOCl-induced SSc treated with As<sub>2</sub>O<sub>3</sub>. In HOCl-induced SSc, advanced oxidation protein products can elicit the apoptosis of endothelial cells and cause vascular damage (6). In vivo treatment of mice with HOCl-induced SSc with As<sub>2</sub>O<sub>3</sub> reduced the levels of advanced oxidation protein products, and, consequently, the concentration of nitrates and sVCAM-1, which are markers of vascular activation and injury in murine and human SSc (22,23), reflecting the beneficial effect of arsenic on the vascular component of the disease.

Another major beneficial effect of As<sub>2</sub>O<sub>3</sub> in mice with HOCl-induced SSc is the inhibition of skin and lung fibrosis. Smad2 and Smad3, transcription factors that are constitutively up-regulated in human SSc fibroblasts, activate the promoter COL1A2 in SSc fibroblasts and the synthesis of collagen (24,25). In this study, the expression of phospho-Smad2/3 was down-regulated in the skin of mice with HOCl-induced SSc treated with As<sub>2</sub>O<sub>3</sub> compared to untreated mice with HOCl-induced SSc, consistent with recent data showing that As<sub>2</sub>O<sub>3</sub> alters the phosphorylation of Smad2/3 in fibroblasts (24). Moreover, transforming growth factor  $\beta$ -induced Smad2/3 phosphorylation is inhibited by NAC, GSH, and L-cysteine, a thiol antioxidant, emphasizing the role of ROS in the activation of the Smad2/3 pathway (26). Thus, in the murine model of SSc used in the present study, the decreased phosphorylation of Smad2/3 was a consequence of the reduced oxidative damages observed in the skin of mice with HOCl-induced SSc following the selective killing of diseased fibroblasts by arsenic. Globally, the decreased phosphorylation of Smad2/3 contrib-

utes to inhibiting an excessive deposition of collagen that leads to fibrosis.

The breach of natural tolerance and the development of an autoimmune reaction are key features of SSc in both humans and rodents. In the present study, As<sub>2</sub>O<sub>3</sub> exerted an immunoregulatory effect in mice with HOCl-induced SSc, reflected by a reduction in B, CD4, and CD8 T cell numbers in the spleens of treated mice, and by a decrease in serum anti-topo I antibody levels. The beneficial effect of As<sub>2</sub>O<sub>3</sub> on the immune system also results in a decrease in splenic production of IL-4 and IL-13, 2 closely linked cytokines that trigger the synthesis of collagen in human skin fibroblasts, and whose concentrations are elevated in the serum and the affected skin of SSc patients (27–29).

By deleting fibroblasts in mice with HOCl-induced SSc, As<sub>2</sub>O<sub>3</sub> abrogated the chronic production of ROS and the consequent oxidation of proteins (especially of topo I). Oxidized topo I is particularly immunogenic and is implicated in the breach of immune tolerance in SSc. Therefore, in vivo treatment with As<sub>2</sub>O<sub>3</sub> could inhibit the induction of the autoimmune reaction by limiting the production and the spreading of the autoantigen. However, a direct effect of arsenic on activated T cells leading to an abrogation of the autoimmune response cannot be ruled out. Indeed, previous studies have shown that the elevated concentration of H<sub>2</sub>O<sub>2</sub> in acute promyelocytic leukemia cells renders them extremely susceptible to the proapoptotic effects of As<sub>2</sub>O<sub>3</sub>. The same effects have been observed in other cell lines, and particularly in lymphocytes during systemic autoimmunity (14,30–32).

In conclusion, we propose that the selective cytotoxic action of As<sub>2</sub>O<sub>3</sub> on activated fibroblasts that produce high amounts of H<sub>2</sub>O<sub>2</sub> could be used in the treatment of SSc in addition to hematologic or solid malignancies.

#### ACKNOWLEDGMENT

The authors are indebted to Ms Agnès Colle for typing the manuscript.

#### AUTHOR CONTRIBUTIONS

All authors were involved in drafting the article or revising it critically for important intellectual content, and all authors approved the final version to be published. Dr. Batteux had full access to all of the data in the study and takes responsibility for the integrity of the data and the accuracy of the data analysis. Study conception and design. Kavian, Marut, Servettaz, Nicco, Chéreau, Lemaréchal, Borderie, Dupin, Weill, Batteux.

Acquisition of data. Kavian, Marut, Servettaz, Nicco, Chéreau, Borderie, Dupin, Weill, Batteux.  
 Analysis and interpretation of data. Kavian, Marut, Nicco, Chéreau, Lemaréchal, Weill, Batteux.

#### ROLE OF THE STUDY SPONSOR

Cephalon had no role in the study design or in the collection, analysis, or interpretation of the data, the writing of the manuscript, or the decision to submit the manuscript for publication. Publication of this article was not contingent upon approval by Cephalon.

#### REFERENCES

- Masamune A, Shimosegawa T. Signal transduction in pancreatic stellate cells. *J Gastroenterol* 2009;44:249–60.
- Pongnimitprasert N, El-Benna J, Foglietti MJ, Gougerot-Pocidal MA, Bernard M, Braut-Boucher F. Potential role of the “NADPH oxidases” (NOX/DUOX) family in cystic fibrosis. *Ann Biol Clin (Paris)* 2008;66:621–9.
- Urtasun R, Conde de la Rosa L, Nieto N. Oxidative and nitrosative stress and fibrogenic response. *Clin Liver Dis* 2008;12:769–90, viii.
- Sambo P, Baroni SS, Luchetti M, Paroncini P, Dusi S, Orlandini G, et al. Oxidative stress in scleroderma: maintenance of scleroderma fibroblast phenotype by the constitutive up-regulation of reactive oxygen species generation through the NADPH oxidase complex pathway. *Arthritis Rheum* 2001;44:2653–64.
- Ziegler TR, Panoskaltus-Mortari A, Gu LH, Jonas CR, Farrell CL, Lacey DL, et al. Regulation of glutathione redox status in lung and liver by conditioning regimens and keratinocyte growth factor in murine allogeneic bone marrow transplantation. *Transplantation* 2001;72:1354–62.
- Servettaz A, Goulvestre C, Kavian N, Nicco C, Guilpain P, Chereau C, et al. Selective oxidation of DNA topoisomerase 1 induced systemic sclerosis in the mouse. *J Immunol* 2009;182:5855–64.
- Svegliati Baroni S, Santillo M, Bevilacqua F, Luchetti M, Spadoni T, Mancini M, et al. Stimulatory autoantibodies to the PDGF receptor in systemic sclerosis. *N Engl J Med* 2006;354:2667–76.
- Laurent A, Nicco C, Chereau C, Goulvestre C, Alexandre J, Alves A, et al. Controlling tumor growth by modulating endogenous production of reactive oxygen species. *Cancer Res* 2005;65:948–56.
- Miller WH, Schipper HM, Lee JS, Singer J, Waxman S. Mechanisms of action of arsenic trioxide. *Cancer Res* 2002;62:3893–903.
- Tallman MS, Nabhan C, Feusner JH, Rowe JM. Acute promyelocytic leukemia: evolving therapeutic strategies. *Blood* 2002;99:759–67.
- Sanz MA, Grimwade D, Tallman MS, Lowenberg B, Fenaux P, Estey EH, et al. Management of acute promyelocytic leukemia: recommendations from an expert panel on behalf of the European LeukemiaNet. *Blood* 2009;113:1875–91.
- Chen GQ, Zhu J, Shi XG, Ni JH, Zhong HJ, Si GY, et al. In vitro studies on cellular and molecular mechanisms of arsenic trioxide (As<sub>2</sub>O<sub>3</sub>) in the treatment of acute promyelocytic leukemia: As<sub>2</sub>O<sub>3</sub> induces NB4 cell apoptosis with downregulation of Bcl-2 expression and modulation of PML-RAR  $\alpha$ /PML proteins. *Blood* 1996;88:1052–61.
- Tse WP, Cheng CH, Che CT, Lin ZX. Arsenic trioxide, arsenic pentoxide, and arsenic iodide inhibit human keratinocyte proliferation through the induction of apoptosis. *J Pharmacol Exp Ther* 2008;326:388–94.
- Bobe P, Bonardelle D, Benihoud K, Opolon P, Chelbi-Alix MK. Arsenic trioxide: a promising novel therapeutic agent for lymphoproliferative and autoimmune syndromes in MRL/lpr mice. *Blood* 2006;108:3967–75.
- Dalle-Donne I, Rossi R, Giustarini D, Gagliano N, Lusini L, Milzani A, et al. Actin carbonylation: from a simple marker of protein oxidation to relevant signs of severe functional impairment. *Free Radic Biol Med* 2001;1:1075–83.
- Servettaz A, Guilpain P, Goulvestre C, Chereau C, Hercend C, Nicco C, et al. Radical oxygen species production induced by advanced oxidation protein products predicts clinical evolution and response to treatment in systemic sclerosis. *Ann Rheum Dis* 2007;66:1202–9.
- Preud'homme JL, Rochard E, Gouet D, Danon F, Alcalay M, Touchard G, et al. Isotypic distribution of anti-double-stranded DNA antibodies: a diagnostic evaluation by enzyme-linked immunosorbent assay. *Diagn Clin Immunol* 1988;5:256–61.
- Chou WC, Jie C, Kenedy AA, Jones RJ, Trush MA, Dang CV. Role of NADPH oxidase in arsenic-induced reactive oxygen species formation and cytotoxicity in myeloid leukemia cells. *Proc Natl Acad Sci U S A* 2004;101:4578–83.
- Davison K, Cote S, Mader S, Miller WH. Glutathione depletion overcomes resistance to arsenic trioxide in arsenic-resistant cell lines. *Leukemia* 2003;17:931–40.
- Wang TS, Kuo CF, Jan KY, Huang H. Arsenite induces apoptosis in Chinese hamster ovary cells by generation of reactive oxygen species. *J Cell Physiol* 1996;169:256–68.
- Scott N, Hatlelid KM, MacKenzie NE, Carter DE. Reactions of arsenic(III) and arsenic(V) species with glutathione. *Chem Res Toxicol* 1993;6:102–6.
- Kavian N, Servettaz A, Marut W, Nicco C, Chereau C, Weill B, et al. Sunitinib inhibits the phosphorylation of platelet-derived growth factor receptor  $\beta$  in the skin of mice with scleroderma-like features and prevents the development of the disease. *Arthritis Rheum* 2012;64:1990–2000.
- Pendergrass SA, Hayes E, Farina G, Lemaire R, Farber HW, Whitfield ML, et al. Limited systemic sclerosis patients with pulmonary arterial hypertension show biomarkers of inflammation and vascular injury. *PLoS One* 2010;5:e12106.
- Smith DM, Patel S, Raffoul F, Haller E, Mills GB, Nanjundan M. Arsenic trioxide induces a beclin-1-independent autophagic pathway via modulation of SnO/SklL expression in ovarian carcinoma cells. *Cell Death Differ* 2010;17:1867–81.
- Asano Y, Ihn H, Yamane K, Kubo M, Tamaki K. Impaired Smad7-Smurf-mediated negative regulation of TGF- $\beta$  signaling in scleroderma fibroblasts. *J Clin Invest* 2004;113:253–64.
- Li WQ, Qureshi HY, Liacini A, Dehnade F, Zafarullah M. Transforming growth factor  $\beta$ 1 induction of tissue inhibitor of metalloproteinases 3 in articular chondrocytes is mediated by reactive oxygen species. *Free Radic Biol Med* 2004;37:196–207.
- Hasegawa M, Fujimoto M, Kikuchi K, Takehara K. Elevated serum levels of interleukin 4 (IL-4), IL-10, and IL-13 in patients with systemic sclerosis. *J Rheumatol* 1997;24:328–32.
- Needleman BW, Wigley FM, Stair RW. Interleukin-1, interleukin-2, interleukin-4, interleukin-6, tumor necrosis factor  $\alpha$ , and interferon- $\gamma$  levels in sera from patients with scleroderma. *Arthritis Rheum* 1992;35:67–72.
- Jinnin M, Ihn H, Yamane K, Tamaki K. Interleukin-13 stimulates the transcription of the human  $\alpha$ 2(I) collagen gene in human dermal fibroblasts. *J Biol Chem* 2004;279:41783–91.
- Dai J, Weinberg RS, Waxman S, Jing Y. Malignant cells can be sensitized to undergo growth inhibition and apoptosis by arsenic trioxide through modulation of the glutathione redox system. *Blood* 1999;93:268–77.
- Li YM, Broome JD. Arsenic targets tubulins to induce apoptosis in myeloid leukemia cells. *Cancer Res* 1999;59:776–80.
- Biswas S, Zhao X, Mone AP, Mo X, Vargo M, Jarjoura D, et al. Arsenic trioxide and ascorbic acid demonstrate promising activity against primary human CLL cells in vitro. *Leuk Res* 2010;34:925–31.

## Arsenic Trioxide Prevents Murine Sclerodermatous Graft-versus-Host Disease

Niloufar Kavian,<sup>\*,†,1</sup> Wioleta Marut,<sup>\*,1</sup> Amélie Servettaz,<sup>\*,‡</sup> H el ene Laude,<sup>\*,§</sup> Carole Nicco,<sup>\*,\*</sup> Christiane Ch ereau,<sup>\*,\*</sup> Bernard Weill,<sup>\*,†</sup> and Fr ed eric Batteux<sup>\*,†</sup>

Chronic graft-versus-host disease (GVHD) follows allogeneic hematopoietic stem cell transplantation. It results from alloreactive processes induced by minor MHC incompatibilities triggered by activated APCs, such as plasmacytoid dendritic cells (pDCs), and leading to the activation of CD4<sup>+</sup> T cells. Therefore, we tested whether CD4<sup>+</sup> and pDCs, activated cells that produce high levels of reactive oxygen species, could be killed by arsenic trioxide (As<sub>2</sub>O<sub>3</sub>), a chemotherapeutic drug used in the treatment of acute promyelocytic leukemia. Indeed, As<sub>2</sub>O<sub>3</sub> exerts its cytotoxic effects by inducing a powerful oxidative stress that exceeds the lethal threshold. Sclerodermatous GVHD was induced in BALB/c mice by body irradiation, followed by B10.D2 bone marrow and spleen cell transplantation. Mice were simultaneously treated with daily i.p. injections of As<sub>2</sub>O<sub>3</sub>. Transplanted mice displayed severe clinical symptoms, including diarrhea, alopecia, vasculitis, and fibrosis of the skin and visceral organs. The symptoms were dramatically abrogated in mice treated with As<sub>2</sub>O<sub>3</sub>. These beneficial effects were mediated through the depletion of glutathione and the overproduction of H<sub>2</sub>O<sub>2</sub> that killed activated CD4<sup>+</sup> T cells and pDCs. The dramatic improvement provided by As<sub>2</sub>O<sub>3</sub> in the model of sclerodermatous GVHD that associates fibrosis with immune activation provides a rationale for the evaluation of As<sub>2</sub>O<sub>3</sub> in the management of patients affected by chronic GVHD. *The Journal of Immunology*, 2012, 188: 5142–5149.

Chronic graft-versus-host disease (GVHD) is a major factor of morbidity following allogeneic hematopoietic stem cell transplantation, with variable clinical presentations (1, 2). Chronic GVHD emerges from alloreactive processes between donor-derived immune cells and host cell populations induced by minor MHC incompatibilities between donor and recipient. Its pathophysiology is poorly understood in contrast to that of acute GVHD (1, 3). Donor CD4<sup>+</sup> T cells are involved in the induction of chronic GVHD, but the effector mechanisms through which they mediate tissue inflammation are unclear; the recognition of MHC class II alloantigens on host dendritic cells (DCs) is sufficient to prime donor CD4<sup>+</sup> T cells and induce GVHD (3–5). Moreover, among APCs, plasmacytoid DCs (pDCs) were shown to be pathogenic in GVHD. In the absence of other APCs, pDCs alone can stimulate donor T cells to trigger GVHD, and total-body irradiation is crucial for their maturation and the subsequent priming of alloreactive CD4<sup>+</sup> T cells (6).

Chronic GVHD often mimics autoimmune diseases (7). Sclerodermatous-GVHD (Scl-GVHD) makes up 10–15% of cases of chronic GVHD (8). This clinical form of GVHD resembles systemic sclerosis, because it includes fibrotic changes and chronic inflammation of the skin, lung, and gastrointestinal tract. Several animal models have been developed to help define the pathophysiology of chronic GVHD. One of them is based on the transfer of donor immune cells into sublethally irradiated host mice with mismatched minor MHC histocompatibility Ags, resulting in full donor lymphoid chimerism (9). This model recapitulates the clinical features of Scl-GVHD, with fibrosis of the skin and visceral organs 14 d following the graft.

Activated T cells with a high rate of production of reactive oxygen species (ROS) play a pivotal role in the development of Scl-GVHD. Therefore, we investigated whether a cytotoxic molecule that acts by enhancing ROS production beyond a lethal threshold could be of any help in treating chronic GVHD.

Arsenic trioxide (As<sub>2</sub>O<sub>3</sub>) is an inorganic trivalent salt that exhibits potent antitumor effects in vitro and in vivo, especially in the treatment of hematological malignancies, such as acute promyelocytic leukemia refractory to all-*trans* retinoic acid (10). Several reports suggested that As<sub>2</sub>O<sub>3</sub> can affect many cellular functions, such as proliferation, apoptosis, differentiation, and angiogenesis, in various cell lines. An important cellular event occurring after As<sub>2</sub>O<sub>3</sub> treatment is the elevation of intracellular ROS levels (11). This ROS generation appears to be regulated through several pathways, including NADPH oxidase, mitochondrial electron transport chain, and inhibition of antioxidant enzymes (12–14). The ROS-mediated apoptosis triggered by As<sub>2</sub>O<sub>3</sub> can impact hematological tumor cells; under certain circumstances, it can also affect nontumor cells, such as keratinocytes, fibroblasts, or activated autoimmune lymphocytes (15–17).

In this study, we tested the therapeutic effects of As<sub>2</sub>O<sub>3</sub> in a murine model of Scl-GVHD generated by grafting B10.D2 (H-2<sup>d</sup>) bone marrow and spleen cells into sublethally irradiated BALB/c mice (H-2<sup>d</sup>). We show that As<sub>2</sub>O<sub>3</sub> limits both the acti-

<sup>\*</sup>Laboratoire EA 1833, Facult e de M edecine, Sorbonne Paris Cit e, Universit e Paris Descartes, 75679 Paris Cedex 14, France; <sup>†</sup>Laboratoire d'Immunologie Biologique, H opital Cochin, Assistance Publique H opitaux de Paris, 75014 Paris, France; <sup>‡</sup>Facult e de M edecine de Reims, Service de M edecine Interne, Maladies Infectieuses, Immunologie Clinique, H opital Robert Debr e, 51092 Reims Cedex, France; and <sup>§</sup>Laboratoire de Virologie, H opital Cochin, Assistance Publique H opitaux de Paris, 75014 Paris, France

<sup>1</sup>N.K. and W.M. contributed equally to this work.

Received for publication December 12, 2011. Accepted for publication March 9, 2012.

This work was supported by grants from Assistance Publique H opitaux de Paris (to N.K.) and Redcat (to W.M.).

Address correspondence and reprint requests to Prof. Fr ed eric Batteux, Laboratoire d'Immunologie EA1833, Facult e de M edecine Paris Descartes, 75679 Paris Cedex 14, France. E-mail address: frederic.batteux@cch.aphp.fr

Abbreviations used in this article: As<sub>2</sub>O<sub>3</sub>, arsenic trioxide; BMT, bone marrow transplantation; cDC, conventional dendritic cell; DC, dendritic cell; GSH, glutathione; GVHD, graft-versus-host disease; MFI, mean fluorescence intensity; NAC, *N*-acetyl-cysteine; pDC, plasmacytoid dendritic cell; ROS, reactive oxygen species; Scl-GVHD, sclerodermatous graft-versus-host disease.

Copyright   2012 by The American Association of Immunologists, Inc. 0022-1767/12/\$16.00

variation of the immune system and fibrosis in mice with Scl-GVHD. As<sub>2</sub>O<sub>3</sub> induces apoptosis in alloreactive CD4<sup>+</sup> T cells and activated pDCs, thus limiting the development of GVHD reaction in mice.

## Materials and Methods

### Animals, cells, and chemicals

Specific pathogen-free, 6-wk-old female BALB/c and male B10.D2 mice were purchased from Harlan (Gannat, France) and maintained with food and water ad libitum. They were given humane care, according to the guidelines of our institution (Université Paris Descartes). All cells were cultured as previously reported (18). All chemicals were from Sigma-Aldrich (Saint-Quentin Fallavier, France).

### Experimental procedure in Scl-GVHD mice

**Induction of GVHD in BALB/c mice.** GVHD following bone marrow transplantation (BMT) was induced in BALB/c mice (H-2<sup>d</sup>; Janvier Laboratory, Le Genest Saint Isle, France) by grafting cells from 7–8-week-old female B10.D2 mice (H-2<sup>k</sup>; Janvier Laboratory), as previously described by Jaffee and Claman (19). Briefly, recipient mice were lethally irradiated with 750 cGy from a Gammacel [<sup>137</sup>Cs] source. Three hours later, they were injected i.v. with donor spleen cells (2 × 10<sup>6</sup>/mouse) and bone marrow cells (1 × 10<sup>6</sup>/mouse) suspended in RPMI 1640. A control group of BALB/c recipient mice received BALB/c spleen and bone marrow cells (syngeneic BMT, referred to as control animals). Transplanted animals were maintained in sterile microisolator cages (Lab Products, Langensfeld, Germany) and supplied with autoclaved food and sterile water. Animals were sacrificed by cervical dislocation 4 wk after BMT.

**Treatment of Scl-GVHD mice with As<sub>2</sub>O<sub>3</sub>.** Scl-GVHD and control mice were randomized and treated for 3 wk with i.p. injections of either As<sub>2</sub>O<sub>3</sub> or vehicle alone beginning on day 7 post-BMT (10 mice/group). A stock solution was prepared extemporaneously, as described above. As<sub>2</sub>O<sub>3</sub> was given 5 d/wk at a dose of 5 μg/g body weight, as described by Bobé et al. (17). Control mice received i.p. injections of PBS 5 d/wk. Four weeks after BMT, the animals were sacrificed by cervical dislocation.

### Assessment of collagen accumulation

**Skin thickness.** Skin thickness of the shaved back of mice was measured 1 d before sacrifice with a caliper and expressed in millimeters.

**Histopathological analysis.** Fixed lung and skin pieces were embedded in paraffin. A 5-μm-thick tissue section was stained with H&E or Picrosirius Red. Slides were examined by standard bright-field microscopy (Olympus BX60, Rungis, France) by a pathologist who was blinded to the assignment of the animal group.

**Collagen content in skin and lung.** Skin and lung pieces were diced using a scalpel, put into tubes, thawed, and mixed with pepsin (1:10 weight ratio) and 0.5 M acetic acid overnight at room temperature under stirring. The assay of collagen content was based on the quantitative dye-binding Sircol method (Biocolor, Belfast, Ireland).

### Disease severity score

To determine the incidence and severity of disease, we assigned a score to each mouse using the following criteria: 0: no external sign; 1: piloerection on back and underside, 1: hunched posture or lethargy; 1: weight loss >10%; 0.5: alopecia <1 cm<sup>2</sup>; 1: alopecia >1 cm<sup>2</sup>; 1: vasculitis (one or more purpuric lesions); and 1: eyelid sclerosis (blepharophymosis). The severity score is the sum of these values and ranges from 0 (unaffected) to a maximum of 6. The incidence and severity score was recorded every week by two blinded scientists.

### Flow cytometric analysis of spleen cell subsets

Cell suspensions from spleens were prepared after hypotonic lysis of erythrocytes in potassium acetate solution. Cells were incubated with the appropriate labeled Ab at 4°C for 30 min in PBS with 0.1% sodium azide and 5% normal rat serum. Flow cytometry was performed using a FACSCanto flow cytometer (BD Biosciences, San Jose, CA), according to standard techniques. The mAbs used in this study were anti-B220-PE-Cy7, anti-CD11b-biotin, anti-CD11c-FITC, anti-CD4-PerCP, and anti-CD8-PE-Cy7 (BD Biosciences). Data were analyzed with FlowJo software (Tree Star, Ashland, OR).

### Determination of IL-4 and IL-17 production by splenocytes

Spleen cells were isolated by gentle disruption of the tissues, and the erythrocytes were lysed by hypotonic shock in potassium acetate solution.

Spleen cells were cultured in RPMI 1640 supplemented with antibiotics, GlutaMAX (Invitrogen Life Technologies), and 10% heat-inactivated FCS (Invitrogen Life Technologies) (complete medium). CD4 T cells were isolated from spleen cell suspensions by positive selection using CD4 microbeads and LS columns (Miltenyi Biotec, Paris, France), according to the manufacturer's instructions. CD4 T cell suspensions were then seeded in 96-well flat-bottom plates and cultured (2 × 10<sup>5</sup> cells) in complete medium for 48 h in the presence of 5 μg/ml Con A. Supernatants were collected, and cytokine concentrations were determined by ELISA (for IL-4: eBioscience, San Diego, CA; for IL-17: DuoSet; R&D Systems). Results are expressed in ng/ml.

### Assays of serum anti-DNA topoisomerase 1 autoantibodies

Levels of anti-DNA topoisomerase 1 IgG Abs were detected by ELISA on microtiter plates (ImmunoVision, Springdale, AR). A 1:50 serum dilution was used for the ELISA.

### Effects of As<sub>2</sub>O<sub>3</sub> on B10.D2 CD4 T cells in vitro

Suspensions of spleen cells from a male B10.D2 mouse and a female BALB/c mouse were prepared after hypotonic lysis of erythrocytes. The BALB/c cell suspension was irradiated at 30 Gy. A B10.D2 cell suspension was also prepared and irradiated at 30 Gy for syngeneic control.

B10.D2 cells were labeled with PKH26 dye, according to the manufacturer's instructions (Sigma-Aldrich).

**Measurement of H<sub>2</sub>O<sub>2</sub> concentration in CD4 T cells.** B10.D2 cells labeled with PKH26 were incubated with irradiated BALB/c cells and complete medium for 24 h. After this incubation period, cells were washed without serum and incubated with 5 μM CM-H<sub>2</sub>DCFDA (Sigma-Aldrich) at 37°C for 20 min. After washing, cells were incubated with 10 μM As<sub>2</sub>O<sub>3</sub>, with or without 4 mM N-acetylcysteine (NAC), for 5 h at 37°C. Cells were then washed and labeled with anti-CD4 mAb.

**Measurement of glutathione concentration in CD4 T cells.** B10.D2 cells labeled with PKH26 were incubated with or without irradiated BALB/c cells and complete medium, with or without 10 μM As<sub>2</sub>O<sub>3</sub> and with or without 4 mM NAC, for 24 h. Cells were washed and labeled with 100 μM monochlorobimane at 37°C for 20 min, followed by labeling with anti-CD4 mAb for 20 min.

**Determination of apoptosis in CD4 T cells.** B10.D2 cells labeled with PKH26 were incubated with or without irradiated BALB/c spleen cells and complete medium alone, with 10 μM As<sub>2</sub>O<sub>3</sub> alone, or with 4 mM NAC for 24 h. Cells were then washed and stained with anti-CD4 mAb (eBioscience) at 4°C for 20 min and Yopro-1 (Sigma-Aldrich) at room temperature for 10 min.

### Effects of As<sub>2</sub>O<sub>3</sub> on B10.D2 pDCs in vitro

A suspension of spleen cells from a male B10.D2 mouse was prepared after hypotonic lysis of erythrocytes.

**Measurement of H<sub>2</sub>O<sub>2</sub> concentration in pDCs.** B10.D2 cells were incubated in complete medium, washed without serum, and incubated with 5 μM CM-H<sub>2</sub>DCFDA (Sigma-Aldrich) at 37°C for 20 min. After washing, cells were incubated with 10 μM As<sub>2</sub>O<sub>3</sub>, with or without 4 mM NAC, for 5 h at 37°C. Cells were then washed and labeled with anti-B220, anti-CD11b, and anti-CD11c mAb (BD, Le Pont de Claix, France).

**Measurement of glutathione concentration in pDCs.** B10.D2 cells were incubated with complete medium with or without 10 μM As<sub>2</sub>O<sub>3</sub> and with or without 4 mM NAC for 24 h. Cells were then washed and labeled with 100 μM monochlorobimane at 37°C for 20 min, followed by labeling with anti-B220, anti-CD11b, and anti-CD11c mAb (BD) for 20 min.

**Determination of apoptosis in pDCs.** B10.D2 cells were incubated with complete medium alone, with 10 μM As<sub>2</sub>O<sub>3</sub> alone, or with 10 μM As<sub>2</sub>O<sub>3</sub> and 4 mM NAC for 24 h. Cells were then washed and stained with anti-B220, anti-CD11b, and anti-CD11c mAb (BD) at 4°C for 20 min and Yopro-1 (Sigma-Aldrich) at room temperature for 10 min.

For all flow cytometry analyses, pDCs were defined as B220<sup>+</sup>CD11c<sup>int</sup>CD11b<sup>low</sup>. Data were acquired on a FACSCanto II flow cytometer (BD Biosciences) and analyzed with FlowJo software (Tree Star).

### Measurement of in vitro IFN-α production by pDCs

pDCs were isolated from the spleen of a BALB/c mouse using the pDC isolation kit and MS columns (Miltenyi Biotec). pDCs were then coated in six-well plates and incubated with 10 μg/ml Gardiquimod (InvivoGen, Toulouse, France) and increasing doses of As<sub>2</sub>O<sub>3</sub> (from 0 to 25 μM) or with medium alone for 24 h. Supernatants were harvested, and IFN-α was assayed as described by Dubois et al. (20). Briefly, L929 cells (5 × 10<sup>4</sup>/well; kindly provided by P. Lebon, Laboratoire de Virologie, Hôpital

Cochin, Paris, France) were coated in 96-well plates and cultured in RPMI 1640 at 37°C with 5% CO<sub>2</sub> until confluence. Culture media were discarded, and plates were incubated for an additional 24 h with 50 µl 2-fold serial dilutions (from 1:2 to 1:256 in RPMI 1640) of supernatant samples or with serial dilutions of a standard solution of murine IFN-α. Thereafter, vesicular stomatitis virus was added; the final concentration was 1:400 of a stock solution previously shown to cause complete lysis of L929 cells at a dilution of 1:2000. We considered the dilution that destroyed half of the cell layer at 24 h, and IFN-α units were determined by comparison with cells incubated with 2-fold serial dilutions of mouse IFN-α (kindly provided by P. Lebon).

#### Statistical analysis

All of the quantitative data are expressed as mean ± SEM and were analyzed with Prism 5 (GraphPad), using one-way ANOVA or the Student *t* test, as appropriate. A *p* value <0.05 was considered statistically significant.

## Results

### As<sub>2</sub>O<sub>3</sub> prevented clinical symptoms of systemic sclerosis induced by GVHD

We investigated the effects of As<sub>2</sub>O<sub>3</sub> on the development of Scl-GVHD, a fibrotic variant of GVHD. As<sub>2</sub>O<sub>3</sub> was administered daily from day 7 following BMT, and mice were sacrificed 21 d later. Lethally irradiated BALB/c mice transplanted with bone marrow and spleen cells from B10.D2 mice developed skin fibrosis, as shown by the measurement of ear skin thickening in Fig. 1A. Control BALB/c animals with syngeneic grafts did not develop skin fibrosis or GVHD (Fig. 2). In addition to skin thickening, the engrafted animals displayed alopecia (100% of mice), vasculitis (>80% of mice), or diarrhea (100% of mice). On day 21, the disease severity score of Scl-GVHD mice was ≥5, whereas that of control animals (syngeneic graft) was 0 (Fig. 2B). As<sub>2</sub>O<sub>3</sub> effectively prevented severe GVHD; the mean severity score of treated mice at day 14 was 2.5 ± 0.2 versus 5 ± 0.4 in untreated Scl-GVHD mice (*p* < 0.001, Fig. 2B). Scl-GVHD mice treated with As<sub>2</sub>O<sub>3</sub> displayed a reduction in skin thickness >40% compared with untreated Scl-GVHD mice (*p* = 0.007, Fig. 1B). Moreover, type I collagen content in the skin of Scl-GVHD mice treated

with As<sub>2</sub>O<sub>3</sub> was 45% lower than in untreated Scl-GVHD mice (*p* = 0.002, Fig. 1C). Picrosirius Red staining of ear sections showed important collagen deposits in the ears from Scl-GVHD mice but not in those of Scl-GVHD mice treated with As<sub>2</sub>O<sub>3</sub> (Fig. 1A). Also, type I collagen concentration was higher in the lungs of Scl-GVHD mice than in Scl-GVHD mice treated with As<sub>2</sub>O<sub>3</sub> (data not shown). Altogether, these results show that As<sub>2</sub>O<sub>3</sub> limits the deposition of collagen and prevents the development of alopecia, vasculitis, and diarrhea in Scl-GVHD mice.

### As<sub>2</sub>O<sub>3</sub> altered spleen cell subsets in Scl-GVHD mice

GVHD is caused by a donor T cell antihost reaction. We investigated whether the clinical improvement observed in Scl-GVHD mice treated with As<sub>2</sub>O<sub>3</sub> correlated with quantitative or qualitative alterations in spleen cell subsets. Flow cytometric analysis of splenocytes showed that As<sub>2</sub>O<sub>3</sub> decreased the percentage of CD4<sup>+</sup> T cells (*p* = 0.049 versus untreated Scl-GVHD mice). This reduction involved the CD44<sup>+</sup>CD62L<sup>-</sup> effector memory CD4 subset, because the ratio of CD4<sup>+</sup>CD44<sup>high</sup>CD62L<sup>low</sup>/CD4<sup>+</sup>CD44<sup>low</sup>CD62L<sup>high</sup> cells was 15.7 ± 4.6 in Scl-GVHD mice versus 3.6 ± 0.7 in Scl-GVHD mice treated with arsenic (*p* = 0.001, Fig. 3A–C). Furthermore, the percentage of splenic pDCs, defined as B220<sup>+</sup>CD11c<sup>+</sup>CD11b<sup>low</sup>, was three times lower in arsenic-treated Scl-GVHD mice compared with untreated Scl-GVHD mice (*p* = 0.021, Fig. 3D).

### As<sub>2</sub>O<sub>3</sub> modified the splenic production of cytokines and the serum levels of autoantibodies in Scl-GVHD mice

In addition, we explored the splenic production of IL-4 and IL-17, two cytokines implicated in the development of GVHD in mice (21). Scl-GVHD mice produced more IL-4 and IL-17 than did control mice (IL-4: 0.24 ± 0.023 for Scl-GVHD mice and 0.12 ± 0.021 for control mice, *p* = 0.011; IL-17: 0.64 ± 0.083 for Scl-GVHD mice and 0.37 ± 0.088 for control mice, *p* = 0.042; Fig. 3E, 3F). As<sub>2</sub>O<sub>3</sub> significantly reduced the production of the two cytokines (*p* = 0.043 and *p* = 0.022 for IL-4 and IL-17, respectively, versus nontreated mice, Fig. 3E, 3F). We then investigated

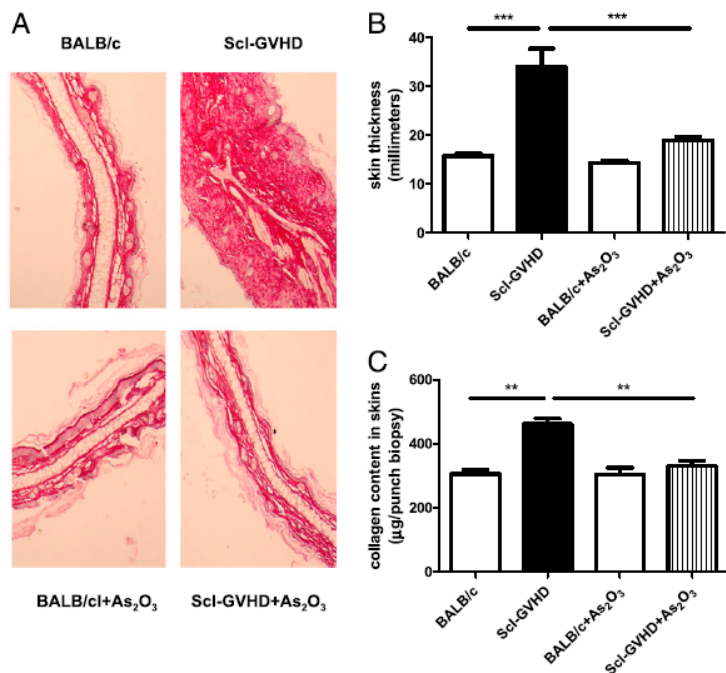
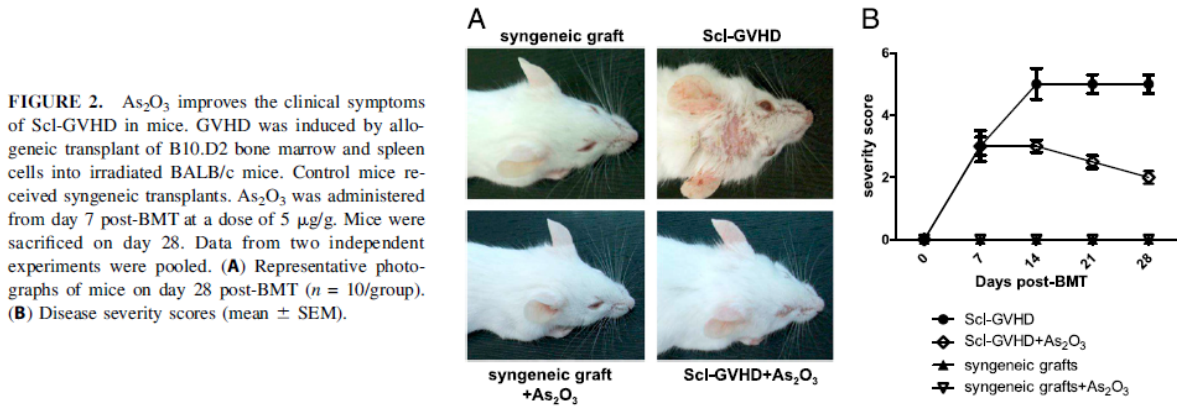


**FIGURE 1.** As<sub>2</sub>O<sub>3</sub> reduces the fibrotic changes in mice with Scl-GVHD. GVHD was induced by allogeneic transplant of B10.D2 bone marrow and spleen cells into irradiated BALB/c mice. Control mice received syngeneic transplants. As<sub>2</sub>O<sub>3</sub> was administered from day 7 post-BMT at a dose of 5 µg/g. Mice were sacrificed on day 28. Data from two independent experiments were pooled (*n* = 10/group). (A) Representative Picrosirius Red staining of the skin (objective ×10). (B) Skin thickness measured with a caliper and expressed in millimeters. (C) Collagen content in skin of mice expressed in µg/punch biopsy. Values are mean ± SEM of data from all mice in the experimental or control groups. \**p* < 0.05, paired Mann–Whitney *U* test.



the presence of anti-DNA topoisomerase 1 Abs, a hallmark of the Scl-GVHD model, which are generally detected 3–9 wk following the onset of disease (9). On the day of sacrifice, 80% of Scl-GVHD mice and only 20% of Scl-GVHD mice treated with  $As_2O_3$  were positive for anti-DNA-topoisomerase 1 Abs ( $p = 0.048$ , Fig. 3G).

*$As_2O_3$  triggered apoptosis of activated B10.D2 CD4<sup>+</sup> T cells by enhancing ROS production*

In vitro, ROS production was higher in B10.D2 CD4<sup>+</sup> T cells stimulated with BALB/c splenocytes than in B10.D2 CD4<sup>+</sup> T cells stimulated with B10.D2 splenocytes (syngeneic controls) (mean fluorescence intensity [MFI] = 1721  $\pm$  40 versus 1186  $\pm$  92,  $p = 0.032$ ). Treatment of stimulated B10.D2 CD4<sup>+</sup> T cells with  $As_2O_3$  further increased their production of  $H_2O_2$  that reached an

MFI of 2172  $\pm$  103 ( $p = 0.031$  versus stimulated B10.D2 CD4<sup>+</sup> T cells without  $As_2O_3$ , Fig. 4A). The enhancement of ROS production was abrogated by incubation with 4 mM NAC (MFI: 1636  $\pm$  87,  $p = 0.021$  versus  $As_2O_3$  alone, Fig. 4A). The level of glutathione (GSH) in B10.D2 CD4<sup>+</sup> T cells was in accordance with those results. Syngeneic stimulated cells displayed elevated levels of GSH (mean of 45  $\pm$  2% of GSH<sup>+</sup> cells), whereas allogeneic stimulated cells had a slight decrease in their GSH content (mean 31  $\pm$  2.5% of positive cells) ( $p = 0.041$ , Fig. 4B). Incubation with 10  $\mu M$   $As_2O_3$  dramatically decreased the GSH content in stimulated B10.D2 CD4<sup>+</sup> T cells (Fig. 4B). In addition, Yopro-1 staining of activated B10.D2 CD4<sup>+</sup> T cells indicated that arsenic dramatically triggered apoptosis in those cells. Apoptosis correlated with ROS production measured by flow cytometry and was downregulated by incubation with 4 mM NAC ( $p = 0.0009$ , Fig. 4C).

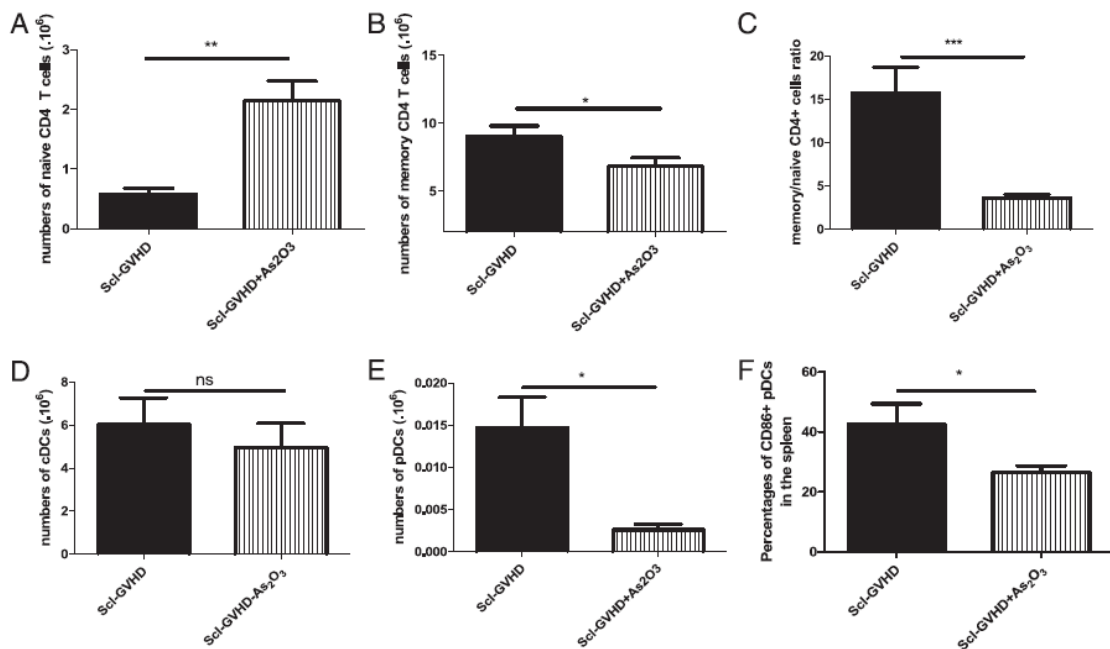


**FIGURE 3.** Treatment of Scl-GVHD mice with  $As_2O_3$  altered the balance between memory and naive CD4<sup>+</sup> T cells and decreased numbers of splenic pDCs. Mice were treated with  $As_2O_3$  from day 7 post-BMT at a dose of 5  $\mu g/g$  ( $n = 10$ /group). Spleen cells were harvested on day 28 post-BMT. **(A)** Numbers of CD4<sup>+</sup> naive T cells in untreated and treated Scl-GVHD mice. **(B)** Numbers of CD4<sup>+</sup> effector memory T cells. **(C)** Effector memory/naive CD4<sup>+</sup> T cell ratio. **(D)** Numbers of splenic pDCs in untreated and treated Scl-GVHD mice. **(E)** Numbers of splenic cDCs in untreated and treated Scl-GVHD mice. **(F)** Percentages of CD86<sup>+</sup> pDCs in untreated and treated Scl-GVHD mice. Values are mean  $\pm$  SEM of data from all mice in the experimental or control groups. \* $p < 0.05$ , \*\* $p < 0.01$ , \*\*\* $p < 0.001$ , paired Mann-Whitney  $U$  test.

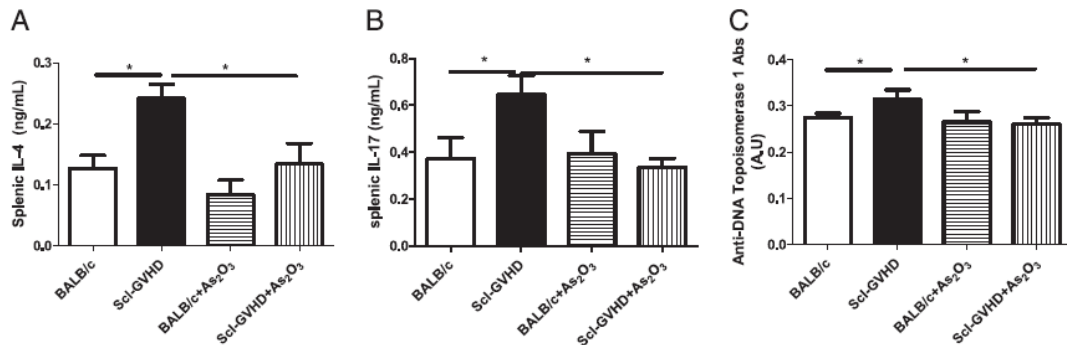


**FIGURE 4.** In vivo treatment with  $\text{As}_2\text{O}_3$  reduced the production of IL-4, IL-17, and autoantibodies in Scl-GVHD mice. Mice were treated with  $\text{As}_2\text{O}_3$  from day 7 post-BMT at a dose of  $5 \mu\text{g/g}$  ( $n = 10/\text{group}$ ). Spleen cells were harvested on day 28 post-BMT, and CD4 T cells were purified as described in *Materials and Methods*. **(A)** IL-4 secretion measured in supernatants of CD4 T cells by ELISA (ng/ml). **(B)** IL-17 secretion measured in supernatants of CD4 T cells by ELISA (ng/ml). **(C)** Anti-DNA-topoisomerase 1 autoantibody concentrations in the sera (A.U.). Values are mean  $\pm$  SEM of data from all mice in the experimental or control groups. \* $p < 0.05$ , paired Mann-Whitney  $U$  test.

*As<sub>2</sub>O<sub>3</sub> also triggered apoptosis of pDCs by enhancing H<sub>2</sub>O<sub>2</sub> production*

We observed the same effects on ROS production and apoptosis in B10.D2 pDCs incubated with  $10 \mu\text{M}$   $\text{As}_2\text{O}_3$ . Indeed, the basal detection MFI of CM-H<sub>2</sub>DCFDA by flow cytometry was  $5405 \pm 12$  for B10.D2 pDCs and  $6527 \pm 25$  when treated with  $\text{As}_2\text{O}_3$ . Adding NAC reduced  $\text{H}_2\text{O}_2$  production by pDCs, as shown by the CM-H<sub>2</sub>DCFDA MFI of  $3675 \pm 15$  (Fig. 5). Monochlorobimane staining was also reduced in pDCs treated with arsenic compared with untreated pDCs (MFI =  $707 \pm 10$  versus  $1583 \pm 80$ ), whereas coaddition of NAC and  $\text{As}_2\text{O}_3$  increased the intracellular content of GSH (MFI =  $1541 \pm 8$ ). The effects of  $\text{As}_2\text{O}_3$  were also studied on conventional DCs (cDCs). There was a tendency toward an increase in  $\text{H}_2\text{O}_2$  production and a decrease in GSH content in cDCs upon treatment with arsenic, but those results did not reach significance (for  $\text{H}_2\text{O}_2$  levels: MFI =  $1,118 \pm 90$  for cDCs alone,  $1,445 \pm 86$  for cDCs +  $\text{As}_2\text{O}_3$ ,  $1,325 \pm 76$  for cDCs +  $\text{As}_2\text{O}_3$  + NAC;  $p = 0.08$  for cDCs versus cDCs +  $\text{As}_2\text{O}_3$ ,  $p = 0.09$  for cDCs +  $\text{As}_2\text{O}_3$  + NAC versus cDCs +  $\text{As}_2\text{O}_3$ ; for GSH levels: MFI =  $24,308 \pm 395$  for cDCs alone,  $21,719 \pm 384$  for cDCs +  $\text{As}_2\text{O}_3$ ,  $23,000 \pm 376$  for cDCs +  $\text{As}_2\text{O}_3$  + NAC;  $p = 0.089$  for cDCs versus cDCs +  $\text{As}_2\text{O}_3$ ,  $p = 0.10$  for cDCs +  $\text{As}_2\text{O}_3$  + NAC versus cDCs +  $\text{As}_2\text{O}_3$ ).

*As<sub>2</sub>O<sub>3</sub> blocked IFN- $\alpha$  production of B10.D2 pDCs*

To assess the specificity of  $\text{As}_2\text{O}_3$  against pDCs, we investigated its effect on the production of IFN- $\alpha$  by splenic pDCs, with and without activation by the TLR7 agonist Gardiquimod. Fig. 6 shows that, in the absence of stimulation of pDCs,  $\text{As}_2\text{O}_3$  has a significant effect on the production of IFN- $\alpha$  only at the highest concentrations tested ( $10$  and  $25 \mu\text{M}$ ). In contrast, after stimulation of TLR7 and incubation with  $10$  and  $25 \mu\text{M}$   $\text{As}_2\text{O}_3$ , the levels of IFN- $\alpha$  in cell supernatants were strongly decreased ( $p = 0.002$  for  $10 \mu\text{M}$   $\text{As}_2\text{O}_3$ ). Incubation with  $5 \mu\text{M}$   $\text{As}_2\text{O}_3$  decreased the concentration of IFN- $\alpha$  in the supernatants  $>2$ -fold, whereas lower doses of  $\text{As}_2\text{O}_3$  had no effect on IFN- $\alpha$  production (Fig. 7).

**Discussion**

This study shows that  $\text{As}_2\text{O}_3$  selectively deletes activated CD4<sup>+</sup> T cells and pDCs that have low levels of GSH and overproduce  $\text{H}_2\text{O}_2$  and, thus, ameliorates Scl-GVHD in mice.

We tested the effects of  $\text{As}_2\text{O}_3$ , a chemotherapeutic drug used in hematological malignancies, on the development of Scl-GVHD in mice. This model of chronic GVHD shares typical features with

systemic sclerosis, including skin and visceral fibrosis and autoimmune manifestations (22).  $\text{As}_2\text{O}_3$  dramatically improved the clinical outcome of sublethally irradiated BALB/c mice transplanted with B10.D2 hematopoietic cells; weight loss, fibrosis, vasculitis, and alopecia were markedly reduced in treated versus untreated mice.

The percentages of effector memory CD4<sup>+</sup> T cells (CD4<sup>+</sup> CD44<sup>high</sup>CD62L<sup>low</sup>) decreased in mice with Scl-GVHD that were treated with arsenic. The pathophysiology of chronic GVHD remains poorly understood, although a large amount of evidence suggests that, in contrast to acute GVHD, which is dependent on CD8<sup>+</sup> T cells, the manifestations observed in chronic GVHD are dependent on the activation of minor histocompatibility Ag-specific donor CD4<sup>+</sup> T cells (4, 23–26). After transplantation of B10.D2 lymphoid cells into irradiated BALB/c mice, naive donor CD4<sup>+</sup> T cells initiate the disease. As a result, donor CD4<sup>+</sup> T cells infiltrate the skin, recruit macrophages and monocytes, and induce fibrosis and destructive changes. Because activated CD4<sup>+</sup> T cells play a pivotal role in the induction of the disease and are decreased by in vivo treatment with arsenic, we investigated the mechanism of action of arsenic on those cells. We show that B10.D2 CD4<sup>+</sup> T cells stimulated with irradiated BALB/c spleen cells display lower GSH contents and produce higher levels of  $\text{H}_2\text{O}_2$  than do unstimulated CD4<sup>+</sup> T cells. These results are in agreement with previous studies showing that, upon activation, T cells overproduce ROS (23, 24). Then, we showed that the high levels of ROS production by activated CD4<sup>+</sup> T cells make them hypersensitive to arsenic-induced apoptosis. Indeed, in vitro treatment with arsenic induced an important decrease in GSH content and a subsequent increase in  $\text{H}_2\text{O}_2$  levels beyond a lethal threshold, inducing cell apoptosis. These data confirm the role of the oxidant/antioxidant balance as a crucial factor that determines cell susceptibility to arsenic (25). Several studies demonstrated that GSH can bind arsenic from attacking its target by formation of a transient  $\text{As}(\text{GS})_3$  complex and that GSH depletion in acute promyelocytic leukemia cells synergizes with  $\text{As}_2\text{O}_3$  in the induction of apoptosis (27).

We next investigated whether an alteration in the profile of cytokine production by splenocytes from mice with Scl-GVHD and treated with  $\text{As}_2\text{O}_3$  could reflect changes in splenic T cell populations. Splenic IL-17 production was lower in arsenic-treated Scl-GVHD mice than in untreated mice. These data are consistent with a large number of recent studies conducted in mice that concluded that Th17 cells are implicated in GVHD development

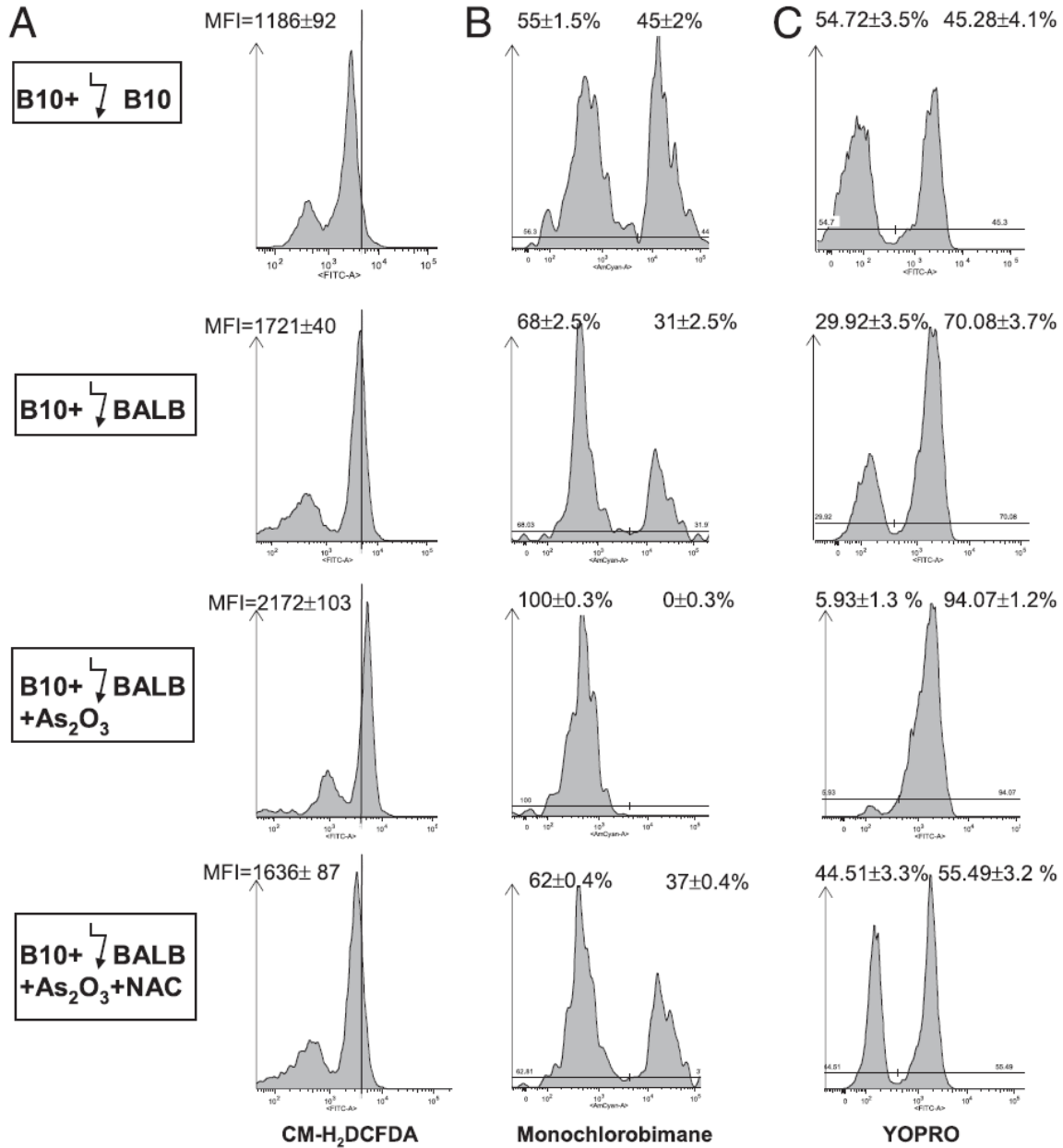


**FIGURE 5.** As<sub>2</sub>O<sub>3</sub> induced apoptosis of activated B10.D2 CD4<sup>+</sup> T cells in culture through ROS production. B10D2 spleen cells were incubated with irradiated B10.D2 splenocytes (↓B10, syngeneic control) or BALB splenocytes (↓BALB) and treated or not with 10 μM As<sub>2</sub>O<sub>3</sub> with or without NAC. Flow cytometry analysis was gated on CD4<sup>+</sup> T cells. Results are representative of four experiments carried out in duplicates. Data were analyzed with FlowJo software. **(A)** Increase in H<sub>2</sub>O<sub>2</sub> generation by As<sub>2</sub>O<sub>3</sub>, measured by flow cytometry using CM-H<sub>2</sub>DCFDA. **(B)** GSH content in B10.D2 CD4<sup>+</sup> T cells, measured by flow cytometry using monochlorobimane staining. **(C)** Induction of apoptosis by As<sub>2</sub>O<sub>3</sub>, measured by flow cytometry using Yopro staining. Mean values were compared using paired Mann–Whitney *U* tests.

in mice. Among them, a study reported that amplification of IL-17 production by the use of the stem cell mobilization factor G-CSF leads to a cutaneous fibrosis occurring late after the graft, as in Scl-GVHD (21). Consistent with those data, another recent article stated that the use of an anti-IL-17 mAb can ameliorate skin symptoms in chronic GVHD (20, 26). Moreover, Nishimori et al. (28) recently showed the beneficial effects of the synthetic retinoid

Am80, which belongs to the same family as all-*trans* retinoic acid, on chronic GVHD. These effects are mediated through the downregulation of Th17 cells. Because other synthetic retinoids, such as N-(4-hydroxyphenyl)retinamide, can induce apoptosis through increased production of ROS, it is possible that Am80 also acts on Th17 cells through the induction of ROS, because As<sub>2</sub>O<sub>3</sub> does in our model (29).

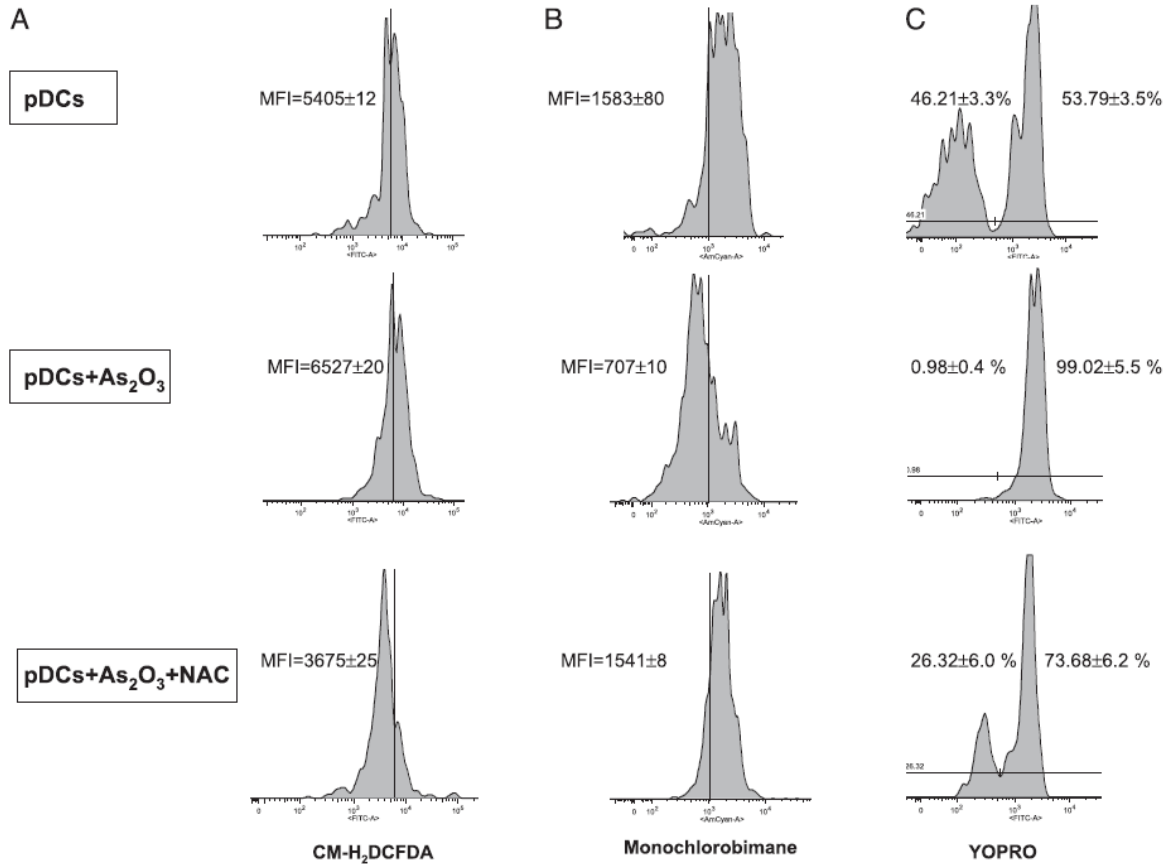


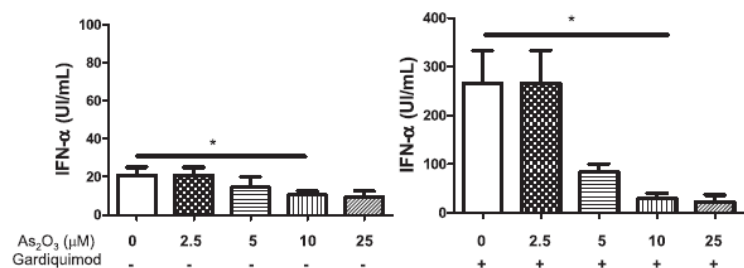
**FIGURE 6.** Effects of in vitro treatment with As<sub>2</sub>O<sub>3</sub> on B10.D2 pDCs. B10.D2 spleen cells were incubated with 10 μM As<sub>2</sub>O<sub>3</sub> with or without NAC for 24 h. Flow cytometry analysis was gated on pDCs subsets defined as B220<sup>+</sup>CD11c<sup>int</sup>CD11b<sup>low</sup>. Results are representative of four experiments carried out in duplicates. Data were analyzed with FlowJo software. **(A)** Induction of ROS formation by As<sub>2</sub>O<sub>3</sub>, measured by flow cytometry using CM-H<sub>2</sub>DCFDA. **(B)** Arsenic induces a decrease in the GSH content in pDCs, measured by flow cytometry using monochlorobimane staining. **(C)** Induction of apoptosis in pDCs by As<sub>2</sub>O<sub>3</sub>, measured by flow cytometry using Yopro staining.

The decrease in splenic CD4<sup>+</sup> effector memory cells in Scl-GVHD mice treated with As<sub>2</sub>O<sub>3</sub> also correlates with a reduction in the Th2 cytokine IL-4 produced in vitro by activated splenocytes. Following the graft of B10.D2 spleen and bone marrow cells into sublethally irradiated BALB/c mice, Zhou et al. (30) observed an increase in the expression of type 2 cytokines in the skin of Scl-GVHD mice compared with syngeneic grafts. Moreover, in other chronic GVHD models, type 2 polarized immune responses are required for the induction of skin GVHD in mice and the development of fibrosis in the skin and visceral organs (31). Thus, the decreased production of IL-4 observed in our study probably contributes to the improvement of skin fibrosis.

As a whole, the alterations in splenic production of cytokines in our model are consecutive to a reduced immune activation after treatment with arsenic and, thus, contribute to the amelioration of Scl-GVHD symptoms.

Chronic GVHD is associated with other autoimmune manifestations, such as the production of autoantibodies in relation to the production of Th2 cytokines. As described by others, we observed the production of anti-DNA-topoisomerase 1 Abs in mice with Scl-GVHD. The levels of these autoantibodies were decreased by As<sub>2</sub>O<sub>3</sub> in our model. Similar effects of As<sub>2</sub>O<sub>3</sub> were reported in a lupus mouse model (MRL/lpr mice), with a decrease in the production of autoantibodies (anti-dsDNA and rheumatoid factors) (17). Consistent with these data, we conclude that As<sub>2</sub>O<sub>3</sub>

**FIGURE 7.** As<sub>2</sub>O<sub>3</sub> targets pDCs and blocks IFN-α production by those cells. pDCs were seeded in six-well plates and coincubated with 10 μg/ml Gardiquimod and/or increasing doses (0–25 μM) of As<sub>2</sub>O<sub>3</sub>. \*p < 0.05.



prevents the development of an autoimmune reaction in Scl-GVHD mice by specifically targeting CD4<sup>+</sup> T cells.

In contrast, the role of APCs in chronic GVHD was recently emphasized by the observation that costimulation of donor T cells through CD80 or CD86 on either host or donor APCs is necessary to induce chronic GVHD (32). pDCs are especially involved in the pathophysiology of GVHD because the adoptive transfer of mature pDCs exacerbates GVHD, and they can stimulate donor T cells to trigger GVHD in the absence of other APCs (6, 33). Yet, the state of maturation of pDCs seems to be crucial in their ability to trigger GVHD. On the one hand, total-body irradiation induces inflammation and maturation of pDCs, which can subsequently activate T cells (6). On the other hand, Banovic et al. (34) showed that precursors of pDCs, but not mature pDCs, can attenuate the symptoms of GVHD, emphasizing the differential functions of pDCs depending on the environment and the model of GVHD. In our hands, the pDC subset was decreased in treated mice compared with untreated mice. As observed for CD4<sup>+</sup> T cells, the increased levels of H<sub>2</sub>O<sub>2</sub> production, along with the decreased GSH content, render pDCs sensitive to As<sub>2</sub>O<sub>3</sub>-induced apoptosis. The action of arsenic on pDCs was confirmed in vitro by the decrease in IFN- $\alpha$  production following stimulation of pDCs by a TLR-7 agonist. This selective effect of arsenic on pDCs could also lead to interesting insights about IFN- $\alpha$ -related diseases, such as systemic lupus erythematosus. Indeed, Bobé et al. (17) showed the beneficial effects of As<sub>2</sub>O<sub>3</sub> in MRL/lpr lupus-prone mice. In accordance with our results, they reported a cytotoxic effect of As<sub>2</sub>O<sub>3</sub> on activated CD4<sup>+</sup> T cells through the reduction in GSH levels, but the beneficial effects observed in their model could also be mediated through regulation of IFN- $\alpha$  production by pDCs.

In summary, our work highlights the beneficial effects of As<sub>2</sub>O<sub>3</sub> in chronic GVHD. As<sub>2</sub>O<sub>3</sub> could be a therapeutic tool in hematologic and solid malignancies, as well as in chronic GVHD (10).

## Acknowledgments

We thank P. Lebon for kindly providing L229 cells and IFN- $\alpha$  standard solution and A. Colle for typing the manuscript.

## Disclosures

The authors have no financial conflicts of interest.

## References

- Lee, S. J., J. P. Klein, A. J. Barrett, O. Ringden, J. H. Antin, J. Y. Cahn, M. H. Carabasi, R. P. Gale, S. Giralt, G. A. Hale, et al. 2002. Severity of chronic graft-versus-host disease: association with treatment-related mortality and relapse. *Blood* 100: 406–414.
- Baird, K., and S. Z. Pavletic. 2006. Chronic graft versus host disease. *Curr. Opin. Hematol.* 13: 426–435.
- Coghill, J. M., S. Sarantopoulos, T. P. Moran, W. J. Murphy, B. R. Blazar, and J. S. Serody. 2011. Effector CD4<sup>+</sup> T cells, the cytokines they generate, and GVHD: something old and something new. *Blood* 117: 3268–3276.
- Korngold, R., and J. Sprent. 1978. Lethal graft-versus-host disease after bone marrow transplantation across minor histocompatibility barriers in mice. Prevention by removing mature T cells from marrow. *J. Exp. Med.* 148: 1687–1698.
- Duffner, U. A., Y. Maeda, K. R. Cooke, P. Reddy, R. Ordemann, C. Liu, J. L. Ferrara, and T. Teshima. 2004. Host dendritic cells alone are sufficient to initiate acute graft-versus-host disease. *J. Immunol.* 172: 7393–7398.
- Koyama, M., D. Hashimoto, K. Aoyama, K. Matsuoka, K. Karube, H. Niuro, M. Harada, M. Tanimoto, K. Akashi, and T. Teshima. 2009. Plasmacytoid dendritic cells prime alloreactive T cells to mediate graft-versus-host disease as antigen-presenting cells. *Blood* 113: 2088–2095.
- Filipovich, A. H., D. Weisdorf, S. Pavletic, G. Socie, J. R. Wingard, S. J. Lee, P. Martin, J. Chien, D. Przepiorka, D. Couriel, et al. 2005. National Institutes of Health consensus development project on criteria for clinical trials in chronic graft-versus-host disease: I. Diagnosis and staging working group report. *Biol. Blood Marrow Transplant.* 11: 945–956.
- Vogelsang, G. B., L. Lee, and D. M. Bensen-Kennedy. 2003. Pathogenesis and treatment of graft-versus-host disease after bone marrow transplant. *Annu. Rev. Med.* 54: 29–52.
- Ruzek, M. C., S. Jha, S. Ledbetter, S. M. Richards, and R. D. Garman. 2004. A modified model of graft-versus-host-induced systemic sclerosis (scleroderma) exhibits all major aspects of the human disease. *Arthritis Rheum.* 50: 1319–1331.
- Sanz, M. A., D. Grimwade, M. S. Tallman, B. Lowenberg, P. Fenaux, E. H. Estey, T. Naoe, E. Lengfelder, T. Büchner, H. Döhner, et al. 2009. Management of acute promyelocytic leukemia: recommendations from an expert panel on behalf of the European LeukemiaNet. *Blood* 113: 1875–1891.
- Miller, W. H., Jr., H. M. Schipper, J. S. Lee, J. Singer, and S. Waxman. 2002. Mechanisms of action of arsenic trioxide. *Cancer Res.* 62: 3893–3903.
- Lynn, S., J. R. Gurr, H. T. Lai, and K. Y. Jan. 2000. NADH oxidase activation is involved in arsenite-induced oxidative DNA damage in human vascular smooth muscle cells. *Circ. Res.* 86: 514–519.
- Smith, K. R., L. R. Klei, and A. Barchowsky. 2001. Arsenite stimulates plasma membrane NADPH oxidase in vascular endothelial cells. *Am. J. Physiol. Lung Cell. Mol. Physiol.* 280: L442–L449.
- Pelicano, H., L. Feng, Y. Zhou, J. S. Carew, E. O. Hileman, W. Plunkett, M. J. Keating, and P. Huang. 2003. Inhibition of mitochondrial respiration: a novel strategy to enhance drug-induced apoptosis in human leukemia cells by a reactive oxygen species-mediated mechanism. *J. Biol. Chem.* 278: 37832–37839.
- Tse, W. P., C. H. Cheng, C. T. Che, and Z. X. Lin. 2008. Arsenic trioxide, arsenic pentoxide, and arsenic iodide inhibit human keratinocyte proliferation through the induction of apoptosis. *J. Pharmacol. Exp. Ther.* 326: 388–394.
- Chen, Y. C., S. Y. Lin-Shiau, and J. K. Lin. 1998. Involvement of reactive oxygen species and caspase 3 activation in arsenite-induced apoptosis. *J. Cell. Physiol.* 177: 324–333.
- Bobé, P., D. Bonardelle, K. Benihoud, P. Popolon, and M. K. Chelbi-Alix. 2006. Arsenic trioxide: A promising novel therapeutic agent for lymphoproliferative and autoimmune syndromes in MRL/lpr mice. *Blood* 108: 3967–3975.
- Kavian, N., A. Servettaz, C. Mongaret, A. Wang, C. Nicco, C. Chéreau, P. Grange, V. Vuiblet, P. Birembaut, M. D. Diebold, et al. 2010. Targeting ADAM-17/notch signaling abrogates the development of systemic sclerosis in a murine model. *Arthritis Rheum.* 62: 3477–3487.
- Jaffee, B. D., and H. N. Claman. 1983. Chronic graft-versus-host disease (GVHD) as a model for scleroderma. I. Description of model systems. *Cell. Immunol.* 77: 1–12.
- Dubois, M. F., V. Mezger, M. Morange, C. Ferrieux, P. Lebon, and O. Bensaude. 1988. Regulation of the heat-shock response by interferon in mouse L cells. *J. Cell. Physiol.* 137: 102–109.
- Hill, G. R., S. D. Olver, R. D. Kuns, A. Varelias, N. C. Raffelt, A. L. Don, K. A. Markey, Y. A. Wilson, M. J. Smyth, Y. Iwakura, et al. 2010. Stem cell mobilization with G-CSF induces type 17 differentiation and promotes scleroderma. *Blood* 116: 819–828.
- McCormick, L. L., Y. Zhang, E. Tootell, and A. C. Gilliam. 1999. Anti-TGF- $\beta$  treatment prevents skin and lung fibrosis in murine sclerodermatous graft-versus-host disease: a model for human scleroderma. *J. Immunol.* 163: 5693–5699.
- Chu, Y. W., and R. E. Gress. 2008. Murine models of chronic graft-versus-host disease: insights and unresolved issues. *Biol. Blood Marrow Transplant.* 14: 365–378.
- Shlomchik, W. D. 2007. Graft-versus-host disease. *Nat. Rev. Immunol.* 7: 340–352.
- Kappel, L. W., G. L. Goldberg, C. G. King, D. Y. Suh, O. M. Smith, C. Ligh, A. M. Holland, J. Grubin, N. M. Mark, C. Liu, et al. 2009. IL-17 contributes to CD4-mediated graft-versus-host disease. *Blood* 113: 945–952.
- Kansu, E. 2004. The pathophysiology of chronic graft-versus-host disease. *Int. J. Hematol.* 79: 209–215.
- Davison, K., S. Côté, S. Mader, and W. H. Miller. 2003. Glutathione depletion overcomes resistance to arsenic trioxide in arsenic-resistant cell lines. *Leukemia* 17: 931–940.
- Nishimori, H., Y. Maeda, T. Teshima, H. Sugiyama, K. Kobayashi, Y. Yamasuji, S. Kadohisa, H. Uryu, K. Takeuchi, T. Tanaka, et al. 2012. Synthetic retinoid Am80 ameliorates chronic graft-versus-host disease by down-regulating Th1 and Th17. *Blood* 119: 285–295.
- Asumendi, A., M. C. Morales, A. Alvarez, J. Aréchaga, and G. Pérez-Yarza. 2002. Implication of mitochondria-derived ROS and cardiolipin peroxidation in N-(4-hydroxyphenyl)retinamide-induced apoptosis. *Br. J. Cancer* 86: 1951–1956.
- Zhou, L., D. Askew, C. Wu, and A. C. Gilliam. 2007. Cutaneous gene expression by DNA microarray in murine sclerodermatous graft-versus-host disease, a model for human scleroderma. *J. Invest. Dermatol.* 127: 281–292.
- Wynn, T. A. 2004. Fibrotic disease and the T(H)1/T(H)2 paradigm. *Nat. Rev. Immunol.* 4: 583–594.
- Anderson, B. E., J. M. McNiff, D. Jain, B. R. Blazar, W. D. Shlomchik, and M. J. Shlomchik. 2005. Distinct roles for donor- and host-derived antigen-presenting cells and costimulatory molecules in murine chronic graft-versus-host disease: requirements depend on target organ. *Blood* 105: 2227–2234.
- MacDonald, K. P., V. Rowe, C. Filippich, R. Thomas, A. D. Clouston, J. K. Welply, D. N. Hart, J. L. Ferrara, and G. R. Hill. 2003. Donor pretreatment with progenipoietin-1 is superior to granulocyte colony-stimulating factor in preventing graft-versus-host disease after allogeneic stem cell transplantation. *Blood* 101: 2033–2042.
- Banovic, T., K. A. Markey, R. D. Kuns, S. D. Olver, N. C. Raffelt, A. L. Don, M. A. Degli-Esposti, C. R. Engwerda, K. P. MacDonald, and G. R. Hill. 2009. Graft-versus-host disease prevents the maturation of plasmacytoid dendritic cells. *J. Immunol.* 182: 912–920.

## Sunitinib Inhibits the Phosphorylation of Platelet-Derived Growth Factor Receptor $\beta$ in the Skin of Mice With Scleroderma-like Features and Prevents the Development of the Disease

Niloufar Kavian,<sup>1</sup> Amélie Servettaz,<sup>2</sup> Wioleta Marut,<sup>1</sup> Carole Nicco,<sup>1</sup> Christiane Chéreau,<sup>3</sup> Bernard Weill,<sup>1</sup> and Frédéric Batteux<sup>3</sup>

**Objective.** Systemic sclerosis (SSc) is characterized by fibrosis of the skin and visceral organs, vascular dysfunction, and immunologic dysregulation. Platelet-derived growth factors (PDGFs) have been implicated in the development of fibrosis and dysregulation of vascular function. We investigated the effects of sunitinib and sorafenib, two tyrosine kinase inhibitors that interfere with PDGF signaling, in a mouse model of diffuse SSc.

**Methods.** SSc was induced in BALB/c mice by subcutaneous injections of HOCl daily for 6 weeks. Mice were randomized to treatment with sunitinib, sorafenib, or vehicle. The levels of native and phosphorylated PDGF receptor  $\beta$  (PDGFR $\beta$ ) and vascular endothelial growth factor receptor (VEGFR) in the skin were assessed by Western blot and immunohistochemical analyses. Skin and lung fibrosis were evaluated by histologic and biochemical methods. Autoantibodies were

detected by enzyme-linked immunosorbent assay, and spleen cell populations were analyzed by flow cytometry.

**Results.** Phosphorylation of PDGFR $\beta$  and VEGFR was higher in fibrotic skin from HOCl-injected mice with SSc than from PBS-injected mice. Injections of HOCl induced cutaneous and lung fibrosis, increased the proliferation rate of fibroblasts in areas of fibrotic skin, increased splenic B cell and T cell counts, and increased anti-DNA topoisomerase I autoantibody levels in BALB/c mice. All of these features were reduced by sunitinib but not by sorafenib. Sunitinib significantly reduced the phosphorylation of both PDGF and VEGF receptors.

**Conclusion.** Inhibition of the hyperactivated PDGF and VEGF pathways by sunitinib prevented the development of fibrosis in HOCl-induced murine SSc and may represent a new SSc treatment for testing in clinical trials.

Supported by the European Union Seventh Framework Programme (FP7/2007-2013 grant 215009) and University Paris-Descartes. Dr. Kavian's work was supported by a grant from the Fondation pour la Recherche Médicale. Dr. Servettaz' work was supported by grants from Actelion and the Association des Sclérodermiques de France.

<sup>1</sup>Niloufar Kavian, MD, PharmD, Wioleta Marut, MS, Carole Nicco, PhD, Bernard Weill, MD, PhD: Université Paris Descartes, EA1833, Hôpital Cochin, AP-HP, Paris, France; <sup>2</sup>Amélie Servettaz, MD, PhD: Université Paris Descartes, EA1833, Hôpital Cochin, AP-HP, Paris, France, and Centre Hospitalier Universitaire de Reims and Hôpital Robert Debré, Reims, France; <sup>3</sup>Christiane Chéreau, PharmD, Frédéric Batteux, MD, PhD: Université Paris Descartes, EA1833, ERTi, Hôpital Cochin, AP-HP, Paris, France, and Centre Hospitalier Universitaire de Reims and Hôpital Robert Debré, Reims, France.

Drs. Kavian and Servettaz contributed equally to this work. Address correspondence to Frédéric Batteux, MD, PhD, Laboratoire d'Immunologie, Faculté de Médecine Paris Descartes, 27 Rue du Faubourg St. Jacques, 75679 Paris Cedex 14, France. E-mail: frederic.batteux@cch.aphp.fr.

Submitted for publication February 7, 2011; accepted in revised form December 15, 2011.

Systemic sclerosis (SSc) is a connective tissue disorder characterized by fibrosis of the skin and visceral organs, vascular dysfunction, and immunologic dysregulation associated with autoantibodies (1). To date, the mechanisms that determine the clinical manifestations of the disease remain unclear (2–4).

Platelet-derived growth factors (PDGFs) are potent mitogens and chemoattractants for cells of mesenchymal and neuroectodermal origin (5). Members of the PDGF family play a major role during embryonic development and contribute to the maintenance of connective tissue in adults (6). Increased levels of PDGF and PDGF receptors (PDGFRs) have been found in skin and lung biopsy samples from patients with scleroderma (7–9). Moreover, sera from patients with SSc may contain autoantibodies directed toward PDGFRs (10). These

antibodies can induce the production of reactive oxygen species that activate the MAP kinase/ERK-1/2 pathway and lead to fibroblast proliferation (11). Transforming growth factor  $\beta$  (TGF $\beta$ ) and interleukin-1 $\alpha$  (IL-1 $\alpha$ ) can also trigger PDGFR signaling through increasing either PDGFR levels or PDGF synthesis by fibroblasts (12). Thus, SSc skin and lung fibroblasts are more sensitive to mitogenic stimulation by PDGF than normal fibroblasts are. The functional significance of the activation of PDGF signaling in fibroblasts has not been fully evaluated in scleroderma, but it may contribute to their enhanced proliferative, migratory, and contractile potential both in vitro and in vivo (13).

Protein tyrosine kinase inhibitors (TKIs) are a new class of therapeutic agents that were initially developed for the treatment of cancers (14,15). They can inhibit proliferative signals via the blockade of the tyrosine kinases Bcr-Abl or c-Kit. Sunitinib and sorafenib also block the tyrosine kinase activity of PDGFRs, as well as the VEGF/VEGFR pathway, which plays a role in the pathogenesis of SSc (16). The aim of this study was to investigate the effects of sunitinib and sorafenib in the HOCl-induced mouse model of SSc (17). We found that these TKIs prevent fibrosis development, immune activation, and endothelial dysfunction in SSc, and thus appear to be attractive therapeutic tools for this disease.

## MATERIALS AND METHODS

**Animals, cells, and chemicals.** Six-week-old female BALB/c mice were purchased from Harlan and were given humane care according to our institutional guidelines. The project was approved by the Regional Ethics Committee on Animal Experimentation. All chemicals were obtained from Sigma, except for sunitinib, which was from Pfizer, and sorafenib, which was from Bayer Health Care.

**Experimental procedure.** *Induction of SSc.* Mice were randomly distributed into experimental and control groups ( $n = 14$  per group). A total of 200  $\mu$ l of substances that generate HOCl was injected intradermally into the back of the mice every day for 6 weeks, as previously described (17). Control groups received injections of 200  $\mu$ l of sterilized phosphate buffered saline (PBS).

*Treatment with TKIs.* Each mouse receiving subcutaneous injections was randomized to receive 6 weeks of oral treatment (by gavage) with sunitinib (50 mg/kg/day), sorafenib (50 mg/kg/day), or vehicle alone. The dosage of 50 mg/kg/day was chosen as being consistent with the report from the European Medicines Agency on sunitinib malate and sorafenib tosylate.

One week after the end of the injections and treatment, the animals were euthanized by cervical dislocation. Lungs were collected, and biopsies of the skin of the back were performed with a punch (6 mm in diameter). Samples for

determination of collagen content were stored at  $-80^{\circ}\text{C}$ . Samples for histopathologic analysis were fixed in 10% formalin.

**Immunofluorescence analysis of skin sections.** Diseased skin was taken from each mouse in each treated and untreated group. Formalin-fixed paraffin-embedded skin sections were dewaxed, and an enzymatic antigen retrieval method was used to overcome antigen masking. Slides were washed for 1 hour at room temperature with sodium borohydride and then blocked with mouse serum. Slides were stained overnight at  $4^{\circ}\text{C}$  with a 1:200 dilution of anti-PDGFR $\beta$ , anti-phosphorylated PDGFR $\beta$ , anti-VEGFR, or anti-phosphorylated VEGFR monoclonal antibodies or with isotype control (all from Santa Cruz Biotechnology). A secondary fluorescein isothiocyanate (FITC)-labeled antibody was then applied, and after washing in PBS, slides were examined using an Olympus microscope equipped with an epifluorescence system. Photographs were captured with an Olympus DP70 camera and analyzed with accompanying controller software as previously described (18).

**Western blot experiments.** Proteins for pPDGFR/PDGFR analysis were extracted from purified primary skin fibroblasts; those for pVEGFR/VEGFR analysis were extracted from the skin. Proteins (30  $\mu$ g per sample) were subjected to immunoprecipitation with PDGFR $\beta$  antibodies and VEGFR antibodies, respectively, using a protein G immunoprecipitation kit (Sigma-Aldrich). Samples were then subjected to 10% polyacrylamide gel electrophoresis, transferred onto nitrocellulose membranes, blocked for 2 hours with 5% dry milk in Tris buffered saline-Tween (TBST), and then incubated overnight at  $4^{\circ}\text{C}$  with anti-PDGFR $\beta$  antibody, anti-phosphorylated PDGFR $\beta$  antibody Tyr<sup>1021</sup>, anti-VEGFR (fetal liver kinase 1) antibody, or anti-phosphorylated VEGFR antibody Tyr<sup>996</sup>. The membranes were then washed and incubated for 1 hour at room temperature with a horseradish peroxidase-conjugated secondary antibody (all from Santa Cruz Biotechnology).

For  $\alpha$ -smooth muscle actin ( $\alpha$ -SMA) Western blots, primary skin fibroblasts were treated with several doses of sorafenib or sunitinib. Cell pellets were then thawed and mixed in radioimmunoprecipitation assay buffer and stored at  $-80^{\circ}\text{C}$ . Proteins were then subjected to 10% polyacrylamide gel electrophoresis, transferred onto nitrocellulose membranes, blocked for 1 hour with 5% dry milk in TBST, and then incubated overnight at  $4^{\circ}\text{C}$  with an anti- $\alpha$ -SMA antibodies diluted 1:2,000 (clone 1A4; Sigma-Aldrich). As an internal control, we used  $\beta$ -actin.

**Assessment of dermal thickness.** The thickness of the skin of the shaved back of each mouse was measured with calipers, and the results were expressed in millimeters. Measurements were performed every week and on the day of euthanization by the same operator (NK). Two sides on the back of each mouse were measured, and the mean was calculated and recorded.

**Histopathologic analysis.** A 5- $\mu$ m-thick tissue section was prepared from the midportion of paraffin-embedded lung and skin pieces and stained with hematoxylin and eosin. Slides were examined under standard brightfield microscopy (Olympus BX60 microscope) by a pathologist (FB) who was blinded to the group assignment of the animal.

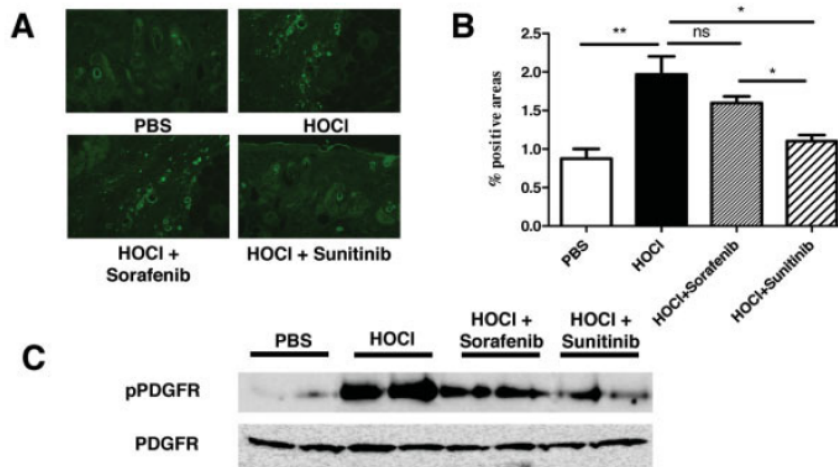


**Figure 1.** Effects of sunitinib and sorafenib on the levels of platelet-derived growth factor receptor (PDGFR) and phosphorylated PDGFR in the skin of mice exposed to HOCl. **A**, Detection of pPDGFR by immunofluorescence in skin sections from a representative mouse from each of the 4 experimental groups ( $n = 7$  per group): phosphate buffered saline (PBS) injected, HOCl injected, HOCl injected and sorafenib treated, and HOCl injected and sunitinib treated. Original magnification  $\times 40$ . **B**, Quantification of pPDGFR staining in skin sections, as determined using ImageJ software. Values are the mean  $\pm$  SEM of 7 mice per group. \* =  $P < 0.05$ ; \*\* =  $P < 0.01$  by Mann-Whitney unpaired U test. NS = not significant. **C**, Levels of native and phosphorylated PDGFR, as determined by Western blotting of protein extracts from purified fibroblasts isolated from mouse skin.  $\beta$ -actin was used as an internal control. Levels of pPDGFR were increased in skin fibroblasts from HOCl-injected mice. Sunitinib down-regulated the phosphorylation of PDGFR. Results are from 2 representative mice ( $n = 7$  per group).

**Measurement of collagen content in skin and lung tissues.** Skin and lung pieces were diced using a sharp scalpel and were mixed with pepsin (1:10 weight ratio) and 0.5M acetic acid overnight at room temperature, with constant stirring. The collagen content assay was based on the quantitative dye-binding Sircol method (Biocolor) (19).

**Isolation of skin fibroblasts and proliferation assays.** Skin fibroblasts were extracted as previously described. Primary fibroblasts ( $2 \times 10^5$ /well) were seeded in 96-well plates and incubated for 48 hours with 150  $\mu$ l of culture medium or a solution of sorafenib (0.75–100 mg/ml) or sunitinib (0.16–25 mg/ml). Cell proliferation was determined by pulsing the cells with  $^3\text{H}$ -thymidine (1  $\mu\text{Ci}$ /well) during the last 16 hours of culture. Results were expressed as absolute counts per minute or as the ratio of the absolute counts per minute with sorafenib or with sunitinib to the absolute counts per minute with medium alone.

**Detection of serum antibodies.** Levels of anti-DNA topoisomerase I IgG (anti-topo I IgG) antibodies were detected using DNA topo I-coated enzyme-linked immunosorbent assay (ELISA) microplates (ImmunoVision). A 1:50 serum dilution was used for the determination of anti-topo I IgG antibodies.

**Flow cytometric analysis of spleen cell subsets.** Cell suspensions from spleens were prepared after hypotonic lysis of erythrocytes. Cells were incubated with the appropriate labeled antibodies for 45 minutes at 4°C in PBS with 0.1% sodium azide and 5% normal rat serum. Cells were then analyzed with a FACSCanto flow cytometer (BD Biosciences). The antibodies used in this study were FITC-conjugated anti-CD11b, phycoerythrin (PE)-conjugated anti-B220, allophycocyanin (APC)-Cy7-conjugated anti-CD4, PE-Cy7-

conjugated anti-CD8, PerCP-Cy-conjugated anti-CD3, and FITC-conjugated anti-B7.1 monoclonal antibodies (BD PharMingen).

**ELISA determination of IL-6 and TGF $\beta$  production by B cells.** B cells were isolated from splenocytes with CD45R (B220) microbeads and MS columns according to the manufacturer's instructions (Miltenyi Biotec). B cell suspensions were then seeded ( $1 \times 10^6$  cells) in 96-well flat-bottomed plates and cultured for 48 hours in complete medium in the presence of 10  $\mu\text{g}/\text{ml}$  of lipopolysaccharide (Sigma-Aldrich). Supernatants were collected, and IL-6 and TGF $\beta$  concentrations determined by ELISA (eBioscience). Results are expressed in nanograms per milliliter.

**ELISA determination of soluble vascular cell adhesion molecule (sVCAM) in serum.** Levels of sVCAM in mouse serum were measured by ELISA. A 1:800 serum dilution and a mouse sVCAM/CD106 DuoSet kit were used according to the manufacturer's instructions (R&D Systems).

**Statistical analysis.** All quantitative data were expressed as the mean  $\pm$  SEM. Data were compared using a nonparametric Mann-Whitney test or Student's paired *t*-test. When the analysis included more than 2 groups, one-way analysis of variance was used. *P* values less than 0.05 were considered significant.

## RESULTS

**High levels of phosphorylated PDGFR $\beta$  in skin fibroblasts from mice with HOCl-induced fibrosis.** Higher amounts of phosphorylated PDGFR $\beta$  were

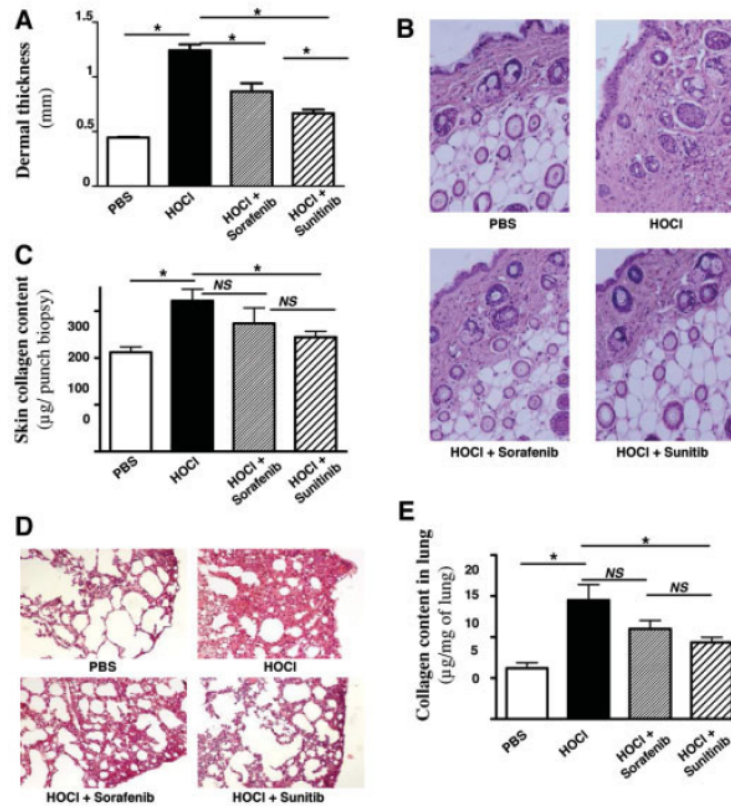


**Figure 2.** Effects of sunitinib and sorafenib on skin and lung collagen contents following subcutaneous injections of an HOCl-generating agent or phosphate buffered saline (PBS) in BALB/c mice ( $n = 7$  per group). Skin and lungs were collected at the time of euthanization. **A**, Dermal thickness in the injected areas of skin from the 4 experimental groups of BALB/c mice. **B**, Representative sections of injected skin from BALB/c mice. Fibrosis was inhibited by sunitinib more than by sorafenib. Hematoxylin and eosin stained; original magnification  $\times 20$ . **C**, Collagen content in skin samples obtained with a 6-mm punch biopsy, as measured by the quantitative dye-binding Sircol method. **D**, Representative sections of lung from BALB/c mice. Lung fibrosis was inhibited by sunitinib more than by sorafenib. Hematoxylin and eosin stained; original magnification  $\times 20$ . **E**, Collagen content in the lung, as measured by the quantitative dye-binding Sircol method. Sunitinib inhibited both skin and lung fibrosis. Values in **A**, **C**, and **E** are the mean  $\pm$  SEM of 7 mice per group.  $*$  =  $P < 0.05$  by Mann-Whitney unpaired U test. NS = not significant.

found in fibrotic areas of skin from HOCl-injected mice than in skin from PBS-injected mice, as demonstrated by immunohistochemistry (Figures 1A and B) and by Western blotting using protein extracts from fibroblasts (Figure 1C). Treatment of mice with HOCl-induced SSc with the TKI sunitinib abrogated the phosphorylation of PDGFR $\beta$  in skin fibroblasts, whereas phosphorylated PDGFRs could still be detected in the skin of mice with SSc treated with sorafenib (Figures 1A–C). No significant difference in the expression of nonphosphorylated PDGFRs in mice exposed to HOCl versus control mice exposed to PBS was observed (Figure 1C).

**Better prevention of skin fibrosis in HOCl-injected mice by sunitinib than by sorafenib.** As previously observed, subcutaneous injections of HOCl in

BALB/c mice increased dermal thickness and the concentration of acid- and pepsin-soluble type I collagen in the skin as compared with injections of PBS ( $P < 0.001$  for dermal thickness and  $P = 0.003$  for collagen concentration in the skin) (Figures 2A and C). Histopathologic analysis confirmed the presence of dermal fibrosis (Figure 2B).

To evaluate whether the inhibition of tyrosine kinases affects the development of dermal fibrosis in this model of SSc, mice exposed to HOCl were simultaneously treated with sorafenib or sunitinib, two different TKIs that interfere with the PDGF pathway.

Sorafenib moderately reduced the dermal thickness ( $P = 0.001$ ) and the accumulation of collagen ( $P = 0.529$ ) induced by HOCl as compared with untreated

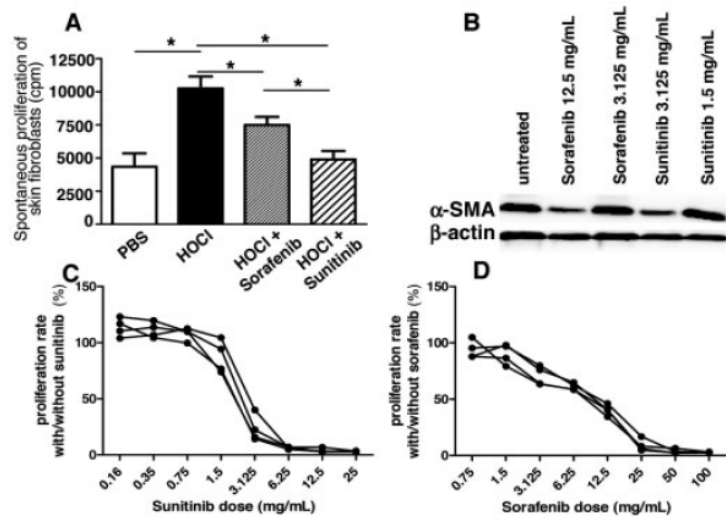


**Figure 3.** Proliferative properties of skin fibroblasts. **A**, Fibroblasts were isolated from injected areas of skin from the 4 experimental groups obtained at the time of euthanization, and cell proliferation was determined by measurement of  $^3\text{H}$ -thymidine ( $1 \mu\text{Ci}/\text{well}$ ) incorporation during the last 16 hours of culture. Fibroblasts from HOCl-injected mice treated with sunitinib showed a lower proliferation rate than those from HOCl-injected mice treated with vehicle alone. Values are the mean  $\pm$  SEM. \* =  $P < 0.05$  by Mann-Whitney unpaired U test. PBS = phosphate buffered saline. **B–D**, Fibroblasts from HOCl-injected mice were isolated and treated in vitro with various doses of sunitinib or sorafenib. Western blotting for the expression of  $\alpha$ -smooth muscle actin ( $\alpha$ -SMA) was performed in untreated cells and in cells treated with 2 different concentrations of sorafenib or sunitinib (**B**).  $\beta$ -actin was used as an internal control. The fibroblast proliferation rate was measured in 4 HOCl-injected mice after exposure to increasing concentrations of sunitinib (**C**) or sorafenib (**D**). Results in **C** and **D** are expressed as the ratio of proliferation with sunitinib or sorafenib, respectively, to the proliferation with medium alone.

mice exposed to HOCl (Figures 2A and C). These results were confirmed by histopathologic analysis of skin biopsy samples stained with hematoxylin and eosin (Figure 2B), which showed a moderate decrease in dermal thickness in HOCl-injected BALB/c mice treated with sorafenib.

In contrast, sunitinib significantly reduced dermal thickness and accumulation of collagen in the skin of HOCl-injected mice ( $P = 0.0003$  and  $P = 0.039$ , respectively, versus untreated HOCl-injected mice) (Figures 2A and C). These results were confirmed by histopathologic analysis (Figure 2B).

**Better prevention of lung fibrosis in HOCl-injected mice by sunitinib than by sorafenib.** In addition to skin fibrosis, HOCl-injected mice developed lung fibrosis, as shown by histopathologic analysis (Figure 2D) and by the higher concentration of type I collagen in the lungs of HOCl-injected mice than in PBS-injected mice ( $P < 0.001$ ) (Figure 2E). Sorafenib did not abrogate the development of lung fibrosis induced by HOCl, as shown by histopathologic analysis and by the accumulation of type I collagen in lungs ( $P = 0.139$  versus untreated HOCl-injected mice) (Figures 2D and E).

In contrast, sunitinib significantly reduced the concentration of type I collagen in the lungs as compared with untreated HOCl-injected mice ( $P = 0.012$ ) (Figure 2E). These findings were confirmed by histopathologic analysis of lung biopsy sections stained with hematoxylin and eosin (Figure 2D), which showed a more marked decrease in lung fibrosis in BALB/c mice treated with sunitinib than in untreated HOCl-injected mice.

Analysis of bronchoalveolar lavage fluid from 4 mice showed a significant increase in the numbers of total leukocytes ( $P = 0.029$ ), neutrophils ( $P = 0.028$ ), monocytes ( $P = 0.036$ ), and lymphocytes ( $P = 0.032$ ) in HOCl-injected mice, which were decreased with sunitinib ( $P = 0.079$ ,  $P = 0.88$ , and  $P = 0.048$ , respectively) (data not shown).

**Normalization of the rate of dermal fibroblast proliferation by sunitinib and sorafenib treatment.** We next investigated whether treatment with various TKIs modified the growth of fibroblasts isolated from the fibrotic skin of mice with SSc. As previously reported, skin fibroblasts isolated from HOCl-injected mice displayed a higher rate of proliferation than did fibroblasts

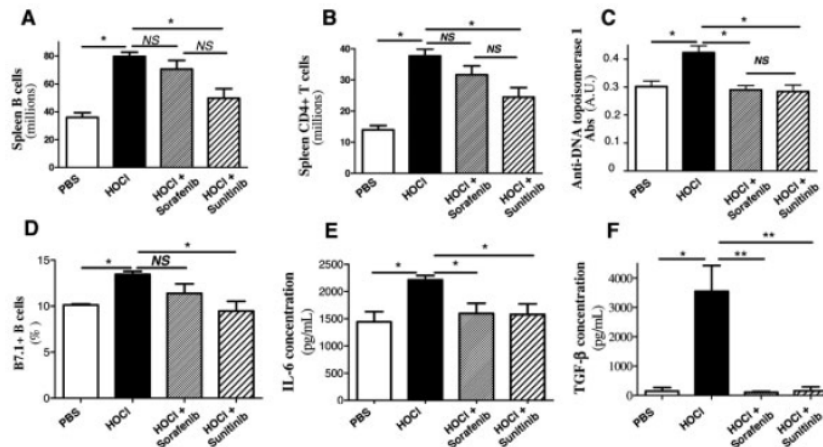


**Figure 4.** Effects of sunitinib and sorafenib on spleen cells, anti-DNA topoisomerase I (anti-topo I) autoantibody production, and interleukin-6 (IL-6) and transforming growth factor  $\beta$  (TGF $\beta$ ) production. BALB/c mice were injected daily for 6 weeks with either an HOCl-generating agent or phosphate buffered saline (PBS) and treated with sunitinib, sorafenib, or vehicle alone. Spleens and sera were collected at the time of euthanization, and cells were enumerated by flow cytometry. **A**, Total numbers of B220+ cells in the spleen. **B**, Total numbers of CD4+ T cells in the spleen. **C**, Levels of anti-topo I antibodies (Abs), as determined by enzyme-linked immunosorbent assay in sera, expressed in arbitrary units (AU). **D**, Percentages of B7.1+ B cells in the spleen. **E**, Concentrations of IL-6 in supernatants from B cells stimulated for 48 hours with lipopolysaccharide (LPS). **F**, Concentrations of TGF $\beta$  in supernatants from B cells stimulated for 48 hours with LPS. Sunitinib treatment decreased splenic B cell and CD4+ T cell numbers, the concentration of anti-topo I antibodies, and the level of activation of B cells. Values are the mean  $\pm$  SEM of 7 mice per group. \* =  $P < 0.05$ ; \*\* =  $P < 0.01$  by Mann-Whitney unpaired U test. NS = not significant.

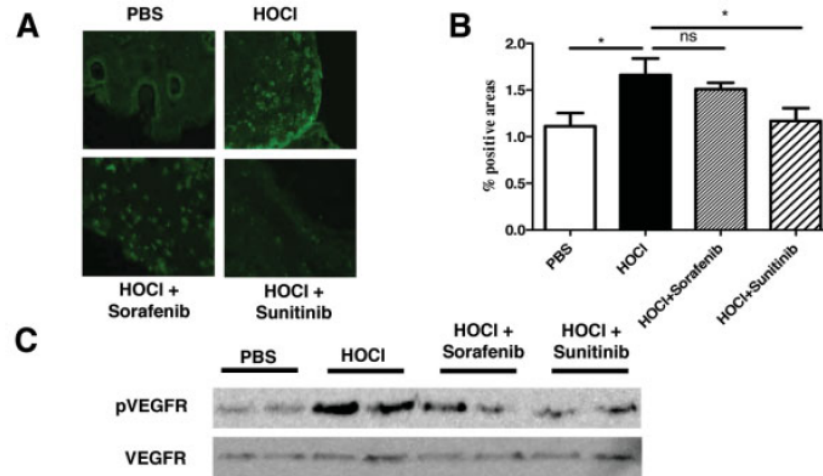


**Figure 5.** Effects of sunitinib and sorafenib on the levels of phosphorylated vascular endothelial growth factor receptor (pVEGFR) in the skin of mice injected with HOCl. **A**, Immunohistochemistry of skin sections obtained from a representative mouse from each of the 4 experimental groups ( $n = 7$  per group). Slides were stained with anti-pVEGFR monoclonal antibody. Original magnification  $\times 40$ . PBS = phosphate buffered saline. **B**, Quantification of pVEGFR staining in skin sections, as determined using ImageJ software. Values are the mean  $\pm$  SEM of 7 mice per group. \* =  $P < 0.05$  by Mann-Whitney unpaired U test. NS = not significant. **C**, Levels of native and phosphorylated VEGFR, as determined by Western blotting of protein extracts from the skin. Sunitinib reduced the levels of pVEGFR in the skin of HOCl-injected mice. Results are from 2 representative mice ( $n = 7$  per group).

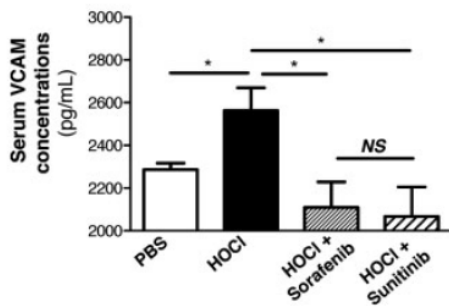


**Figure 6.** Effects of sunitinib and sorafenib on serum concentrations of soluble vascular cell adhesion molecule (sVCAM). BALB/c mice were injected daily for 6 weeks with either an HOCl-generating agent or phosphate buffered saline (PBS) and treated with sunitinib, sorafenib, or vehicle alone. Sera were collected at the time of euthanization, and concentrations of sVCAM were determined by enzyme-linked immunosorbent assay. Soluble VCAM concentrations were lower in sera from HOCl-injected mice treated with sunitinib than in those from HOCl-injected mice treated with vehicle alone. Values are the mean  $\pm$  SEM of 7 mice per group. \* =  $P < 0.05$  by Mann-Whitney unpaired U test. NS = not significant.

from mice injected with PBS ( $P = 0.007$ ) (Figure 3A). The rate of proliferation of fibroblasts isolated from HOCl-injected mice treated with sorafenib or sunitinib was lower than that of fibroblasts isolated from HOCl-injected mice treated with PBS ( $P = 0.028$  for sorafenib and  $P < 0.001$  for sunitinib) (Figure 3A). Sunitinib was more efficient than sorafenib in reducing the rate of dermal fibroblast proliferation ( $P = 0.019$ ) (Figure 3A).

We then analyzed the in vitro effects of both TKIs on fibroblast proliferation. At low doses (0.16–0.75 mg/ml), sunitinib had no effect, whereas at 3.125 mg/ml, the proliferation rate was reduced by 75% (Figure 3C). In vitro treatment with sorafenib also had major effects on fibroblast proliferation, but effective doses were 4 times higher than the effective doses of sunitinib (Figure 3D). Indeed, the 50% inhibition concentration ( $IC_{50}$ ) of sunitinib was 2.75 mg/ml, whereas for sorafenib, the  $IC_{50}$  was 9.75 mg/ml ( $P = 0.029$ ). These results were confirmed by Western blotting showing  $\alpha$ -SMA expression in fibroblasts after in vitro exposure to different doses of sorafenib or sunitinib (Figure 3B).

**Decreased serum levels of HOCl-induced anti-topo I autoantibodies by sunitinib and sorafenib treatment.** We next tested the effects of the two TKIs on the specific autoimmune response to DNA topo I that characterizes the diffuse cutaneous SSc phenotype. IgG antibodies directed toward DNA topo I were found, as usual, in the sera of mice exposed to HOCl for 6 weeks

( $P < 0.001$  versus PBS-injected mice) (Figure 4C). As previously observed, no significant levels of other autoantibodies, such as anti-DNA IgG antibodies, anti-cardiolipin IgG antibodies, or rheumatoid factors, could be detected in the sera of HOCl-injected mice (data not shown).

Both sunitinib and sorafenib prevented the development of anti-topo I IgG antibodies in mice exposed to HOCl ( $P < 0.001$  for comparison of each TKI versus untreated mice) (Figure 4C).

**Decreased expansion of splenic B cells in HOCl-injected mice by sunitinib, but not sorafenib, treatment.**

We next investigated the effects of the 2 TKIs on the different spleen cell populations. Daily subcutaneous exposure to HOCl for 6 weeks increased the numbers of splenic B220+ B cells and CD4+ T cells in the HOCl-injected mice as compared to PBS-injected mice ( $P < 0.001$  for each comparison) (Figures 4A and B). Sunitinib prevented the increase in splenic B cell and CD4+ T cell numbers in mice exposed to HOCl ( $P = 0.002$  and  $P = 0.004$ , respectively, versus untreated mice) (Figures 4A and B). Moreover, treatment with sunitinib reduced the expression of B7.1 on splenic B cells ( $P = 0.0089$ ). Sorafenib tended to decrease B cell and CD4+ T cell numbers and B7.1 expression on B cells, but these results didn't achieve significance ( $P = 0.095$ ,  $P = 0.48$ , and  $P = 0.21$ , respectively) (Figures 4A, B, and D).

**Reduced production of IL-6 and TGF $\beta$  by B cells in HOCl-injected mice by sunitinib, but not sorafenib, treatment.** Since sunitinib and sorafenib exerted beneficial effects on autoantibody production and B cell activation, we tested their actions on the production of profibrotic cytokines by B cells. Both sorafenib and sunitinib decreased the production of IL-6 ( $P = 0.032$  and  $P = 0.029$ , respectively) and TGF $\beta$  ( $P = 0.097$  and  $P = 0.010$ , respectively) (Figures 4E and F).

**Significant reduction of phosphorylated VEGFR concentrations in the skin of mice with HOCl-induced fibrosis by sunitinib treatment.** Since VEGF signaling has been found to be abnormal in SSc patients, we investigated the level of phosphorylation of VEGF receptors in the fibrotic skin of HOCl-injected mice and the effect of the two TKIs on this pathway. Higher levels of phosphorylated VEGFRs were detected in the diseased areas of skin from HOCl-injected mice than in skin from control mice (Figure 5). Sunitinib prevented the phosphorylation of this receptor, since no phosphorylated VEGFRs were found in the diseased areas of skin from HOCl-injected mice treated with sunitinib, as assessed by immunohistochemistry and Western blotting

(Figure 5). In contrast, sorafenib had only a weak effect (Figure 5).

**Prevention of increased serum levels of VCAM by sunitinib and sorafenib treatment.** Elevated serum levels of markers of endothelial cell damage such as sVCAM are observed in SSc. This was confirmed in mice exposed to HOCl as compared with those exposed to PBS ( $P = 0.037$ ) (Figure 6). Sunitinib and sorafenib prevented the increase in sVCAM in mice exposed to HOCl ( $P = 0.015$  for sunitinib versus vehicle alone and  $P = 0.010$  for sorafenib versus vehicle alone) (Figure 6).

## DISCUSSION

In the present study, we describe the hyperactivation of PDGFR $\beta$  and VEGFR in areas of fibrotic skin obtained from mice with HOCl-induced SSc. In addition, we show that TKIs targeting the PDGF and VEGF pathways can represent effective treatments in SSc by abrogating the fibrotic process, endothelial damage, and autoimmune activation that characterize the disease.

PDGFs and their receptors are physiologically involved in the embryogenesis of many organs and in the formation of blood vessels (6). They are also implicated in various diseases. Autocrine or paracrine activation of PDGF signaling pathways has been demonstrated in certain type of cancers and has been shown to affect tumor growth, angiogenesis, invasion, and metastasis. PDGFs and their receptors also play a role in vascular disorders, such as atherosclerosis and pulmonary hypertension, as well as in fibrotic diseases, including pulmonary fibrosis, liver cirrhosis, and cardiac fibrosis.

We first assessed the presence of high levels of PDGFR $\beta$  and its phosphorylation in the fibrotic skin of HOCl-injected mice. The elevated rate of phosphorylation, which reflects receptor hyperactivation, is consistent with the role played by PDGF in several fibrotic diseases. For example, high levels of phosphorylated PDGFRs have been reported in a histologic study of 2 patients with SSc (20). In other studies in which the phosphorylation levels were not investigated, elevated expression of PDGFs or PDGFRs in various tissues obtained from SSc patients have been reported. In contrast, PDGF is almost undetectable in healthy skin or lung (7,8). Similarly, elevated levels of PDGF-A and PDGF-B have been found in bronchoalveolar lavage fluid from scleroderma patients (9). PDGFRs and their signaling pathway may be activated not only by the binding of PDGF, but also by the autoantibodies found in SSc patients (10). Another possible mechanism, which has been observed in SSc fibroblasts, is that TGF $\beta$  released by platelets or infiltrating mononuclear cells

increases the expression of PDGFRs and enhances the mitogenic effect of PDGF-A (21). Taken together, those data strongly suggest a crucial role of the PDGF signaling pathway in the pathogenesis of SSc.

We therefore undertook an investigation of the potential inhibiting effects of 2 TKIs that interfere with the PDGF signaling pathway: sunitinib and sorafenib. Sunitinib was more effective than the same dosage of sorafenib in preventing skin and lung fibrosis in the HOCl-induced SSc model. The higher capacity of sunitinib over sorafenib to prevent fibrosis was associated with a stronger reduction of the phosphorylation rates of PDGFR $\beta$  and VEGFRs. Sorafenib can in fact reduce some features of autoimmunity and abrogate endothelial cell damage, but because of its low capacity to prevent fibrosis, the drug, when administered at a dosage of 50 mg/kg/day, is not able to prevent the development of disease; in contrast, sunitinib acts simultaneously on the vascular, immune, and fibrotic features of the disease.

Many differences between sorafenib and sunitinib can account for the superiority of the latter drug in our experiments. First, sorafenib has a shorter half-life (22), being 30–40 hours, whereas the half-life of sunitinib is 80–100 hours. Second, sunitinib is metabolized as the active metabolite SU012662, increasing the duration of the effects of the molecule. SU012662 is 2-fold less potent than sunitinib, but it inhibits PDGF and VEGF receptors and contributes to the pharmacologic activity of sunitinib. Third, sorafenib and sunitinib do not have identical activity on their target receptors (23). With regard to PDGFR $\beta$ , for example, the  $IC_{50}$  of sorafenib is 1129 nM, whereas it is 75 nM for sunitinib (i.e., >15-fold less). Moreover, the two TKIs do not have identical kinase selectivity, as they both are multikinase inhibitors. Sunitinib has a wider spectrum of inhibition than sorafenib and could inhibit additional receptors, possibly affecting the development of scleroderma in our model (23). Despite these differences, however, it is possible that sorafenib would have been more potent in SSc at higher doses, and further studies are needed to confirm the effects of sorafenib on fibrosis and vascular dysfunctions.

The reduction of dermal fibrosis induced by the profibrotic drug bleomycin has been observed in studies using other TKIs that target PDGFRs, such as imatinib, dasatinib, and nilotinib (24,25). However, the effects on lung fibrosis have not yet been studied. Sorafenib, in contrast, has been shown to attenuate intrahepatic fibrogenesis, hydroxyproline accumulation, and collagen deposition in 2 rat models of liver fibrosis (26). Our study is the first to show clearcut effectiveness of sunitinib on

the development of lung fibrosis in experimental SSc. A study of 5 SSc patients with lung fibrosis treated with a combination of imatinib and cyclophosphamide reported variable results among the patients (27). However, the small number of patients and the absence of a control group render the interpretation of these data difficult (27).

The skin and lungs of patients with SSc contain myofibroblasts, a cell population that produces high amounts of collagen, expresses  $\alpha$ -SMA, and displays an excessive rate of proliferation (28–30). The same observation has been made in the mouse model of HOCl-induced SSc (18). The reduction of fibroblast proliferation by sunitinib and sorafenib in fibrotic areas of the skin of mice exposed to HOCl is consistent with the inhibitory role of other TKIs: imatinib has been shown to inhibit the proliferation of normal and sclerodermatous human fibroblasts in the presence or absence of PDGF or TGF $\beta$  in vitro (8,20). Moreover, treatment with dasatinib and nilotinib was shown to strongly decrease the number of myofibroblasts in bleomycin-induced dermal fibrosis (25).

In addition to the inhibition of fibroblast proliferation and myofibroblast differentiation, we suggest that 2 other mechanisms can also lead to the reduction of skin fibrosis by sunitinib and, to a lesser extent, sorafenib in our SSc model. First, by inhibiting the phosphorylation of PDGFRs, sunitinib and sorafenib may directly decrease collagen production by fibroblasts. This phenomenon has been observed in 2 models of liver fibrosis in which sorafenib treatment directly reduced collagen production by hepatic stellate cells in vitro (26). Dasatinib and nilotinib, 2 other TKIs that interfere with the PDGF pathway, have been shown to decrease collagen synthesis in dermal fibroblasts from bleomycin-treated mice or from scleroderma patients (25). Alternatively, sunitinib and sorafenib can indirectly mediate a reduction in collagen deposition by decreasing the expression of tissue inhibitor of metalloproteinases 1 (TIMP-1), thereby potentially enhancing extracellular matrix degradation. Such a phenomenon, which is caused by an alteration in the balance between matrix metalloproteinase 13 and TIMP-1, has been observed in hepatic stellate cells treated with sorafenib and in dermal fibroblasts exposed to dasatinib or nilotinib (26).

As in patients with diffuse cutaneous SSc, the mice with HOCl-induced SSc develop anti-topo I autoantibodies, and increased numbers of B cells and CD4+ T cells are found in the spleens of these mice. Both sunitinib and sorafenib prevent the development of these autoantibodies as well as the B cell production of IL-6 and TGF $\beta$ . However, only sunitinib significantly

limits the expansion of B cells and CD4+ T cells in the spleen and B cell activation through down-regulation of B7.1. To our knowledge, the effects of sunitinib on the immune system have not previously been reported.

Imatinib may induce a reversible dose-dependent lymphopenia and hypogammaglobulinemia, inhibit the development of dendritic cells derived from human CD34+ progenitor cells, and inhibit the expansion of memory cytotoxic T lymphocytes without affecting primary T cell or B cell responses (31,32). These effects of imatinib may be linked to the inhibition of the Abl protein tyrosine kinase, but the exact mechanism remains unclear. Sunitinib only slightly interferes with Abl, but it strongly inhibits the VEGF receptor. VEGFs play a key role in activating naive T cells (33). VEGFR-1, which is expressed in monocyte/macrophages at both the messenger RNA and protein levels, is involved in the migration of these cells and in the initiation and perpetuation of chronic inflammation (34,35). Mice lacking VEGFR-1 do not develop type II collagen arthritis because they display a decreased inflammatory response of monocyte/macrophages and decreased hematopoietic proliferation (35).

Based on these findings, we hypothesize that the effects of sunitinib on the immune cells observed in our SSc model may be dependent on the inhibition of the phosphorylation of VEGFR. Moreover, sunitinib strongly inhibits B7.1 expression on B cells. The effects of B7.1 downstream signaling on B cell/T cell cooperation may also explain why sunitinib is more effective than sorafenib in preventing disease progression. Indeed, experiments using SCID mice have clearly demonstrated that the immune system is required for the systemic spreading of the disease in the HOCl model of SSc (17).

In addition to fibroblast hyperproliferation and collagen hyperproduction, SSc is characterized by vascular abnormalities. High levels of soluble VCAM, a marker of damage to the endothelium, are found in the sera of SSc patients (36) and in sera from mice with HOCl-induced SSc. Sunitinib and, to a lesser extent, sorafenib prevent the elevation of VCAM in the sera of these mice. Little is known about the events that initiate vascular injury, prevent its repair, and lead to loss of angiogenesis (37). Early stages of SSc are characterized by an exaggerated angiogenic response, which is later followed by fibrosis (38,39). One of the predominant growth factors associated with vascular endothelial proliferation, migration, and survival is VEGF (40). VEGF binds to 2 major receptors, VEGFR-1 and VEGFR-2. The VEGF-A/VEGFR-2 signaling pathway promotes the proliferation, survival, adhesion, and migration of

endothelial cells. Several groups of investigators have reported the up-regulation of VEGF-A and its receptors VEGFRs in sclerodermatous skin (41–43), consistent with the data reported herein.

Taken together, all of these studies indicate a dysregulation of the VEGF/VEGFR axis in SSc. This dysregulation varies with the stage of the disease but is undisputable. A chronic and uncontrolled activation of VEGF-A/VEGFR-2 signaling may play a role in the microangiopathy of SSc (41). In addition, a prolonged exposure to VEGF and uncontrolled activation of VEGFRs can induce the formation of irregularly abnormal vessels with reduced blood flow in vitro (44). Both sunitinib and sorafenib block the kinase activity associated with VEGFRs. The beneficial effects following the use of these 2 drugs on the markers of endothelium damage emphasize the above hypothesis that excessive activation of the VEGFR signaling pathway may trigger the endothelial dysfunction in SSc.

In conclusion, the findings of this study emphasize the pivotal role of the PDGF/PDGFR $\beta$  signaling pathway in SSc by showing a steady phosphorylated state of PDGFR $\beta$  in the fibrotic skin of a mouse model of SSc. In addition, the results of this work strengthen the hypothesis that the uncontrolled activation of the VEGF/VEGFR pathway could be deleterious in this disease and could be directly involved in the microangiopathy of SSc. Our findings also suggest that some TKIs that target both PDGFRs and VEGFRs could be a new and attractive therapeutic tool for use in SSc by acting on the fibrotic, immune, and vascular components of the disease.

#### ACKNOWLEDGMENT

The authors are indebted to Ms Agnes Colle for typing the manuscript.

#### AUTHOR CONTRIBUTIONS

All authors were involved in drafting the article or revising it critically for important intellectual content, and all authors approved the final version to be published. Dr. Batteux had full access to all of the data in the study and takes responsibility for the integrity of the data and the accuracy of the data analysis.

**Study conception and design.** Kavian, Servettaz, Weill, Batteux.

**Acquisition of data.** Kavian, Marut, Nicco, Chéreau.

**Analysis and interpretation of data.** Kavian, Servettaz, Marut, Nicco, Chéreau, Batteux.

#### REFERENCES

- Gabrielli A, Avvedimento EV, Krieg T. Scleroderma. *N Engl J Med* 2009;360:1989–2003.
- Mukerjee D, St George D, Coleiro B, Knight C, Denton CP, Davar J, et al. Prevalence and outcome in systemic sclerosis associated pulmonary arterial hypertension: application of a registry approach. *Ann Rheum Dis* 2003;62:1088–93.
- Matucci-Cerinic M, Denton CP, Furst DE, Mayes MD, Hsu VM, Carpentier P, et al. Bosentan treatment of digital ulcers related to systemic sclerosis: results from the RAPIDS-2 randomised, double-blind, placebo-controlled trial. *Ann Rheum Dis* 2011;70:32–8.
- Launay D, Sitbon O, Le Pavec J, Savale L, Tcherakian C, Yaici A, et al. Long-term outcome of systemic sclerosis-associated pulmonary arterial hypertension treated with bosentan as first-line monotherapy followed or not by the addition of prostanoids or sildenafil. *Rheumatology (Oxford)* 2010;49:490–500.
- Fredriksson L, Li H, Eriksson U. The PDGF family: four gene products form five dimeric isoforms. *Cytokine Growth Factor Rev* 2004;15:197–204.
- Andrae J, Gallini R, Betsholtz C. Role of platelet-derived growth factors in physiology and medicine. *Genes Dev* 2008;22:1276–312.
- Gay S, Jones JR, Huang GQ, Gay R. Immunohistologic demonstration of platelet-derived growth factor (PDGF) and sis-oncogene expression in scleroderma. *J Invest Dermatol* 1989;92:301–3.
- Soria A, Cario-Andre M, Lepreux S, Rezvani HR, Pasquet JM, Pain C, et al. The effect of imatinib (Gleevec) on scleroderma and normal dermal fibroblasts: a preclinical study. *Dermatology* 2008;216:109–17.
- Ludwicka A, Ohba T, Trojanowska M, Yamakage A, Strange C, Smith EA, et al. Elevated levels of platelet derived growth factor and transforming growth factor- $\beta$ 1 in bronchoalveolar lavage fluid from patients with scleroderma. *J Rheumatol* 1995;22:1876–83.
- Svegliati Baroni S, Santillo M, Bevilacqua F, Luchetti M, Spadoni T, Mancini M, et al. Stimulatory autoantibodies to the PDGF receptor in systemic sclerosis. *N Engl J Med* 2006;354:2667–76.
- Svegliati S, Cancellato R, Sambo P, Luchetti M, Paroncini P, Orlandini G, et al. Platelet-derived growth factor and reactive oxygen species (ROS) regulate Ras protein levels in primary human fibroblasts via ERK1/2. *J Biol Chem* 2005;280:36474–82.
- Trojanowska M. Role of PDGF in fibrotic diseases and systemic sclerosis. *Rheumatology (Oxford)* 2008;47:2–4.
- Tingstrom A, Heldin CH, Rubin K. Regulation of fibroblast-mediated collagen gel contraction by platelet-derived growth factor, interleukin-1 $\alpha$  and transforming growth factor- $\beta$ 1. *J Cell Sci* 1992;102:315–22.
- Virgili A, Koptyra M, Dasgupta Y, Glodkowska-Mrowka E, Stoklosa T, Nacheva EP, et al. Imatinib sensitivity in BCR-ABL1-positive chronic myeloid leukemia cells is regulated by the remaining normal ABL1 allele. *Cancer Res* 2011;71:5381–6.
- Mahmood ST, Agresta S, Vigil C, Zhao X, Han G, D'Amato G, et al. Phase II study of sunitinib malate, a multitargeted tyrosine kinase inhibitor in patients with relapsed or refractory soft tissue sarcomas: focus on 3 prevalent histologies: leiomyosarcoma, liposarcoma, and malignant fibrous histiocytoma. *Int J Cancer* 2011;129:1963–9.
- Pendergrass SA, Hayes E, Farina G, Lemaire R, Farber HW, Whitfield ML, et al. Limited systemic sclerosis patients with pulmonary arterial hypertension show biomarkers of inflammation and vascular injury. *PLoS One* 2010;5:e12106.
- Servettaz A, Goulvestre C, Kavian N, Nicco C, Guilpain P, Chereau C, et al. Selective oxidation of DNA topoisomerase I induced systemic sclerosis in the mouse. *J Immunol* 2009;182:5855–64.
- Kavian N, Servettaz A, Mongaret C, Wang A, Nicco C, Chereau C, et al. Targeting ADAM-17/Notch signaling abrogates the development of systemic sclerosis in a murine model. *Arthritis Rheum* 2010;62:3477–87.
- Burdick MD, Murray LA, Keane MP, Xue YY, Zisman DA,

- Belperio JA, et al. CXCL11 attenuates bleomycin-induced pulmonary fibrosis via inhibition of vascular remodeling. *Am J Respir Crit Care Med* 2005;171:261–8.
20. Chung L, Fiorentino DF, BenBarak MJ, Adler AS, Mariano MM, Paniagua RT, et al. Molecular framework for response to imatinib mesylate in systemic sclerosis. *Arthritis Rheum* 2009;60:584–91.
  21. Yamakage A, Kikuchi K, Smith EA, LeRoy EC, Trojanowska M. Selective upregulation of platelet-derived growth factor  $\alpha$  receptors by transforming growth factor  $\beta$  in scleroderma fibroblasts. *J Exp Med* 1992;175:1227–34.
  22. Clark JW, Eder JP, Ryan D, Lathia C, Lenz HJ. Safety and pharmacokinetics of the dual action Raf kinase and vascular endothelial growth factor receptor inhibitor, BAY 43-9006, in patients with advanced, refractory solid tumors. *Clin Cancer Res* 2005;11:5472–80.
  23. Kumar R, Crouthamel MC, Rominger DH, Gontarek RR, Tummino PJ, Levin RA, et al. Myelosuppression and kinase selectivity of multikinase angiogenesis inhibitors. *Br J Cancer* 2009;101:1717–23.
  24. Akhmetshina A, Venalis P, Dees C, Busch N, Zwerina J, Schett G, et al. Treatment with imatinib prevents fibrosis in different preclinical models of systemic sclerosis and induces regression of established fibrosis. *Arthritis Rheum* 2009;60:219–24.
  25. Akhmetshina A, Dees C, Pilecky M, Maurer B, Axmann R, Jungel A, et al. Dual inhibition of c-abl and PDGF receptor signaling by dasatinib and nilotinib for the treatment of dermal fibrosis. *FASEB J* 2008;22:2214–22.
  26. Wang Y, Gao J, Zhang D, Zhang J, Ma J, Jiang H. New insights into the antifibrotic effects of sorafenib on hepatic stellate cells and liver fibrosis. *J Hepatol* 2010;53:132–44.
  27. Sabnani I, Zucker MJ, Rosenstein ED, Baran DA, Arroyo LH, Tsang P, et al. A novel therapeutic approach to the treatment of scleroderma-associated pulmonary complications: safety and efficacy of combination therapy with imatinib and cyclophosphamide. *Rheumatology (Oxford)* 2009;48:49–52.
  28. Rajkumar VS, Howell K, Csiszar K, Denton CP, Black CM, Abraham DJ. Shared expression of phenotypic markers in systemic sclerosis indicates a convergence of pericytes and fibroblasts to a myofibroblast lineage in fibrosis. *Arthritis Res Ther* 2005;7:R1113–23.
  29. Kirk TZ, Mark ME, Chua CC, Chua BH, Mayes MD. Myofibroblasts from scleroderma skin synthesize elevated levels of collagen and tissue inhibitor of metalloproteinase (TIMP-1) with two forms of TIMP-1. *J Biol Chem* 1995;270:3423–8.
  30. Yamamoto T, Nishioka K. Animal model of sclerotic skin. V: increased expression of a smooth muscle actin in fibroblastic cells in bleomycin-induced scleroderma. *Clin Immunol* 2002;102:77–83.
  31. Appel S, Boehmler AM, Grunebach F, Muller MR, Ruf A, Weck MM, et al. Imatinib mesylate affects the development and function of dendritic cells generated from CD34<sup>+</sup> peripheral blood progenitor cells. *Blood* 2004;103:538–44.
  32. Mumprecht S, Matter M, Pavelic V, Ochsenbein AF. Imatinib mesylate selectively impairs expansion of memory cytotoxic T cells without affecting the control of primary viral infections. *Blood* 2006;108:3406–13.
  33. Kim YS, Hong SW, Choi JP, Shin TS, Moon HG, Choi EJ, et al. Vascular endothelial growth factor is a key mediator in the development of T cell priming and its polarization to type 1 and type 17 T helper cells in the airways. *J Immunol* 2009;183:5113–20.
  34. Barleon B, Sozzani S, Zhou D, Weich HA, Mantovani A, Marme D. Migration of human monocytes in response to vascular endothelial growth factor (VEGF) is mediated via the VEGF receptor flt-1. *Blood* 1996;87:3336–43.
  35. Murakami M, Iwai S, Hiratsuka S, Yamauchi M, Nakamura K, Iwakura Y, et al. Signaling of vascular endothelial growth factor receptor-1 tyrosine kinase promotes rheumatoid arthritis through activation of monocytes/macrophages. *Blood* 2006;108:1849–56.
  36. Kuryliszyn-Moskal A, Klimiuk PA, Sierakowski S. Soluble adhesion molecules (sVCAM-1, sE-selectin), vascular endothelial growth factor (VEGF) and endothelin-1 in patients with systemic sclerosis: relationship to organ systemic involvement. *Clin Rheumatol* 2005;24:111–6.
  37. Konttinen YT, Mackiewicz Z, Ruuttila P, Ceponis A, Sukura A, Povilenaite D, et al. Vascular damage and lack of angiogenesis in systemic sclerosis skin. *Clin Rheumatol* 2003;22:196–202.
  38. Distler O, Del Rosso A, Giacomelli R, Cipriani P, Conforti ML, Guiducci S, et al. Angiogenic and angiostatic factors in systemic sclerosis: increased levels of vascular endothelial growth factor are a feature of the earliest disease stages and are associated with the absence of fingertip ulcers. *Arthritis Res* 2002;4:R11.
  39. Guiducci S, Distler O, Distler JH, Matucci-Cerinic M. Mechanisms of vascular damage in SSc—implications for vascular treatment strategies. *Rheumatology (Oxford)* 2008;47:v18–20.
  40. Ferrara N. The role of VEGF in the regulation of physiological and pathological angiogenesis. *EXS* 2005;94:209–31.
  41. Jinnin M, Makino T, Kajihara I, Honda N, Makino K, Ogata A, et al. Serum levels of soluble vascular endothelial growth factor receptor-2 in patients with systemic sclerosis. *Br J Dermatol* 2010;162:751–8.
  42. Distler O, Distler JH, Scheid A, Acker T, Hirth A, Rethage J, et al. Uncontrolled expression of vascular endothelial growth factor and its receptors leads to insufficient skin angiogenesis in patients with systemic sclerosis. *Circ Res* 2004;95:109–16.
  43. Davies CD, Jeziorska M, Freemont AJ, Herrick AL. The differential expression of VEGF, VEGFR-2, and GLUT-1 proteins in disease subtypes of systemic sclerosis. *Hum Pathol* 2006;37:190–7.
  44. Dor Y, Djonov V, Abramovitch R, Itin A, Fishman GI, Carmeliet P, et al. Conditional switching of VEGF provides new insights into adult neovascularization and pro-angiogenic therapy. *EMBO J* 2002;21:1939–47.



## The organotelluride catalyst LAB027 prevents colon cancer growth in the mice

R Coriat<sup>1,3</sup>, W Marut<sup>1,3</sup>, M Leconte<sup>1</sup>, LB Ba<sup>2</sup>, A Vienne<sup>1</sup>, C Chéreau<sup>1</sup>, J Alexandre<sup>1</sup>, B Weill<sup>1</sup>, M Doering<sup>2</sup>, C Jacob<sup>2</sup>, C Nicco<sup>1,3</sup> and F Batteux<sup>\*,1,3</sup>

Organotellurides are newly described redox-catalyst molecules with original pro-oxidative properties. We have investigated the *in vitro* and *in vivo* antitumoral effects of the organotelluride catalyst LAB027 in a mouse model of colon cancer and determined its profile of toxicity *in vivo*. LAB027 induced an overproduction of H<sub>2</sub>O<sub>2</sub> by both human HT29 and murine CT26 colon cancer cell lines *in vitro*. This oxidative stress was associated with a decrease in proliferation and survival rates of the two cell lines. LAB027 triggered a caspase-independent, ROS-mediated cell death by necrosis associated with mitochondrial damages and autophagy. LAB027 also synergized with the cytotoxic drug oxaliplatin to augment its cytostatic and cytotoxic effects on colon cancer cell lines but not on normal fibroblasts. The opposite effects of LAB027 on tumor and on non-transformed cells were linked to differences in the modulation of reduced glutathione metabolism between the two types of cells. In mice grafted with CT26 tumor cells, LAB027 alone decreased tumor growth compared with untreated mice, and synergized with oxaliplatin to further decrease tumor development compared with mice treated with oxaliplatin alone. LAB027 an organotelluride catalyst compound synergized with oxaliplatin to prevent both *in vitro* and *in vivo* colon cancer cell proliferation while decreasing the *in vivo* toxicity of oxaliplatin. No *in vivo* adverse effect of LAB027 was observed in this model.

Cell Death and Disease (2011) 2, e191; doi:10.1038/cddis.2011.73; published online 11 August 2011

Subject Category: Cancer

All living organisms need to maintain a healthy intracellular redox balance in order to survive and to proliferate.<sup>1</sup> Reactive oxygen species (ROS) are natural by-products of aerobic metabolism whose production correlates with normal cell proliferation through the activation of growth-related signaling pathways.<sup>2</sup> Exposure to low levels of ROS can stimulate the growth of many types of mammalian cells, whereas scavengers of ROS suppress normal cell proliferation in human and rodent fibroblasts.<sup>3,4</sup> Furthermore, growth factors trigger the production of hydrogen peroxide (H<sub>2</sub>O<sub>2</sub>) that leads to mitogen-activated protein kinase activation and DNA synthesis, a phenomenon inhibited by antioxidant molecules.<sup>5,6</sup> Several observations suggest that ROS also participate in carcinogenesis. First, ROS production is increased in cancer cells, and an oxidative stress can induce DNA damages that lead to genomic instability and possibly stimulate cancer progression.<sup>7</sup> Second, elevated ROS levels are responsible for the activation of transcription factors, such as NF- $\kappa$ B and AP-1 during tumor progression.<sup>8</sup> Several studies have shown that different types of cancer cells such as colon, liver, lung, kidney, prostate and skin cancer cells<sup>9–11</sup> display a high proliferation rate associated with an increased endogenous production of ROS and a downregulation of their antioxidant enzymatic systems.

On the other hand, ROS can also induce the apoptosis/necrosis of cancer cells. Indeed, most anticancer drugs kill their target cells, at least in part, through the generation of high amounts of intracellular ROS that stimulate pro-apoptotic signal molecules.<sup>12,13</sup> Several anticancer agents, such as 5-fluorouracil,<sup>14</sup> platinum,<sup>9,12</sup> arsenic trioxide,<sup>15</sup> paclitaxel,<sup>16</sup> and anthracyclines<sup>17</sup> increase the intra-cellular levels of ROS. Tumor cells generate higher levels of ROS compared with normal cells and are therefore more sensitive to the additional oxidative stress caused by anticancer agents.<sup>9,12,18</sup>

Cells also contain a variety of free radical scavenging systems that protect them from the effects of drugs that generate ROS. Catalase and glutathione peroxidase are enzymes that detoxify H<sub>2</sub>O<sub>2</sub>. High levels of reduced glutathione, the cofactor of glutathione peroxidase, have been associated with the multidrug resistance phenotype in tumor cells.<sup>19</sup> Therefore, compounds that target such protective mechanisms could enhance the activity of anticancer agents and reverse the multidrug resistance phenotype. For example, buthionine sulfoximine (BSO), a glutathione synthesis inhibitor, can increase the cytotoxicity of melphalan by preventing glutathione peroxidase activity.<sup>20</sup> Conversely, *N*-acetylcysteine protects normal cells from the cytotoxic effects of anticancer drugs by preventing the elevation of

<sup>1</sup>Université Paris Descartes, Faculté de Médecine, Hôpital Cochin, Assistance Publique-Hôpitaux de Paris (AP-HP), Laboratoire d'immunologie, EA 1833, Paris, France and <sup>2</sup>Division of Bioorganic Chemistry, School of Pharmacy, Saarland University, PO Box 151150, D-66123, Saarbruecken, Germany

\*Corresponding author: F Batteux, Laboratoire d'immunologie, UPRES EA 1833, Université Paris Descartes, 24 rue du faubourg St. Jacques, 75679 Paris cedex 14, France. Tel: +33 015 841 2007; Fax: +33 015 841 2008; E-mail: frederic.batteux@cch.aphp.fr

<sup>3</sup>These authors contributed equally to this work.

**Keywords:** tellurium; colon cancer; mice; reactive oxygen species; oxaliplatin

**Abbreviations:** DHE, dihydroethidium; H<sub>2</sub>DCFDA, dichlorodihydrofluorescein diacetate; H<sub>2</sub>O<sub>2</sub>, hydrogen peroxide; ROS, reactive oxygen species

Received 25.11.10; revised 27.5.11; accepted 14.6.11; Edited by V De Laurenzi

intracellular  $\text{H}_2\text{O}_2$  through its reductive properties.<sup>9</sup> SOD enzymes can also affect tumor cell proliferation via their effects on peroxide levels. Thus, the overexpression of SOD in human cancer cell lines or the use of nonpeptidyl mimic of SOD increases  $\text{H}_2\text{O}_2$  production and reduces tumor growth.<sup>9,16,21,22</sup>

Killing cancer cells through the oxidative stress may require compounds that generate ROS and, more appropriately, catalysts that convert the intracellular ROS into a cocktail of cytotoxic chemical species that selectively kills cancer cells.<sup>18,23</sup> Compounds that contain quinones and tellurium are cytotoxic at low concentrations.<sup>24</sup> The LAB027 compound that associates a quinone core along with two tellurium atoms can thus be considered as the prototype of pro-oxidative tellurium compounds. However, LAB027 as well as the other multifunctional redox catalysts synthesized so far have always been tested alone and *in vitro*.

Colon cancer cells are highly sensitive to the oxidative stress<sup>18</sup> and are currently treated by 5FU, oxaliplatin and irinotecan, that generate an intracellular stress in cancer cells. The capacity of organotelluride catalysts to generate an intracellular oxidative burst alone and in combination with a pro-oxidative cytotoxic drug, prompted us to test these molecules against colon cancer *in vitro* and *in vivo*. Therefore, we investigated the antitumoral activity of the organotelluride catalyst LAB027 alone and in combination with oxaliplatin *in vitro* and *in vivo* in an animal model of colon cancer. Because of the therapeutic potential of this compound, an evaluation of its profile of toxicity profile has also been performed.

## Results

**LAB027 exerts pro-oxidative effects *in vitro*.** Incubation of mouse CT26 and human HT29 colon cancer cell lines with increasing amounts of LAB027, dose-dependently increased the production of  $\text{O}_2^{\bullet-}$  (CT26:  $P < 0.05$  with  $2 \mu\text{M}$  LAB027;

HT29:  $P < 0.05$  with  $1 \mu\text{M}$  LAB027) (Figure 1). A dose-dependent increase in the production of  $\text{H}_2\text{O}_2$  was also observed (CT26:  $P < 0.05$  with  $2 \mu\text{M}$  LAB027; HT29:  $P < 0.05$  with  $2 \mu\text{M}$  LAB027) (Figure 1). Incubation of NIH3T3 fibroblasts with increasing amounts of LAB027 had no effects on the production of  $\text{O}_2^{\bullet-}$  ( $P = \text{NS}$ ), but dose dependently increased the production of  $\text{H}_2\text{O}_2$  by 500% (NIH3T3:  $P < 0.05$  with  $1 \mu\text{M}$  LAB027) (Figure 1). Incubation of W138 fibroblasts with increasing amounts of LAB027 had no effects on the production of  $\text{O}_2^{\bullet-}$  ( $P = \text{NS}$ ), but dose-dependently increased the production of  $\text{H}_2\text{O}_2$  by 260% (W138:  $P < 0.05$  with  $1 \mu\text{M}$  LAB027) (Figure 1).

**LAB027 alters the activities of antioxidant enzymes *in vitro*.** Incubation of CT26 and HT29 cells with increasing amounts of LAB027 did not significantly alter SOD, catalase and glutathione reductase activities ( $P = \text{NS}$  compared with untreated cells) (Supplementary Figure 2). By contrast, incubation of NIH3T3 or W138 fibroblasts with increasing amounts of LAB027 dose-dependently increased the production of SOD ( $P < 0.001$  for NIH3T3 and  $P < 0.001$  for W138 with  $4 \mu\text{M}$  LAB027) and glutathione reductase activities ( $P < 0.001$  for NIH3T3 and  $P < 0.001$  for W138 with  $4 \mu\text{M}$  LAB027) versus untreated cells (Supplementary Figure 2) but had no effect on catalase levels.

**LAB027 exerts cytostatic and cytotoxic effects *in vitro*.** Incubation of CT26 or HT29 cells with increasing amounts of LAB027 dose-dependently decreased their proliferative rates and their viability (Figures 2a and b). At  $1 \mu\text{M}$ , LAB027 decreased CT26 and HT29 proliferation rates by 54% and 57%, respectively ( $P < 0.001$  for CT26 and  $P < 0.001$  for HT29), and decreased their viability by 31 and 27%, respectively ( $P < 0.001$  for CT26 and  $P < 0.05$  for HT29). Incubation of NIH3T3 or W138 fibroblasts with increasing amounts of LAB027, dose-dependently decreased their proliferation rates and their viability. At

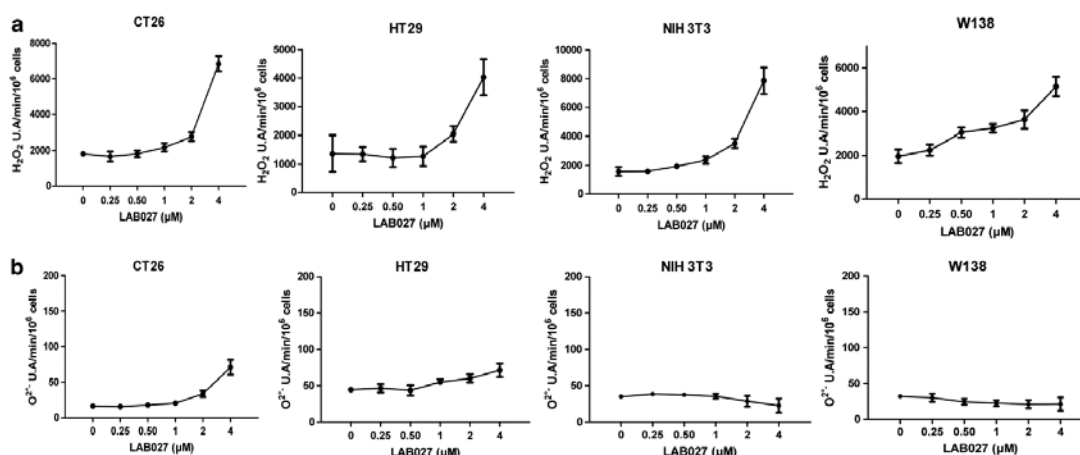


**Figure 1** Production of hydrogen peroxide (a) and of superoxide anions (b) by CT26, HT29, NIH3T3 and W138 cells incubated with increasing concentrations of LAB027. Results are the mean  $\pm$  S.E.M. of three experiments performed in triplicates

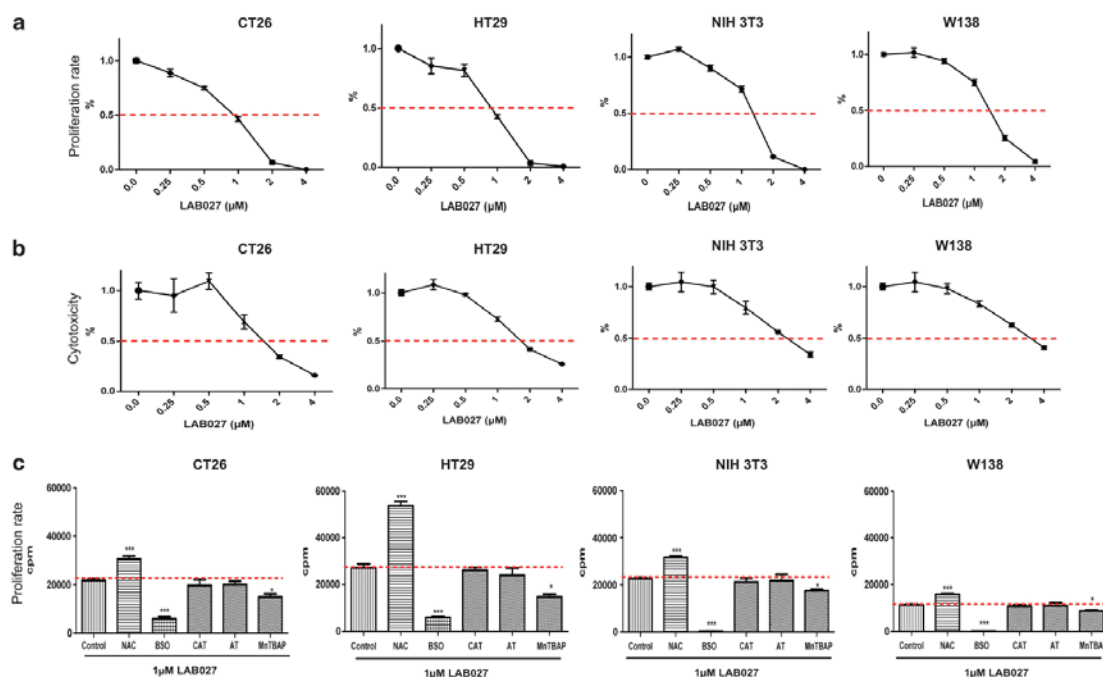


**Figure 2** Proliferation rates (a) and cytotoxicity (b) of CT26, HT29, NIH3T3 and W138 cells incubated with various concentrations of LAB027. Results are the mean  $\pm$  S.E.M. of three experiments performed in triplicates. Proliferation (c) of CT26, HT29, NIH3T3 and W138 cell lines following incubation with 1  $\mu$ M LAB027 alone, or associated with either 400  $\mu$ M *N*-acetylcysteine, 400  $\mu$ M DL-buthionine-(S,R)-sulfoximine (BSO), 200  $\mu$ M 3-amino-1,2,4-triazole (AT), 50 units/ml catalase PEG (CAT) or with 100  $\mu$ M MnTBAP. Cellular proliferation was measured by thymidine incorporation. Error bars represent S.E.M.

1  $\mu$ M LAB027 decreased NIH3T3 and W138 proliferation rates by 28 and 25%, respectively ( $P < 0.001$  for NIH3T3 and  $P < 0.001$  for W138), and decreased their viability by 20 and 17%, respectively ( $P < 0.05$  for NIH3T3 and  $P < 0.05$  for W138) (Figures 2a and b). LAB027 was significantly more cytostatic and cytotoxic in CT26 and in HT29 tumor cells lines compared with non-tumoral NIH3T3 and W138 fibroblasts (cytostatic effect of 1  $\mu$ M LAB027: CT26 versus NIH3T3,  $P < 0.001$ ; CT26 versus W138,  $P < 0.001$ ; HT29 versus NIH3T3,  $P < 0.001$ ; HT29 versus W138,  $P < 0.001$ ; cytotoxic effect of 2  $\mu$ M LAB027: CT26 versus NIH3T3,  $P < 0.001$ ; CT26 versus W138,  $P < 0.001$ ; HT29 versus NIH3T3,  $P < 0.001$ ; HT29 versus W138,  $P < 0.001$ ). The antiproliferative effect of 1  $\mu$ M LAB027 on CT26, HT29 NIH3T3 and W138 cells was significantly abrogated *in vitro* by 400  $\mu$ M *N*-acetylcysteine ( $P < 0.05$ ;  $P < 0.02$ ;  $P < 0.05$ ;  $P < 0.05$ , respectively). By contrast, the SOD mimic MnTBAP that produces  $H_2O_2$  through the dismutation of  $O_2^{\bullet -}$ , significantly increased the antiproliferative activities of 1  $\mu$ M LAB027 on CT26 ( $P < 0.05$ ), on HT29 ( $P < 0.02$ ), on NIH3T3 ( $P < 0.05$ ) and on W138 ( $P < 0.05$ ). Incubation of 1  $\mu$ M LAB027 with the gamma-glutamylcysteine synthetase inhibitor BSO that depletes intracellular GSH, significantly augmented the cytotoxicity of LAB027 in all cell lines ( $P < 0.001$ ). By contrast, blocking catalase by aminotriazole or increasing its intracellular levels by incubation with

PEG-catalase had no effects on cell survival or proliferation whatever the cell type considered (Figure 2c).

**Cytotoxic pathways engaged by LAB027.** To determine the pathway through which LAB027 promotes tumor cell death, we examined by western blot the cleavage of caspase-3 and caspase-8 proteins 24 h after incubation of HT29 tumor cells with increasing amounts of LAB027. Although the expression of cleaved caspase-8 fragments was dose-dependently upregulated in HT29 cells treated with LAB027, no caspase-3 cleavage was observed in LAB027-treated HT29 cells at any concentration tested (Figure 3a). Incubation of HT29, CT26 or NIH 3T3 cells with either caspase-3-specific inhibitor Ac-DEVD-FMK, or with caspase-8 inhibitor Z-IETD-FMK or with the broad-spectrum caspase inhibitor Z-VAD-FMK along with LAB027 did not modify the cytotoxic effects of LAB027 (Figure 3b), whereas the latter two caspases inhibitors effectively inhibited caspase-8 cleavage at the concentration tested (not shown). Early intracellular events that occur during cell death are associated with mitochondrial changes mediated by members of the Bcl-2 family of proteins, including antiapoptotic Bcl-2, Bcl-xL and pro-apoptotic Bax, Bad proteins. In addition, treatment of HT29 cells with LAB027 triggered an autophagic process (Figure 3) as demonstrated by ATG8 induction and cleavage, and by autophagic

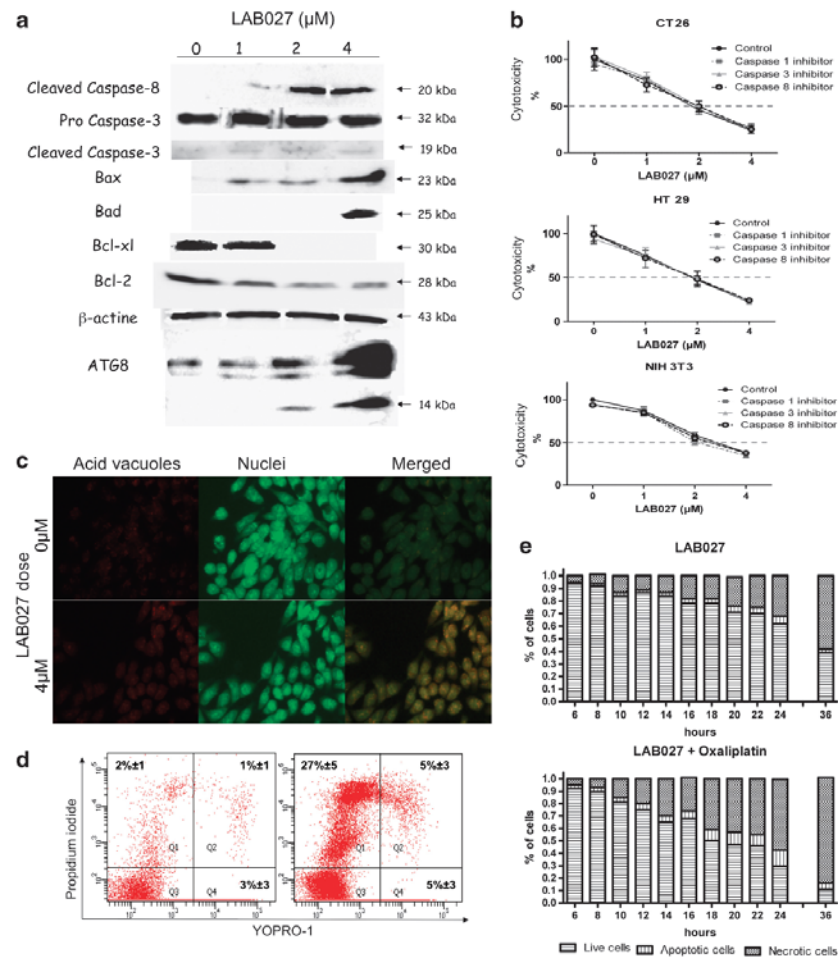


**Figure 3** Pro-apoptotic effects of LAB027 (a). HT29 cells were treated or not with increasing concentrations of LAB027 for 24 h. Expressions of cleaved caspase-8, pro-caspase-3 and cleaved caspase-3, Bax, Bad, Bcl-xL, Bcl-2 and ATG8 proteins were analyzed by western blot. Proliferation rates (b) of CT26, HT29 and NIH3T3 cells incubated with various concentrations of LAB027 alone or associated with either 40  $\mu$ M DEVD-FMK (caspase-3 inhibitor) or 40  $\mu$ M IETD-FMK (caspase-8 inhibitor) 40  $\mu$ M ZVAD-FMK (broad-spectrum caspase inhibitor). Results are means  $\pm$  S.E.M. of three independent experiments. (c) Immunofluorescence microscopy of HT29 cells stained with acridine orange and treated for 24 h or not with 4  $\mu$ M LAB027. An increased number of cells with stained acidic vesicular organelles (orange fluorescence) in 4  $\mu$ M LAB027 treated cells was observed. (d) Fluorescence-activated cell sorting analysis of cell death. Apoptosis/necrosis was analyzed by flow cytometry using the Membrane Permeability/Dead Cell Apoptosis Kit with YO-PRO-1 and Propidium iodide on HT29 treated (right panel) or not (left panel) with 4  $\mu$ M LAB027 for 24 h. Necrotic cells are PI positive and YO-PRO-1 positive or negative. Apoptotic cells are PI negative and YO-PRO-1 positive. Viable cells are negative for both dyes. One representative experiment of three is shown. (e) Kinetic apoptosis/necrosis evolution in HT29 cells treated with 4  $\mu$ M LAB027 alone or with oxaliplatin 0.5  $\mu$ M

vacuolization as demonstrated by acridine orange staining. To clarify the mode of cell death, LAB027-treated HT29 cells were stained with PI and YO-PRO-1. After 24-h incubation with 4  $\mu$ M LAB027, 5%  $\pm$  3 HT29 were positive for YO-PRO-1 alone and 33%  $\pm$  7 HT29 were positive for PI alone or with YO-PRO-1 showing a necrotic process (Figure 3d). A kinetic analysis of the mode of cell death between 6 and 24 h indicated that LAB027 induces cell death mainly through a necrotic process (Figure 3e).

**LAB027 synergized with oxaliplatin to trigger ROS production and exert cytostatic effects on colon**

**cancer cell lines *in vitro*.** Co-incubation of CT26 or HT29 cells with 5 or 0.5  $\mu$ M oxaliplatin and increasing concentrations of LAB027, augmented the production of H<sub>2</sub>O<sub>2</sub> up to 323% (CT26) or 1215% (HT29) at the highest concentration of LAB027 tested. By contrast, co-incubation of mouse NIH3T3 fibroblasts with 5  $\mu$ M oxaliplatin and LAB027 did not augment the production of H<sub>2</sub>O<sub>2</sub> versus oxaliplatin alone (Figure 4). Moreover, co-incubation of CT26, HT29 or NIH3T3 cells with oxaliplatin (5  $\mu$ M with CT26 cells and NIH3T3 cells; 0.5  $\mu$ M with HT29 cells) with increasing concentrations of LAB027 did not augment the production of O<sub>2</sub><sup>•-</sup> versus oxaliplatin alone (Figure 4).

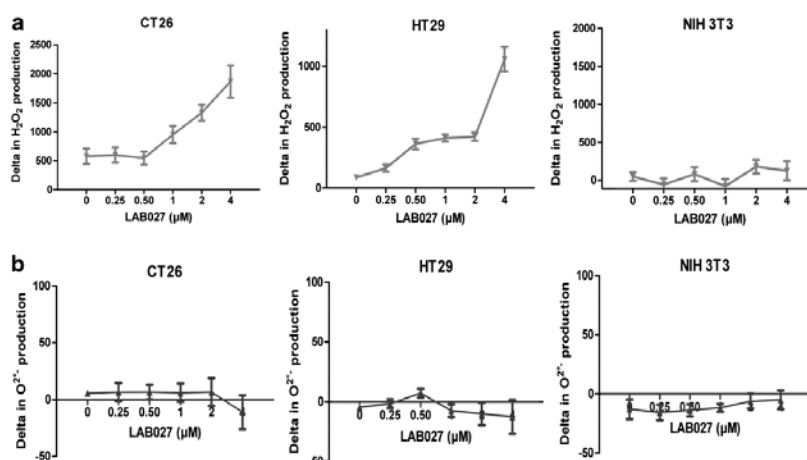


**Figure 4** Production of hydrogen peroxide (a) and superoxide anions (b) by oxaliplatin-treated CT26, HT29 and NIH3T3 cells incubated with increasing concentrations of LAB027. Differences (delta) in  $H_2O_2$  production (a) and in  $O_2^{\bullet-}$  production (b) between oxaliplatin-treated cells and untreated cells are shown. Results are the mean  $\pm$  S.E.M. of three experiments performed in triplicate

Incubation of HT29 colon cancer cells with  $1 \mu M$  LAB027 along with  $0.5 \mu M$  oxaliplatin significantly increased the antiproliferative potential of LAB027 by 31% ( $P < 0.05$ ) and the antiproliferative potential of oxaliplatin by 23% ( $P < 0.05$ ). By contrast, incubation of mouse NIH3T3 fibroblasts with  $1 \mu M$  LAB027 along with  $5 \mu M$  oxaliplatin did not significantly modify the antiproliferative potential of LAB027 ( $P = 0.68$ ) or of oxaliplatin ( $P = 0.85$ ) administered alone (Figure 5). A kinetic analysis of the mode of cell death induced by co-incubation of LAB027 with oxaliplatin was performed on HT29 cells. The percentages of necrotic cells among apoptotic + necrotic cells were 81%, 84% and 84% after 6, 12 and 24 h incubation, respectively, with LAB027 alone compared with 60, 80 and 83% after 6, 12 and 24 h incubation, respectively, with oxaliplatin + LAB027 (Figure 3e).

**Imbalance of GSH metabolism in tumor cells.** In normal NIH3T3 cells, increasing the oxidative stress by incubation with  $4 \mu M$  LAB027 augmented intracellular GSH levels by 311% (Figure 5). Adding  $5 \mu M$  oxaliplatin to LAB027, further increased GSH synthesis by 80%. Interestingly, incubating CT26 or HT29 colon cancer cells with LAB027 alone or in association with oxaliplatin failed to increase GSH synthesis (Figure 5). In order to determine whether this phenomenon was linked to a differential effect of LAB027 on GSH efflux in normal and tumor cells, we measured the GSH released from CT26, HT29 or NIH3T3 upon incubation with increasing concentrations of LAB027 alone or in association with oxaliplatin. Increasing concentrations of LAB027 significantly induced GSH release, but no difference was observed between normal and tumor cells (Supplementary Figure 3).

Co-incubation of oxaliplatin and LAB027 with the glutathione reductase inhibitor BSO that depletes the cells in reduced glutathione, significantly increased the antiproliferative potential of oxaliplatin + LAB027 in all cell lines

( $P < 0.001$ ). In addition, incubation with NAC, a precursor of GSH significantly increased cell proliferation ( $P < 0.001$  for HT29 and CT26 and  $P < 0.05$  for 3T3). By contrast, blocking catalase with aminotriazol or increasing its intracellular levels with PEG-catalase had no effect on cell survival and proliferation whatever the cell type considered (Figure 5).

**Effect of LAB027 on the growth of CT26 tumor cells implanted in mice treated with oxaliplatin.** To determine whether LAB027 could inhibit tumor growth *in vivo*, we treated mice bearing CT26 tumors with either oxaliplatin or LAB027, or with the association of oxaliplatin and LAB027 (Figure 6a). Mice treated with oxaliplatin alone developed significantly smaller tumors than untreated mice ( $-58\%$ ,  $P < 0.001$  versus untreated mice on day 27). LAB027 also inhibited tumor growth when administered alone ( $-25\%$  on day 27,  $P < 0.05$  versus untreated mice). Mice treated simultaneously with LAB027 and oxaliplatin had significantly smaller tumors than untreated mice on day 27 ( $-75\%$ ,  $P < 0.001$ ). Furthermore, the administration of LAB027 amplified the antitumor effect observed with oxaliplatin alone ( $-41\%$  versus oxaliplatin-treated mice,  $P < 0.05$  on day 27). In order to determine whether the immune system has a role in the antitumoral effects induced by LAB027 alone or in combination with oxaliplatin, we performed the same experiment using immunodeficient SCID mice. In SCID mice implanted with CT26, LAB027 inhibited tumor growth when administered alone ( $-24\%$  at day 27,  $P < 0.05$  versus untreated mice). SCID mice treated simultaneously with LAB027 and oxaliplatin had significantly smaller tumors than untreated mice at day 27 ( $-78\%$ ,  $P < 0.001$ ). The administration of LAB027 amplified the antitumor effect observed with oxaliplatin alone ( $-56\%$  versus oxaliplatin-treated mice,  $P < 0.05$  at day 27).

***In vivo* effects of LAB027 on the toxicity of oxaliplatin and on the susceptibility of mice to bacterial**

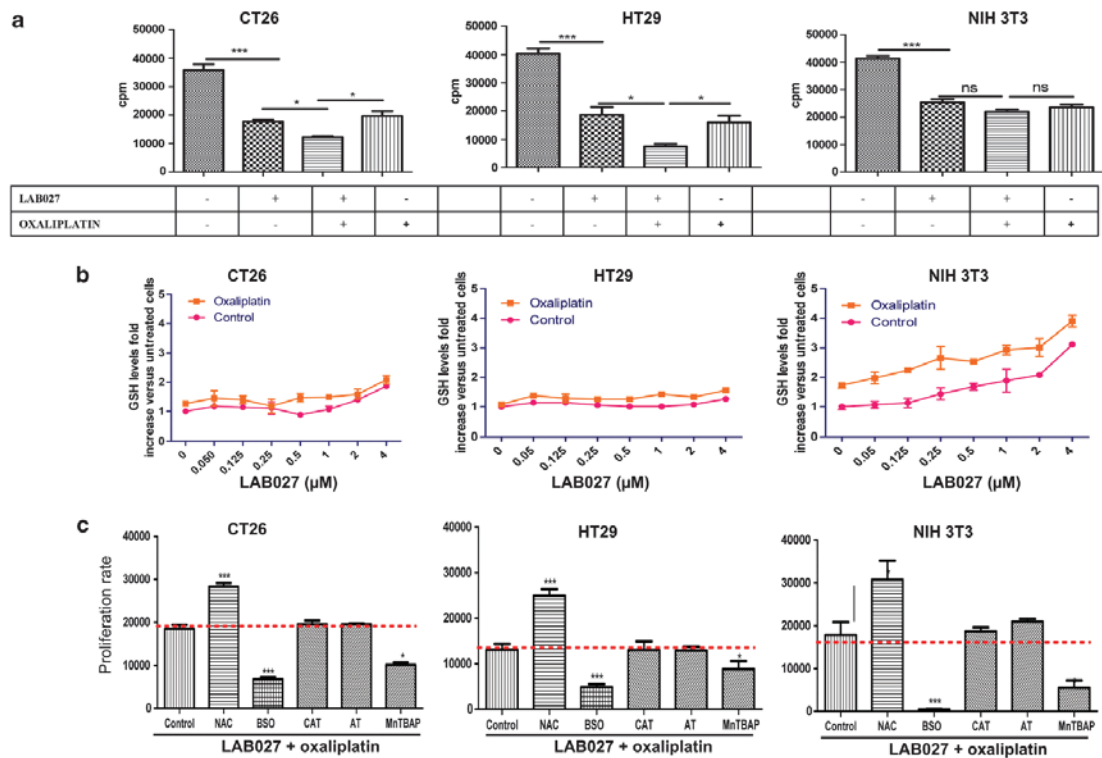


**Figure 5** Proliferation (a) of CT26, HT29 and NIH3T3 cells treated with LAB027 alone or in association with oxaliplatin. Error bars represent S.E.M. LAB027 concentration was 1  $\mu$ M for all the cells tested. Intracellular levels of reduced glutathione (b) in CT26 cells, HT29 cells and NIH3T3 cells treated with various concentrations of LAB027. Results are the mean  $\pm$  S.E.M. of three experiments each performed in triplicate. Proliferation (c) of CT26, HT29 and NIH3T3 cell lines following incubation with 1  $\mu$ M LAB027 plus oxaliplatin alone, or associated with either 400  $\mu$ M *N*-acetylcysteine, 400  $\mu$ M DL-buthionine-[S,R]-sulfoximine (BSO), 200  $\mu$ M 3-amino-1,2,4-triazole (AT), 50 units/ml catalase PEG (CAT) or with 100  $\mu$ M MnTBAP. Oxaliplatin concentration was respectively 5, 0.5 and 5  $\mu$ M for CT26, HT29 and NIH3T3 cells. Cellular proliferation was measured by thymidine incorporation. Error bars represent S.E.M.

**infection.** We next investigated the effects of LAB027 on the toxicity of oxaliplatin in BALB/c mice. The toxicity on liver was evaluated by measuring serum concentrations of ALAT, LDH and alkaline phosphatases. Kidney function was assessed on serum BUN and creatinin (Supplementary Figure 4). None of these parameters were altered in the serum of mice treated with oxaliplatin or LAB027 alone, or in the serum of mice treated with both LAB027 and oxaliplatin. After 14 days the first injection of oxaliplatin, a significant decrease in the absolute numbers of peripheral leukocytes, neutrophils and platelets was observed *versus* control mice treated with PBS (Figure 6b). LAB027 alone had no hematological toxicity compared with untreated control mice. Furthermore, the administration of LAB027 in association with oxaliplatin significantly decreased the hematological toxicity of oxaliplatin. Indeed, the counts of peripheral leukocytes ( $P=0.027$ ), neutrophils ( $P=0.008$ ) and platelets ( $P=0.035$ ) in the blood of mice treated with LAB027 and oxaliplatin were higher than in the blood of mice treated with oxaliplatin alone. Because bacterial infection is the main complication of neutropenia, the susceptibility of mice to intraperitoneal inoculation of *E. coli* was tested

following the administration of oxaliplatin alone or in association with LAB027 (Figure 6c). In all, 40% of control mice treated with PBS survived 28 h after *E. coli* inoculation. However, no animal treated with oxaliplatin before *E. coli* inoculation, survived more than 22 h following the bacterial challenge. In contrast, 55% of mice treated with oxaliplatin and LAB027 survived 28 h following intraperitoneal inoculation of *E. coli* ( $P=0.044$ ).

## Discussion

This study provides pre-clinical evidence that the organotelluride catalyst LAB027, a prototypical member of family of the 'sensor/effector' multifunctional redox catalyst agents, is a new candidate molecule to treat colon cancer either alone or in combination with oxaliplatin.

Previous experiments have shown that 'sensor/effector' agents can act as cytotoxic molecules *in vitro*.<sup>25</sup> These agents are catalytic molecules that recognize a particular intracellular state of cells – such as an oxidative stress – and selectively kill the cells that are under this state. In our hands, tumor cells display an elevated basal level of ROS that is amplified by

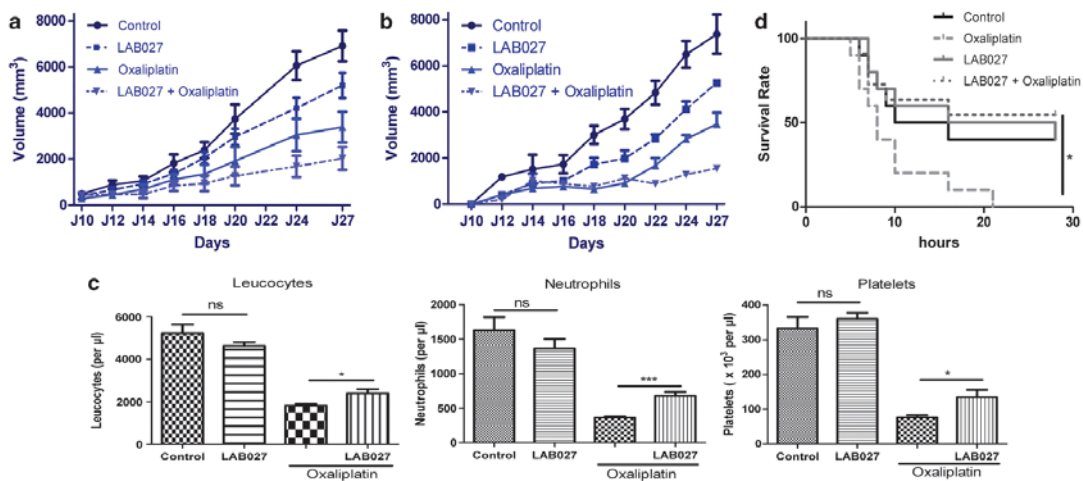


**Figure 6** Tumor growth following implantation of  $2 \times 10^6$  CT26 cells in BALB/c mice (a) or in SCID mice (b). Mice were treated as described in the 'Materials and Methods section' (seven mice/group). Biological toxicity (c): leukocytes, neutrophils and platelets count in the blood of mice on day 14, following two i.v. injections of oxaliplatin (10 mg/kg) on days 1 and 7 and two injections of LAB027 (10 mg/kg) on days 1 and 7. Survival rate of mice (d) following intraperitoneal injection of  $10^7$  *E. coli* in BALB/c mice. Mice were treated as described in the 'Material and Method section' (10 mice/group)

LAB027 to generate a lethal oxidative burst. The most likely explanation for this amplifying effect is an association of oxygen radical and  $H_2O_2$  formation at the quinone and oxidation of cellular thiols catalyzed by tellurium in the presence of  $H_2O_2$ . Those chemical reactions are likely to increase the oxidative stress in tumor cells with a high initial level of  $H_2O_2$ , and ultimately push those cells over a critical 'life and death' (redox) threshold.<sup>24</sup> This also accounts for the differences of toxicity of the LAB027 compound in tumor and normal cells. Moreover in tumor cells, the levels of antioxidant enzyme activities are low and not modified by LAB027. In normal cells, the basal levels of antioxidant enzyme activities are higher and are still raised by LAB027, thus preventing cell death.<sup>9</sup> The differences between normal and tumor cells in terms of basal oxidative stress and antioxidant enzyme levels have already been used to selectively kill tumor cells *in vitro*. Thus, SOD mimics favor the dismutation of superoxide anions overproduced by tumor cells, and consecutively raise the production of  $H_2O_2$  up to a cytotoxic level that is not reached in normal cells with low basal levels of  $H_2O_2$ .<sup>9,16</sup> The mechanism of action of LAB027 is different; it induces by itself an oxidative stress that is amplified by the pre-existing oxidative stress in tumor cells.  $H_2O_2$  and not  $O_2^{\bullet-}$  has a key role in the death induced by LAB027, as *N*-acetylcysteine but not the SOD mimic MnTBAP significantly decreases LAB027 toxicity. Incubation of LAB027 with the gamma-glutamylcysteine synthetase inhibitor BSO that depletes the cells in reduced glutathione significantly increases the cytotoxicity of LAB027 in all cell lines. By contrast, blocking catalase with aminotriazol or increasing its intracellular levels with PEG-catalase, has no effects on cell survival and proliferation whatever the cell type considered. These results indicate that  $H_2O_2$ -mediated LAB027 toxicity is controlled by the glutathione pathway rather than by the catalase pathway, as already observed with several chemotherapeutic drugs.

The role of ROS in tumor cell death induced by LAB027 is emphasized by the effects of the compound on the mitochondrial release of pro-apoptotic molecules. Members of the Bcl-2 family control the permeability of the mitochondrial outer membrane to various pro-apoptotic proteins.<sup>26</sup> In our hands, LAB027 exerts its powerful cytotoxic effect by inhibiting the expression of Bcl-2 and Bcl-xL, two antiapoptotic molecules, and increasing the expression of Bax and Bad, two pro-apoptotic molecules. This alteration in the mitochondrial membrane composition leads to the mitochondrial collapse, but is not followed by caspase-3 cleavage as usually observed during apoptosis.<sup>26</sup> Those results are in line with the ineffectiveness of caspase-3 inhibitors to abrogate LAB027-induced cell death and with the necrotic mode of death induced by LAB027 as demonstrated by YOPRO-1/PI staining of LAB027-treated cells. ROS have been reported to induce cell death by necrosis and/or apoptosis depending on the rate of ROS production, the duration of the oxidative burst and the cell type considered.<sup>27</sup> In our hands, LAB027 triggers a caspase-independent, ROS-mediated cell death by necrosis. LAB027 also induces an autophagic process as demonstrated by ATG-8 induction and cleavage, and by the phenomenon of vacuolization. Indeed,  $H_2O_2$  can trigger the formation of autophagosomes through the oxidation of a critical cysteine residue on HsAtg4A. The resulting inactivation of HsAtg4A leads to the accumulation of Atg8-PE on the phagophore membrane and to the formation of autophagosomes.<sup>28</sup> However, it is not clear whether this mechanism is involved in cell death, or counteracts the toxic effects of LAB027 and favours cell survival by removal of harmful protein aggregates and damaged mitochondria, which are sources of altered proteins.<sup>29</sup>

The chemotherapeutic treatment of colon cancer usually requires the use of several drugs. Oxaliplatin is one of the most frequently used.<sup>30,31</sup> In our hands, the augmentation of

the antiproliferative effects of oxaliplatin on colon cancer cells when associated with LAB027, is linked to the increased intracellular concentration of  $H_2O_2$ . However, a similar increase in  $H_2O_2$  concentration is observed in NIH3T3 fibroblasts treated by oxaliplatin and LAB027, and no antiproliferative effect is observed. This is explained by the increase in GSH levels that occurs in normal 3T3 fibroblasts but not in colon cancer cells. Because of its role in  $H_2O_2$  detoxification, the glutathione pathway represents a major component of cellular defense against cytotoxic drugs as oxaliplatin. These results are in agreement with the effect of LAB027 on glutathione reductase levels, an enzyme that restores the pool of reduced GSH and whose level is increased in normal but not in tumor cells. The role of glutathione reductase is also emphasized by the synergistic effect of the gamma-glutamylcysteine synthetase inhibitor BSO with LAB027 and oxaliplatin on tumor cells. The effect is still more dramatic on normal cells.

Thus, our data confirm that oxaliplatin exerts its anti-tumoral effects at least partly through the induction of an oxidative stress and emphasizes the role of reduced glutathione in the control of oxaliplatin cytotoxicity.<sup>32</sup> In tumor cells, high levels of reduced glutathione, the cofactor of glutathione peroxidase, have been associated with a multidrug resistance phenotype.<sup>19</sup> Compounds that target such protective mechanisms could enhance the activity of anticancer agents and reverse the multidrug resistance phenotype. For example, BSO, an inhibitor of glutathione synthesis, can increase the cytotoxicity of melphalan by preventing glutathione peroxidase activity and increasing  $H_2O_2$  levels.<sup>20</sup> However, BSO depletes glutathione in both normal and cancer cells, which increases melphalan's hematological toxicity and prevents any enhancement of the therapeutic index of this anticancer agent.<sup>33,34</sup> Conversely, *N*-acetylcysteine protects normal cells from the cytotoxic effects of anticancer drugs by preventing the elevation of intracellular  $H_2O_2$  through its reductive properties,<sup>9</sup> but abrogates the effectiveness of chemotherapeutic drugs. We have already observed that, as LAB027, mangafodipir prevents the hematological toxicity of oxaliplatin, but enhances its antitumoral activity against colon cancer both *in vitro* and *in vivo*.<sup>16</sup> The differential cytotoxic effects of mangafodipir on normal and cancer cells also result from differences in the redox status of those cells. Mangafodipir induces an overproduction of  $H_2O_2$  through the dismutation of superoxide anions, but decreases the toxicity of  $H_2O_2$  in normal cells through its glutathione reductase-like activity. Both mangafodipir and LAB027 increase the therapeutic index of oxaliplatin *in vitro* and *in vivo*, prevent hematologic toxicity and the death of animals injected with a lethal concentration of bacteria. Moreover, arsenic trioxide, one of the prototypical 'sensor/effector' chemotherapeutic agents, exerts its antitumoral activity through the induction of an oxidative burst without inducing leucopenia.<sup>15</sup>

Only a small number of studies have previously explored the antitumoral role of tellurium compounds. Only one tellurium-based compound, AS101, has been tested so far. AS101 (ammonium trichloro(dioxoethylene-O,O') tellurate), a tellurium (IV) compound, is endowed with antitumor properties in several murine models.<sup>35,36</sup> Phase I clinical trials on patients with advanced cancer treated with AS101 have

shown an increased production and secretion of a variety of cytokines, leading to a clear dominance of Th1 responses with a concurrent decrease in Th2 responses.<sup>37</sup> The predominance of Th1 responses is related to the antitumor activity of AS101. In addition, AS101, as a tellurium (IV) compound, can interact with thiols to form a Te-S bond. The ability of AS101 to interact with cysteine residue can alter protein functions,<sup>38</sup> increase intracellular ROS and favor the induction of apoptosis.<sup>39</sup> However, all the activities of AS101 are associated with little toxicity, and this drug is safe for clinical applications.<sup>40</sup>

The present study provides the first pre-clinical evidence that the organotelluride catalyst, LAB027 is a potential drug to treat colon cancer either alone or in combination with oxaliplatin through a mechanism that involves mainly necrosis. Tumor cell death is associated with the overproduction of intracellular ROS but with no elevation of reduced glutathione levels as observed in normal cells. This difference may explain the limited kidney, liver and hematological toxicity of this compound *in vivo*. Finally, this report shows for the first time that 'sensor/effector' pro-oxidative agents could represent effective and safe options to treat patients with colon cancer.

#### Materials and Methods

**Animals.** BALB/c and BALB/c SCID female mice between 6 and 8 weeks of age were used in all experiments (Harlan, Gannat, France). All mice were housed in autoclaved cages with sterile food and water. Animals received humane care in compliance with institutional guidelines.

**LAB027 synthesis.** The synthesis of LAB027 is described in detail in Supplementary files (Supplementary data and Supplementary Figure 1).

**Chemicals, cell lines and culture.** All chemicals were from Sigma (Saint Quentin Fallavier, France) except for oxaliplatin (Eloxatine, Sanofi-Pharma, Paris, France). CT26 (mouse colon carcinoma), HT29 (human colon carcinoma), NIH 3T3 (mouse fibroblast) and W138 (human lung fibroblast) were obtained from American Type Culture Collection (Manassas, VA, USA). All cell lines were cultured in DMEM/ glutamax-1 supplemented with 10% heat-inactivated FCS and antibiotics (Life Technologies, Cergy Pontoise, France). All cell lines were routinely tested for Mycoplasma infection.

**Cellular production of  $O_2^{\bullet -}$  and  $H_2O_2$ .** Cells ( $2 \times 10^4$  cells/well) were seeded in 96-well plates (Costar, Corning, Inc., Corning, NY) and incubated for 48 h in culture medium alone or added with various concentrations of LAB027 alone or in combination with oxaliplatin. Levels of intracellular superoxide anion  $O_2^{\bullet -}$  and  $H_2O_2$  were assessed spectrophotometrically (Packard Bioscience, Boston, MA, USA) by oxidation of dihydroethidium (DHE) (Molecular Probes, Leiden, The Netherlands) and of 2',7'-dichlorodihydrofluorescein diacetate ( $H_2DCFDA$ ) (Molecular Probes), respectively, as previously described.<sup>16</sup> The levels of  $O_2^{\bullet -}$  or  $H_2O_2$  were calculated in each sample as follows: ROS rate (arbitrary units/min/ $10^6$  cells) = (fluorescence intensity (arbitrary units) at T60 minutes - fluorescence intensity (arbitrary units) at T0)/60 min/number of viable cells as measured by the crystal violet assay.

**Determination of enzymatic activities.** The SOD activity in tumor or normal cells was evaluated by the method of Beauchamp and Fridovich<sup>40</sup> and expressed as units/ $10^6$  cells. The catalase activity in tumor or normal cells was determined according to Aebi<sup>41</sup> and expressed as units/ $10^6$  cells. The glutathione reductase assay was performed by the method of Carlberg and Mannervik<sup>42</sup> and expressed as nmol/min/ $10^6$  cells. Levels of extracellular GSH were measured by the method of Baker *et al.*<sup>43</sup> and expressed as nmol/ $10^6$  cells.

***In vitro* cell proliferation and viability assays.** CT26, HT29, NIH 3T3 or W138 cells ( $2 \times 10^4$  cells/well) were seeded into 96-well plates and incubated for

48 h in complete DMEM medium with varying amounts of LAB027 alone or with oxaliplatin. Cell proliferation was determined by pulsing the cells with [<sup>3</sup>H] thymidine (1  $\mu$ Ci/well) during the last 16 h of culture. Cell viability was evaluated by the crystal violet assay.<sup>16</sup> Results are expressed as percentages of viable cells compared with untreated cells (that have 100% viability).

**Levels of intracellular and extracellular reduced glutathione.** The levels of intracellular glutathione were assessed spectrofluorometrically by monochlorobimane staining.<sup>44</sup> Briefly, tumor cells ( $2 \times 10^4$ /well) or normal NIH3T3 ( $2 \times 10^4$ /well) were seeded in 96-well plates and incubated for 48 h in complete medium with LAB027 alone or in combination with oxaliplatin at concentrations described in figure legends. Cells were washed once with PBS and then incubated with 50  $\mu$ M monochlorobimane in PBS. The fluorescence intensity was measured after 15 min at 37 °C. Excitation and emission wavelengths were 380 and 485 nm, respectively. The intracellular glutathione level was expressed as arbitrary units of fluorescence intensity/number of adherent cells as measured by the crystal violet assay. Extracellular reduced glutathione was assayed in culture supernatants using the method of Baker *et al*.<sup>45</sup>

**Immunoblotting of cell lysates.** HT29 cells were treated or not with 1, 2 or 4  $\mu$ M LAB027 for 24 h then lysed in ice-cold RIPA.<sup>9</sup> Protein (50  $\mu$ g) extracts were analyzed by immunoblotting after 10–15% SDS-PAGE using of rabbit polyclonal anti-mouse pro- and active caspase-3 (1:1500, Abcam 47131, Paris, France), rabbit polyclonal anti-mouse caspase-8, mouse polyclonal anti-mouse Bcl-2, Bcl-xL and Bax primary antibodies (1:200, Santa Cruz Biotechnology, Inc., Santa Cruz, CA, USA), Bad primary antibody (1:100, Santa Cruz Biotechnology), ATG-8 primary antibody (1:500, Sigma-Aldrich, Saint-Quentin Fallavier, France) and mouse monoclonal anti- $\beta$ -actin (1:50000, Sigma). After washing, membranes were incubated with a 1:1000 goat anti-rabbit or goat anti-mouse secondary antibody (Sigma-Aldrich). The membranes were developed in Super Signal West Pico Chemiluminescent Substrate (Pierce, CO, USA). Images of blots were obtained using Fujifilm LAS3000 digital imager analyzed with Fujifilm Multi-Gauge Imaging software (Fujifilm, Tokyo, Japan).

**Modulation of the catalase and glutathione reductase pathways.** HT29, CT26, NIH 3T3 or W138 cells ( $2 \times 10^4$  cells/well) were pre-incubated for 2 h with either 400  $\mu$ Mol/l *N*-acetyl cysteine (NAC), or with 50 units/ml PEG-catalase, or with 200  $\mu$ Mol/l aminotriazol (ATZ, a catalase inhibitor) or with 400  $\mu$ Mol/l *L*-buthionine-SR-sulfoximine (BSO, a gamma-glutamylcysteine synthetase inhibitor). Those concentrations were chosen because they significantly modulated either reduced glutathione concentration (BSO, NAC) or catalase activity (PEG-catalase, ATZ) (not shown). The cells were then incubated with 1  $\mu$ M LAB027 alone or in combination with oxaliplatin for 48 h. Cell proliferation was assayed by pulsing the cells with [<sup>3</sup>H] thymidine (1  $\mu$ Ci/well) during the last 16 h of culture.

**Study of caspase inhibition.** HT29 cells ( $2 \times 10^4$  cells/well) were pre-incubated for 2 h with either 40  $\mu$ M caspase-3-specific inhibitor Ac-DEVD-FMK or with 40  $\mu$ M caspase-8 inhibitor Z-IETD-FMK, or with the broad-spectrum 40  $\mu$ M caspase inhibitor Z-VAD-FMK. The cells were then incubated with LAB027 for 48 h. Cell viability was evaluated by the crystal violet assay. Results are expressed as percentages of viable cells compared with untreated cells (100% viability).

**Fluorescence-activated cell sorting analysis of cell death.** Apoptosis and necrosis were analyzed by the fluorescence-activated cell sorting (FACS) Canto II flow cytometer (Becton Dickinson, Franklin Lakes, NJ, USA), using the Membrane Permeability/Dead Cell Apoptosis Kit with YO-PRO-1 and Propidium iodide (PI) for Flow Cytometry (Invitrogen, Cergy Pontoise, France) under the manufacturer's recommendations. Briefly,  $5 \times 10^5$  HT29 cells were incubated with 4  $\mu$ M LAB027 for a period of time indicated in the legends of figures. After the incubation period, cells were collected and stained for 30 min on ice with 1.5  $\mu$ M PI and 0.1  $\mu$ M YO-PRO-1. Cells were washed two times and analyzed by flow cytometry.

**Acridine orange staining for autophagy detection.** Acridine orange (Sigma) staining was performed according to Kanzawa *et al*.<sup>45</sup> Briefly, HT29 cells were treated or not for 24 h with 4  $\mu$ M LAB027. After the incubation period, cells were washed twice with phosphate-buffered saline and stained with 1  $\mu$ M acridine orange for 15 min at 37 °C. Cells were washed and analyzed by fluorescence

microscopy using 490-nm band-pass blue excitation filters and a 515-nm long-pass barrier filter.

***In vivo* antitumor activity of LAB027.** CT26 ( $2 \times 10^6$ ) cells were injected subcutaneously into the back of BALB/c or BALB/c SCID mice. When the tumors reached a mean size of 200–500 mm<sup>3</sup>, mice were randomized (day 10) in each experimental and control groups depending on tumor size, in order to start the treatment with a similar mean size in each group. One group of seven mice was treated by intraperitoneal oxaliplatin (10 mg/kg/week) starting on day 10. One group of seven mice was treated by intravenous LAB027 (10 mg/kg/week) starting on day 10. One group of seven mice was treated with intravenous LAB027 (10 mg/kg/week) and intraperitoneal oxaliplatin (10 mg/kg/week) starting on day 10. One control group of seven mice was injected with PBS. Tumor size was measured with a calliper rule every 2 days. Tumor volume was calculated as follows: TV (mm<sup>3</sup>) = (L  $\times$  W<sup>2</sup>)/2, where L is the longest and W the shortest radius of the tumor in millimeters. Results were expressed as means of tumor volumes  $\pm$  S.E.M. ( $n = 7$  in each group).

***In vivo* analysis of blood, liver and kidney toxicity.** Mice were injected with PBS alone or intraperitoneal, oxaliplatin alone, or intravenous LAB027 alone or intraperitoneal oxaliplatin in association with intravenous LAB027 at days 0 and 7. Five mice were treated in each group. After 14 days of the first injection, mice were killed by cervical dislocation. Blood samples were then collected from each mouse. Leukocytes, neutrophils and platelets were enumerated using a Malassez cell after hypotonic red blood cell lysis. Liver enzymes ALAT, LDH, alkaline phosphatases, BUN and creatinine were assayed using a multiparametric analyzer (Hitachi 747, Roche Diagnostics, Meylan, France).

**Susceptibility of mice to bacterial infection.** BALB/c female mice were injected with vehicle alone (PBS), or intraperitoneal oxaliplatin alone, or intravenous LAB027 alone or intraperitoneal oxaliplatin and intravenous LAB027 days 0 and seven. Five mice were treated in each group. After 14 days of the first injection, mice were injected i.p with a lethal dose of  $10^7$  *E. coli* on day 9. The survival rate of mice was evaluated during 24 h following *E. coli* injection. A total of 10 mice were treated in each group in two independent experiments.

**Statistical analysis.** The statistical significance of differences between experimental treated groups and untreated controls was analyzed by Student's *t*-test for comparison of means. A level of  $P < 0.05$  was accepted as significant. \* $P < 0.05$ ; \*\*\* $P < 0.01$  versus controls.

#### Conflict of Interest

The authors declare no conflict of interest.

**Acknowledgements.** This research has been funded by a grant from the European Community's Seventh Framework Program (FP7/2007-2013) under grant agreement no (215009). The authors thank Ms Agnes Colle for editing the manuscript and Ms Marie Mianowski for reviewing the manuscript.

1. Halliwell B, Gutteridge JM. *Free Radicals in Biology and Medicine*. Oxford University Press: UK, 2007.
2. Benhar M, Engelberg D, Levitzki A. ROS, stress-activated kinases and stress signaling in cancer. *EMBO Rep* 2002; 3: 420–425.
3. Burdon RH. Superoxide and hydrogen peroxide in relation to mammalian cell proliferation. *Free Radic Biol Med* 1995; 18: 775–794.
4. Murrell GA, Francis MJ, Bromley L. Modulation of fibroblast proliferation by oxygen free radicals. *Biochem J* 1990; 265: 659–665.
5. Bae YS, Kang SW, Seo MS, Baines IC, Tekle E, Chock PB *et al*. Epidermal growth factor (EGF)-induced generation of hydrogen peroxide. Role in EGF receptor-mediated tyrosine phosphorylation. *J Biol Chem* 1997; 272: 217–221.
6. Sundaresan M, Yu ZX, Ferrans VJ, Irani K, Finkel T. Requirement for generation of H<sub>2</sub>O<sub>2</sub> for platelet-derived growth factor signal transduction. *Science (New York, NY)* 1995; 270: 296–299.
7. Jackson AL, Loeb LA. The contribution of endogenous sources of DNA damage to the multiple mutations in cancer. *Mutat Res* 2001; 477: 7–21.
8. Gupta A, Rosenberger SF, Bowden GT. Increased ROS levels contribute to elevated transcription factor and MAP kinase activities in malignant progressed mouse keratinocyte cell lines. *Carcinogenesis* 1999; 20: 2063–2073.

9. Laurent A, Nicco C, Chereau C, Goulvestre C, Alexandre J, Alves A *et al*. Controlling tumor growth by modulating endogenous production of reactive oxygen species. *Cancer Res* 2005; 65: 948–956.
10. Mates JM, Segura JA, Alonso FJ, Marquez J. Intracellular redox status and oxidative stress: implications for cell proliferation, apoptosis, and carcinogenesis. *Arch Toxicol* 2008; 82: 273–299.
11. Oberley TD, Oberley LW. Antioxidant enzyme levels in cancer. *Histol Histopathol* 1997; 12: 525–535.
12. Benhar M, Dalyot I, Engelberg D, Levitzki A. Enhanced ROS production in oncogenically transformed cells potentiates c-Jun N-terminal kinase and p38 mitogenactivated protein kinase activation and sensitization to genotoxic stress. *Mol Cell Biol* 2001; 21: 6913–6926.
13. Jabs T. Reactive oxygen intermediates as mediators of programmed cell death in plants and animals. *Biochem Pharmacol* 1999; 57: 231–245.
14. Hwang PM, Bunz F, Yu J, Rago C, Chan TA, Murphy MP *et al*. Ferredoxin reductase affects p53-dependent, 5-fluorouracil-induced apoptosis in colorectal cancer cells. *Nat Med* 2001; 7: 1111–1117.
15. Jing Y, Dai J, Chalmers-Redman RM, Tatton WG, Waxman S. Arsenic trioxide selectively induces acute promyelocytic leukemia cell apoptosis via a hydrogen peroxide-dependent pathway. *Blood* 1999; 94: 2102–2111.
16. Alexandre J, Nicco C, Chereau C, Laurent A, Weill B, Goldwasser F *et al*. Improvement of the therapeutic index of anticancer drugs by the superoxide dismutase mimic mangafodipir. *J Natl Cancer Inst* 2006; 98: 236–244.
17. Hussain SP, Amstad P, He P, Robles A, Lupold S, Kaneko I *et al*. p53-induced up-regulation of MnSOD and GPx but not catalase increases oxidative stress and apoptosis. *Cancer Res* 2004; 64: 2350–2356.
18. Trachootham D, Alexandre J, Huang P. Targeting cancer cells by ROS-mediated mechanisms: a radical therapeutic approach? *Nat Rev* 2009; 8: 579–591.
19. Hamaguchi K, Godwin AK, Yakushiji M, O'Dwyer PJ, Ozols RF, Hamilton TC. Cross-resistance to diverse drugs is associated with primary cisplatin resistance in ovarian cancer cell lines. *Cancer Res* 1993; 53: 5225–5232.
20. Skapek SX, Colvin OM, Griffith OW, Elion GB, Bigner DD, Friedman HS. Enhanced melphalan cytotoxicity following buthionine sulfoximine-mediated glutathione depletion in a human medulloblastoma xenograft in athymic mice. *Cancer Res* 1988; 48: 2764–2767.
21. Cullen JJ, Weydert C, Hinkhouse MM, Ritchie J, Domann FE, Spitz D *et al*. The role of manganese superoxide dismutase in the growth of pancreatic adenocarcinoma. *Cancer Res* 2003; 63: 1297–1303.
22. Zhang Y, Zhao W, Zhang HJ, Domann FE, Oberley LW. Overexpression of copper zinc superoxide dismutase suppresses human glioma cell growth. *Cancer Res* 2002; 62: 1205–1212.
23. Hileman EO, Liu J, Albitar M, Keating MJ, Huang P. Intrinsic oxidative stress in cancer cells: a biochemical basis for therapeutic selectivity. *Cancer Chemother Pharmacol* 2004; 53: 209–219.
24. Mecklenburg S, Shaaban S, Ba LA, Burkholz T, Schneider T, Diesel B *et al*. Exploring synthetic avenues for the effective synthesis of selenium- and tellurium-containing multifunctional redox agents. *Org Biomol Chem* 2009; 7: 4753–4762.
25. Shabaan S, Ba LA, Abbas M, Burkholz T, Denkert A, Gohr A *et al*. Multicomponent reactions for the synthesis of multifunctional agents with activity against cancer cells. *Chem Commun (Camb, England)* 2009; 40: 4702–4704.
26. Joza N, Kroemer G, Penninger JM. Genetic analysis of the mammalian cell death machinery. *Trends Genet* 2002; 18: 142–149.
27. Orrenius S, Gogvadze V, Zhivotovskiy B. Mitochondrial oxidative stress: implications for cell death. *Annu Rev Pharmacol Toxicol* 2007; 47: 143–183.
28. Scherz-Shouval R, Shvets E, Fass E, Shorer H, Gil L, Elazar Z. Reactive oxygen species are essential for autophagy and specifically regulate the activity of Atg4. *EMBO J* 2007; 26: 1749–1760.
29. Azad MB, Chen Y, Gibson SB. Regulation of autophagy by reactive oxygen species (ROS): implications for cancer progression and treatment. *Antioxid Redox Signal* 2009; 11: 777–790.
30. Beauchamp C, Fridovich I. Superoxide dismutase: improved assays and an assay applicable to acrylamide gels. *Anal Biochem* 1971; 44: 276–287.
31. Diaz-Rubio E, Sastre J, Zaniboni A, Labianca R, Cortes-Funes H, de Braud F *et al*. Oxaliplatin as single agent in previously untreated colorectal carcinoma patients: a phase multicentric study. *Ann Oncol* 1998; 9: 105–108.
32. Godwin AK, Meister A, O'Dwyer PJ, Huang CS, Hamilton TC, Anderson ME. High resistance to cisplatin in human ovarian cancer cell lines is associated with marked increase of glutathione synthesis. *Proc Natl Acad Sci U S A* 1992; 89: 3070–3074.
33. Bailey HH, Mulcahy RT, Tutsch KD, Arzooonian RZ, Alberti D, Tombes MB *et al*. Phase clinical trial of intravenous L-buthionine sulfoximine and melphalan: an attempt at modulation of glutathione. *J Clin Oncol* 1994; 12: 194–205.
34. Bailey HH, Ripple G, Tutsch KD, Arzooonian RZ, Alberti D, Feierabend C *et al*. Phase study of continuous-infusion L-SR-buthionine sulfoximine with intravenous melphalan. *J Natl Cancer Inst* 1997; 89: 1789–1796.
35. Hayun M, Naor Y, Weil M, Albeck M, Peled A, Don J *et al*. The immunomodulator AS10 induces growth arrest and apoptosis in multiple myeloma: association with the Akt/survivin pathway. *Biochem Pharmacol* 2006; 72: 1423–1431.
36. Sredni B, Caspi RR, Klein A, Kalechman Y, Danziger Y, Ben Ya'akov M *et al*. A new immunomodulating compound (AS-101) with potential therapeutic application. *Nature* 1987; 330: 173–176.
37. Sredni B, Tichler T, Shani A, Catane R, Kaufman B, Strassmann G *et al*. Predominance of TH1 response in tumor-bearing mice and cancer patients treated with AS101. *J Natl Cancer Inst* 1996; 88: 1276–1284.
38. Okun E, Dikshtein Y, Carmely A, Saida H, Frei G, Sela BA *et al*. The organotellurium compound ammonium trichloro(dioxoethylene-*o,o'*)tellurate reacts with homocysteine to form homocystine and decreases homocysteine levels in hyperhomocysteinemic mice. *FEBS J* 2007; 274: 3159–3170.
39. Frei GM, Kremer M, Hanschmann KM, Krause S, Albeck M, Sredni B *et al*. Antitumor effects in mycosis fungoides of the immunomodulatory, tellurium-based compound AS101. *Br J Dermatol* 2008; 158: 578–586.
40. Sredni B, Xu RH, Albeck M, Gafter U, Gal R, Shani A *et al*. The protective role of the immunomodulator AS101 against chemotherapy-induced alopecia studies on human animal models. *Int J Cancer* 1996; 65: 97–103.
41. Aebi H. Catalase *in vitro*. *Methods Enzymol* 1984; 105: 121–126.
42. Carlberg I, Mannervik B. Glutathione reductase. *Methods Enzymol* 1985; 113: 484–490.
43. Baker MA, Cerniglia GJ, Zaman A. Microtiter plate assay for the measurement of glutathione and glutathione disulfide in large numbers of biological samples. *Anal Biochem* 1990; 190: 360–365.
44. Rice GC, Bump EA, Shrieve DC, Lee W, Kovacs M. Quantitative analysis of cellular glutathione by flow cytometry utilizing monochlorobimane: some applications to radiation and drug resistance *in vitro* and *in vivo*. *Cancer Res* 1986; 46: 6105–6110.
45. Kanzawa T, Kondo Y, Ito H, Kondo S, Germano I. Induction of autophagic cell death in malignant glioma cells by arsenic trioxide. *Cancer Res* 2003; 63: 2103–2108.



Cell Death and Disease is an open-access journal published by Nature Publishing Group. This work is licensed under the Creative Commons Attribution-NonCommercial-NoDerivs 3.0 Unported License. To view a copy of this license visit <http://creativecommons.org/licenses/by-nc-nd/3.0/>

Supplementary Information accompanies the paper on Cell Death and Disease website (<http://www.nature.com/cddis>)

## REFERENCES

1. Gabrielli A, Avvedimento EV, Krieg T: Scleroderma. *The New England journal of medicine* 2009, 360(19):1989-2003.
2. LeRoy EC, Black C, Fleischmajer R, Jablonska S, Krieg T, Medsger TA, Jr., Rowell N, Wollheim F: Scleroderma (systemic sclerosis): classification, subsets and pathogenesis. *The Journal of rheumatology* 1988, 15(2):202-205.
3. Varga J: Systemic sclerosis: an update. *Bulletin of the NYU hospital for joint diseases* 2008, 66(3):198-202.
4. Lunardi C, Bason C, Navone R, Millo E, Damonte G, Corrocher R, Puccetti A: Systemic sclerosis immunoglobulin G autoantibodies bind the human cytomegalovirus late protein UL94 and induce apoptosis in human endothelial cells. *Nature medicine* 2000, 6(10):1183-1186.
5. Simonini G, Cerinic MM, Generini S, Zoppi M, Anichini M, Cesaretti C, Pignone A, Falcini F, Lotti T, Cagnoni M: Oxidative stress in Systemic Sclerosis. *Molecular and cellular biochemistry* 1999, 196(1-2):85-91.
6. Herrick AL, Matucci Cerinic M: The emerging problem of oxidative stress and the role of antioxidants in systemic sclerosis. *Clinical and experimental rheumatology* 2001, 19(1):4-8.
7. Sambo P, Baroni SS, Luchetti M, Paroncini P, Dusi S, Orlandini G, Gabrielli A: Oxidative stress in scleroderma: maintenance of scleroderma fibroblast phenotype by the constitutive up-regulation of reactive oxygen species generation through the NADPH oxidase complex pathway. *Arthritis and rheumatism* 2001, 44(11):2653-2664.
8. Ihn H, Yamane K, Kubo M, Tamaki K: Blockade of endogenous transforming growth factor beta signaling prevents up-regulated collagen synthesis in scleroderma fibroblasts: association with increased expression of transforming growth factor beta receptors. *Arthritis and rheumatism* 2001, 44(2):474-480.
9. Kissin EY, Lemaire R, Korn JH, Lafyatis R: Transforming growth factor beta induces fibroblast fibrillin-1 matrix formation. *Arthritis and rheumatism* 2002, 46(11):3000-3009.
10. Bhattacharyya S, Wei J, Varga J: Understanding fibrosis in systemic sclerosis: shifting paradigms, emerging opportunities. *Nature reviews* 2012, 8(1):42-54.
11. Wei J, Bhattacharyya S, Tourtellotte WG, Varga J: Fibrosis in systemic sclerosis: emerging concepts and implications for targeted therapy. *Autoimmunity reviews* 2011, 10(5):267-275.
12. Bhattacharyya S, Wei J, Varga J: Understanding fibrosis in systemic sclerosis: shifting paradigms, emerging opportunities. *Nature reviews*, 8(1):42-54.
13. Blobel GC, Schiemann WP, Lodish HF: Role of transforming growth factor beta in human disease. *The New England journal of medicine* 2000, 342(18):1350-1358.
14. Dong C, Zhu S, Wang T, Yoon W, Li Z, Alvarez RJ, ten Dijke P, White B, Wigley FM, Goldschmidt-Clermont PJ: Deficient Smad7 expression: a putative molecular defect in scleroderma. *Proceedings of the National Academy of Sciences of the United States of America* 2002, 99(6):3908-3913.
15. Moustakas A, Heldin CH: Non-Smad TGF-beta signals. *Journal of cell science* 2005, 118(Pt 16):3573-3584.
16. Pannu J, Asano Y, Nakerakanti S, Smith E, Jablonska S, Blaszczyk M, ten Dijke P, Trojanowska M: Smad1 pathway is activated in systemic sclerosis fibroblasts and is targeted by imatinib mesylate. *Arthritis and rheumatism* 2008, 58(8):2528-2537.

17. Mori Y, Chen SJ, Varga J: Expression and regulation of intracellular SMAD signaling in scleroderma skin fibroblasts. *Arthritis and rheumatism* 2003, 48(7):1964-1978.
18. Verrecchia F, Mauviel A, Farge D: Transforming growth factor-beta signaling through the Smad proteins: role in systemic sclerosis. *Autoimmunity reviews* 2006, 5(8):563-569.
19. Kawakami T, Ihn H, Xu W, Smith E, LeRoy C, Trojanowska M: Increased expression of TGF-beta receptors by scleroderma fibroblasts: evidence for contribution of autocrine TGF-beta signaling to scleroderma phenotype. *The Journal of investigative dermatology* 1998, 110(1):47-51.
20. Kubo M, Ihn H, Yamane K, Tamaki K: Up-regulated expression of transforming growth factor beta receptors in dermal fibroblasts in skin sections from patients with localized scleroderma. *Arthritis and rheumatism* 2001, 44(3):731-734.
21. Katsumoto TR, Whitfield ML, Connolly MK: The pathogenesis of systemic sclerosis. *Annual review of pathology*, 6:509-537.
22. Yamamoto T: Scleroderma--pathophysiology. *Eur J Dermatol* 2009, 19(1):14-24.
23. Varga JA, Trojanowska M: Fibrosis in systemic sclerosis. *Rheumatic diseases clinics of North America* 2008, 34(1):115-143; vii.
24. Ruperez M, Lorenzo O, Blanco-Colio LM, Esteban V, Egido J, Ruiz-Ortega M: Connective tissue growth factor is a mediator of angiotensin II-induced fibrosis. *Circulation* 2003, 108(12):1499-1505.
25. Grigoryev DN, Mathai SC, Fisher MR, Girgis RE, Zaiman AL, Houston-Harris T, Cheadle C, Gao L, Hummers LK, Champion HC *et al*: Identification of candidate genes in scleroderma-related pulmonary arterial hypertension. *Transl Res* 2008, 151(4):197-207.
26. Sternlicht MD, Werb Z: How matrix metalloproteinases regulate cell behavior. *Annual review of cell and developmental biology* 2001, 17:463-516.
27. Wang CT, Jing H: [Current progress of matrix metalloproteinases in systemic inflammatory reaction following cardiopulmonary bypass]. *Sheng li ke xue jin zhan [Progress in physiology]* 2011, 42(2):145-147.
28. Peng WJ, Yan JW, Wan YN, Wang BX, Tao JH, Yang GJ, Pan HF, Wang J: Matrix Metalloproteinases: A Review of Their Structure and Role in Systemic Sclerosis. *Journal of clinical immunology* 2012.
29. Kuroda K, Shinkai H: Gene expression of types I and III collagen, decorin, matrix metalloproteinases and tissue inhibitors of metalloproteinases in skin fibroblasts from patients with systemic sclerosis. *Archives of dermatological research* 1997, 289(10):567-572.
30. Kim WU, Min SY, Cho ML, Hong KH, Shin YJ, Park SH, Cho CS: Elevated matrix metalloproteinase-9 in patients with systemic sclerosis. *Arthritis research & therapy* 2005, 7(1):R71-79.
31. Holmbeck K, Bianco P, Caterina J, Yamada S, Kromer M, Kuznetsov SA, Mankani M, Robey PG, Poole AR, Pidoux I *et al*: MT1-MMP-deficient mice develop dwarfism, osteopenia, arthritis, and connective tissue disease due to inadequate collagen turnover. *Cell* 1999, 99(1):81-92.
32. Baroni SS, Santillo M, Bevilacqua F, Luchetti M, Spadoni T, Mancini M, Fraticelli P, Sambo P, Funaro A, Kazlauskas A *et al*: Stimulatory autoantibodies to the PDGF receptor in systemic sclerosis. *The New England journal of medicine* 2006, 354(25):2667-2676.
33. Svegliati S, Cancellato R, Sambo P, Luchetti M, Paroncini P, Orlandini G, Discepoli G, Paterno R, Santillo M, Cuzzo C *et al*: Platelet-derived growth factor and reactive oxygen species (ROS) regulate Ras protein levels in primary human fibroblasts via

- ERK1/2. Amplification of ROS and Ras in systemic sclerosis fibroblasts. *The Journal of biological chemistry* 2005, 280(43):36474-36482.
34. Hayashida T, Poncelet AC, Hubchak SC, Schnaper HW: TGF-beta1 activates MAP kinase in human mesangial cells: a possible role in collagen expression. *Kidney international* 1999, 56(5):1710-1720.
  35. Yamamoto T, Nishioka K: Role of monocyte chemoattractant protein-1 and its receptor,CCR-2, in the pathogenesis of bleomycin-induced scleroderma. *The Journal of investigative dermatology* 2003, 121(3):510-516.
  36. Denton CP, Shi-Wen X, Sutton A, Abraham DJ, Black CM, Pearson JD: Scleroderma fibroblasts promote migration of mononuclear leucocytes across endothelial cell monolayers. *Clinical and experimental immunology* 1998, 114(2):293-300.
  37. Distler O, Pap T, Kowal-Bielecka O, Meyringer R, Guiducci S, Landthaler M, Scholmerich J, Michel BA, Gay RE, Matucci-Cerinic M *et al*: Overexpression of monocyte chemoattractant protein 1 in systemic sclerosis: role of platelet-derived growth factor and effects on monocyte chemotaxis and collagen synthesis. *Arthritis and rheumatism* 2001, 44(11):2665-2678.
  38. Kawaguchi Y, Hara M, Wright TM: Endogenous IL-1alpha from systemic sclerosis fibroblasts induces IL-6 and PDGF-A. *The Journal of clinical investigation* 1999, 103(9):1253-1260.
  39. Doucet C, Brouty-Boye D, Pottin-Clemenceau C, Canonica GW, Jasmin C, Azzarone B: Interleukin (IL) 4 and IL-13 act on human lung fibroblasts. Implication in asthma. *The Journal of clinical investigation* 1998, 101(10):2129-2139.
  40. Emura M, Nagai S, Takeuchi M, Kitaichi M, Izumi T: In vitro production of B cell growth factor and B cell differentiation factor by peripheral blood mononuclear cells and bronchoalveolar lavage T lymphocytes from patients with idiopathic pulmonary fibrosis. *Clinical and experimental immunology* 1990, 82(1):133-139.
  41. Wallace WA, Ramage EA, Lamb D, Howie SE: A type 2 (Th2-like) pattern of immune response predominates in the pulmonary interstitium of patients with cryptogenic fibrosing alveolitis (CFA). *Clinical and experimental immunology* 1995, 101(3):436-441.
  42. Booth M, Mwatha JK, Joseph S, Jones FM, Kadzo H, Ileri E, Kazibwe F, Kemijumbi J, Kariuki C, Kimani G *et al*: Periportal fibrosis in human *Schistosoma mansoni* infection is associated with low IL-10, low IFN-gamma, high TNF-alpha, or low RANTES, depending on age and gender. *J Immunol* 2004, 172(2):1295-1303.
  43. Hasegawa M, Fujimoto M, Kikuchi K, Takehara K: Elevated serum levels of interleukin 4 (IL-4), IL-10, and IL-13 in patients with systemic sclerosis. *The Journal of rheumatology* 1997, 24(2):328-332.
  44. Postlethwaite AE: Role of T cells and cytokines in effecting fibrosis. *International reviews of immunology* 1995, 12(2-4):247-258.
  45. Yamamoto T, Takagawa S, Katayama I, Yamazaki K, Hamazaki Y, Shinkai H, Nishioka K: Animal model of sclerotic skin. I: Local injections of bleomycin induce sclerotic skin mimicking scleroderma. *The Journal of investigative dermatology* 1999, 112(4):456-462.
  46. McGaha TL, Le M, Koderia T, Stoica C, Zhu J, Paul WE, Bona CA: Molecular mechanisms of interleukin-4-induced up-regulation of type I collagen gene expression in murine fibroblasts. *Arthritis and rheumatism* 2003, 48(8):2275-2284.
  47. Ong CJ, Ip S, Teh SJ, Wong C, Jirik FR, Grusby MJ, Teh HS: A role for T helper 2 cells in mediating skin fibrosis in tight-skin mice. *Cellular immunology* 1999, 196(1):60-68.

48. Fertin C, Nicolas JF, Gillery P, Kalis B, Banchereau J, Maquart FX: Interleukin-4 stimulates collagen synthesis by normal and scleroderma fibroblasts in dermal equivalents. *Cellular and molecular biology* 1991, 37(8):823-829.
49. Zurawski SM, Vega F, Jr., Huyghe B, Zurawski G: Receptors for interleukin-13 and interleukin-4 are complex and share a novel component that functions in signal transduction. *The EMBO journal* 1993, 12(7):2663-2670.
50. Belperio JA, Dy M, Burdick MD, Xue YY, Li K, Elias JA, Keane MP: Interaction of IL-13 and C10 in the pathogenesis of bleomycin-induced pulmonary fibrosis. *American journal of respiratory cell and molecular biology* 2002, 27(4):419-427.
51. Nakashima T, Jinnin M, Yamane K, Honda N, Kajihara I, Makino T, Masuguchi S, Fukushima S, Okamoto Y, Hasegawa M *et al*: Impaired IL-17 signaling pathway contributes to the increased collagen expression in scleroderma fibroblasts. *J Immunol*, 188(8):3573-3583.
52. Yoshizaki A, Yanaba K, Iwata Y, Komura K, Ogawa A, Akiyama Y, Muroi E, Hara T, Ogawa F, Takenaka M *et al*: Cell adhesion molecules regulate fibrotic process via Th1/Th2/Th17 cell balance in a bleomycin-induced scleroderma model. *J Immunol*, 185(4):2502-2515.
53. Grassegger A, Schuler G, Hessenberger G, Walder-Hantich B, Jabkowski J, MacHeiner W, Salmhofer W, Zahel B, Pinter G, Herold M *et al*: Interferon-gamma in the treatment of systemic sclerosis: a randomized controlled multicentre trial. *The British journal of dermatology* 1998, 139(4):639-648.
54. Hein R, Behr J, Hundgen M, Hunzelmann N, Meurer M, Braun-Falco O, Urbanski A, Krieg T: Treatment of systemic sclerosis with gamma-interferon. *The British journal of dermatology* 1992, 126(5):496-501.
55. Xu SW, Howat SL, Renzoni EA, Holmes A, Pearson JD, Dashwood MR, Bou-Gharios G, Denton CP, du Bois RM, Black CM *et al*: Endothelin-1 induces expression of matrix-associated genes in lung fibroblasts through MEK/ERK. *The Journal of biological chemistry* 2004, 279(22):23098-23103.
56. Abraham DJ, Vancheeswaran R, Dashwood MR, Rajkumar VS, Pantelides P, Xu SW, du Bois RM, Black CM: Increased levels of endothelin-1 and differential endothelin type A and B receptor expression in scleroderma-associated fibrotic lung disease. *The American journal of pathology* 1997, 151(3):831-841.
57. Morelli S, Ferri C, Di Francesco L, Baldoncini R, Carlesimo M, Bottoni U, Properzi G, Santucci A: Plasma endothelin-1 levels in patients with systemic sclerosis: influence of pulmonary or systemic arterial hypertension. *Annals of the rheumatic diseases* 1995, 54(9):730-734.
58. Shi-Wen X, Chen Y, Denton CP, Eastwood M, Renzoni EA, Bou-Gharios G, Pearson JD, Dashwood M, du Bois RM, Black CM *et al*: Endothelin-1 promotes myofibroblast induction through the ETA receptor via a rac/phosphoinositide 3-kinase/Akt-dependent pathway and is essential for the enhanced contractile phenotype of fibrotic fibroblasts. *Molecular biology of the cell* 2004, 15(6):2707-2719.
59. Cotton SA, Herrick AL, Jayson MI, Freemont AJ: TGF beta--a role in systemic sclerosis? *The Journal of pathology* 1998, 184(1):4-6.
60. Yamakage A, Kikuchi K, Smith EA, LeRoy EC, Trojanowska M: Selective upregulation of platelet-derived growth factor alpha receptors by transforming growth factor beta in scleroderma fibroblasts. *The Journal of experimental medicine* 1992, 175(5):1227-1234.
61. Needleman BW, Choi J, Burrows-Mezu A, Fontana JA: Secretion and binding of transforming growth factor beta by scleroderma and normal dermal fibroblasts. *Arthritis and rheumatism* 1990, 33(5):650-656.

62. Yamane K, Ihn H, Tamaki K: Epidermal growth factor up-regulates expression of transforming growth factor beta receptor type II in human dermal fibroblasts by phosphoinositide 3-kinase/Akt signaling pathway: Resistance to epidermal growth factor stimulation in scleroderma fibroblasts. *Arthritis and rheumatism* 2003, 48(6):1652-1666.
63. Querfeld C, Eckes B, Huerkamp C, Krieg T, Sollberg S: Expression of TGF-beta 1, -beta 2 and -beta 3 in localized and systemic scleroderma. *Journal of dermatological science* 1999, 21(1):13-22.
64. Higley H, Persichitte K, Chu S, Waegell W, Vancheeswaran R, Black C: Immunocytochemical localization and serologic detection of transforming growth factor beta 1. Association with type I procollagen and inflammatory cell markers in diffuse and limited systemic sclerosis, morphea, and Raynaud's phenomenon. *Arthritis and rheumatism* 1994, 37(2):278-288.
65. Fredriksson L, Li H, Eriksson U: The PDGF family: four gene products form five dimeric isoforms. *Cytokine & growth factor reviews* 2004, 15(4):197-204.
66. Andrae J, Gallini R, Betsholtz C: Role of platelet-derived growth factors in physiology and medicine. *Genes & development* 2008, 22(10):1276-1312.
67. Bonner JC: Regulation of PDGF and its receptors in fibrotic diseases. *Cytokine & growth factor reviews* 2004, 15(4):255-273.
68. Olson LE, Soriano P: Increased PDGFRalpha activation disrupts connective tissue development and drives systemic fibrosis. *Developmental cell* 2009, 16(2):303-313.
69. Ludwicka A, Ohba T, Trojanowska M, Yamakage A, Strange C, Smith EA, Leroy EC, Sutherland S, Silver RM: Elevated levels of platelet derived growth factor and transforming growth factor-beta 1 in bronchoalveolar lavage fluid from patients with scleroderma. *The Journal of rheumatology* 1995, 22(10):1876-1883.
70. Schermuly RT, Dony E, Ghofrani HA, Pullamsetti S, Savai R, Roth M, Sydykov A, Lai YJ, Weissmann N, Seeger W *et al*: Reversal of experimental pulmonary hypertension by PDGF inhibition. *The Journal of clinical investigation* 2005, 115(10):2811-2821.
71. Distler JH, Jungel A, Huber LC, Schulze-Horsel U, Zwerina J, Gay RE, Michel BA, Hauser T, Schett G, Gay S *et al*: Imatinib mesylate reduces production of extracellular matrix and prevents development of experimental dermal fibrosis. *Arthritis and rheumatism* 2007, 56(1):311-322.
72. Akhmetshina A, Venalis P, Dees C, Busch N, Zwerina J, Schett G, Distler O, Distler JH: Treatment with imatinib prevents fibrosis in different preclinical models of systemic sclerosis and induces regression of established fibrosis. *Arthritis and rheumatism* 2009, 60(1):219-224.
73. Kavian N, Servettaz A, Marut W, Nicco C, Chereau C, Weill B, Batteux F: Sunitinib inhibits the phosphorylation of platelet-derived growth factor receptor beta in the skin of mice with scleroderma-like features and prevents the development of the disease. *Arthritis and rheumatism* 2012, 64(6):1990-2000.
74. Biondi ML, Marasini B, Bianchi E, Agostoni A: Plasma free and intraplatelet serotonin in patients with Raynaud's phenomenon. *International journal of cardiology* 1988, 19(3):335-339.
75. Welsh DJ, Harnett M, MacLean M, Peacock AJ: Proliferation and signaling in fibroblasts: role of 5-hydroxytryptamine<sub>2A</sub> receptor and transporter. *American journal of respiratory and critical care medicine* 2004, 170(3):252-259.
76. Dees C, Akhmetshina A, Zerr P, Reich N, Palumbo K, Horn A, Jungel A, Beyer C, Kronke G, Zwerina J *et al*: Platelet-derived serotonin links vascular disease and tissue fibrosis. *The Journal of experimental medicine* 2011, 208(5):961-972.

77. Rosenkranz S: TGF-beta1 and angiotensin networking in cardiac remodeling. *Cardiovascular research* 2004, 63(3):423-432.
78. Bataller R, Schwabe RF, Choi YH, Yang L, Paik YH, Lindquist J, Qian T, Schoonhoven R, Hagedorn CH, Lemasters JJ *et al*: NADPH oxidase signal transduces angiotensin II in hepatic stellate cells and is critical in hepatic fibrosis. *The Journal of clinical investigation* 2003, 112(9):1383-1394.
79. Watanabe T, Barker TA, Berk BC: Angiotensin II and the endothelium: diverse signals and effects. *Hypertension* 2005, 45(2):163-169.
80. Mezzano SA, Ruiz-Ortega M, Egido J: Angiotensin II and renal fibrosis. *Hypertension* 2001, 38(3 Pt 2):635-638.
81. Kato J, Koda M, Kishina M, Tokunaga S, Matono T, Sugihara T, Ueki M, Murawaki Y: Therapeutic effects of angiotensin II type 1 receptor blocker, irbesartan, on non-alcoholic steatohepatitis using FLS-ob/ob male mice. *International journal of molecular medicine*, 30(1):107-113.
82. Burstein B, Nattel S: Atrial fibrosis: mechanisms and clinical relevance in atrial fibrillation. *Journal of the American College of Cardiology* 2008, 51(8):802-809.
83. Hunyady L, Catt KJ: Pleiotropic AT1 receptor signaling pathways mediating physiological and pathogenic actions of angiotensin II. *Molecular endocrinology (Baltimore, Md)* 2006, 20(5):953-970.
84. Botzoris V, Drosos AA: Management of Raynaud's phenomenon and digital ulcers in systemic sclerosis. *Joint Bone Spine*, 78(4):341-346.
85. Takahashi T, Kalka C, Masuda H, Chen D, Silver M, Kearney M, Magner M, Isner JM, Asahara T: Ischemia- and cytokine-induced mobilization of bone marrow-derived endothelial progenitor cells for neovascularization. *Nature medicine* 1999, 5(4):434-438.
86. Carmeliet P: Mechanisms of angiogenesis and arteriogenesis. *Nature medicine* 2000, 6(4):389-395.
87. Hassoun PM, Thappa V, Landman MJ, Fanburg BL: Endothelin 1: mitogenic activity on pulmonary artery smooth muscle cells and release from hypoxic endothelial cells. *Proc Soc Exp Biol Med* 1992, 199(2):165-170.
88. Kahaleh B, Matucci-Cerinic M: Raynaud's phenomenon and scleroderma. Dysregulated neuroendothelial control of vascular tone. *Arthritis and rheumatism* 1995, 38(1):1-4.
89. Smyth AE, Bell AL, Bruce IN, McGrann S, Allen JA: Digital vascular responses and serum endothelin-1 concentrations in primary and secondary Raynaud's phenomenon. *Annals of the rheumatic diseases* 2000, 59(11):870-874.
90. Jeremy JY, Rowe D, Emsley AM, Newby AC: Nitric oxide and the proliferation of vascular smooth muscle cells. *Cardiovascular research* 1999, 43(3):580-594.
91. Matucci Cerinic M, Kahaleh MB: Beauty and the beast. The nitric oxide paradox in systemic sclerosis. *Rheumatology (Oxford)* 2002, 41(8):843-847.
92. Yamaguchi Y, Okazaki Y, Seta N, Satoh T, Takahashi K, Ikezawa Z, Kuwana M: Enhanced angiogenic potency of monocytic endothelial progenitor cells in patients with systemic sclerosis. *Arthritis research & therapy* 2010, 12(6):R205.
93. Anderegg U, Saalbach A, Haustein UF: Chemokine release from activated human dermal microvascular endothelial cells--implications for the pathophysiology of scleroderma? *Archives of dermatological research* 2000, 292(7):341-347.
94. Cerinic MM, Valentini G, Sorano GG, D'Angelo S, Cuomo G, Fenu L, Generini S, Cinotti S, Morfini M, Pignone A *et al*: Blood coagulation, fibrinolysis, and markers of endothelial dysfunction in systemic sclerosis. *Seminars in arthritis and rheumatism* 2003, 32(5):285-295.

95. Kraling BM, Maul GG, Jimenez SA: Mononuclear cellular infiltrates in clinically involved skin from patients with systemic sclerosis of recent onset predominantly consist of monocytes/macrophages. *Pathobiology* 1995, 63(1):48-56.
96. Ruzek MC, Jha S, Ledbetter S, Richards SM, Garman RD: A modified model of graft-versus-host-induced systemic sclerosis (scleroderma) exhibits all major aspects of the human disease. *Arthritis and rheumatism* 2004, 50(4):1319-1331.
97. Seibold JR, Giorno RC, Claman HN: Dermal mast cell degranulation in systemic sclerosis. *Arthritis and rheumatism* 1990, 33(11):1702-1709.
98. Yamamoto T, Takahashi Y, Takagawa S, Katayama I, Nishioka K: Animal model of sclerotic skin. II. Bleomycin induced scleroderma in genetically mast cell deficient WBB6F1-W/W(V) mice. *The Journal of rheumatology* 1999, 26(12):2628-2634.
99. Mathai SK, Gulati M, Peng X, Russell TR, Shaw AC, Rubinowitz AN, Murray LA, Siner JM, Antin-Ozerkis DE, Montgomery RR *et al*: Circulating monocytes from systemic sclerosis patients with interstitial lung disease show an enhanced profibrotic phenotype. *Laboratory investigation; a journal of technical methods and pathology*, 90(6):812-823.
100. Higashi-Kuwata N, Jinnin M, Makino T, Fukushima S, Inoue Y, Muchemwa FC, Yonemura Y, Komohara Y, Takeya M, Mitsuya H *et al*: Characterization of monocyte/macrophage subsets in the skin and peripheral blood derived from patients with systemic sclerosis. *Arthritis research & therapy*, 12(4):R128.
101. Roelofs MF, Joosten LA, Abdollahi-Roodsaz S, van Lieshout AW, Sprong T, van den Hoogen FH, van den Berg WB, Radstake TR: The expression of toll-like receptors 3 and 7 in rheumatoid arthritis synovium is increased and costimulation of toll-like receptors 3, 4, and 7/8 results in synergistic cytokine production by dendritic cells. *Arthritis and rheumatism* 2005, 52(8):2313-2322.
102. van Lieshout AW, Vonk MC, Bredie SJ, Joosten LB, Netea MG, van Riel PL, Lafyatis R, van den Hoogen FH, Radstake TR: Enhanced interleukin-10 production by dendritic cells upon stimulation with Toll-like receptor 4 agonists in systemic sclerosis that is possibly implicated in CCL18 secretion. *Scandinavian journal of rheumatology* 2009, 38(4):282-290.
103. Farina GA, York MR, Di Marzio M, Collins CA, Meller S, Homey B, Rifkin IR, Marshak-Rothstein A, Radstake TR, Lafyatis R: Poly(I:C) drives type I IFN- and TGFbeta-mediated inflammation and dermal fibrosis simulating altered gene expression in systemic sclerosis. *The Journal of investigative dermatology*, 130(11):2583-2593.
104. Roumm AD, Whiteside TL, Medsger TA, Jr., Rodnan GP: Lymphocytes in the skin of patients with progressive systemic sclerosis. Quantification, subtyping, and clinical correlations. *Arthritis and rheumatism* 1984, 27(6):645-653.
105. Varga J, Abraham D: Systemic sclerosis: a prototypic multisystem fibrotic disorder. *The Journal of clinical investigation* 2007, 117(3):557-567.
106. Artlett CM: Immunology of systemic sclerosis. *Front Biosci* 2005, 10:1707-1719.
107. Mavalia C, Scaletti C, Romagnani P, Carossino AM, Pignone A, Emmi L, Pupilli C, Pizzolo G, Maggi E, Romagnani S: Type 2 helper T-cell predominance and high CD30 expression in systemic sclerosis. *The American journal of pathology* 1997, 151(6):1751-1758.
108. Valentini G, Baroni A, Esposito K, Naclerio C, Buommino E, Farzati A, Cuomo G, Farzati B: Peripheral blood T lymphocytes from systemic sclerosis patients show both Th1 and Th2 activation. *Journal of clinical immunology* 2001, 21(3):210-217.

109. Lakos G, Melichian D, Wu M, Varga J: Increased bleomycin-induced skin fibrosis in mice lacking the Th1-specific transcription factor T-bet. *Pathobiology* 2006, 73(5):224-237.
110. Tanaka C, Fujimoto M, Hamaguchi Y, Sato S, Takehara K, Hasegawa M: Inducible costimulator ligand regulates bleomycin-induced lung and skin fibrosis in a mouse model independently of the inducible costimulator/inducible costimulator ligand pathway. *Arthritis and rheumatism*, 62(6):1723-1732.
111. Chizzolini C, Rezzonico R, Ribbens C, Burger D, Wollheim FA, Dayer JM: Inhibition of type I collagen production by dermal fibroblasts upon contact with activated T cells: different sensitivity to inhibition between systemic sclerosis and control fibroblasts. *Arthritis and rheumatism* 1998, 41(11):2039-2047.
112. Chizzolini C, Parel Y, De Luca C, Tyndall A, Akesson A, Scheja A, Dayer JM: Systemic sclerosis Th2 cells inhibit collagen production by dermal fibroblasts via membrane-associated tumor necrosis factor alpha. *Arthritis and rheumatism* 2003, 48(9):2593-2604.
113. Saito E, Fujimoto M, Hasegawa M, Komura K, Hamaguchi Y, Kaburagi Y, Nagaoka T, Takehara K, Tedder TF, Sato S: CD19-dependent B lymphocyte signaling thresholds influence skin fibrosis and autoimmunity in the tight-skin mouse. *The Journal of clinical investigation* 2002, 109(11):1453-1462.
114. Hasegawa M, Hamaguchi Y, Yanaba K, Bouaziz JD, Uchida J, Fujimoto M, Matsushita T, Matsushita Y, Horikawa M, Komura K *et al*: B-lymphocyte depletion reduces skin fibrosis and autoimmunity in the tight-skin mouse model for systemic sclerosis. *The American journal of pathology* 2006, 169(3):954-966.
115. Sato S, Hasegawa M, Fujimoto M, Tedder TF, Takehara K: Quantitative genetic variation in CD19 expression correlates with autoimmunity. *J Immunol* 2000, 165(11):6635-6643.
116. Matsushita T, Hasegawa M, Yanaba K, Kodera M, Takehara K, Sato S: Elevated serum BAFF levels in patients with systemic sclerosis: enhanced BAFF signaling in systemic sclerosis B lymphocytes. *Arthritis and rheumatism* 2006, 54(1):192-201.
117. Zhang J, Roschke V, Baker KP, Wang Z, Alarcon GS, Fessler BJ, Bastian H, Kimberly RP, Zhou T: Cutting edge: a role for B lymphocyte stimulator in systemic lupus erythematosus. *J Immunol* 2001, 166(1):6-10.
118. Groom J, Kalled SL, Cutler AH, Olson C, Woodcock SA, Schneider P, Tschopp J, Cachero TG, Batten M, Wheway J *et al*: Association of BAFF/BLyS overexpression and altered B cell differentiation with Sjogren's syndrome. *The Journal of clinical investigation* 2002, 109(1):59-68.
119. Scala E, Pallotta S, Frezzolini A, Abeni D, Barbieri C, Sampogna F, De Pita O, Puddu P, Paganelli R, Russo G: Cytokine and chemokine levels in systemic sclerosis: relationship with cutaneous and internal organ involvement. *Clinical and experimental immunology* 2004, 138(3):540-546.
120. Wynn TA: Fibrotic disease and the T(H)1/T(H)2 paradigm. *Nature reviews* 2004, 4(8):583-594.
121. Okano Y: Antinuclear antibody in systemic sclerosis (scleroderma). *Rheumatic diseases clinics of North America* 1996, 22(4):709-735.
122. Walker JG, Fritzler MJ: Update on autoantibodies in systemic sclerosis. *Current opinion in rheumatology* 2007, 19(6):580-591.
123. Moroi Y, Peebles C, Fritzler MJ, Steigerwald J, Tan EM: Autoantibody to centromere (kinetochore) in scleroderma sera. *Proceedings of the National Academy of Sciences of the United States of America* 1980, 77(3):1627-1631.

124. Earnshaw WC, Machlin PS, Bordwell BJ, Rothfield NF, Cleveland DW: Analysis of anticentromere autoantibodies using cloned autoantigen CENP-B. *Proceedings of the National Academy of Sciences of the United States of America* 1987, 84(14):4979-4983.
125. Reveille JD, Solomon DH: Evidence-based guidelines for the use of immunologic tests: anticentromere, Scl-70, and nucleolar antibodies. *Arthritis and rheumatism* 2003, 49(3):399-412.
126. Hamaguchi Y: Autoantibody profiles in systemic sclerosis: predictive value for clinical evaluation and prognosis. *The Journal of dermatology*, 37(1):42-53.
127. Kuwana M, Kaburaki J, Mimori T, Tojo T, Homma M: Autoantibody reactive with three classes of RNA polymerases in sera from patients with systemic sclerosis. *The Journal of clinical investigation* 1993, 91(4):1399-1404.
128. Van Eenennaam H, Vogelzangs JH, Lugtenberg D, Van Den Hoogen FH, Van Venrooij WJ, Pruijn GJ: Identity of the RNase MRP- and RNase P-associated Th/To autoantigen. *Arthritis and rheumatism* 2002, 46(12):3266-3272.
129. Carvalho D, Savage CO, Black CM, Pearson JD: IgG antiendothelial cell autoantibodies from scleroderma patients induce leukocyte adhesion to human vascular endothelial cells in vitro. Induction of adhesion molecule expression and involvement of endothelium-derived cytokines. *The Journal of clinical investigation* 1996, 97(1):111-119.
130. Alderuccio F, Witherden D, Toh BH, Barnett A: Autoantibody to gp50, a glycoprotein shared in common between fibroblasts and lymphocytes, in progressive systemic sclerosis. *Clinical and experimental immunology* 1989, 78(1):26-30.
131. Ronda N, Gatti R, Giacosa R, Raschi E, Testoni C, Meroni PL, Buzio C, Orlandini G: Antifibroblast antibodies from systemic sclerosis patients are internalized by fibroblasts via a caveolin-linked pathway. *Arthritis and rheumatism* 2002, 46(6):1595-1601.
132. Chizzolini C, Raschi E, Rezzonico R, Testoni C, Mallone R, Gabrielli A, Facchini A, Del Papa N, Borghi MO, Dayer JM *et al*: Autoantibodies to fibroblasts induce a proadhesive and proinflammatory fibroblast phenotype in patients with systemic sclerosis. *Arthritis and rheumatism* 2002, 46(6):1602-1613.
133. Terrier B, Tamby MC, Camoin L, Guilpain P, Berezne A, Tamas N, Broussard C, Hotellier F, Humbert M, Simonneau G *et al*: Antifibroblast antibodies from systemic sclerosis patients bind to  $\alpha$ -enolase and are associated with interstitial lung disease. *Annals of the rheumatic diseases* 2010, 69(2):428-433.
134. Tan FK, Arnett FC, Antohi S, Saito S, Mirarchi A, Spiera H, Sasaki T, Shoichi O, Takeuchi K, Pandey JP *et al*: Autoantibodies to the extracellular matrix microfibrillar protein, fibrillin-1, in patients with scleroderma and other connective tissue diseases. *J Immunol* 1999, 163(2):1066-1072.
135. Classen JF, Henrohn D, Rorsman F, Lennartsson J, Lauwerys BR, Wikstrom G, Rorsman C, Lenglez S, Franck-Larsson K, Tomasi JP *et al*: Lack of evidence of stimulatory autoantibodies to platelet-derived growth factor receptor in patients with systemic sclerosis. *Arthritis and rheumatism* 2009, 60(4):1137-1144.
136. Riemekasten G, Philippe A, Nather M, Slowinski T, Muller DN, Heidecke H, Matucci-Cerinic M, Czirjak L, Lukitsch I, Becker M *et al*: Involvement of functional autoantibodies against vascular receptors in systemic sclerosis. *Annals of the rheumatic diseases*, 70(3):530-536.
137. Smith V, Van Praet JT, Vandooren B, Van der Cruyssen B, Naeyaert JM, Decuman S, Elewaut D, De Keyser F: Rituximab in diffuse cutaneous systemic sclerosis: an open-

- label clinical and histopathological study. *Annals of the rheumatic diseases*, 69(1):193-197.
138. Lafyatis R, Kissin E, York M, Farina G, Viger K, Fritzler MJ, Merkel PA, Simms RW: B cell depletion with rituximab in patients with diffuse cutaneous systemic sclerosis. *Arthritis and rheumatism* 2009, 60(2):578-583.
  139. Bosello S, De Santis M, Lama G, Spano C, Angelucci C, Tolusso B, Sica G, Ferraccioli G: B cell depletion in diffuse progressive systemic sclerosis: safety, skin score modification and IL-6 modulation in an up to thirty-six months follow-up open-label trial. *Arthritis research & therapy*, 12(2):R54.
  140. Daoussis D, Liossis SN, Tsamandas AC, Kalogeropoulou C, Kazantzi A, Sirinian C, Karampetsou M, Yiannopoulos G, Andonopoulos AP: Experience with rituximab in scleroderma: results from a 1-year, proof-of-principle study. *Rheumatology (Oxford, England)*, 49(2):271-280.
  141. Ranque B, Mouthon L: Geoepidemiology of systemic sclerosis. *Autoimmunity reviews*, 9(5):A311-318.
  142. Agarwal SK: The genetics of systemic sclerosis. *Discovery medicine*, 10(51):134-143.
  143. Tan FK, Stivers DN, Foster MW, Chakraborty R, Howard RF, Milewicz DM, Arnett FC: Association of microsatellite markers near the fibrillin 1 gene on human chromosome 15q with scleroderma in a Native American population. *Arthritis and rheumatism* 1998, 41(10):1729-1737.
  144. Green MC, Sweet HO, Bunker LE: Tight-skin, a new mutation of the mouse causing excessive growth of connective tissue and skeleton. *The American journal of pathology* 1976, 82(3):493-512.
  145. Harrison RE, Flanagan JA, Sankelo M, Abdalla SA, Rowell J, Machado RD, Elliott CG, Robbins IM, Olschewski H, McLaughlin V *et al*: Molecular and functional analysis identifies ALK-1 as the predominant cause of pulmonary hypertension related to hereditary haemorrhagic telangiectasia. *Journal of medical genetics* 2003, 40(12):865-871.
  146. Fonseca C, Lindahl GE, Ponticos M, Sestini P, Renzoni EA, Holmes AM, Spagnolo P, Pantelidis P, Leoni P, McHugh N *et al*: A polymorphism in the CTGF promoter region associated with systemic sclerosis. *The New England journal of medicine* 2007, 357(12):1210-1220.
  147. Broen JC, Coenen MJ, Radstake TR: Genetics of systemic sclerosis: an update. *Current rheumatology reports*, 14(1):11-21.
  148. Dieude P, Boileau C, Guedj M, Avouac J, Ruiz B, Hachulla E, Diot E, Cracowski JL, Tiev K, Sibilia J *et al*: Independent replication establishes the CD247 gene as a genetic systemic sclerosis susceptibility factor. *Annals of the rheumatic diseases*, 70(9):1695-1696.
  149. Sharif R, Mayes MD, Tan FK, Gorlova OY, Hummers LK, Shah AA, Furst DE, Khanna D, Martin J, Bossini-Castillo L *et al*: IRF5 polymorphism predicts prognosis in patients with systemic sclerosis. *Annals of the rheumatic diseases*, 71(7):1197-1202.
  150. Graham RR, Kyogoku C, Sigurdsson S, Vlasova IA, Davies LR, Baechler EC, Plenge RM, Koeuth T, Ortmann WA, Hom G *et al*: Three functional variants of IFN regulatory factor 5 (IRF5) define risk and protective haplotypes for human lupus. *Proceedings of the National Academy of Sciences of the United States of America* 2007, 104(16):6758-6763.
  151. Sigurdsson S, Nordmark G, Goring HH, Lindroos K, Wiman AC, Sturfelt G, Jonsen A, Rantapaa-Dahlqvist S, Moller B, Kere J *et al*: Polymorphisms in the tyrosine kinase

- 2 and interferon regulatory factor 5 genes are associated with systemic lupus erythematosus. *American journal of human genetics* 2005, 76(3):528-537.
152. Gourh P, Arnett FC, Tan FK, Assassi S, Divecha D, Paz G, McNearney T, Draeger H, Reveille JD, Mayes MD *et al*: Association of TNFSF4 (OX40L) polymorphisms with susceptibility to systemic sclerosis. *Annals of the rheumatic diseases*, 69(3):550-555.
  153. Nietert PJ, Silver RM: Systemic sclerosis: environmental and occupational risk factors. *Current opinion in rheumatology* 2000, 12(6):520-526.
  154. Ferri C, Giuggioli D, Sebastiani M, Panfilo S, Abatangelo G, Zakrzewska K, Azzi A: Parvovirus B19 infection of cultured skin fibroblasts from systemic sclerosis patients: comment on the article by Ray *et al*. *Arthritis and rheumatism* 2002, 46(8):2262-2263; author reply 2263-2264.
  155. Magro CM, Nuovo G, Ferri C, Crowson AN, Giuggioli D, Sebastiani M: Parvoviral infection of endothelial cells and stromal fibroblasts: a possible pathogenetic role in scleroderma. *Journal of cutaneous pathology* 2004, 31(1):43-50.
  156. Ray NB, Nieva DR, Seftor EA, Khalkhali-Ellis Z, Naides SJ: Induction of an invasive phenotype by human parvovirus B19 in normal human synovial fibroblasts. *Arthritis and rheumatism* 2001, 44(7):1582-1586.
  157. Lunardi C, Dolcino M, Peterlana D, Bason C, Navone R, Tamassia N, Beri R, Corrocher R, Puccetti A: Antibodies against human cytomegalovirus in the pathogenesis of systemic sclerosis: a gene array approach. *PLoS medicine* 2006, 3(1):e2.
  158. Muryoi T, Kasturi KN, Kafina MJ, Cram DS, Harrison LC, Sasaki T, Bona CA: Antitopoisomerase I monoclonal autoantibodies from scleroderma patients and tight skin mouse interact with similar epitopes. *The Journal of experimental medicine* 1992, 175(4):1103-1109.
  159. Jimenez SA, Christner PJ: Murine animal models of systemic sclerosis. *Current opinion in rheumatology* 2002, 14(6):671-680.
  160. Chen SJ, Ning H, Ishida W, Sodin-Semrl S, Takagawa S, Mori Y, Varga J: The early-immediate gene EGR-1 is induced by transforming growth factor-beta and mediates stimulation of collagen gene expression. *The Journal of biological chemistry* 2006, 281(30):21183-21197.
  161. Lakos G, Takagawa S, Chen SJ, Ferreira AM, Han G, Masuda K, Wang XJ, DiPietro LA, Varga J: Targeted disruption of TGF-beta/Smad3 signaling modulates skin fibrosis in a mouse model of scleroderma. *The American journal of pathology* 2004, 165(1):203-217.
  162. Servettaz A, Goulvestre C, Kavian N, Nicco C, Guilpain P, Chereau C, Vuiblet V, Guillevin L, Mouthon L, Weill B *et al*: Selective oxidation of DNA topoisomerase 1 induces systemic sclerosis in the mouse. *J Immunol* 2009, 182(9):5855-5864.
  163. Batteux F, Kavian N, Servettaz A: New insights on chemically induced animal models of systemic sclerosis. *Current opinion in rheumatology*, 23(6):511-518.
  164. Le Hir M, Martin M, Haas C: A syndrome resembling human systemic sclerosis (scleroderma) in MRL/lpr mice lacking interferon-gamma (IFN-gamma) receptor (MRL/lprgammaR-/-). *Clinical and experimental immunology* 1999, 115(2):281-287.
  165. Maurer B, Busch N, Jungel A, Pileckyte M, Gay RE, Michel BA, Schett G, Gay S, Distler J, Distler O: Transcription factor fos-related antigen-2 induces progressive peripheral vasculopathy in mice closely resembling human systemic sclerosis. *Circulation* 2009, 120(23):2367-2376.
  166. Asano Y, Stawski L, Hant F, Highland K, Silver R, Szalai G, Watson DK, Trojanowska M: Endothelial Fli1 deficiency impairs vascular homeostasis: a role in scleroderma vasculopathy. *The American journal of pathology*, 176(4):1983-1998.

167. Wei J, Melichian D, Komura K, Hinchcliff M, Lam AP, Lafyatis R, Gottardi CJ, MacDougald OA, Varga J: Canonical Wnt signaling induces skin fibrosis and subcutaneous lipoatrophy: a novel mouse model for scleroderma? *Arthritis and rheumatism*, 63(6):1707-1717.
168. Christner PJ, Artlett CM, Conway RF, Jimenez SA: Increased numbers of microchimeric cells of fetal origin are associated with dermal fibrosis in mice following injection of vinyl chloride. *Arthritis and rheumatism* 2000, 43(11):2598-2605.
169. Christner PJ, Peters J, Hawkins D, Siracusa LD, Jimenez SA: The tight skin 2 mouse. An animal model of scleroderma displaying cutaneous fibrosis and mononuclear cell infiltration. *Arthritis and rheumatism* 1995, 38(12):1791-1798.
170. Gentiletti J, McCloskey LJ, Artlett CM, Peters J, Jimenez SA, Christner PJ: Demonstration of autoimmunity in the tight skin-2 mouse: a model for scleroderma. *J Immunol* 2005, 175(4):2418-2426.
171. McCormick LL, Zhang Y, Tootell E, Gilliam AC: Anti-TGF-beta treatment prevents skin and lung fibrosis in murine sclerodermatous graft-versus-host disease: a model for human scleroderma. *J Immunol* 1999, 163(10):5693-5699.
172. Gershwin ME, Abplanalp H, Castles JJ, Ikeda RM, van der Water J, Eklund J, Haynes D: Characterization of a spontaneous disease of white leghorn chickens resembling progressive systemic sclerosis (scleroderma). *The Journal of experimental medicine* 1981, 153(6):1640-1659.
173. D'Autreaux B, Toledano MB: ROS as signalling molecules: mechanisms that generate specificity in ROS homeostasis. *Nature reviews* 2007, 8(10):813-824.
174. Temple MD, Perrone GG, Dawes IW: Complex cellular responses to reactive oxygen species. *Trends in cell biology* 2005, 15(6):319-326.
175. Slaughter RL, Edwards DJ: Recent advances: the cytochrome P450 enzymes. *The Annals of pharmacotherapy* 1995, 29(6):619-624.
176. Geiszt M, Leto TL: The Nox family of NAD(P)H oxidases: host defense and beyond. *The Journal of biological chemistry* 2004, 279(50):51715-51718.
177. Zelko IN, Mariani TJ, Folz RJ: Superoxide dismutase multigene family: a comparison of the CuZn-SOD (SOD1), Mn-SOD (SOD2), and EC-SOD (SOD3) gene structures, evolution, and expression. *Free radical biology & medicine* 2002, 33(3):337-349.
178. Dalle-Donne I, Rossi R, Giustarini D, Gagliano N, Lusini L, Milzani A, Di Simplicio P, Colombo R: Actin carbonylation: from a simple marker of protein oxidation to relevant signs of severe functional impairment. *Free radical biology & medicine* 2001, 31(9):1075-1083.
179. Stratford N, Murphy P: Effect of lipid and propofol on oxidation of haemoglobin by reactive oxygen species. *British journal of anaesthesia* 1997, 78(3):320-322.
180. Cooke MS, Evans MD, Dizdaroglu M, Lunec J: Oxidative DNA damage: mechanisms, mutation, and disease. *Faseb J* 2003, 17(10):1195-1214.
181. Babior BM, Kipnes RS, Curnutte JT: Biological defense mechanisms. The production by leukocytes of superoxide, a potential bactericidal agent. *The Journal of clinical investigation* 1973, 52(3):741-744.
182. Grisham MB: Reactive oxygen species in immune responses. *Free radical biology & medicine* 2004, 36(12):1479-1480.
183. Laurent A, Nicco C, Chereau C, Goulvestre C, Alexandre J, Alves A, Levy E, Goldwasser F, Panis Y, Soubrane O *et al*: Controlling tumor growth by modulating endogenous production of reactive oxygen species. *Cancer research* 2005, 65(3):948-956.

184. Robinson MJ, Cobb MH: Mitogen-activated protein kinase pathways. *Current opinion in cell biology* 1997, 9(2):180-186.
185. Davis RJ: Signal transduction by the JNK group of MAP kinases. *Cell* 2000, 103(2):239-252.
186. Rao GN, Lassegue B, Griendling KK, Alexander RW, Berk BC: Hydrogen peroxide-induced c-fos expression is mediated by arachidonic acid release: role of protein kinase C. *Nucleic acids research* 1993, 21(5):1259-1263.
187. Ushio-Fukai M, Alexander RW: Reactive oxygen species as mediators of angiogenesis signaling: role of NAD(P)H oxidase. *Molecular and cellular biochemistry* 2004, 264(1-2):85-97.
188. Bose KS, Vyas P, Singh M: Plasma non-enzymatic antioxidants-vitamin C, E, beta-carotenes, reduced glutathione levels and total antioxidant activity in oral sub mucous fibrosis. *European review for medical and pharmacological sciences*, 16(4):530-532.
189. Percy ME: Catalase: an old enzyme with a new role? *Canadian journal of biochemistry and cell biology = Revue canadienne de biochimie et biologie cellulaire* 1984, 62(10):1006-1014.
190. Meister A: Glutathione metabolism. *Methods in enzymology* 1995, 251:3-7.
191. Avouac J, Borderie D, Ekindjian OG, Kahan A, Allanore Y: High DNA oxidative damage in systemic sclerosis. *The Journal of rheumatology*, 37(12):2540-2547.
192. Srivastava KD, Rom WN, Jagirdar J, Yie TA, Gordon T, Tchou-Wong KM: Crucial role of interleukin-1beta and nitric oxide synthase in silica-induced inflammation and apoptosis in mice. *American journal of respiratory and critical care medicine* 2002, 165(4):527-533.
193. Gossart S, Cambon C, Orfila C, Seguelas MH, Lepert JC, Rami J, Carre P, Pipy B: Reactive oxygen intermediates as regulators of TNF-alpha production in rat lung inflammation induced by silica. *J Immunol* 1996, 156(4):1540-1548.
194. Yamamoto T, Takagawa S, Katayama I, Mizushima Y, Nishioka K: Effect of superoxide dismutase on bleomycin-induced dermal sclerosis: implications for the treatment of systemic sclerosis. *The Journal of investigative dermatology* 1999, 113(5):843-847.
195. Cardenas A, Abian J, Bulbena O, Rosello J, Gelpi E: Determination of oxidation products of N-phenyllinoleamide: Spanish toxic oil syndrome studies. *Journal of chromatography* 1988, 426(1):83-91.
196. Allanore Y, Borderie D, Lemarechal H, Ekindjian OG, Kahan A: Acute and sustained effects of dihydropyridine-type calcium channel antagonists on oxidative stress in systemic sclerosis. *The American journal of medicine* 2004, 116(9):595-600.
197. Solans R, Motta C, Sola R, La Ville AE, Lima J, Simeon P, Montella N, Armadans-Gil L, Fonollosa V, Vilardell M: Abnormalities of erythrocyte membrane fluidity, lipid composition, and lipid peroxidation in systemic sclerosis: evidence of free radical-mediated injury. *Arthritis and rheumatism* 2000, 43(4):894-900.
198. Sambo P, Jannino L, Candela M, Salvi A, Donini M, Dusi S, Luchetti MM, Gabrielli A: Monocytes of patients with systemic sclerosis (scleroderma) spontaneously release in vitro increased amounts of superoxide anion. *The Journal of investigative dermatology* 1999, 112(1):78-84.
199. Dooley A, Gao B, Bradley N, Abraham DJ, Black CM, Jacobs M, Bruckdorfer KR: Abnormal nitric oxide metabolism in systemic sclerosis: increased levels of nitrated proteins and asymmetric dimethylarginine. *Rheumatology (Oxford)* 2006, 45(6):676-684.

200. Dooley A, Low SY, Holmes A, Kidane AG, Abraham DJ, Black CM, Bruckdorfer KR: Nitric oxide synthase expression and activity in the tight-skin mouse model of fibrosis. *Rheumatology (Oxford, England)* 2008, 47(3):272-280.
201. Chung MP, Monick MM, Hamzeh NY, Butler NS, Powers LS, Hunninghake GW: Role of repeated lung injury and genetic background in bleomycin-induced fibrosis. *American journal of respiratory cell and molecular biology* 2003, 29(3 Pt 1):375-380.
202. Yoshimura S, Nishimura Y, Nishiura T, Yamashita T, Kobayashi K, Yokoyama M: Overexpression of nitric oxide synthase by the endothelium attenuates bleomycin-induced lung fibrosis and impairs MMP-9/TIMP-1 balance. *Respirology (Carlton, Vic)* 2006, 11(5):546-556.
203. Cotton SA, Herrick AL, Jayson MI, Freemont AJ: Endothelial expression of nitric oxide synthases and nitrotyrosine in systemic sclerosis skin. *The Journal of pathology* 1999, 189(2):273-278.
204. Yamamoto T, Katayama I, Nishioka K: Nitric oxide production and inducible nitric oxide synthase expression in systemic sclerosis. *The Journal of rheumatology* 1998, 25(2):314-317.
205. Beckman JS, Koppenol WH: Nitric oxide, superoxide, and peroxynitrite: the good, the bad, and ugly. *The American journal of physiology* 1996, 271(5 Pt 1):C1424-1437.
206. Takagi K, Kawaguchi Y, Hara M, Sugiura T, Harigai M, Kamatani N: Serum nitric oxide (NO) levels in systemic sclerosis patients: correlation between NO levels and clinical features. *Clinical and experimental immunology* 2003, 134(3):538-544.
207. Urtasun R, Conde de la Rosa L, Nieto N: Oxidative and nitrosative stress and fibrogenic response. *Clinics in liver disease* 2008, 12(4):769-790, viii.
208. Servettaz A, Guilpain P, Goulvestre C, Chereau C, Hercend C, Nicco C, Guillevin L, Weill B, Mouthon L, Batteux F: Radical oxygen species production induced by advanced oxidation protein products predicts clinical evolution and response to treatment in systemic sclerosis. *Annals of the rheumatic diseases* 2007, 66(9):1202-1209.
209. Kawaguchi Y, Takagi K, Hara M, Fukasawa C, Sugiura T, Nishimagi E, Harigai M, Kamatani N: Angiotensin II in the lesional skin of systemic sclerosis patients contributes to tissue fibrosis via angiotensin II type 1 receptors. *Arthritis and rheumatism* 2004, 50(1):216-226.
210. Wang W, Huang XR, Canlas E, Oka K, Truong LD, Deng C, Bhowmick NA, Ju W, Bottinger EP, Lan HY: Essential role of Smad3 in angiotensin II-induced vascular fibrosis. *Circulation research* 2006, 98(8):1032-1039.
211. Dooley A, Bruckdorfer KR, Abraham DJ: Modulation of fibrosis in systemic sclerosis by nitric oxide and antioxidants. *Cardiology research and practice* 2012, 2012:521958.
212. Martinez-Salgado C, Fuentes-Calvo I, Garcia-Cenador B, Santos E, Lopez-Novoa JM: Involvement of H- and N-Ras isoforms in transforming growth factor-beta1-induced proliferation and in collagen and fibronectin synthesis. *Experimental cell research* 2006, 312(11):2093-2106.
213. Malcarne VL, Hansdottir I, McKinney A, Upchurch R, Greenbergs HL, Henstorf GH, Furst DE, Clements PJ, Weisman MH: Medical signs and symptoms associated with disability, pain, and psychosocial adjustment in systemic sclerosis. *The Journal of rheumatology* 2007, 34(2):359-367.
214. Riemekasten G, Philippe A, Nather M, Slowinski T, Muller DN, Heidecke H, Matucci-Cerinic M, Czirjak L, Lukitsch I, Becker M *et al*: Involvement of functional autoantibodies against vascular receptors in systemic sclerosis. *Annals of the rheumatic diseases* 2011, 70(3):530-536.

215. de Gasparo M, Catt KJ, Inagami T, Wright JW, Unger T: International union of pharmacology. XXIII. The angiotensin II receptors. *Pharmacological reviews* 2000, 52(3):415-472.
216. Dragun D, Muller DN, Brasen JH, Fritsche L, Nieminen-Kelha M, Dechend R, Kintscher U, Rudolph B, Hoebeke J, Eckert D *et al*: Angiotensin II type 1-receptor activating antibodies in renal-allograft rejection. *The New England journal of medicine* 2005, 352(6):558-569.
217. Wallukat G, Homuth V, Fischer T, Lindschau C, Horstkamp B, Jupner A, Baur E, Nissen E, Vetter K, Neichel D *et al*: Patients with preeclampsia develop agonistic autoantibodies against the angiotensin AT1 receptor. *The Journal of clinical investigation* 1999, 103(7):945-952.
218. Xia Y, Ramin SM, Kellems RE: Potential roles of angiotensin receptor-activating autoantibody in the pathophysiology of preeclampsia. *Hypertension* 2007, 50(2):269-275.
219. Servettaz A, Goulvestre C, Kavian N, Nicco C, Guilpain P, Chéreau C, Vuiblet V, Guillevin L, Mouthon L, Weill B *et al*: Selective oxidation of DNA topoisomerase 1 induced systemic sclerosis in the mouse. *J Immunol* 2009, 182(9):5855-5864.
220. Dalle-Donne I, Rossi R, Giustarini D, Gagliano N, Lusini L, Milzani A, Di Simplicio P, Colombo R: Actin carbonylation: from a simple marker of protein oxidation to relevant signs of severe functional impairment. *Free radical biology & medicine* 2001, 1:1075-1083.
221. Burdick MD, Murray LA, Keane MP, Xue YY, Zisman DA, Belperio JA, Strieter RM: CXCL11 attenuates bleomycin-induced pulmonary fibrosis via inhibition of vascular remodeling. *Am J Respir Crit Care Med* 2005, 171:261–268.
222. Sue RD, Belperio JA, Burdick MD, Murray LA, Xue YY, Dy MC, Kwon JJ, Keane MP, Strieter RM: CXCR2 is critical to hyperoxia-induced lung injury. *J Immunol* 2004, 172:3860–3868.
223. Servettaz A, Kavian N, Nicco C, Deveaux V, Chereau C, Wang A, Zimmer A, Lotersztajn S, Weill B, Batteux F: Targeting the cannabinoid pathway limits the development of fibrosis and autoimmunity in a mouse model of systemic sclerosis. *The American journal of pathology* 2010, 177(1):187-196.
224. Marut WK, Kavian N, Servettaz A, Nicco C, Ba LA, Doering M, Chereau C, Jacob C, Weill B, Batteux F: The Organotelluride Catalyst (PHTE)(2)NQ Prevents HOCl-Induced Systemic Sclerosis in Mouse. *The Journal of investigative dermatology* 2012.
225. Kavian N, Servettaz A, Mongaret C, Wang A, Nicco C, Chereau C, Grange P, Vuiblet V, Birembaut P, Diebold MD *et al*: Targeting ADAM-17/notch signaling abrogates the development of systemic sclerosis in a murine model. *Arthritis and rheumatism* 2010, 62(11):3477-3487.
226. Sastry KV, Moudgal RP, Mohan J, Tyagi JS, Rao GS: Spectrophotometric determination of serum nitrite and nitrate by copper-cadmium alloy. *Analytical biochemistry* 2002, 306(1):79-82.
227. Delclaux C, Dinh-Xuan AT: [Art--and artefacts--of exhaled NO measurement in asthma]. *Revue des maladies respiratoires* 2005, 22(2 Pt 1):209-211.
228. Shimizu K, Ogawa F, Muroi E, Hara T, Komura K, Bae SJ, Sato S: Increased serum levels of nitrotyrosine, a marker for peroxynitrite production, in systemic sclerosis. *Clinical and experimental rheumatology* 2007, 25(2):281-286.
229. Tiev KP, Hua-Huy T, Kettaneh A, Allanore Y, Le-Dong NN, Duong-Quy S, Cabane J, Dinh-Xuan AT: Alveolar concentration of nitric oxide predicts pulmonary function deterioration in scleroderma. *Thorax* 2012, 67(2):157-163.

230. Gruschwitz MS, Hornstein OP, von Den Driesch P: Correlation of soluble adhesion molecules in the peripheral blood of scleroderma patients with their in situ expression and with disease activity. *Arthritis and rheumatism* 1995, 38(2):184-189.
231. Takagi K, Kawaguchi Y, Kawamoto M, Ota Y, Tochimoto A, Gono T, Katsumata Y, Takagi M, Hara M, Yamanaka H: Activation of the activin A-ALK-Smad pathway in systemic sclerosis. *Journal of autoimmunity* 2011, 36(3-4):181-188.
232. Smaldone S, Olivieri J, Gusella GL, Moroncini G, Gabrielli A, Ramirez F: Ha-Ras stabilization mediates pro-fibrotic signals in dermal fibroblasts. *Fibrogenesis & tissue repair* 2011, 4(1):8.
233. Sato S, Fujimoto M, Hasegawa M, Takehara K: Altered blood B lymphocyte homeostasis in systemic sclerosis: expanded naive B cells and diminished but activated memory B cells. *Arthritis and rheumatism* 2004, 50(6):1918-1927.
234. Needleman BW, Wigley FM, Stair RW: Interleukin-1, interleukin-2, interleukin-4, interleukin-6, tumor necrosis factor alpha, and interferon-gamma levels in sera from patients with scleroderma. *Arthritis and rheumatism* 1992, 35(1):67-72.
235. Iborra S, Soto M, Stark-Aroeira L, Castellano E, Alarcon B, Alonso C, Santos E, Fernandez-Malave E: H-ras and N-ras are dispensable for T-cell development and activation but critical for protective Th1 immunity. *Blood* 2011, 117(19):5102-5111.
236. Forstermann U, Gath I, Schwarz P, Closs EI, Kleinert H: Isoforms of nitric oxide synthase. Properties, cellular distribution and expressional control. *Biochemical pharmacology* 1995, 50(9):1321-1332.
237. Sigusch HH, Campbell SE, Weber KT: Angiotensin II-induced myocardial fibrosis in rats: role of nitric oxide, prostaglandins and bradykinin. *Cardiovascular research* 1996, 31(4):546-554.
238. Berlett BS, Friguet B, Yim MB, Chock PB, Stadtman ER: Peroxynitrite-mediated nitration of tyrosine residues in Escherichia coli glutamine synthetase mimics adenylation: relevance to signal transduction. *Proceedings of the National Academy of Sciences of the United States of America* 1996, 93(5):1776-1780.
239. Tiev KP, Le-Dong NN, Duong-Quy S, Hua-Huy T, Cabane J, Dinh-Xuan AT: Exhaled nitric oxide, but not serum nitrite and nitrate, is a marker of interstitial lung disease in systemic sclerosis. *Nitric oxide : biology and chemistry / official journal of the Nitric Oxide Society* 2009, 20(3):200-206.
240. Coriat R, Marut W, Leconte M, Ba LB, Vienne A, Chereau C, Alexandre J, Weill B, Doering M, Jacob C *et al*: The organotelluride catalyst LAB027 prevents colon cancer growth in the mice. *Cell death & disease*, 2:e191.
241. Busch C, Jacob C, Anwar A, Burkholz T, Aicha Ba L, Cerella C, Diederich M, Brandt W, Wessjohann L, Montenarh M: Diallylpolysulfides induce growth arrest and apoptosis. *International journal of oncology* 2010, 36(3):743-749.
242. Takagi K, Kawaguchi Y, Kawamoto M, Ota Y, Tochimoto A, Gono T, Katsumata Y, Takagi M, Hara M, Yamanaka H: Activation of the activin A-ALK-Smad pathway in systemic sclerosis. *Journal of autoimmunity*, 36(3-4):181-188.
243. Smaldone S, Olivieri J, Gusella GL, Moroncini G, Gabrielli A, Ramirez F: Ha-Ras stabilization mediates pro-fibrotic signals in dermal fibroblasts. *Fibrogenesis & tissue repair*, 4(1):8.
244. Iborra S, Soto M, Stark-Aroeira L, Castellano E, Alarcon B, Alonso C, Santos E, Fernandez-Malave E: H-ras and N-ras are dispensable for T-cell development and activation but critical for protective Th1 immunity. *Blood*, 117(19):5102-5111.
245. Servettaz A, Kavian N, Nicco C, Deveaux V, Chereau C, Wang A, Zimmer A, Lotersztajn S, Weill B, Batteux F: Targeting the cannabinoid pathway limits the

development of fibrosis and autoimmunity in a mouse model of systemic sclerosis.  
*The American journal of pathology*, 177(1):187-196.